



<https://theses.gla.ac.uk/>

Theses Digitisation:

<https://www.gla.ac.uk/myglasgow/research/enlighten/theses/digitisation/>

This is a digitised version of the original print thesis.

Copyright and moral rights for this work are retained by the author

A copy can be downloaded for personal non-commercial research or study, without prior permission or charge

This work cannot be reproduced or quoted extensively from without first obtaining permission in writing from the author

The content must not be changed in any way or sold commercially in any format or medium without the formal permission of the author

When referring to this work, full bibliographic details including the author, title, awarding institution and date of the thesis must be given

Enlighten: Theses

<https://theses.gla.ac.uk/>  
[research-enlighten@glasgow.ac.uk](mailto:research-enlighten@glasgow.ac.uk)

# **Gyroplane Handling Qualities Assessment Using Flight Testing and Simulation Techniques**

**Marat Bagiev**

Thesis submitted to the Faculty of Engineering, University of Glasgow, for the Degree of Doctor of Philosophy. All aspects of the work contained herein are original in content except where indicated.

This thesis is based on research conducted between October 2001 and October 2004 at the Department of Aerospace Engineering, University of Glasgow.

August 2005

© Marat Bagiev, 2005

ProQuest Number: 10390726

All rights reserved

INFORMATION TO ALL USERS

The quality of this reproduction is dependent upon the quality of the copy submitted.

In the unlikely event that the author did not send a complete manuscript and there are missing pages, these will be noted. Also, if material had to be removed, a note will indicate the deletion.



ProQuest 10390726

Published by ProQuest LLC (2017). Copyright of the Dissertation is held by the Author.

All rights reserved.

This work is protected against unauthorized copying under Title 17, United States Code  
Microform Edition © ProQuest LLC.

ProQuest LLC.  
789 East Eisenhower Parkway  
P.O. Box 1346  
Ann Arbor, MI 48106 – 1346

GLASGOW  
UNIVERSITY  
LIBRARY:

# *Abstract*

Handling qualities are without doubt one of the primary objectives of the design of modern rotary-wing aircraft, where improved handling qualities increase mission effectiveness and flight safety, and reduce pilot workload. This dissertation provides results of an assessment of gyroplane handling qualities using flight testing and simulation techniques. Since at the time of writing, there are no direct handling qualities requirements and criteria developed for light gyroplanes anywhere in the world, objective handling qualities of the G-UNIV research gyroplane are estimated using criteria from numerous fixed and rotary wing aircraft specifications.

To obtain subjective handling qualities gyroplane test manoeuvres must be designed. In this thesis inverse simulation is proposed as a preliminary tool in designing gyroplane manoeuvres. A high fidelity, individual blade/blade element coupled rotor-fuselage mathematical model of a gyroplane, GSIM is developed and successfully coupled with a generic inverse simulation algorithm GENISA to form an inverse simulation package GENISA/GSIM. Two gyroplane manoeuvres, slalom and acceleration-deceleration, are designed based on those from the Aeronautical Design Standard ADS-33E-PRF. A flight test programme for the G-UNIV research gyroplane is conducted to demonstrate the use of the designed gyroplane manoeuvres and obtain subjective handling qualities.

Preliminary recommendations are proposed regarding suitability of handling qualities criteria of fixed and rotary wing aircraft. In addition, this dissertation proposes two handling qualities criteria for a light gyroplane, roll quickness and pilot attack criteria for the slalom manoeuvre.

# *Acknowledgements*

I would like to express my sincere gratitude to my supervisors, Dr Douglas Thomson and Dr Stewart Houston, for their constant support, guidance and supervision throughout the research programme and writing of this dissertation. I am greatly indebted to Robert Gilmour and the team of technicians who worked hard to prepare the research gyroplane for the flight tests. I am also grateful to Prof Frank Coton and Dr George Barakos for their assistance with rotor blade aerodynamics. I would like to thank the staff and students in the Department of Aerospace Engineering and the personnel in the Faculty Office for creating a wonderful atmosphere to work in. Special thanks go to Dr Richard Green who proofread the manuscript. I wish to thank the Universities UK for the Overseas Research Students Award and the University of Glasgow for the Scholarship.

Finally, I would like to dedicate this dissertation to my parents, Robert and Claudia, for their constant love, support and encouragement.

# Contents

<b>Abstract</b>	ii
<b>Acknowledgements</b>	iii
<b>Contents</b>	iv
<b>List of Tables</b>	viii
<b>List of Figures</b>	x
<b>Nomenclature</b>	xvi
<b>Chapter 1 Introduction</b>	1
1.1 Background and Motivation	1
1.2 Main Aim of the Thesis	5
1.3 Thesis Objectives	7
1.4 Thesis Structure	11
<b>Chapter 2 A Review of Techniques for Handling Qualities Assessment</b>	13
2.1 Introduction	13
2.2 Handling Qualities	13
2.3 British Civil Airworthiness Requirements for Light Gyroplanes	22
2.4 Aeronautical Design Standard ADS-33E-PRF	26
2.5 Specifications and Standards Review	33
2.5.1 BCAR Section S, JAR/FAR-23, JAR/FAR-27, JAR-VLA and JAR-VLR	34
2.5.2 MIL-H-8501A	35
2.5.3 MIL-F-8785C and DEF STAN 00-970	35

2.5.4 MIL-F-83300	40
2.5.5 AGARD-R-577-70	43
2.5.6 DEF STAN 00-970 Rotorcraft	45
2.5.7 MIL-HDBK-1797	47
2.6 Chapter Summary	50
<b>Chapter 3 Objective Assessment of Gyroplane</b>	
<b>Handling Qualities</b>	51
3.1 Introduction	51
3.2 Longitudinal Handling Qualities	51
3.2.1 BCAR Section T	56
3.2.2 MIL-F-8785C and DEF STAN 00-970	57
3.2.3 MIL-F-83300 and AGARD-R-577-70	59
3.2.4 DEF STAN 00-970 Rotorcraft	60
3.2.5 ADS-33E-PRF	62
3.2.6 MIL-HDBK-1797	66
3.3 Lateral-Directional Handling Qualities	68
3.3.1 BCAR Section T	70
3.3.2 MIL-F-8785C and DEF STAN 00-970	72
3.3.3 MIL-F-83300 and AGARD-R-577-70	72
3.3.4 DEF STAN 00-970 Rotorcraft	74
3.3.5 ADS-33E-PRF	75
3.4 Chapter Summary	79
<b>Chapter 4 Development of a Gyroplane Simulation</b>	
<b>Model GSIM</b>	82
4.1 Introduction	82
4.2 Overview of the Gyroplane Simulation Model	83
4.3 Aircraft Rigid Body Dynamics	86
4.4 Rotor Forces and Moments	89
4.4.1 Blade Element Kinematics	90
4.4.1.1 Blade Element Velocity	91
4.4.1.2 Blade Element Acceleration	97

4.4.2 Blade Aerodynamic Forces	99
4.4.3 Blade Inertial Forces	102
4.4.4 Total Forces and Moments	102
4.5 Blade Flapping Dynamics	104
4.6 Rotor Dynamic Inflow Model	106
4.7 Fuselage Aerodynamic Forces and Moments	112
4.8 Empennage Aerodynamic Forces and Moments	114
4.9 Validation of the GSIM	116
4.10 Chapter Summary	125
<b>Chapter 5 Gyroplane Inverse Simulation</b>	<b>126</b>
5.1 Introduction	126
5.2 Evolution of Rotorcraft Inverse Simulation	127
5.3 Generic Inverse Simulation Algorithm GENISA	130
5.4 Mathematical Modelling of Gyroplane Manoeuvres	134
5.4.1 Slalom Manoeuvre	137
5.4.2 Acceleration-Deceleration Manoeuvre	139
5.5 Inverse Simulation as a Preliminary Tool in Designing Gyroplane Manoeuvres	143
5.5.1 Slalom Manoeuvre	144
5.5.2 Acceleration-Deceleration Manoeuvre	152
5.6 Validation of the Inverse Simulation Package GENISA/GSIM	158
5.6.1 Slalom Manoeuvre	158
5.6.2 Acceleration-Deceleration Manoeuvre	163
5.7 Chapter Summary	165
<b>Chapter 6 Flight Testing Technique for Gyroplane Manoeuvres</b>	<b>167</b>
6.1 Introduction	167
6.2 Description of the G-UNIV Research Gyroplane	167
6.3 Flight Test Instrumentation	168
6.4 Ground Preparations	173
6.4.1 Calculation of Mass and Centre of Gravity	173
6.4.2 Calculation of Moments of Inertia	173

6.4.3 Calibration of the Flight Test Instrumentation	174
6.4.4 Airspeed Calculation Technique	176
6.4.5 Calculation of the Engine Power	178
6.5 Design of Flight Test Manoeuvres	179
6.5.1 Slalom Manoeuvre	179
6.5.2 Acceleration-Deceleration Manoeuvre	182
6.6 Chapter Summary	186
<b>Chapter 7 Flight Testing of the G-UNIV Gyroplane for Subjective Assessment of Handling Qualities and Criteria Design</b>	<b>188</b>
7.1 Introduction	188
7.2 Flight Tests of the G-UNIV Gyroplane for Handling Qualities and Workload Assessment	188
7.2.1 Slalom Manoeuvre	190
7.2.2 Acceleration-Deceleration Manoeuvre	201
7.3 Examples of a Design of Handling Qualities Criteria for Light Gyroplanes	205
7.4 Chapter Summary	208
<b>Chapter 8 Conclusions and Recommendations</b>	<b>210</b>
8.1 Introductory Remarks	210
8.2 Conclusions	211
8.3 Recommendations for Future Work	214
8.4 Concluding Remarks	216
<b>Appendices</b>	<b>217</b>
<b>References</b>	<b>234</b>

# List of Tables

2.1 Design and airworthiness standards considered in the thesis	23
2.2 Short period damping ratio limits, adapted from MIL-F-8785C (1980)	38
2.3 Minimum Dutch roll frequency and damping, adapted from MIL-F-8785C (1980)	38
3.1 Characteristics of the short period response of the G-UNIV gyroplane	54
3.2 The undamped natural frequency and acceleration sensitivity of the short period oscillation of the G-UNIV gyroplane	57
3.3 Assessment of the short period damping ratio of the G-UNIV gyroplane	58
3.4 The G-UNIV metrics against DEF STAN 00-970 Rotorcraft (1984) pitch short term initial response and dynamic stability criteria (Active Flight Phases, Aggressive Manoeuvres)	61
3.5 Longitudinal frequency sweeps characteristics of the G-UNIV gyroplane	64
3.6 Characteristics of the short period response of the G-UNIV gyroplane	66
3.7 Characteristics of the Dutch roll response of the G-UNIV gyroplane	68
3.8 Assessment of the Dutch roll frequency and damping ratio of the G-UNIV gyroplane	72
3.9 The G-UNIV metrics against DEF STAN 00-970 Rotorcraft (1984) roll short term initial response and dynamic stability criteria (Active Flight Phases, Aggressive Manoeuvres)	74
3.10 Lateral frequency sweeps characteristics of the G-UNIV gyroplane	77
4.1 Gyroplane mathematical model description	85
4.2 Levels of rotor mathematical modelling, reproduced from Padfield (1996)	85

5.1 Estimation of the time and distance for the different acceleration-deceleration courses	157
6.1 Measured parameters and corresponding transducers	170
6.2 Desired and adequate performance for slalom manoeuvre, reproduced from the ADS-33E-PRF (2000)	180
6.3 Desired and adequate performance for acceleration-deceleration manoeuvre, reproduced from the ADS-33E-PRF (2000)	185
7.1 Slalom courses with various length and width	191
7.2 Pilot subjective HQRs and WRs for the slalom courses	193
7.3 Acceleration-deceleration courses with various speed ranges	201
7.4 Pilot subjective HQRs and WRs for the acceleration-deceleration courses	202
A1.1 Pitch short term initial response and dynamic stability criteria - Active Flight Phases, adapted from DEF STAN 00-970 Rotorcraft (1984)	221
A1.2 Roll short term initial response and dynamic stability criteria - Active Flight Phases, adapted from DEF STAN 00-970 Rotorcraft (1984)	223
A2.1 Physical characteristics of the G-UNIV research gyroplane	224
A2.2 Coordinates (in metres) of the G-UNIV gyroplane subsystems used in the simulation	225
A3.1 Specifications of the VSG 2000 angular rate sensors	226
A3.2 Specifications of the AD01-RP, AD01-Y angle sensors	226
A3.3 Specifications of the C3A-02 3-axes accelerometer	227
A3.4 Specifications of the Seika B1 single axis accelerometer	227
A3.5 Specifications of the Sensortech pressure transducers	228
A3.6 Specifications of the AccuStar II/DAS 20 dual axis clinometer	228
A3.7 Specifications of the GARMIN eTrex Summit Personal Navigator	229

# List of Figures

1.1 UK gyroplanes accident statistics for the decade 1992-2001 ( <i>Anon., 2002</i> )	2
1.2 Average rate of fatal accidents per million hours flown 1992-2001 ( <i>Anon., 2002</i> )	2
1.3 VPM M16 research gyroplane (reg. G-BWGI)	4
1.3 Glasgow University research gyroplane (reg. G-UNIV)	4
2.1 The Cooper-Harper handling qualities rating scale ( <i>Cooper and Harper, 1969</i> )	16
2.2 The Bedford workload scale ( <i>Ellis and Roscoe, 1982, cited Geddie et al, 2001</i> )	18
2.3 Longitudinal short period oscillation – pilot opinion contours, adapted from O’Hara ( <i>1967</i> )	19
2.4 Definitions of bandwidth and phase delay, adapted from ADS-33E-PRF ( <i>2000</i> )	28
2.5 Requirements for small-amplitude pitch attitude changes (All Other MTEs), adapted from ADS-33E-PRF ( <i>2000</i> )	30
2.6 Requirements for small-amplitude roll attitude changes (All Other MTEs), adapted from ADS-33E-PRF ( <i>2000</i> )	30
2.7 Requirements for moderate-amplitude roll attitude changes (All Other MTEs), adapted from ADS-33E-PRF ( <i>2000</i> )	31
2.8 Limits on pitch (roll) oscillations – hover and low speed, adapted from ADS-33E-PRF ( <i>2000</i> )	32
2.9 Lateral-directional oscillatory requirements, adapted from ADS-33E-PRF ( <i>2000</i> )	33

2.10 Short period frequency requirements – Category B Flight Phases, Class I, adapted from MIL-F-8785C (1980)	37
2.11 Short-term longitudinal response requirements, VFR, adapted from MIL-F-83300 (1970)	41
2.12 Lateral-directional oscillatory requirements, adapted from MIL-F-83300 (1970)	42
2.13 Longitudinal dynamic stability criteria, adapted from AGARD-R-577-70 (1970)	44
2.14 Lateral-directional dynamic stability criteria, adapted from AGARD-R-577-70 (1970)	44
2.15 Transient response characteristics, adapted from DEF STAN 00-970 Rotorcraft (1984)	46
2.16 Short period dynamic requirements for Category B Flight Phases, adapted from MIL-HDBK-1797 (1997)	49
2.17 Bandwidth requirements for Category C Flight Phases, adapted from MIL-HDBK-1797 (1997)	49
3.1 Definition of control stick and pedals positions and directions	52
3.2 Pitch rate response of the G-UNIV gyroplane to a pulse input	53
3.3 Short period mode of the G-UNIV gyroplane in the s-plane in comparison with the VPM M16 gyroplane, a Piper Cherokee aeroplane and a Puma helicopter	54
3.4 Short period frequency and damping ratio of the G-UNIV gyroplane against requirements of the longitudinal short period thumb print criterion (O'Hara, 1967)	55
3.5 Short period frequency and acceleration sensitivity of the G-UNIV gyroplane against MIL-F-8785C (1980) requirements for Category B Flight Phases	58
3.6 The G-UNIV data points against MIL-F-83300 (1970) short-term longitudinal response requirements	59
3.7 The G-UNIV data points against AGARD-R-577-70 (1970) longitudinal dynamic stability criteria	60
3.8 Longitudinal frequency sweeps of the G-UNIV gyroplane at 50 mph	63
3.9 Longitudinal sweep power spectrums of the G-UNIV gyroplane	63

3.10 The G-UNIV data points against ADS-33E-PRF (2000) requirements for small-amplitude pitch attitude changes (all other MTEs)	65
3.11 The G-UNIV data points against ADS-33E-PRF (2000) limits on pitch oscillations (hover and low speed)	65
3.12 The G-UNIV data points against MIL-HDBK-1797 (1997) short period dynamic requirements for Category B Flight Phases	67
3.13 The G-UNIV data points against MIL-HDBK-1797 (1997) and ADS-33E-PRF (2000) bandwidth requirements	67
3.14 Roll and yaw rate response of the G-UNIV gyroplane to a rudder doublet	69
3.15 Dutch roll mode of the G-UNIV gyroplane in the s-plane in comparison with a Piper Cherokee aeroplane and Bo 105, Lynx and Puma helicopters	70
3.16 Roll rate response of the G-UNIV gyroplane to a pulse input	71
3.17 The G-UNIV data points against MIL-F-83300 (1970) lateral-directional oscillatory requirements	73
3.18 The G-UNIV data points against AGARD-R-577-70 (1970) lateral-directional dynamic stability criteria	73
3.19 Lateral frequency sweeps of the G-UNIV gyroplane at 50 mph	76
3.20 Lateral sweep power spectrums of the G-UNIV gyroplane	76
3.21 The G-UNIV data points against ADS-33E-PRF (2000) requirements for small-amplitude roll attitude changes (all other MTEs)	78
3.22 The G-UNIV data points against DLR (Pausder and Blanken, 1992) and ADS-33E-PRF (2000) bandwidth requirements	78
3.23 The G-UNIV data points against ADS-33E-PRF (2000) lateral-directional oscillatory requirements	80
4.1 Transformation from <i>body</i> to <i>pivot</i> axes	92
4.2 Transformation from <i>pivot</i> to <i>disc</i> axes	93
4.3 Transformation from <i>disc</i> to <i>shaft</i> axes	95
4.4 Transformation from <i>shaft</i> to <i>blade</i> axes	96
4.5 Aerodynamic forces and incident velocities of a blade element	100
4.6 Lift coefficient of the NACA 8-H-12 aerofoil section	118
4.7 Drag coefficient of the NACA 8-H-12 aerofoil section	118
4.8 Comparison of steady state results for pitch attitude	120

4.9 Comparison of steady state results for roll attitude	120
4.10 Comparison of steady state results for longitudinal rotor tilt	121
4.11 Comparison of steady state results for lateral rotor tilt	121
4.12 Comparison of steady state results for rotor speed	122
5.1 Suggested course for slalom manoeuvre, reproduced from the ADS-33E-PRF (2000)	138
5.2 Track for the slalom manoeuvre	138
5.3 Suggested course for acceleration-deceleration manoeuvre, reproduced from the ADS-33E-PRF (2000)	141
5.4 Piecewise polynomial representation of an acceleration profile for the acceleration-deceleration manoeuvre	141
5.5 Comparison of inverse simulation results for the G-UNIV gyroplane flying minimum slalom manoeuvre with constrained sideslip rate and constrained heading rate ( $h = 20$ m; $V_f = 70$ mph; $AR=0.067$ ; $L=450$ m; $y_{\max} = 15$ m; $t_m = 14.4$ sec)	146
5.6 Comparison of lateral rotor tilt perturbations predicted by inverse simulation for the 50 mph slalom with various ARs	148
5.7 Comparison of roll attitude perturbations predicted by inverse simulation for the 50 mph slalom with various ARs	148
5.8 Comparison of lateral rotor tilt perturbations predicted by inverse simulation for the AR 0.11 slalom with various airspeeds	150
5.9 Comparison of roll attitude perturbations predicted by inverse simulation for the AR 0.11 slalom with various airspeeds	150
5.10 Predicted flight envelope for the G-UNIV gyroplane minimum slalom course from inverse simulation results	151
5.11 Suggested levels of aggressiveness for the G-UNIV gyroplane minimum slalom course from inverse simulation results	151
5.12 Acceleration profiles for the acceleration-deceleration manoeuvre with different levels of aggressiveness	154
5.13 Airspeed profiles for the acceleration-deceleration manoeuvre with different levels of aggressiveness	154

5.14 Inverse simulation results for engine power perturbations of the G-UNIV gyroplane flying the acceleration-deceleration manoeuvre	155
5.15 Comparison of inverse simulation results for pitch attitude of the G-UNIV gyroplane and Lynx helicopter flying the acceleration-deceleration manoeuvre	156
5.16 Inverse simulation results for pitch attitude of the Lynx helicopter flying the acceleration-deceleration manoeuvre with two different acceleration profiles	156
5.17 GPS tracking for the gyroplane slalom manoeuvre [AR 0.13, L 225 m, W 30 m, 70 mph]	159
5.18 GPS tracking for the gyroplane slalom manoeuvre [AR 0.2, L 300 m, W 60 m, 70 mph]	159
5.19 Comparison of flight test data and inverse simulation results for the slalom manoeuvre [AR 0.13, L 225, W 30 m, 70 mph, Trial 1]	160
5.20 Comparison of flight test data and inverse simulation results for the slalom manoeuvre [AR 0.2, L 300 m, W 60 m, 70 mph, Trial 2]	161
5.21 Comparison of flight test data and inverse simulation results for the 40-60-40 mph acceleration-deceleration manoeuvre	164
6.1 Glasgow University research gyroplane (reg. G-UNIV)	168
6.2 The GPS receiver installed in the instrumentation pallet	172
6.3 The G-UNIV gyroplane instrumentation setup	172
6.4 Control stick transducer calibration surface for longitudinal channel	175
6.5 Control stick transducer calibration surface for lateral channel	175
6.6 ROTAX TYPE 618 engine performance	178
6.7 Suggested course for slalom manoeuvre, reproduced from the ADS-33E-PRF (2000)	180
6.8 Course for gyroplane minimum slalom manoeuvre	181
6.9 Suggested course for acceleration-deceleration manoeuvre, reproduced from the ADS-33E-PRF (2000)	184
7.1 The G-UNIV gyroplane at Carlisle airfield during pre-flight engine runs	190
7.2 Pilot HQRs for the slalom manoeuvre	194
7.3 Pilot WRs for the slalom manoeuvre	194

7.4 Flight test results for the G-UNIV research gyroplane flying the slalom manoeuvre [AR 0.1, 35 mph, Trial 1, HQR 4, WR 3]	196
7.5 Flight test results for the G-UNIV research gyroplane flying the slalom manoeuvre [AR 0.13, 70 mph, Trial 2, HQR 7, WR 7]	196
7.6 Flight test results for the G-UNIV research gyroplane flying the slalom manoeuvre [AR 0.2, L 300 m, 50 mph, Trial 2, HQR 6, WR 6]	197
7.7 Suggested levels of aggressiveness for the slalom course predicted by inverse simulation in comparison with pilot HQRs	198
7.8 Maximum lateral rotor tilt for the 35 mph slalom	199
7.9 Maximum lateral rotor tilt for the 50 mph slalom	200
7.10 Maximum lateral rotor tilt for the 70 mph slalom	200
7.11 Pilot HQRs for the acceleration-deceleration manoeuvre	203
7.12 Pilot WRs for the acceleration-deceleration manoeuvre	203
7.13 Flight test results for the G-UNIV research gyroplane flying the acceleration-deceleration manoeuvre [40-60-40 mph, HQR 2, WR 2]	204
7.14 Suggested roll attitude quickness Levels for gyroplane slalom manoeuvre in comparison with those of ADS-33E-PRF	207
7.15 Suggested pilot attack Levels for gyroplane slalom manoeuvre	207
A3.1 GARMIN eTrex Summit Personal Navigator ( <i>Garmin, 2005</i> )	229
A4.1 Measurement of longitudinal c.g. position	231
A4.2 Measurement of vertical c.g. position	231

# Nomenclature

## Notes

- i. Where a vector has both subscript and superscript, the subscript refers to a position/location in an axis set and the superscript is the axis set.
- ii. Unless explicitly stated, all quantities are given in standard SI units.

## General

$a$	local speed of sound
$\mathbf{a}$	translational acceleration vector
$a_x, a_y, a_z$	linear accelerations in body axes
$c$	blade chord length
$C_l, C_d$	lift and drag coefficients
$C_x, C_y, C_z$	force vector components
$dL, dD$	differential lift and drag forces
$\mathbf{f}, \mathbf{F}$	force vectors
$g$	acceleration due to gravity
$g_r$	tail rotor gear ratio
$h$	height
$I_R$	moment of inertia of the rotor
$I_{xx}, I_{yy}, I_{zz}$	aircraft roll, pitch and yaw moments of inertia in body axes
$I_{xz}$	product of inertia in body axes
$I_\beta$	blade flapping moment of inertia

$J$	Jacobian
$K_\beta$	spring stiffness
$l_{shaft}, h_{shaft}$	longitudinal and vertical rotor shaft offsets
$L, M, N$	aircraft external aerodynamic moments
$L$	length of the slalom course, wheelbase
$L, L_{nl}$	inflow gains matrices
$m$	aircraft mass
$M$	Mach number
$M$	moment vector, apparent mass matrix
$M_\beta$	blade mass moment
$n_{int}$	number of intermediate integrations per discretisation interval
$n_z$	load factor
$n_\alpha, n/\alpha$	acceleration sensitivity parameter
$p, q, r$	aircraft roll, pitch and yaw rates as a perturbation from trim
$p_{pk}$	peak roll rate
$P, Q, R$	aircraft roll, pitch and yaw rates
$P_{dyn}$	dynamic air pressure
$P_{static}$	static air pressure
$P_{total}$	total air pressure
$Q_e$	engine torque
$Q_R$	rotor aerodynamic torque
$Q_{tr}$	tail rotor torque
$r$	position vector
$R$	rotor radius
$t_a, t_d$	acceleration and deceleration periods
$t_k$	time point in inverse simulation
$t_m$	time taken to complete the slalom manoeuvre
$T$	transformation matrix
$T_{air}$	air temperature

$T_{prop}$	propeller thrust
$u, v, w$	aircraft velocity components as a perturbation from trim
$\mathbf{u}$	translational velocity vector, control vector
$\mathbf{u}_{error}$	control error vector
$U, V, W$	aircraft velocity components
$U_p$	perpendicular component of blade velocity
$U_t$	tangential component of blade velocity
$v_0, v_{ls}, v_{lc}$	uniform, longitudinal and lateral inflow components
$v_l$	rotor induced velocity
$V$	mass-flow parameter matrix
$V_f$	aircraft flight velocity
$V_m$	mass-flow parameter
$\dot{V}_{max}, \dot{V}_{min}$	maximum values of acceleration and deceleration
$V_T$	resultant flow through the rotor disc
$W$	width of the slalom course, aircraft weight
$\mathbf{x}$	state vector
$x, y, z$	distances along axes
$x_e, y_e, z_e$	displacements relative to an earth fixed inertial frame
$X, Y, Z$	aircraft external aerodynamic forces
$\mathbf{y}$	output vector
$\mathbf{y}_{desired}$	desired output vector
$\mathbf{y}_{error}$	output error vector
$y_{max}, y_{min}$	maximum and minimum lateral distances from the centreline of the slalom course

### Greek Symbols

$\alpha$	angle of attack
$\mathbf{a}$	rotational acceleration vector

$\alpha_{vane}$	$\alpha$ -vane angle
$\beta$	aircraft sideslip angle, blade flap angle
$\beta_{vane}$	$\beta$ -vane angle
$\chi$	rotor wake angle
$\delta$	difference between azimuth angles in disc and wind set of axes
$\delta_{rud}$	rudder angle
$\delta u$	control perturbation size
$\Delta t$	inverse simulation discretisation interval
$\Delta\phi_{pk}$	change in roll attitude
$\Delta\Phi_{2\omega_{180}}$	phase angle at twice the neutral stability frequency
$\Delta\eta$	net lateral stick displacement
$\varepsilon$	convergence tolerance
$\phi, \theta, \psi$	aircraft roll, pitch and yaw attitudes as a perturbation from trim
$\phi_{shaft}, \theta_{shaft}$	longitudinal and lateral rotor shaft angles
$\phi$	inflow angle
$\Phi, \Theta, \Psi$	aircraft roll, pitch and yaw attitudes
$\dot{\eta}_{pk}$	peak lateral stick displacement derivative
$\lambda_n, \lambda_{1s}, \lambda_{1c}$	non-dimensionalised inflow components
$\mu$	non-dimensionalised resultant forward disc velocity
$\mu_x, \mu_y, \mu_z$	non-dimensionalised disc velocity components
$\theta$	blade pitch angle
$\rho$	air density
$\tau_{dl}$	period of Dutch roll oscillation
$\tau_p$	bandwidth time delay parameter
$\tau_{sp}$	period of short period oscillation
$\omega$	rotational velocity vector
$\omega_{180}$	neutral stability frequency
$\omega_{BW}$	bandwidth parameter
$\omega_{BW_{gain}}$	gain-limited bandwidth parameter

$\omega_{BW_{phase}}$	phase-limited bandwidth parameter
$\omega_d$	Dutch roll undamped natural frequency
$\omega_n$	undamped natural frequency
$\omega_{sp}$	short period undamped natural frequency
$\Omega$	rotorspeed
$\Omega_{prop}$	propeller speed
$\Psi_{az}$	shaft azimuth angle
$\zeta$	damping ratio
$\zeta_d$	Dutch roll damping ratio
$\zeta_{sp}$	short period damping ratio

### Subscripts and Superscripts

<i>b.e.</i>	blade element
<i>blade</i>	blade axes set
<i>body</i>	body axes set
<i>c.g.</i>	centre of gravity
<i>disc</i>	disc axes set
<i>fin</i>	fin
<i>fus</i>	fuselage
<i>hub</i>	rotor hub
<i>pitot</i>	pitot
<i>pivot</i>	pivot axes set
<i>p.p.</i>	pivot point
<i>P</i>	power
<i>R</i>	rotor
<i>shaft</i>	shaft axes set
<i>tp</i>	tailplane

**Abbreviations**

ACAH	Attitude Command/Attitude Hold
ADS	Aeronautical Design Standard
AR	Aspect Ratio
BCAR	British Civil Airworthiness Requirements
CAA	Civil Aviation Authority
CAP	Control Anticipation Parameter
CFD	Computational Fluid Dynamics
c.g.	centre of gravity
c.p.	centre of pressure
DAQ	Data Acquisition
DLR	German Aerospace Centre
DVE	Degraded Visual Environment
EAS	Equivalent Airspeed
FAA	Federal Aviation Administration
FAR	Federal Aviation Regulations
GENISA	Generic Inverse Simulation Algorithm
GPS	Global Positioning System
GSIM	Gyroplane Simulation Model
GVE	Good Visual Environment
HELINV	Helicopter Inverse Simulation
HGS	Helicopter Generic Simulation
HIBROM	Helicopter Individual Blade Rotor Model
HQR	Handling Qualities Rating
IFR	Instrument Flight Rules
JAA	Joint Aviation Authorities
JAR	Joint Aviation Requirements
LER	Leading-Edge Roughness
MTE	Mission Task Element
OFE	Operational Flight Envelope
PIO	Pilot Induced Oscillation
PSD	Power Spectral Density

RASCAL	Rotorcraft Aeromechanic Simulation for Control Analysis
SCU	Signal Conditioning Unit
SFE	Service Flight Envelope
TAS	True Airspeed
UCE	Usable Cue Environment
VCR	Visual Cue Ratings
VFR	Visual Flight Rules
VMC	Visual Meteorological Conditions
V/STOL	Vertical and/or Short Takeoff and Landing
VTOL	Vertical Takeoff and Landing
WR	Workload Rating

# Chapter 1

## Introduction

### 1.1 Background and Motivation

Light gyroplanes, or autogyros, are attracting a great amount of current interest in the general aviation community all around the world. Not only do gyroplanes have low operating cost, but also their design provides for easy maintenance, and in theory at least, they should be simple to operate and fly. Unfortunately, gyroplanes have not had the benefit of a “design evolution” as experienced by other rotorcraft types. Their design today (including materials, propulsion, aerodynamics etc.) is much the same as it was seven decades ago. Until recently there have been few attempts to improve the technologies associated with gyroplanes and few theoretical advances. In particular, there has to date been no published research in the area of gyroplane handling qualities. Contrast this with other types of rotorcraft, where handling qualities are central to design standards (*Padfield, 1996; Padfield and Meyer, 2003; Fortenbaugh et al, 2004; Meyer and Padfield, 2005* for example), as they strongly affect mission effectiveness and pilot workload, and thereby flight safety. The major influence of handling qualities on the flight safety of aeroplanes and helicopters was stressed by Hodgkinson (*1995*) and Padfield (*1996*) respectively, and although much simpler than the aeroplane and helicopter, the link between flight safety and handling qualities of the gyroplane has also been established (*PRA, 2004*).

Despite this, in most countries there are no special design and airworthiness standards for light gyroplanes as they are usually categorised as ultralight or experimental aircraft. This is a possible contributory factor in an increasing accident rate, particularly in the

UK. For example, between 1989 and 1991, the gyroplane fatal accident rate in the UK was 6 per 1000 flying hours, whereas the overall general aviation rate during 1990 was 0.015 per 1000 flying hours (Anon., 1991). According to the “Aviation Safety Review 1992 – 2001” (Anon., 2002) for the decade 1992 – 2001 there have been 29 reportable accidents to UK gyroplanes. These reportable accidents resulted in 5 fatalities and 2 serious injuries (Figure 1.1). The average rate of fatal accidents per million hours flown is 109. The fatal accident rate for the same period for public transport helicopters is 1.8, for airline aeroplanes (maximum takeoff weight < 5700 kg) is 36.1, and for airline aeroplanes (maximum takeoff weight > 5700 kg) it is zero (Figure 1.2).

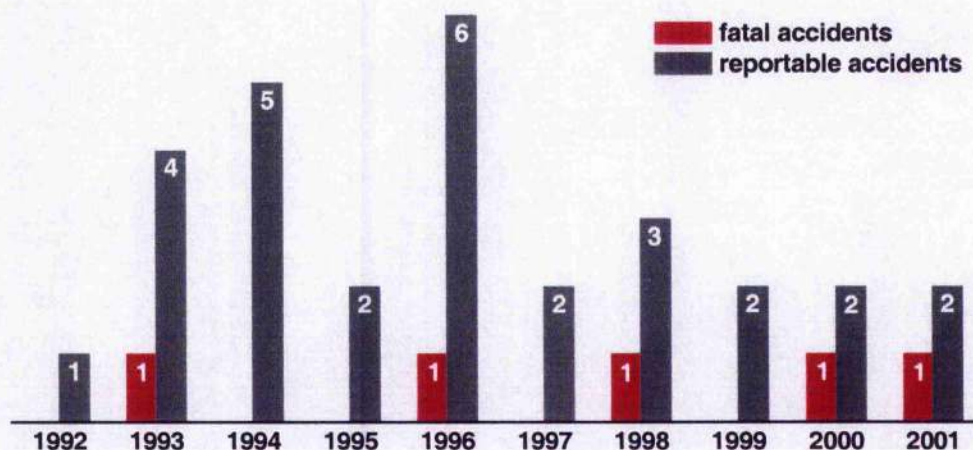


**Figure 1.1** UK gyroplanes accident statistics for the decade 1992-2001 (Anon., 2002)

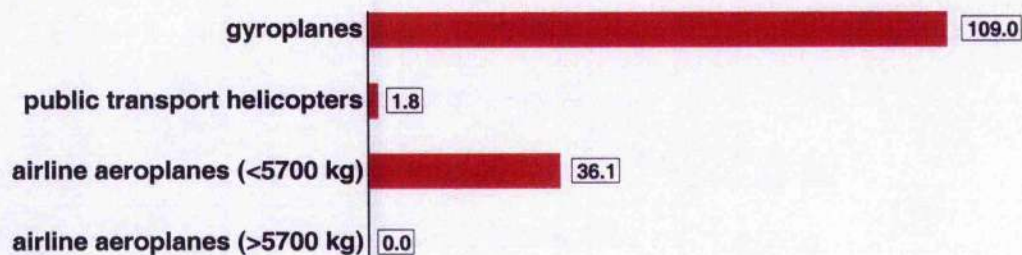


**Figure 1.2** Average rate of fatal accidents per million hours flown 1992-2001 (Anon., 2002)

To address this problem the UK Civil Aviation Authority (CAA) has developed a new airworthiness standard for light gyroplanes: “British Civil Airworthiness Requirements, Section T, Light Gyroplane Design Requirements” (*BCAR Section T, 1993*), and its superseding, “British Civil Airworthiness Requirements, Section T, Light Gyroplanes” (*BCAR Section T, 1995; BCAR Section T, 2003*). However, this standard is not prescriptive regarding direct criteria for handling qualities except simple requirements for dynamic stability, which are primarily based on those from airworthiness requirements for small light aeroplanes, *BCAR Section S (2003)* and aviation regulations for small rotorcraft, *JAR/FAR-27 (JAR-27, 2004; FAR-27, 1983)*.

The University of Glasgow has been involved in the process of developing *BCAR Section T* requirements since 1993. Numerous studies have been conducted, including research on gyroplane stability (*Houston, 1996; 1998*), aerodynamics (*Coton et al, 1998; Houston and Thomson, 2001*), simulation (*Houston, 2000; 2002*), flight testing (*Spathopoulos, 2001; Houston and Thomson, 2004*) and handling qualities (*Houston et al, 2001; Bagiev et al, 2003; 2004*). The aircraft used in this research were the VPM M16 gyroplane, registration G-BWGI (Figure 1.3) in the initial stages and more recently the Montgomery-Parsons research gyroplane, registration G-UNIV (Figure 1.4). This Montgomery-Parsons research gyroplane is owned by the Department of Aerospace Engineering, University of Glasgow for study and flight test purposes. In fact, the research gyroplane is a converted original two-seat Montgomery-Parsons gyroplane. Due to its uniqueness, this research gyroplane referred throughout the dissertation as the G-UNIV research gyroplane (a thorough description of the G-UNIV research gyroplane is provided in Chapter 6).

However, despite recent research at Glasgow, comparatively little is known about gyroplane handling qualities, and to date, to the author’s best knowledge, there are no direct handling qualities requirements and criteria developed for light gyroplanes anywhere in the world. Consequently, there are no techniques for assessment of gyroplane handling qualities currently available. Given that there is an obvious need to improve gyroplane safety, the question therefore arises: how can gyroplane handling qualities be estimated and how can handling qualities requirements and criteria for gyroplanes be designed?



**Figure 1.3** VPM M16 research gyroplane (reg. G-BWGI)

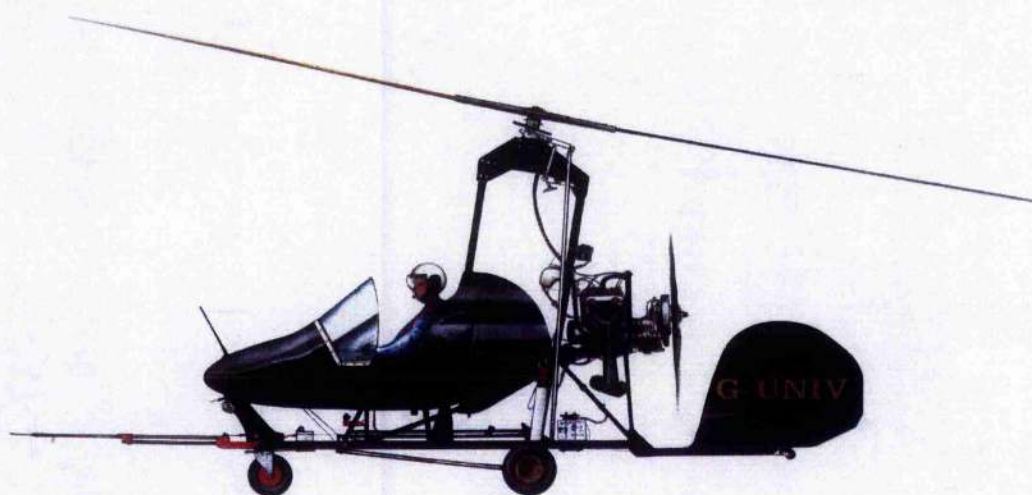


**Figure 1.4** Glasgow University research gyroplane (reg. G-UNIV)

## 1.2 Main Aim of the Thesis

There are two generally accepted distinct methods of assessment levels of handling qualities: objective and subjective. The objective assessment of handling qualities can be obtained from quantitative criteria, such as a simple short period thumb print criterion (*O'Hara, 1967*), or more sophisticated criteria from various design and airworthiness standards. It should be emphasised that the quantitative criteria do not depend on the pilot's qualitative opinion; and metrics, which form quantitative criteria of handling qualities, are based primarily on the stability and controllability characteristics of the aircraft, which are derived from the flight test data.

Since there are no handling qualities criteria for gyroplanes available, except perhaps the simple dynamic stability requirements from BCAR Section T, the only reasonable way to estimate the handling qualities of a light gyroplane is to apply existing criteria for other types of flight vehicles, such as helicopters, aeroplanes and V/STOL aircraft, either in their current form or in modified form. By doing so, not only can levels of gyroplane handling qualities be estimated, but also general information regarding the concept of designing gyroplane's own handling qualities criteria can be obtained.

The subjective qualitative assessment of handling qualities is usually obtained from the test pilot's opinion in a form of handling qualities ratings from the Cooper-Harper scale (*Cooper and Harper, 1969*). For rotorcraft, this assessment is often made on the basis of flight testing specially designed flight tasks, or manoeuvres. A new concept of mission task elements (MTEs) was introduced in the US handling qualities standard for military rotorcraft, ADS-33E-PRF (2000), which states, that the "MTEs provide a basis for an overall assessment of the rotorcraft's ability to perform certain critical tasks, and result in an assigned level of handling qualities" (*ADS-33E-PRF, 2000, p.25*). To obtain assigned (or subjective) levels, the ADS-33E-PRF requires using the Cooper-Harper handling qualities rating scale. The obvious question then arises: can these MTEs be applied to the gyroplane problem?

The basic premise of this research is that the subjective assessment of handling qualities of gyroplanes *can* be obtained using the MTEs approach proposed by the ADS-33E-PRF document. A justification for this assertion is that the ADS-33E-PRF standard does not provide any categorisation according to rotorcraft size, which makes this document universal, and allows using it as a basis for developing handling qualities requirements for light gyroplanes. To test this assertion one of the research objectives is to develop manoeuvres, or MTEs, suitable for gyroplane operations, then to test fly them using the fully instrumented G-UNIV research gyroplane to demonstrate their use and obtain subjective assessments of handling qualities ratings using the Cooper-Harper scale and workload ratings using the Bedford workload scale (*Ellis and Roscoe, 1982, cited Geddie et al, 2001*). The author knows of no other instance of the Cooper-Harper rating scale and the Bedford workload scale being applied to a light gyroplane flight testing.

Since, to the author's knowledge, a gyroplane has never been flight tested before using the MTEs concept from ADS-33E-PRF standard, and a flight test programme for handling qualities assessment usually includes aggressive manoeuvring at the edges of the aircraft flight envelope, safety issues must be the primary aspect to be considered. Simulation of the gyroplane flight dynamics is therefore essential to reduce the flight test effort required and increase flight safety. In this thesis, an inverse simulation is proposed as a preliminary tool in the process of designing gyroplane MTEs for handling qualities study. A state-of-the-art, high fidelity mathematical model of a gyroplane was developed to incorporate into the inverse simulation algorithm. In such a manner, the thesis provides the first published results of a gyroplane inverse simulation. The inverse simulation package developed is unique and posed a significant challenge both in the development of the gyroplane mathematical model and its implementation in the inverse simulation algorithm.

The main aim of the research therefore can be stated as follows:

*Assessment and study of gyroplane handling qualities using flight testing and simulation techniques.*

It should be stated in the very beginning of the thesis, that to create handling qualities requirements and criteria for gyroplanes, extensive flight tests and simulation are

necessary. It would be unreasonable to expect this to be possible in the context of a three-year PhD study. It might take years to construct a suitable database of flight test results to allow any firm conclusions to be drawn, and thus to develop new criteria. Nonetheless, the work contained in this dissertation represents a major contribution in achieving this goal. Meyer and Padfield (2005, p.34) stated that “developing handling qualities is a long and iterative process where not all aspects can be considered or fixed initially due to the lack of information, time or resources”. The thesis should be considered as a preliminary methodology for the objective and subjective assessment of the handling qualities of gyroplanes, and one of the main objectives is to give guidance on how to develop new criteria for light gyroplanes. Thus, in this thesis only the very first steps of this time-consuming process of developing new handling qualities requirements for gyroplanes are presented.

Since the thesis is covering a wide range of areas of research, such as handling qualities and workload, design and airworthiness standards, mathematical modelling, inverse simulation, and flight testing, it was decided to present the relevant literature review in the corresponding chapters. The following section provides a description of additional objectives of the thesis with a further discussion of methodology implemented and results obtained.

### **1.3 Thesis Objectives**

There are four additional objectives of the thesis, which are now detailed.

#### *i) Objective Assessment of Gyroplane Handling Qualities*

It has been stated that the only reasonable way to estimate the handling qualities of a light gyroplane is to apply already existing criteria for other types of flight vehicles, such as helicopters, aeroplanes and V/STOL aircraft. Therefore, the first part of the thesis concentrates on the reviewing design and airworthiness standards. It should be stated at this point that only dynamic stability characteristics related to short period and Dutch roll modes are considered and used throughout the dissertation, as these are most

influential in handling qualities characteristics. Chapter 2 provides a more detailed discussion regarding dynamic stability modes. The dissertation does not provide a comprehensive review of all of the standards. Instead, it focuses on particular parts of these documents, which are related to handling qualities requirements and criteria for the short period and Dutch roll modes.

Objective handling qualities of the G-UNIV research gyroplane were estimated using BCAR Section T, and numerous fixed and rotary wing aircraft specifications, as presented in Chapter 3. The assessment is based on the flight test data obtained from the previous studies of the G-UNIV gyroplane (*Spathopoulos, 2001; Houston and Thomson, 2004*).

For instance, a very similar process of developing handling qualities criteria for a civil tiltrotor is currently underway (*Padfield and Meyer, 2003; Meyer and Padfield, 2005*), sponsored by European Commission. This project is focused on developing handling qualities criteria through analysis and piloted simulation at Eurocopter SPHERE (Marignane, France) and HELIFLIGHT (University of Liverpool, UK) facilities. Another example is a programme of the Bell/Agusta BA609 civil tiltrotor, which made its first flight on March 2003, and is currently in the process of certification (*Fortenbaugh et al, 1999; Fortenbaugh, 2004*). Since there are no handling qualities criteria for tiltrotors developed, in both examples handling qualities criteria from various standards for aeroplanes, rotorcraft and V/STOL aircraft were considered in the assessment of handling qualities of the civil tiltrotors.

#### *ii) Development of Inverse Simulation Package for Preliminary Design of Gyroplane Manoeuvres*

In contrast to conventional simulation, the inverse simulation algorithm calculates the pilot control inputs that will force an aircraft to fly a specified manoeuvre. Rotorcraft inverse simulation was first developed by Thomson (1986), and since this time, the University of Glasgow has become a centre of excellence in the development and

research of the inverse simulation problem. Inverse simulation has become a very useful tool in estimating rotorcraft handling qualities. Since the ADS-33E-PRF defines test manoeuvres in the form of precisely defined MTEs, a mathematical representation of these MTEs (Thomson and Bradley, 1997a; 1997b) can therefore be used as an input for the inverse simulation algorithm to calculate the pilot control inputs, which allows estimating of workload and handling qualities. Using this technique, Thomson and Bradley (Thomson and Bradley, 1997b) proposed the inverse simulation as a tool for a preliminary assessment of helicopter handling qualities. In this work, they made an important conclusion that validity of inverse simulation is equivalent to validity of conventional simulation based on the same helicopter model.

The second objective of the current research is to develop an inverse simulation package for preliminary design of gyroplane manoeuvres. As demonstrated in Chapter 5, use is made of the existing modified generic inverse simulation algorithm GENISA, proposed originally by Rutherford and Thomson (1996). A high fidelity, individual blade/blade element coupled rotor-fuselage mathematical model of a gyroplane, GSIM (Gyroplane Simulation Model), is developed to incorporate into the modified GENISA. Combined blade element momentum theory was applied to calculate forces and moments of the gyroplane's autorotating rotor. The GSIM model utilises the dynamic inflow model of Pitt and Peters (1981) improved later by Peters and HaQuang (1988). Blade flapping dynamics is based on centre-spring equivalent rotor approach (Padfield, 1996), and is described by a second order nonlinear differential equation. Lookup tables of force and moment coefficients obtained from wind tunnel tests are used to calculate forces and moments of the fuselage, tailplane and fin.

Using the inverse simulation package, behaviour of the G-UNIV gyroplane flying slalom and acceleration-deceleration manoeuvres with different levels of aggressiveness is investigated. Obtained results are essential in the stage of designing gyroplane slalom and acceleration-deceleration manoeuvres. In addition, based on the inverse simulation results, a flight envelope and levels of aggressiveness for the gyroplane slalom manoeuvre are predicted, which must play an assisting role in designing gyroplane slalom manoeuvre.

### *iii) Subjective Assessment of Gyroplane Handling Qualities by Conducting a Series of Flight Tests*

Recently, UK Department for Transport published Safety Recommendation 2003-01 (Anon., 2003), which states that “it is recommended that the CAA should review the pitch stability requirements of BCAR Section T in the light of current research, and amend the Requirements as necessary. The CAA should consider the need for an independent qualified *pilot assessment of the handling qualities* of different gyroplane types currently approved for the issue of a Permit to Fly against the standards of BCAR Section T, as amended”. It is obvious that the research in the field of gyroplane handling qualities is of current interest to the aviation authorities mainly because of the bad accident statistics for such type of aircraft.

As indicated above, a new concept of MTEs from the ADS-33E-PRF (2000) standard is used as a basis for the technique of subjective assessment of gyroplane handling qualities. At first, a flight test technique for handling qualities assessment of a light gyroplane must be developed. A detailed description of the test gyroplane, including onboard instrumentation and ground preparations for the flight test programme is provided in Chapter 6. In addition, gyroplane slalom and acceleration-deceleration manoeuvres are designed based on those from ADS-33E-PRF.

A series of flight tests of the G-UNIV research gyroplane were conducted to demonstrate that the slalom and acceleration-deceleration manoeuvres from the ADS-33E-PRF (2000) standard can be modified and applied to a light gyroplane. Thirty slalom and six acceleration-deceleration courses with various levels of aggressiveness were flown during the flight test programme for handling qualities study. After each test flight the test pilot assigned handling qualities ratings using the Cooper-Harper rating scale (Cooper and Harper, 1969) and workload ratings using the Bedford workload scale (Ellis and Roscoe, 1982, cited Geddie et al, 2001). Therefore, a database of subjective pilot assessments were formed and analysed. Chapter 7 presents the results obtained during the flight test programme, as well as results of an investigation of the effect of manoeuvre aggressiveness on pilot subjective handling qualities and workload ratings. Mounting such a flight test programme was challenging, as flying such tightly prescribed manoeuvres using a gyroplane has never previously been attempted.

*iv) Preliminary Recommendations Regarding the Structure and Organisation of Gyroplane Handling Qualities Requirements and Criteria*

In developing handling qualities criteria for gyroplanes, it is natural to look at the techniques used for other rotorcraft and aeroplanes. An extensive literature search and analysis was therefore undertaken to review the existing handling qualities criteria for fixed and rotary wing aircraft in the context of the future needs for light gyroplane handling qualities requirements. The question that naturally arises is how can we modify existing fixed and rotary wing aircraft criteria with an aim to develop new criteria for gyroplanes? The fourth objective of this thesis is to answer this question.

Preliminary recommendations are proposed regarding suitability of handling qualities criteria of fixed and rotary wing aircraft. Chapters 2 and 3 provide a detailed discussion of a possible structure and organisation of the gyroplane handling qualities requirements. In addition, the thesis proposes two handling qualities criteria for a light gyroplane, the roll quickness criterion and pilot attack criterion for the slalom manoeuvre. These criteria are presented in Chapter 7, and based on the flight test data obtained from the flight tests of the G-UNIV research gyroplane.

### **1.3 Thesis Structure**

The thesis structure is as follows. Chapter 2 consists of a review of techniques of handling qualities assessment, providing general information about handling qualities and pilot workload at first, and then followed by a comprehensive review and discussion of the existing civil and military airworthiness and design standards. Chapter 3 presents results of the objective assessment of the G-UNIV research gyroplane handling qualities against criteria of the standards reviewed in the previous chapter. The assessment is based on the flight test data obtained from the previous studies of the G-UNIV gyroplane (*Spathopoulos, 2001; Houston and Thomson, 2004*).

A thorough description of the development and validation of the gyroplane simulation model GSIM is provided in Chapter 4. Chapter 5 starts with a description of the modified inverse simulation algorithm GENISA. In addition, a process of mathematical modelling of gyroplane manoeuvres is presented and discussed. A validation of the developed inverse simulation package GENISA/GSIM is also provided. It should be noted that the simulation results were compared with the flight data obtained from the flight test programme for handling qualities study, which is discussed in detail in the following Chapters 6 and 7.

Chapter 6 introduces a flight testing technique developed to assess and study subjective handling qualities of the G-UNIV research gyroplane. A description of the test gyroplane, onboard instrumentation and ground preparations for the flight tests is presented. The second part of the chapter is devoted to a designing process of gyroplane manoeuvres, slalom and acceleration-deceleration, for the study of handling qualities. Chapter 7 provides flight test results for the G-UNIV gyroplane's slalom and acceleration-deceleration manoeuvres. Subjective assessments of handling qualities and pilot workload are also provided. The final section of the chapter proposes examples of designing handling qualities criteria for a light gyroplane. Chapter 8 presents research conclusions and recommendations for future work.

In addition, five appendices are included. Appendix 1 provides a brief review of definitions of MIL-F-8785C (1980) specification and DEF STAN 00-970 Rotorcraft (1984) standard. Appendix 2 presents physical characteristics of the G-UNIV research gyroplane and coordinates of the gyroplane subsystems. Appendix 3 lists specifications of the test instrumentation installed onboard the G-UNIV test gyroplane. A technique of experimental measurement of centre of gravity position is described in detail in Appendix 4. Finally, Appendix 5 provides examples of flight trials instruction forms used during the flight test programme.

## ***Chapter 2***

# **A Review of Techniques for Handling Qualities Assessment**

### **2.1 Introduction**

The chapter starts with a general discussion of handling qualities, and then provides a description of principles of subjective and objective assessment of handling qualities and workload. This is followed by a comprehensive review and discussion of the British Civil Airworthiness Requirements for Light Gyroplanes and Aeronautical Design Standard ADS-33E-PRF. Finally, a detailed survey of existing airworthiness and design standards is presented. The aim of this chapter is therefore to determine if any existing handling qualities criteria are directly applicable to a light gyroplane and, if not, then to reveal what elements of existing criteria can be applied with, or without, modification.

### **2.2 Handling Qualities**

Handling qualities are without doubt one of the primary objectives of the design of modern rotary-wing aircraft, where improved handling qualities increase mission effectiveness and flight safety, and reduce pilot workload. It is very difficult to define unambiguously the term "handling qualities" for the reason that they evolved from the early days when they were primarily based on the pilot opinion, to the present where they consist of a complex set of qualitative and quantitative assessments of mission effectiveness. These assessments are influenced by a wide range of parameters

including aircraft stability and controllability, cockpit ergonomics, mission requirements, pilot's background and physical state, and external environment (Etkin, 1972). Cooper and Harper (1969) gave the definition for handling qualities as:

*“those qualities or characteristics of an aircraft that govern the ease and precision with which a pilot is able to perform the tasks required in support of an aircraft role”.*

Padfield (1996, p.335) noted that this definition is still relevant, but needs to be revised to meet modern and future needs. Padfield (1996, p.336; 1998, p.413) and Mitchell *et al* (2004, p.13) have raised an open question about terminology in this area: does the term “handling qualities” mean the same as “flying qualities”? Most specifications and design standards use the latter term (MIL-F-8785C, 1980; MIL-F-83300, 1970; DEF STAN 00-970, 2003), some of them use both (MIL-H-8501A, 1961; MIL-HDBK-1797, 1997), and some use the former term (AGARD-R-577-70, 1970; DEF STAN 00-970 Rotorcraft, 1984; ADS-33E-PRF, 2000). Much the same can be said about the literature in this field, which shows that there is still disagreement between specialists regarding this issue. One of the attempts to define a distinction was made by Key (1988, cited Padfield, 1996, p.336), who proposed associating flying qualities with the aircraft's stability and control characteristics, or the internal attributes, and handling qualities with the task and environment included, or external influences. Thomson (2005) acceded with such an approach, and gave an example to illustrate this distinction: two identical aircraft have the same flying qualities, however if one of these aircraft has degraded cockpit ergonomics then this aircraft will have poorer handling qualities because the pilot will face much greater difficulty in completing the task. Presumably, Key's definition is thorough and proper, however to avoid any misunderstanding this dissertation will use an approach used by Mitchell *et al* (2004), where the term “handling qualities” were used throughout the contents of the paper, and original terminology was kept when referring to the specifications and standards.

Etkin (1972, p.510) stated that “research in the field of aircraft handling qualities is undertaken for two primary reasons. These are (i) to formulate a set of design criteria which if met will ensure that a new flight vehicle will have adequate handling qualities and (ii) to better understand how the various vehicle and mission parameters affect the

human pilot". It should be emphasised that the objectives of this dissertation are wholly consistent with these points.

Handling qualities studies have been a very active area of research since the very early days of aviation. A large number of papers have been published on this topic, including theoretical and experimental development. O'Hara (1967) made one of the first detailed surveys of handling qualities. Perhaps the most comprehensive papers on historical development of handling qualities are those by Ashkenas (1984) and Philips (1989). Recently Mitchell *et al* (2004) have published comprehensive review of the development of handling qualities, which contains a detailed timeline for handling qualities evolution and discussion of the handling and flying qualities specifications.

The subjective scale proposed by Cooper and Harper (1969) for measuring handling qualities has become the worldwide standard and now is well known as the Cooper-Harper handling qualities rating scale (Figure 2.1). The Cooper-Harper handling qualities rating (TIQR) depends only on one pilot's qualitative assessment obtained from the decision tree. Therefore, during flight tests or simulation experiments, an aircraft performance is usually assessed by a number of pilots. For example, it suggested in ADS-33E-PRF (2000) standard that the required manoeuvres must be flown by at least three test pilots. In addition, it is very important to note that the Cooper-Harper rating scale allows assigning a handling qualities rating specific to one particular aircraft and particular manoeuvre flown. Thorough discussion on the Cooper-Harper rating scale and suggestions for its application to rotorcraft handling qualities assessment was presented by Padfield (1996, p. 431).

There is a commonly used relationship between the qualitative HQRs obtained from the Cooper-Harper scale and the quantitative levels of handling qualities used in flying and handling qualities specifications and standards: Level 1 is equivalent to the range of HQRs between 1 and 3.5; Level 2 is equivalent to HQRs between 3.5 and 6.5; and Level 3 is equivalent to HQRs between 6.5 and 8.5 (ADS-33E-PRF, 2000, p.73). HQRs 9 and 10 from the Cooper-Harper scale are below Level 3, indicating that there are major deficiencies in the aircraft; and, respectively, intense pilot compensation is required to retain control during the task, and control might be lost during some parts of the manoeuvre.

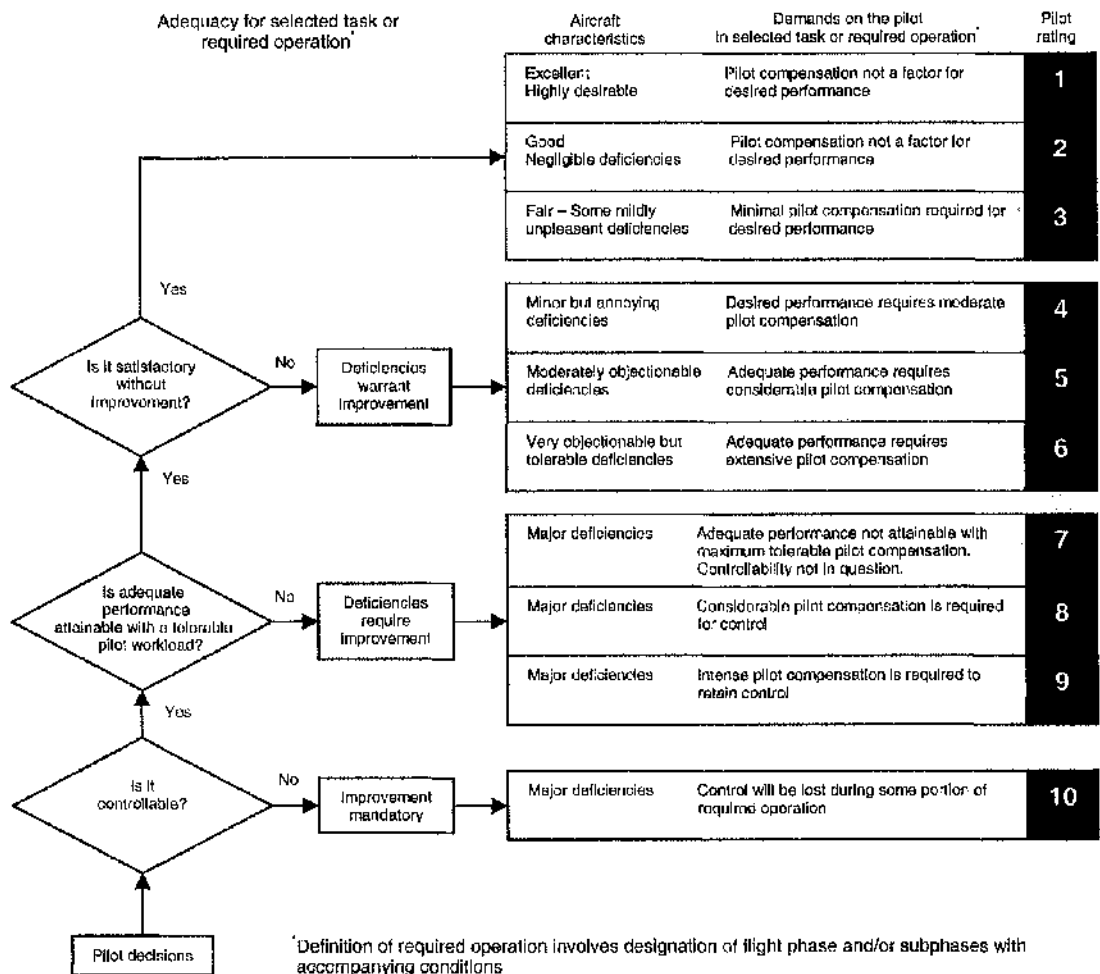


**Figure 2.1** The Cooper-Harper handling qualities rating scale  
(Cooper and Harper, 1969)

Padfield (1996, p. 433) demonstrated that pilot workload and task performance are the factors, which contribute to the HQRs from the Cooper-Harper scale. Moreover, it was emphasised that “workload should be the driver” in assessing the HQRs. According to Geddie *et al* (2001), “workload can be defined as the portion of human resources an operator expends when performing a specified task”. The pilot workload can also be measured using different subjective assessment techniques. The subjective estimation of the workload has been a very active area of research for the past few decades. Many different approaches and techniques have been developed and used successfully in

various studies. For example, Geddie *et al* (2001) provided a detailed description and discussion of the most successful techniques of subjective workload assessment, including NASA-TLX (NASA Task Load Index), SWAT (Subjective Workload Assessment Technique), MCH (Modified Cooper-Harper scale), ZEIS (Sequential Judgement Scale), SWORD (Subjective Workload Dominance Technique) and Bedford workload scale. For the reason that the Bedford workload scale (Ellis and Roscoe, 1982, cited Geddie *et al*, 2001) is based on the Cooper-Harper scale and uses the same decision tree approach as shown in Figure 2.2, it was decided to use it in the current work in conjunction with the Cooper-Harper scale to obtain subjective assessment of handling qualities and pilot workload during the flight test programme of the G-UNIV research gyroplane.

Objective assessment of handling qualities and workload, which does not depend on a pilot's qualitative opinion, can be obtained from quantitative criteria, which are specified in various standards and specifications. The quantitative metrics of handling qualities are based primarily on the stability and controllability characteristics of the aircraft. Only dynamic stability characteristics related to short period and Dutch roll modes will be considered and used throughout the thesis. The rationale behind this decision is that it will not be possible to cover all the static and dynamic stability characteristics and therefore only these two most influential in aircraft handling qualities are considered. Houston and Thomson (2001) demonstrated that there is strong evidence that light gyroplanes have classical short period and Dutch roll responses. In addition, Chapter 3 will provide analysis of short period and Dutch roll modes of the G-UNIV gyroplane using flight test data. Nevertheless, further simulation and flight experiments are required to provide more evidence.

O'Hara (1967) indicated a large influence of the short period and Dutch roll modes on the aircraft's handling qualities. The study (O'Hara, 1967) revealed investigation results for the effects of variations of undamped natural frequency and damping ratio on pilot subjective opinion. The summary of these results is the following:

- 1) *There is a frequency below which handling is not classed "satisfactory", and a lower frequency below which the handling will not be "acceptable."*

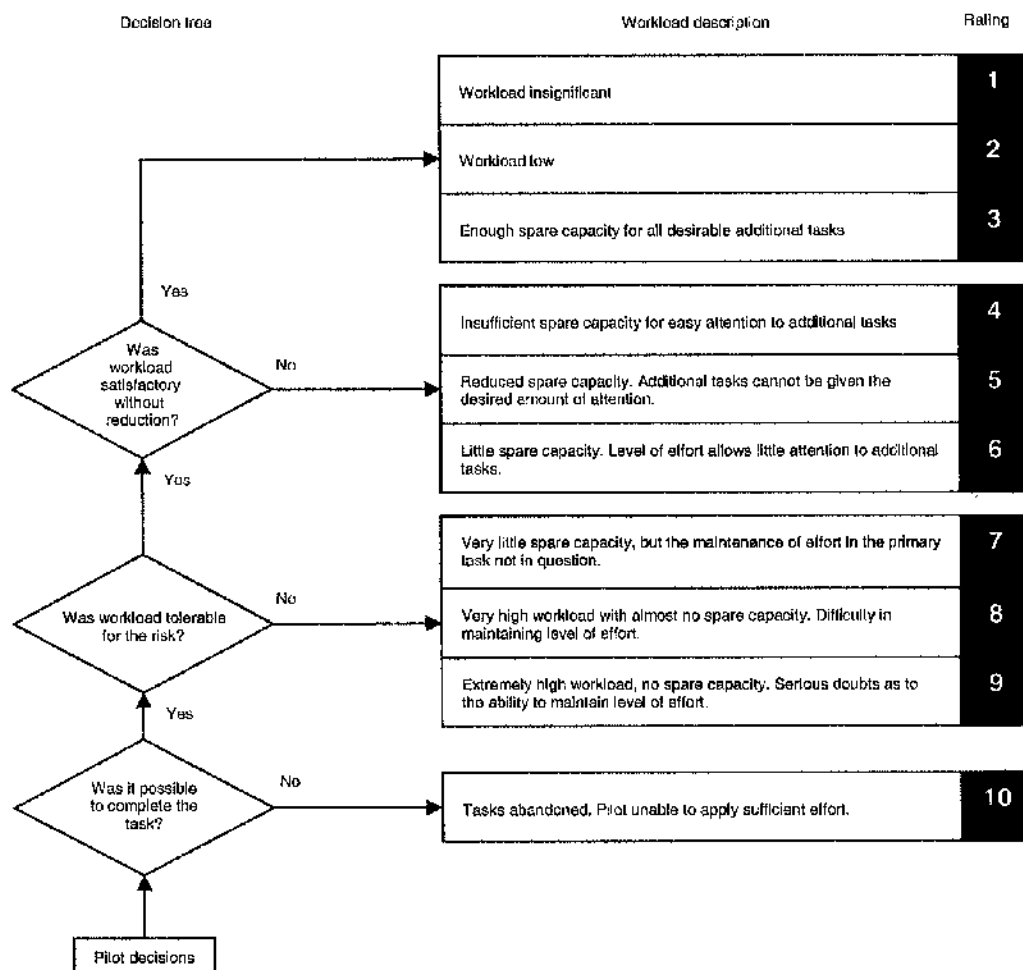


**Figure 2.2** The Bedford workload scale  
(Ellis and Roscoe, 1982, cited Geddie et al, 2001)

- 2) For frequencies greater than the minimum, there is a minimum damping ratio, defining the lower limit of satisfactory handling, and a lower minimum defining the limit of acceptability.
- 3) For frequencies greater than the minimum, there is a maximum damping ratio defining the limit of satisfactory handling and a higher maximum ratio defining the limit of acceptability.

Figure 2.3 depicts these results in the frequency-damping plot, also known as the thumb print criterion. In spite of the fact that this criterion has found wide practical application, there are some disadvantages inherent in it. First, this criterion is not universal; it cannot be applied to all types of aircraft. Second, the short period frequency and damping are not the only parameters which influence pilot assessment of longitudinal handling qualities. For example, Chalk and Wilson (1969) suggested that the boundaries on Figure 2.3 must depend on acceleration sensitivity parameter  $\Delta n_z / \Delta \alpha$ , or  $n_\alpha$ . The acceleration sensitivity is the steady state normal acceleration change per unit change in angle of attack for an increment in pitch control deflection at constant speed. Chalk and Wilson (1969) gave an indicative example of this criterion, where the frequency-damping chart has two sets of boundaries, one for low  $n_\alpha$  numbers, and another one, shifted upwards, for higher numbers of the acceleration sensitivity. The acceleration sensitivity parameter along with other parameters influencing longitudinal handling qualities assessment will be discussed in detail in the following sections.

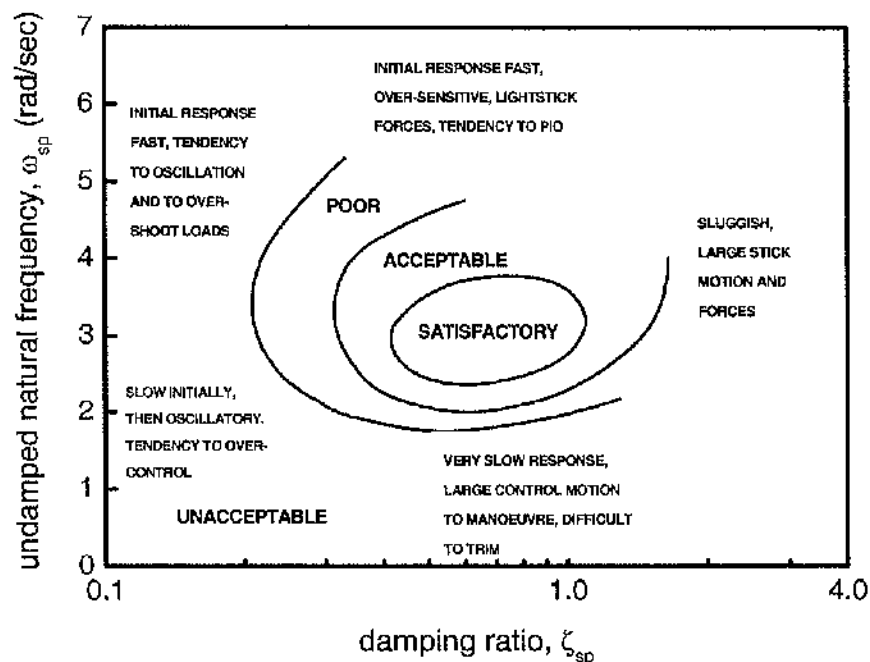


Figure 2.3 Longitudinal short period oscillation – pilot opinion contours, adapted from O'Hara (1967)

The second dynamic mode of interest in this dissertation is the Dutch roll mode, which represents a short period oscillation involving yaw, roll and sideslip; therefore, it significantly affects lateral-directional handling qualities (O'Hara, 1967). As was noted by Cook (1997, p.226), the Dutch roll can be considered as the lateral-directional equivalent of the longitudinal short period mode. It will be demonstrated later in Chapter 3 that the short period and Dutch roll undamped natural frequencies of the G-UNIV gyroplane are indeed similar.

In general, phugoid oscillations do not critically affect the handling characteristics of aircraft because low frequencies associated with phugoid, or long period, dynamic mode lie within the bandwidth of the average human pilot (Cook, 1997, p.204). For example, early research (Soule, 1937; Gilbuth, 1943) indicated that the damping of phugoid mode oscillations of conventional aeroplanes does not affect the pilot handling qualities ratings. However, Houston and Thomson (2001) came to the conclusion, based on simulation and flight test results of the VPM M16 gyroplane, that the light gyroplane has significantly higher frequency of phugoid oscillations and, furthermore, rotor speed degree of freedom couples into these oscillations. This combination might cause "PIO tendency, a subject of much discussion among gyroplane pilots, [which] is most probably caused by this relatively high frequency, lightly damped or even unstable phugoid" (Houston and Thomson, 2001, p.104). Moreover, the research has revealed that the vertical location of the c.g. position of the gyroplane in relation to the propeller thrust line has influence on the frequency of phugoid oscillations. For example, raising the c.g. from 2 in (~0.05 m) below the propeller thrust line to 2 in (~0.05 m) above can double the damping across the speed range, and reduce the frequency of oscillation. These results were obtained for a VPM M16 test gyroplane, and are likely to be the same for other similar types of light gyroplanes.

Despite of the fact that the phugoid mode appears to be influential in handling and workload characteristics of a light gyroplane, it is not discussed further in this dissertation. The higher than usual frequency of the VPM M16 gyroplane phugoid oscillations is close to the short period frequency. Moreover, during the first phase of the G-UNIV gyroplane flight tests (Houston and Thomson, 2004) an unusual oscillatory mode with the frequency even closer to short period was observed (this phenomenon

will be discussed in detail in Chapter 3). Therefore, to locate the phugoid mode, a carefully organised flight test technique must be prepared to test the available G-UNIV research gyroplane. The flight data gathered from previous flight tests do not provide enough information, which could give new insight into the phugoid mode. The flight test programme, within the framework of the current research, was concentrated on gyroplane manoeuvres designed to assess handling qualities and workload, and because of the limits of flight time, investigations on phugoid mode were not included on the list.

In developing handling qualities criteria for gyroplanes, it is natural to look at the techniques used for other types of aircraft, including aeroplanes, rotorcraft and V/STOL. Although basing gyroplane handling qualities criteria on rotorcraft regulations may seem the natural choice it should be noted that gyroplane flight dynamics are more akin to those of fixed wing than rotary wing aircraft. An extensive literature search and analysis were therefore undertaken to review the future needs for light gyroplane handling qualities requirements. Unfortunately, as was noted by Houston and Thomson (2001, p.73), there is only a limited number of documents and papers available, which are related to the fundamentals of gyroplane aerodynamics and flight dynamics. The technical report by Houston and Thomson (2001) provides probably the most comprehensive review of literature linked to gyroplane development and research.

The gyroplane paved the way for the development of the helicopter. For this reason, the early work of the 1920s on rotary-wing aircraft was concentrated primarily to research of dynamics and aerodynamics of gyroplanes available at that period. The most seminal research is that of Glauert (1926; 1927), who developed fundamentals of the rotor theory based on the study of experimental data for gyroplane aerodynamics. In addition, Lock (1927), and Lock and Townend (1928) extended Glauert's theory using wind tunnel test results of a model gyroplane. The research activity in NACA (now NASA) in the early 1930s has generated a great number of technical reports, which presented results of study of gyroplane aeromechanics and data obtained from wind tunnel testing (Wheatley, 1932; 1933; 1934; 1935; 1936a; 1936b; 1937a; 1937b; Wheatley and Windler, 1935; Wheatley and Hood, 1936; Wheatley and Bioletti, 1936a; 1936b; 1937; Bailey, 1938; Bailey and Gustafson, 1939). Basic information on gyroplane historical development is available in some published books on helicopter theory (Johnson, 1980;

Prouty, 1990; Leishman, 2000). A large number of papers have been produced as a result of the research of gyroplane aerodynamics and flight dynamics carried out in the University of Glasgow since early 1990s (Houston, 1996; 1998; 2000; 2002; Coton et al, 1998; Houston et al, 2001; Spathopoulos, 2001; Houston and Thomson, 1999; 2001; 2004; Bagiev et al, 2003; 2004). A considerably extensive paper on historical and theoretical development of gyroplanes was contributed recently by Leishman (2003).

The design and certification standards for aeroplanes, rotorcraft and V/STOL aircraft that are considered relevant to the research of handling qualities of a light gyroplane are presented in Table 2.1. The basic premise of the research presented in this dissertation, therefore, is that the existing flying and handling qualities specifications for fixed and rotary wing aircraft can be modified to suit a light rotorcraft such as a gyroplane. The following sections will review the standards and specifications listed in Table 2.1 with the aim of highlighting the handling qualities requirements and criteria, which can be applied with, or without, modifications to a light gyroplane. A considerable emphasis is placed on the review of the British Civil Airworthiness Requirements for Light Gyroplanes and Aeronautical Design Standard ADS-33E-PRF as the most appropriate standards for a light gyroplane application.

### **2.3 British Civil Airworthiness Requirements for Light Gyroplanes**

The UK Civil Aviation Authority (CAA) developed a new design standard for light gyroplanes "British Civil Airworthiness Requirements, Section T, Light Gyroplane Design Requirements" (BCAR Section T, 1993), and "British Civil Airworthiness Requirements, Section T, Light Gyroplanes" (BCAR Section T, 1995; BCAR Section T, 2003). However, this standard is not prescriptive regarding direct criteria for handling qualities except simple requirements for dynamic stability. At this point, it should be emphasised that neither of the existing civil regulations for different types of flying vehicles uses handling qualities requirements similar to those of the military specifications and standards. Nevertheless, it is the author's opinion that in the future, proper handling qualities criteria must be developed and included in civil airworthiness requirements because handling qualities strongly influence pilot workload and flight safety.

**Table 2.1** Design and airworthiness standards considered in the thesis

Standard	Description	Aeroplane	Rotorcraft, V/STOL	Gyroplane
BCAR Section T	UK CAA BCAR Section T, Light Gyroplanes (CAP 643)			AS*
BCAR Section S	UK CAA BCAR Section S, Small Light Aeroplanes (CAP 482)	AS		
JAR-VLA	Requirements for Very Light Aeroplanes	AS		
JAR-VLR	Requirements for Very Light Rotorcraft		AS	
JAR/FAR-23	Requirements for Normal, Utility, Aerobatic, and Commuter Category Aeroplanes	AS		
JAR/FAR-27	Requirements for Small Rotorcraft		AS	
MIL-F-8785C	Military Specification, Flying Qualities of Piloted Airplanes	DS*/AS		
MIL-H-8501A	Military Specification, Helicopter Flying and Ground Qualities		DS/AS	
MIL-F-83300	Military Specification, Flying Qualities of Piloted V/STOL Aircraft		DS/AS	
DEF STAN 00-970	UK DEF STAN 00-970, Design and Airworthiness Requirements for Service Aircraft, Flight	DS/AS		
DEF STAN 00-970 Rotorcraft	UK DEF STAN 00-970, Design and Airworthiness Requirements for Service Aircraft, Rotorcraft		DS/AS	
AGARD-R-577-70	V/STOL Handling Qualities Criteria		DS	
MIL-HDBK-1797	Department of Defence Handbook, Flying Qualities of Piloted Aircraft (Superseding MIL-F-1797A)	DS/AS		
ADS-33E-PRF	Aeronautical Design Standard, Performance Specification, Handling Qualities Requirements for Military Rotorcraft		DS/AS	

\* AS – Airworthiness Standard, DS – Design Standard

Since 1993 the University of Glasgow has been involved in the process of developing requirements for BCAR Section T, investigating gyroplane stability (Houston, 1996; Houston, 1998), aerodynamics (Coton et al, 1998; Houston and Thomson, 2001) and handling qualities (Houston et al, 2001; Bagiev et al, 2003; 2004); conducting simulation studies (Houston, 2000; 2002) and flight test research (Spathopoulos, 2001; Houston and Thomson, 2004). The aircraft used in this study were the VPM M16 gyroplane and, more recently, the Montgomerie-Parsons research gyroplane (registration G-UNIV).

In general, BCAR Section T has been based on BCAR Section S (2003), with rotorcraft requirements included, which coincide with JAR/FAR-27 (JAR-27, 2004; FAR-27, 1983) regulations. There are only three paragraphs in BCAR Section T related to handling qualities: Controllability and Manoeuvrability, Stability, and Ground Handling Characteristics. Since the Stability paragraph provides requirements on dynamic stability, it is now discussed in detail. The Dynamic Stability section T 181 states, that

- a) *Any short-period oscillations occurring under any permissible flight condition must be heavily damped with the primary controls fixed or free.*
- b) *The gyroplane, under smooth air conditions, must exhibit no dangerous behaviour at any speed between the speed for best rate of climb and never exceed speed, when all controls are fixed or free for a period of 5 seconds.*

Paragraph AMC (Acceptable Means of Compliance) T 181 defines in detail dynamic stability requirements as

*Longitudinal, lateral or directional oscillations with controls fixed or free and following a single disturbance in smooth air, should at least meet the following criteria:*

- a) *Any oscillation having a period of less than 5 seconds should damp to one half amplitude in not more than one cycle. There should be no tendency for undamped small amplitude oscillations to persist.*

- b) *Any oscillation having a period between 5 and 10 seconds should damp to one half amplitude in not more than two cycles. There should be no tendency for undamped small amplitude oscillations to persist.*
  
- c) *Any oscillation having a period between 10 and 20 seconds should be damped, and in no circumstances should an oscillation having a period greater than 20 seconds achieve more than double amplitude in less than 20 seconds.*

The BCAR Section T gives a description of how initiate the oscillations:

*The disturbance should be introduced, with the gyroplane in trimmed steady flight and with the other primary controls fixed, by moving one primary flight control sharply to an out-of-trim position and immediately returning it to its original trim position, at which it is then held fixed. For those gyroplanes which do not have a variable trim control the method of exciting the oscillation is the same but the control must be returned to the datum position and held fixed in that position.*

It can be seen from the above description of those parts of the BCAR Section T, which relate to handling qualities, that these gyroplane airworthiness requirements provide only simple dynamic stability criteria, which are mainly based on those from BCAR Section S (2003) and JAR/FAR-27 (JAR-27, 2004; FAR-27, 1983) regulations. Besides, it should be emphasised that only short period mode was specified in this standard, while Dutch roll and phugoid oscillatory modes were referred to as “longitudinal, lateral or directional oscillations”. This can be explained by the fact that existence of these modes in gyroplane flight dynamics still has not been definitely proven. On the other side, simulation results (Houston and Thomson, 2001) revealed that the VPM M16 test gyroplane has “marginally stable Dutch roll type of oscillation” and as discussed earlier in this chapter, phugoid mode. Moreover, flight test results of the G-UNIV research gyroplane also indicate presence of these modes (detailed discussion of this topic is presented in Chapter 3). Nevertheless, extensive flight tests and simulation are essential to understand better the dynamic behaviour of a light gyroplane.

As was recommended by Houston and Thomson (2001, p.74), the Dynamic Stability subparagraph of BCAR Section T should “be amended to state that short period oscillations be “damped” and not “heavily damped”, unless “heavily” can be further quantified”. In addition, it can be recommended to specify the limits of damping ratio for short period, and also for phugoid and lateral-directional requirements in a manner used, for example, in MIL-F-8785C (1980) specification or DEF STAN 00-970 (2003) standard.

## 2.4 Aeronautical Design Standard ADS-33E-PRF

The handling qualities specifications for rotorcraft, such as MIL-H-8501A (1961) and DEF STAN 00-970 Rotorcraft (1984), were based on time-domain dynamic stability criteria. The modern US handling qualities standard for military rotorcraft, ADS-33C (1989), and its superseding, ADS-33D (1994), ADS-33D-PRF (1996) and ADS-33E-PRF (2000), includes new response-type mission-oriented concept based on extensive frequency-domain criteria. Mitchell *et al* (2004) called the appearance of this standard as a second revolution in handling qualities. What was started as the US Army research programme for a new experimental helicopter, LHX, in the early 1980s, became the most comprehensive handling qualities standard for rotorcraft after publishing as ADS-33C in 1989.

A number of papers have been published which discuss the application of the ADS-33 standards to a helicopter handling qualities evaluation. For example, the US Army conducted a number of flight tests to determine the handling qualities of the OH-58D helicopter (Ham, 1992; Ham *et al*, 1995). At the same time, the DLR at Braunschweig conducted a partial evaluation of the ADS-33 handling qualities criteria by flight testing the BO 105 research helicopter (Pausder and Blanken, 1992a; 1992b; Ockier and Pausder, 1995; Ockier, 1996).

This standard uses two distinct methods of establishing levels of handling qualities, objective and subjective, or predicted levels and assigned levels. Predicted levels are obtained from quantitative criteria, assigned levels are obtained from test pilots using

the Cooper-Harper HQR scale (Figure 2.1) to estimate the workload and task performance required to perform designated MTEs. The ADS-33E-PRF defines Level 1 as HQRs between 1 and 3.5; Level 2 as HQRs between 3.5 and 6.5; and Level 3 as HQRs between 6.5 and 8.5.

There are some new revolutionary innovations in this standard. For example, the standard does not provide any categorisation according to rotorcraft size. This makes this document universal, and gives the possibility of using it as a basis for light gyroplane requirements. The new concept of response-type and mission task elements (MTE) was introduced. The MTE concept forms the core of the G-UNIV flight test programme presented in this dissertation. Since the basic premise of the flight testing part of this thesis is that the ADS-33E-PRF handling qualities requirements can be modified to suit a light rotorcraft such as a gyroplane, the ultimate aim of this dissertation is to develop gyroplane MTEs based on those from ADS-33E-PRF, and then to document test flights using them on the fully instrumented G-UNIV research gyroplane demonstrating their effectiveness. Two rotorcraft MTEs were selected for consideration, slalom and acceleration-deceleration, which will be discussed in detail in Chapters 5, 6 and 7.

The required response-types depend on the MTEs and the usable cue environment (UCE). The UCE in turn can be obtained from criteria provided in the standard using visual cue ratings (VCR) from pilot assessments. Levels of aggressiveness are graded in ADS-33E-PRF. A degree of pilot attention is also specified, and the standard provides requirements for full and divided pilot attention. Another distinctive feature of the standard is that the requirements are different for hover/low airspeed and forward flight. ADS-33E-PRF also defines new requirements for pitch-roll cross couplings.

Other innovations that may be employed are short-term bandwidth and time delay criteria, which form the basis for requirements for small-amplitude range of rotorcraft manoeuvres. In spite of the fact that these criteria were developed for highly augmented rotorcraft with automatic control systems, it was decided to apply them to the research gyroplane flight data with the aim of investigating the applicability of such an approach of assessing handling qualities of a light gyroplane.

Figure 2.4 illustrates the definition of bandwidth  $\omega_{BW}$  and phase delay  $\tau_p$ . For Rate response-types  $\omega_{BW}$  is lesser of  $\omega_{BW_{gain}}$  and  $\omega_{BW_{phase}}$ , for Attitude Command/Attitude Hold response-types (ACAH)  $\omega_{BW} = \omega_{BW_{phase}}$ . The phase bandwidth  $\omega_{BW_{phase}}$  is the frequency at a phase of 135 degrees, while the gain bandwidth  $\omega_{BW_{gain}}$  can be obtained by adding 6 dB to the neutral stability magnitude. The phase delay  $\tau_p$  is defined by

$$\tau_p = \frac{\Delta\Phi_{2\omega_{180}}}{57.3(2\omega_{180})}, \quad (2.1)$$

where  $\omega_{180}$  is the neutral stability frequency and  $\Delta\Phi_{2\omega_{180}}$  is the phase increase at  $2\omega_{180}$ .

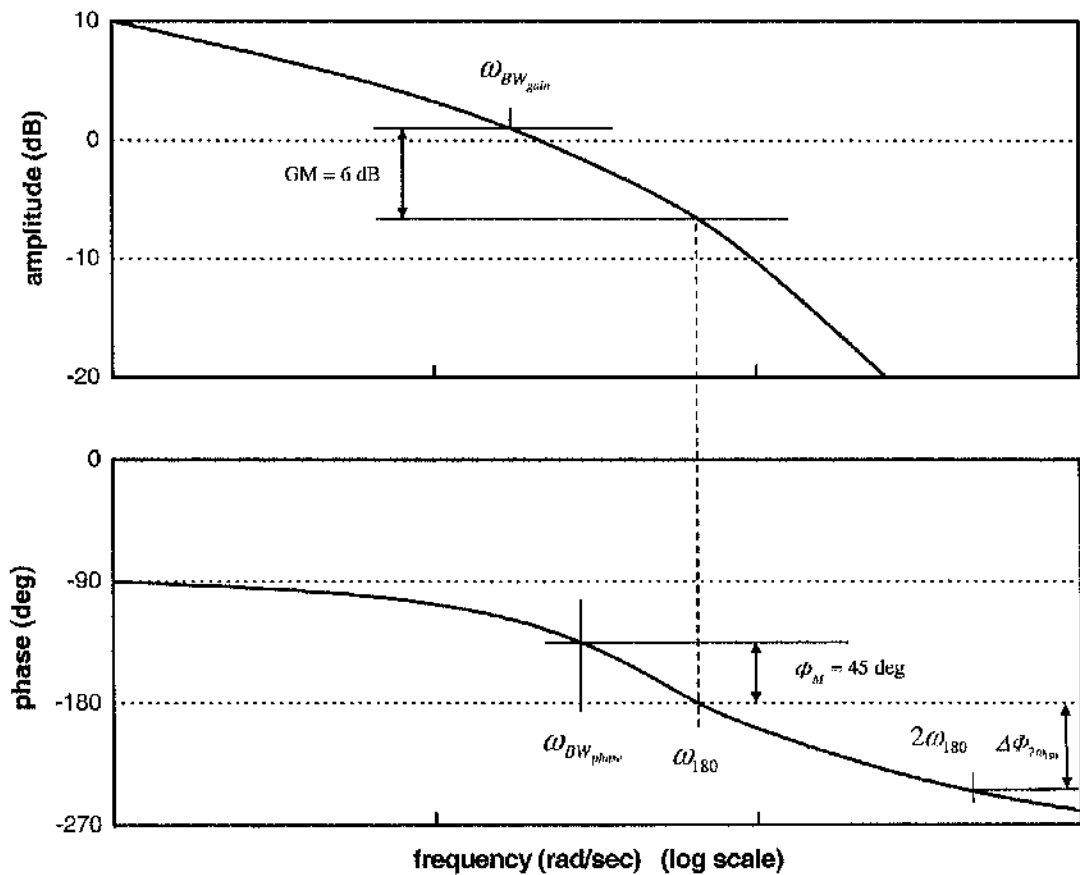


**Figure 2.4** Definitions of bandwidth and phase delay, adapted from ADS-33E-PRF (2000)

Pausder and Blanken (1992a; 1992b) gave background information and detailed explanation of these criteria. In general, an aircraft must have a high bandwidth to transmit the control input. Such an aircraft can be described as sharp, quick, or agile, while an aircraft with low bandwidth is sluggish, with a smooth response (Ham, 1992). Research has shown that pilot handling qualities ratings strongly depend on the shape of phase plot at frequencies beyond the neutral stability frequency  $\omega_{180}$ . This led to definition of the phase delay parameter in the form presented above. A large phase delay can be caused by onboard flight control software, or delays of flight control hydraulic actuators. In addition, an aircraft with large phase delay values can be prone to pilot induced oscillations (PIO). Since light gyroplanes usually do not use any stability augmentation, the phase delay parameter is likely to be ineffective in application to light gyroplanes, whilst the requirements on bandwidth are essential. Further discussions regarding this topic are provided in Chapter 3.

There are different requirements for bandwidth/phase delay criteria, which depend on various task and flight conditions. In addition, ADS-33E-PRF standard defines these criteria for two speed ranges: (i) hover and low speed (up to 45 knots), and (ii) forward flight (greater than 45 knots). The interest here is in requirements for small-amplitude pitch attitude changes - hover and low speed (All Other MTEs, UCE=1, Fully Attended Operations), which completely coincide with those for forward flight (All Other MTEs, VMC (Visual Meteorological Conditions), Fully Attended Operations), and are presented in Figure 2.5. Requirements for small-amplitude roll attitude changes - forward flight (All Other MTEs, UCE=1, Fully Attended Operations) also entirely coincide with those for forward flight (All Other MTEs, VMC, Fully Attended Operations), and are depicted in Figure 2.6.

The ADS-33E-PRF requirements for moderate-amplitude range of attitude changes are based on attitude quickness parameter, which is defined for pitch, roll and heading as the ratio of peak attitude rate to change in attitude angle. Therefore, the attitude quickness can be considered as an agility metric of the aircraft response to a pilot control input (Meyer and Padfield, 2005, p.41). As an example for the roll channel, the attitude quickness is defined as

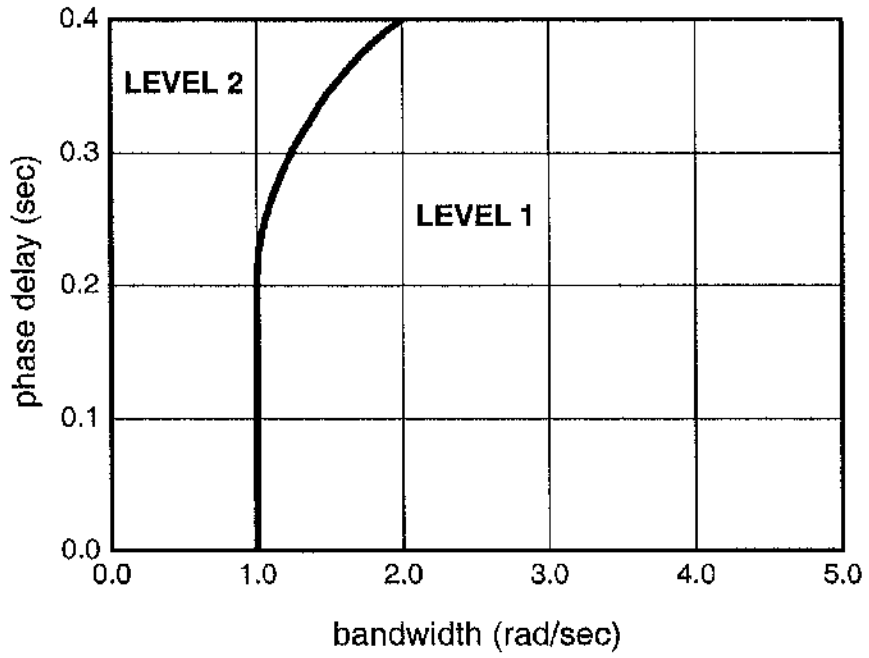


**Figure 2.5** Requirements for small-amplitude pitch attitude changes (All Other MTEs), adapted from ADS-33E-PRF (2000)

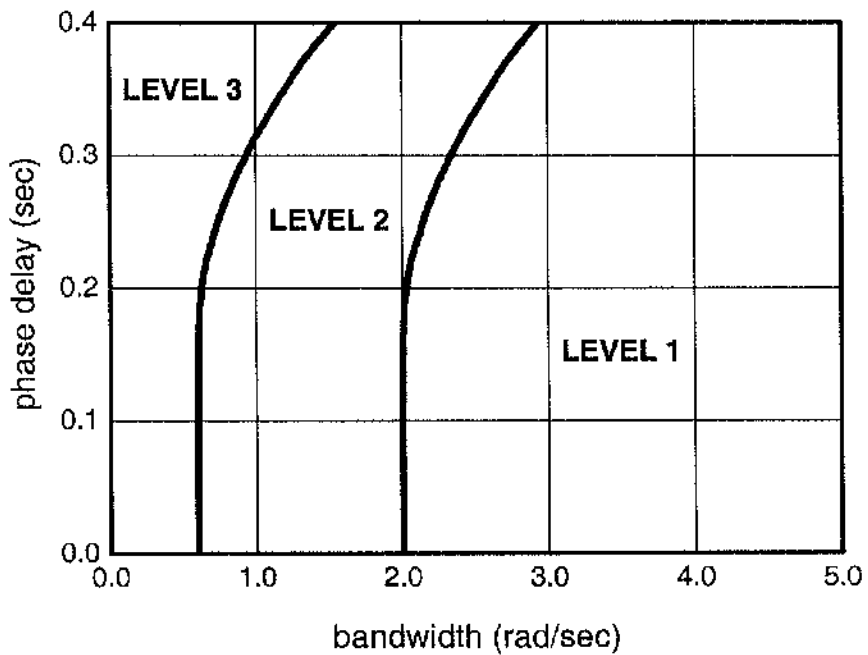


**Figure 2.6** Requirements for small-amplitude roll attitude changes (All Other MTEs), adapted from ADS-33E-PRF (2000)

$$\text{roll attitude quickness} = \frac{p_{pk}}{\Delta\phi_{pk}}, \quad (2.2)$$

where  $p_{pk}$  is the peak roll rate, and  $\Delta\phi_{pk}$  is the change in roll attitude. According to ADS-33E-PRF standard, the roll attitude quickness should satisfy the requirements for moderate-amplitude roll attitude changes depicted in Figure 2.7. It should be noted that ADS-33E-PRF defines roll attitude quickness criteria for full range of speed, while pitch and heading attitude quickness criteria are defined only for hover and low speed.

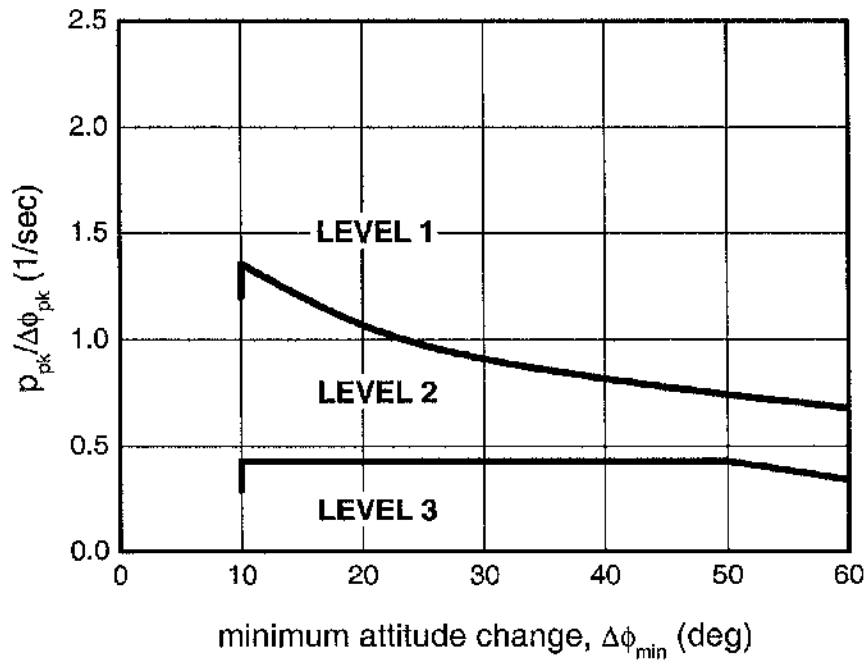


**Figure 2.7** Requirements for moderate-amplitude roll attitude changes (All Other MTEs), adapted from ADS-33E-PRF (2000)

The attitude quickness concept can be easily applied to a light gyroplane. As an example, the roll attitude quickness criteria for the gyroplane slalom manoeuvre have been developed based on pilot subjective assessments of handling qualities. The process of designing of these criteria is presented in detail in Chapter 7.

The ADS-33E-PRF standard limits the oscillations by terms of undamped natural frequency and damping ratio in the same manner as, for example, AGARD-R-577-70 (1970). Figures 2.8 and 2.9 show requirements on pitch and roll oscillations for hover and low speed, and requirements for lateral-directional oscillations respectively.

It should be noted that this is not the first time that handling qualities requirements for military rotorcraft have been adapted to different types of rotorcraft. In addition to examples of designing handling qualities requirements for civil tiltrotors (Fortenbaugh *et al*, 1999; Padfield and Meyer, 2003; Fortenbaugh *et al*, 2004; Meyer and Padfield, 2005) based on military standards for aeroplanes and rotorcraft (this topic is discussed in detail in Section 2.5.4), some other attempts to adapt the handling qualities criteria of the ADS-33 standards for maritime (Tate *et al*, 1995; Padfield, 1998; Carignan and Gubbels, 1998), civil (Charlton and Talbot, 1997), and cargo helicopters (Key *et al*, 1998) were also carried out.

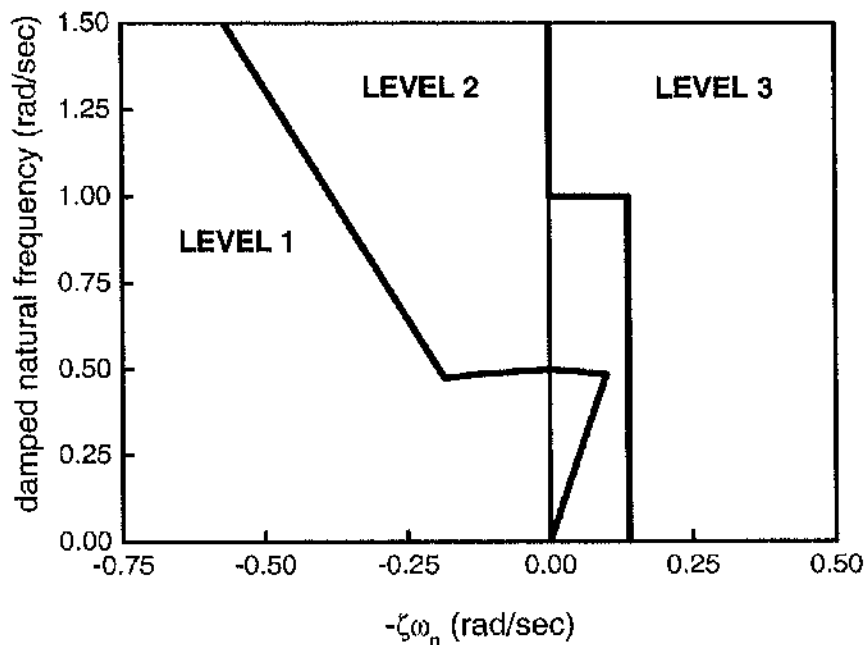


**Figure 2.8** Limits on pitch (roll) oscillations – hover and low speed, adapted from ADS-33E-PRF (2000)



The airworthiness and design standards listed in Table 2.1 are now reviewed with emphasis placed upon the handling qualities requirements.

### 2.5.1 BCAR Section S, JAR/FAR-23, JAR/FAR-27, JAR-VLA and JAR-VLR

As mentioned earlier in the chapter, BCAR Section T is based generally on BCAR Section S (2003) and JAR/FAR-27 (JAR-27, 2004; FAR-27, 1983) specifications. After detailed analysis of these three airworthiness standards, it was revealed that dynamic stability requirements of BCAR Section T are based primarily only on those of JAR/FAR-27 for single-pilot approval. Only minor modifications have been made. BCAR Section S requires only that any short period longitudinal and lateral-directional oscillations must be *heavily damped* with the primary controls free and fixed. European Joint Aviation Authorities requirements for Very Light Rotorcraft, JAR-VLR (2004) specifies only static stability, not any dynamic stability criteria.

Joint Aviation Requirements for Very Light Aeroplanes, JAR-VLA (2004) coincide in requirements for dynamic stability with Joint Aviation Requirements JAR-23 (2004) and Part 23 of the Federal Aviation Regulations (FAR-23, 1993) for Normal, Utility, Aerobatic, and Commuter Category Aeroplanes, which go further and define requirements not only for short period oscillations, but also for Dutch roll and long period, or phugoid, oscillations. In general, the approach used in JAR-VLA and JAR/FAR-23 is similar to that of BCAR Section T, but in contrast to the gyroplane requirements, these airworthiness standards categorise oscillation modes. Such a categorisation is essential in future handling qualities standards for light gyroplanes, though an extensive flight test database is needed to define properly requirements for the short period, Dutch roll and phugoid.

It is well known that military aviation standards and specifications are more detailed in quantitative assessment and more demanding than civil airworthiness regulations. It is reasonable, because military aircraft are usually more agile and manoeuvrable, and designed to complete assigned missions. Moreover, military aircraft actually appear to be a compound system with variety of complex subsystems, and state of the art technology and knowledge are used to design and produce such highly augmented

aircraft. Among the military specifications and standards, the rotary-wing standards are even more demanding due to the fact that rotorcraft as a flight vehicle has more complicated dynamics caused mainly by the rotating rotor. This probably explains the fact that the helicopter flying qualities requirements were the first to appear in 1952 as MIL-H-8501.

### **2.5.2 MIL-H-8501A**

The first helicopter flying and ground handling qualities specification, MIL-H-8501 (1952), and its superseding, MIL-H-8501A (1961), use simple dynamic stability requirements based on time response parameters. The requirements are defined as follows:

- (a) Any vacillation having a period of less than 5 seconds shall damp to one-half amplitude in not more than 2 cycles, and there shall be no tendency for undamped small amplitude oscillations to persist.*
- (b) Any oscillation having a period greater than 5 seconds but less than 10 seconds shall be at least lightly damped.*
- (c) Any oscillation having a period greater than 10 seconds but less than 20 seconds shall not achieve double amplitude in less than 10 seconds.*

Apparently, civil regulations for rotorcraft, such as JAR/FAR-27, JAR-VLR and BCAR Section T, are based on these very first helicopter requirements.

### **2.5.3 MIL-F-8785C and DEF STAN 00-970**

Mitchell *et al* (2004) described the appearance of the new generation of specifications in the late 1950s and early 1960s as the most significant revolution in handling qualities. Simple dynamic criteria were replaced by aeroplane specific modal characteristics, such as short period damping and frequency, phugoid damping, roll time constant, etc.

MIL-F-008785A(USAF) (1968) was issued by the US Air Force and was the first specification which used this innovation. Later, MIL-F-8785B(ASG) (1969) and MIL-F-8785C (1980) superseded the first version. The latter version of this specification, MIL-F-8785C, will be considered in the thesis. MIL-F-8785C specification divides all aeroplanes into four classes (Appendix 1, Section A1.1.1). Obviously, the test gyroplane can be considered as Class I aircraft, therefore only requirements for Class I aeroplanes would be appropriate. In addition, this document defines Flight Phase Categories (Appendix 1, Section A1.1.2). It can be seen that Category A Flight Phases are apparently typical military tasks, and therefore will not be considered in the thesis. MIL-F-8785C definitions of Levels of flying qualities are presented in Appendix 1, Section A1.1.3.

In contrast to the short period frequency and damping criterion (the thumb print criterion) depicted in Figure 2.3, MIL-F-8785C specification uses short period frequency and acceleration sensitivity criteria together with independent damping requirements. For example, for Category B Flight Phases, Class I, the specification requires that the equivalent short period undamped natural frequency should be within the limits shown in Figure 2.10. The requirements for Category C Flight Phases, Class I, are slightly more stringent for Levels 1 and 2.

The acceleration sensitivity  $n_\alpha$  is the steady state normal acceleration change per unit change in angle of attack for an increment in pitch control deflection at constant speed. In fact, the boundaries of flying qualities levels define acceptable ratios between angular and linear accelerations with respect to the angle of attack. It can be seen from the approximate expression of angular acceleration

$$\Delta\ddot{\theta} \approx \omega_{sp}^2 \Delta\alpha \quad (2.3)$$

after dividing it by acceleration increment  $\Delta n_z$

$$\frac{\Delta\ddot{\theta}}{\Delta n_z} \approx \frac{\omega_{sp}^2}{\Delta n_z / \Delta\alpha} = \frac{\omega_{sp}^2}{n_\alpha}, \quad (2.4)$$

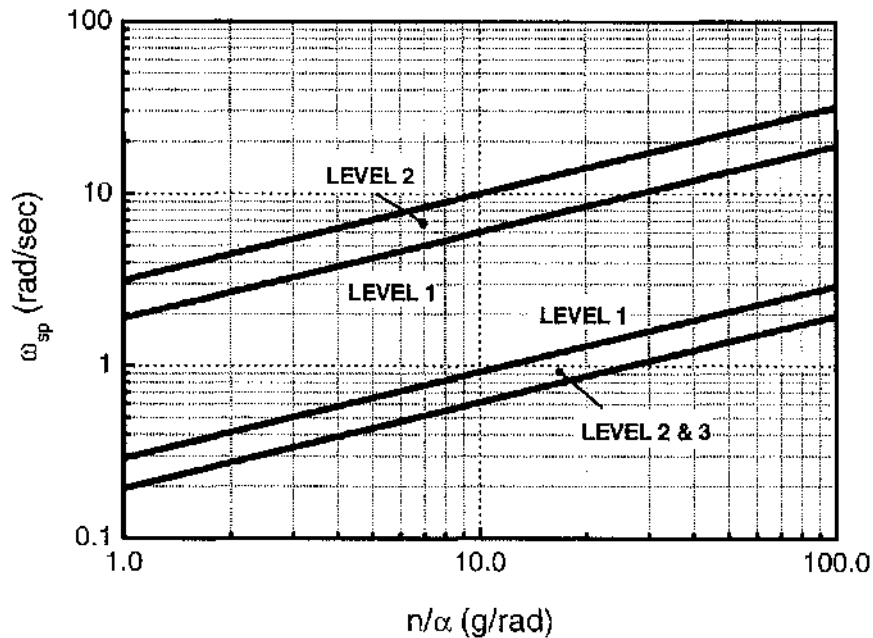


**Figure 2.10** Short period frequency requirements – Category B Flight Phases, Class I, adapted from MIL-F-8785C (1980)

where  $n_\alpha$  is the acceleration sensitivity. Thus, the level boundaries in the criteria chart in logarithmic scale are represented by the constant numbers of the ratio  $\Delta\ddot{\theta}/\Delta n_\alpha$ . Chalk and Wilson (1969) provided more detailed review of this criterion, and discussed other research on short period mode requirements for aeroplanes. As will be demonstrated in Section 2.5.7, the ratio  $\Delta\ddot{\theta}/\Delta n_\alpha$  is nothing else but Control Anticipation Parameter (CAP) proposed by Bihrlé (1966, cited MIL-HDBK-1797, 1997, p.188). In addition, Section 2.5.7 will analyse short period CAP/damping ratio criteria (MIL-HDBK-1797, 1997), which are based on similar principles to those discussed above.

The equivalent short period damping ratio,  $\zeta_{sp}$ , according to the MIL-F-8785C requirements should be within the limits of Table 2.2.

**Table 2.2** Short period damping ratio limits, adapted from MIL-F-8785C (1980)

Level	Category A and C Flight Phases		Category B Flight Phases	
	Minimum	Maximum	Minimum	Maximum
1	0.35	1.30	0.30	2.00
2	0.25	2.00	0.20	2.00
3	0.15	-	0.15	-

The frequency and damping ratio of the lateral-directional oscillations (Dutch roll) following a yaw disturbance input should exceed the minimum values in Table 2.3.

**Table 2.3** Minimum Dutch roll frequency and damping, adapted from MIL-F-8785C (1980)

Level	Phase Category	Class	Min $\zeta_d$	Min $\zeta_d \omega_d$ (rad/sec)	Min $\omega_d$ (rad/sec)
1	A (Air-to-air Combat and Ground Attack)	IV	0.4	-	1.0
	A	I, IV	0.19	0.35	1.0
		II, III	0.19	0.35	0.4
	B	All	0.08	0.15	0.4
C	I, II-C, IV	0.08	0.15	1.0	
	II-L, III	0.08	0.10	0.4	
2	All	All	0.02	0.05	0.4
3	All	All	0	-	0.4

In 2003 UK Ministry of Defence published Issue 3 of the Defence Standard 00-970, "Design and Airworthiness Requirements for Service Aircraft, Flight" (*DEF STAN 00-970, 2003*). This standard defines requirements and provides guidance for the design of military aircraft to meet airworthiness requirements. This standard has a long history that can be traced back to 1916, when "Design Requirements for Aeroplanes" (AP 970), a basic six-page pamphlet, was issued by the Royal Aircraft Factory (later Royal Aircraft Establishment) of Farnborough (*NASA, 2005*). Air Publication (AP) 970 2<sup>nd</sup> Edition dated 1924, and Aviation Publication (AvP) 970 dated 1959 were the next developments of the standard, which led to the Issue 1 of the Defence Standard 00-970 in December 1983 (*DEF STAN 00-970, 2003*).

The structure of DEF STAN 00-970 is generally similar to that of MIL-F-8785C. Moreover, the Flight Phase Categories and Levels of flying qualities are defined in the same manner as in MIL-F-8785C specification. The DEF STAN 00-970 criteria for short period undamped frequency and acceleration sensitivity are also analogous, except that the MIL-F-8785C's Level 1 requirements for Category C Flight Phases are more stringent than those of DEF STAN 00-970. The requirements for the short period damping ratio  $\zeta_{sp}$ , Dutch roll damping ratio  $\zeta_d$  and Dutch roll undamped natural frequency  $\omega_d$ , are also comparable to those of MIL-F-8785C, with minor differences in required values for these parameters.

In conclusion, two points should be emphasised regarding MIL-F-8785C specification and DEF STAN 00-970 standard, which are of interest in the current work. First is that instead of simple short period frequency and damping requirements, known as thumb print criterion, these standards use short period frequency and acceleration sensitivity criterion. As was noted by Cook (*1997, p.213*), the requirements in both MIL-F-8785C and DEF STAN 00-970 are based on the dynamics of classical aeroplanes whose, for example, short term response is described by second order transfer functions. As was demonstrated by Houston and Thomson (*2001*), there is strong evidence that light gyroplanes have a classical, or similar, short period response, though further simulation and flight experiments are required to prove this postulate. Therefore, assuming that the short period dynamics of light gyroplanes can be described by second order transfer

functions, it can be supposed that the short period frequency and acceleration sensitivity criterion is suitable for light gyroplanes.

Secondly, according to MIL-F-8785C and DEF STAN 00-970, short period and lateral-directional oscillations (Dutch roll) damping ratios must be within defined limits (moreover, Dutch roll undamped natural frequency is also specified). Probably gyroplane requirements for short period and lateral-directional oscillations must also be developed in terms of damping ratio for short period and damping ratio/frequency for Dutch roll rather than in terms of “amplitude and cycles”, “damped” and “heavily damped” as specified in MIL-H-8501A, JAR/FAR-23 and BCAR Section T standards.

Therefore, to sum up, the approach used to define the dynamic stability requirements in MIL-F-8785C specification and DEF STAN 00-970 standard can be suggested as a basis for the light gyroplane handling qualities requirements.

#### **2.5.4 MIL-F-83300**

The first specification for V/STOL aircraft, MIL-F-83300 (1970), is based on initial requirements of MIL-F-8785B(ASG) (1969). It is very interesting for the purposes of the thesis to follow the changes and innovations of this V/STOL standard in comparison with previous acroplane specifications. In fact, the V/STOL aircraft, as well as the gyroplane, combines the behaviour of both aeroplanes and rotorcraft, and V/STOL handling qualities specifications use existing aeroplane standards modified to suit a V/STOL aircraft. These modifications might be helpful in designing the handling qualities criteria for light gyroplanes. A modern example of such an approach is a process of developing handling qualities criteria for a civil tiltrotor (Padfield and Meyer, 2003; Meyer and Padfield, 2005). This project is developing handling qualities criteria through analysis and piloted simulation at Eurocopter SPHERE (Marignane, France) and HELIFLIGHT (University of Liverpool, UK) facilities. Another example is a programme of the Bell/Agusta BA609 civil tiltrotor, which made its first flight in March 2003, and is currently in the process of certification as a special condition under FAA regulations (Fortenbaugh et al, 2004). The handling qualities requirements are based on previous flight experience with V-22 and XV-15 tiltrotor aircraft, high-fidelity

simulation evaluations and several military specifications, including MIL-F-8785C (1980), MIL-F-83300 (1970), and ADS-33E-PRF (2000) (Fortenbaugh et al, 1999; Fortenbaugh et al, 2004).

Classification of aircraft and definition of Flying Qualities Levels in MIL-F-83300 are identical to those of MIL-F-8785C, while Flight Phases in addition have the tasks specific to V/STOL aircraft. In contrast to MIL-F-8785C, longitudinal handling qualities are defined not by the terms of short period frequency and acceleration sensitivity, but by short period undamped natural frequency and damping ratio as shown in Figure 2.11. It should be noted that Figure 2.11 shows handling qualities Level boundaries only for VFR (Visual Flight Rules) conditions, which is applicable to a light gyroplane, while the specification also defines Levels for IFR (Instrument Flight Rules) conditions. To achieve Level 3 of Flying Qualities, “an instability will be permitted provided its frequency is less than 1.25 radians per second and its time to double amplitude is greater than 5 seconds” (MIL-F-83300, 1970).

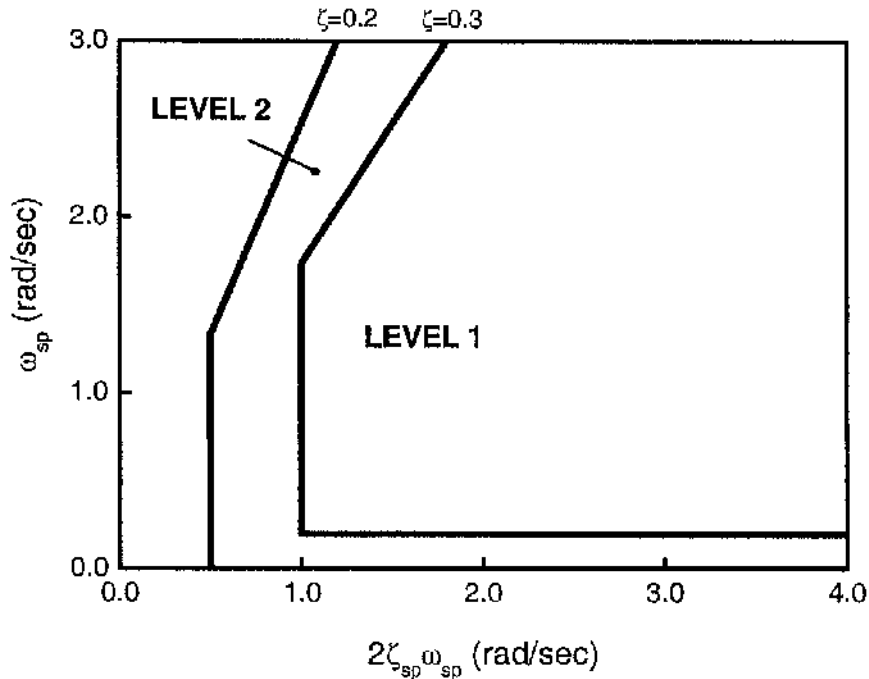


**Figure 2.11** Short-term longitudinal response requirements, VFR, adapted from MIL-F-83300 (1970)

According to MIL-F-83300 specification, the frequency and damping ratio of the lateral-directional oscillations (Dutch roll) following a disturbance input, for example a yaw control doublet, should exceed the minima presented on Figure 2.12. The requirements should be met with controls fixed and with them free for oscillations of any magnitude that might be experienced in operational use. In contrast to short-term longitudinal response requirements, the lateral-directional oscillatory requirements are based not only on undamped natural frequency, but also on frequency of damped oscillation.

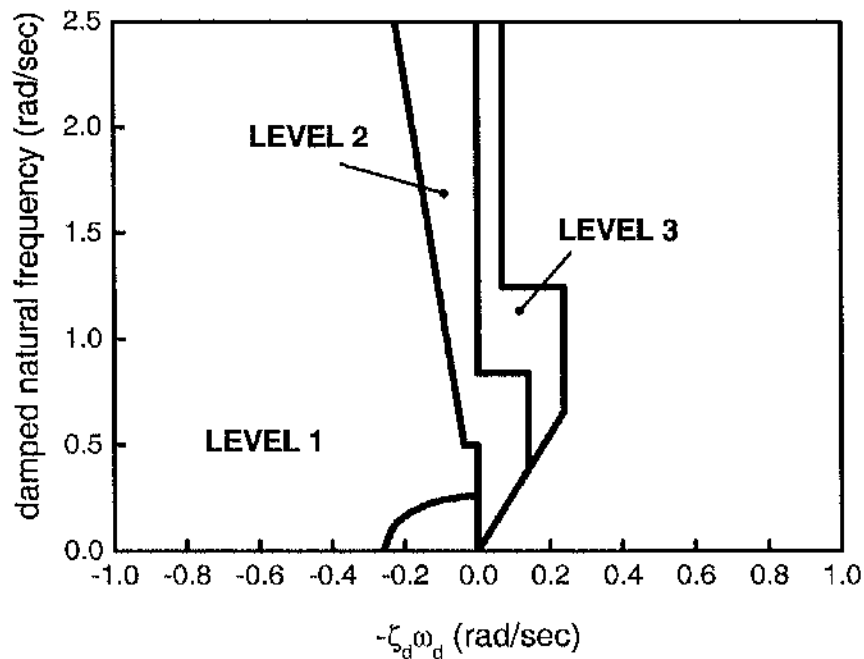


**Figure 2.12** Lateral-directional oscillatory requirements, adapted from MIL-F-83300 (1970)

It can be concluded that the approach used in MIL-F-83300 specification to define both short period longitudinal response requirements and lateral-directional oscillatory requirements might be suitable, in general, for light gyroplanes. Again, extensive flight tests and simulation are necessary to define proper boundaries of handling qualities levels.

### 2.5.5 AGARD-R-577-70

The AGARD Report 577 "V/STOL Handling-Qualities Criteria" (AGARD-R-577-70, 1970) is also relevant. The criteria proposed in this report "can serve as a guide in establishing specifications to be used by a contractor for the design and testing of a particular aircraft" (AGARD-R-577-70, 1970, p.1). Longitudinal dynamic stability requirements are defined in the report as follows:

*The responses of the aircraft should not be divergent (i.e., all roots of the longitudinal characteristic equations should be stable). In addition the damping ratio of the second-order pair of roots that primarily determine the short-term response of angle of attack and pitch attitude following an abrupt pitch control input should be at least 0.3 for the most critical undamped natural frequency.*

*The frequency and damping characteristics of any oscillations superimposed on the normal control modes for VTOL aircraft in hover and V/STOL aircraft at the approach reference speed should meet at least the values shown in Figure 2.13. Any sustained residual oscillations should not degrade the pilot's ability to perform the required tasks.*

Lateral-directional dynamic stability criteria are also defined in AGARD-R-577-70:

*Any roll-yaw oscillations superimposed on the normal control mode due to a disturbance input should exhibit at least the frequency-damping characteristics shown in Figure 2.14 over the speed range specified. Also, there should be no tendency for perceptible small-amplitude oscillations to persist or for pilot-induced oscillations to result from the pilot's attempts to perform the required flight tasks.*

It can be seen from Figure 2.13 that the longitudinal dynamic stability criteria are based on the same principles as those of MIL-F-83300, the only difference is that the y-coordinate in the AGARD-R-577-70 criteria is represented by the damped natural frequency in the same manner as in ADS-33E-PRF. The approach of lateral-directional dynamic stability criteria (Figure 2.14) is similar to that of MIL-F-83300 and ADS-33E-PRF. However, the boundaries of handling qualities levels are different.

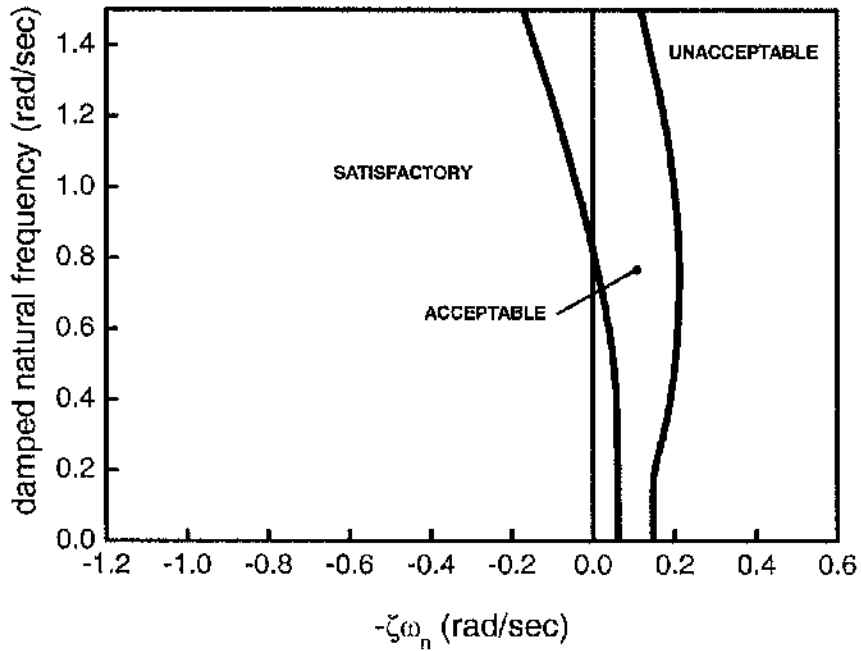


**Figure 2.13** Longitudinal dynamic stability criteria, adapted from AGARD-R-577-70 (1970)

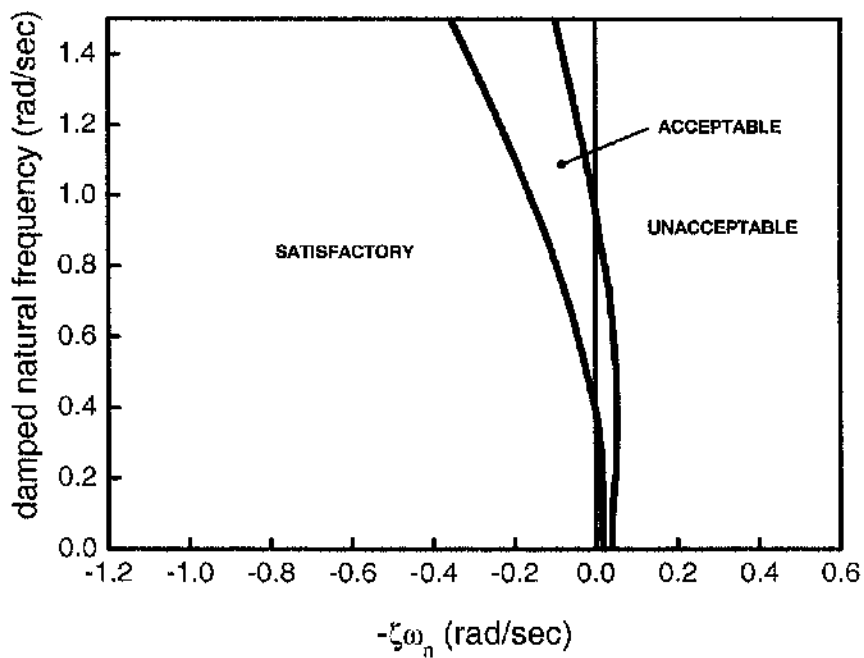


**Figure 2.14** Lateral-directional dynamic stability criteria, adapted from AGARD-R-577-70 (1970)

The next generations of standards and specifications, which will be reviewed in the following subsections, have been developed for applications to highly augmented aircraft. Nevertheless, despite the fact that light gyroplanes usually do not use stability augmentation, it was decided to review all the relevant standards and specifications with the aim of revealing what elements and approaches of designing handling qualities requirements can be applied with, or without, modification to a light gyroplane.

### 2.5.6 DEF STAN 00-970 Rotorcraft

DEF STAN 00-970 (2003), which was described above, has a special part devoted to rotorcraft requirements, Volume 2 - Rotorcraft (*DEF STAN 00-970 Rotorcraft, 1984*). There are three types of Flight Phases defined in this standard: the Active Flight Phase, Attentive Flight Phase, and Passive Flight Phase. The last two phases include automatic flight control, therefore will not be considered for a light gyroplane case. The Active Flight Phase is defined as:

(i) *Pilot Involvement in Flying – High:*

*Continuously flying rotorcraft through the flying controls.*

(ii) *Major Rotorcraft Handling Considerations:*

*Short term stability and response characteristics;*

*Manoeuvrability; Precise transient flight path control.*

The short period stability criteria from DEF STAN 00-970 Rotorcraft are based on time domain response requirements of initial response and dynamic stability (Figure 2.15). The initial response metrics are *responsiveness*, *initial delay* and *sensitivity*. The *responsiveness* of the rotorcraft to control inputs is characterised by the peak value of the time response, as can be seen in Figure 2.15. It must be greater than some minimum value for adequate responsiveness, and not exceed some maximum to avoid over sensitivity. Regarding the *initial delay* the DEF STAN 00-970 Rotorcraft defines that "...within a specified finite time of the initiation of the control input the relevant parameter must have achieved a minimum percentage of the peak value". For example, for Level 1 handling qualities, the value of  $y_1$  at  $T_1$  sec should not be less than 30%

(Figure 2.15). According to the standard, “to avoid *oversensitivity* the parameter response  $y_1\%$  at time  $T_1$  should not exceed some percentage of the peak value, and prior to the end of the control input, the response parameter should not exceed the peak value by more than  $y_2\%$ ” (Figure 2.15).

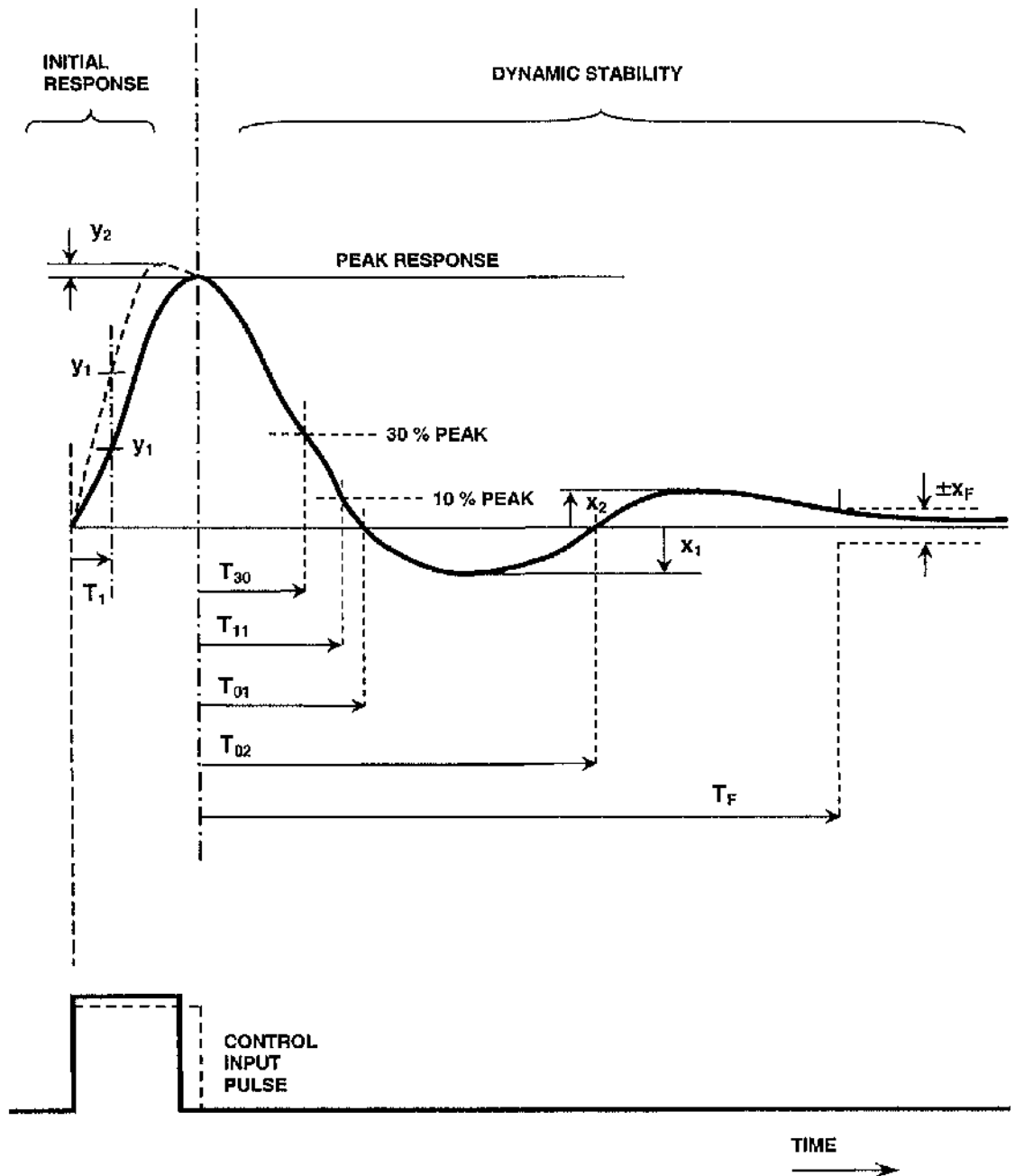


**Figure 2.15** Transient response characteristics, adapted from DEF STAN 00-970 Rotorcraft (1984)

The short term dynamic stability metrics and criteria are presented in Appendix 1, Section A1.2. DEF STAN 00-970 Rotorcraft defines levels of handling qualities for the pitch and roll axes in terms of short period initial response and dynamic stability criteria (Appendix 1, Sections A1.2.2 and A1.2.3, Tables A1.1 and A1.2). As can be noted, the pitch and roll short term criteria are similar except for the peak response.

To sum up the discussion of DEF STAN 00-970 Rotorcraft standard, it should be noted that the concept of short period pitch and roll stability criteria, which is based on time domain requirements of initial response and dynamic stability, can be applied to light gyroplanes with appropriate values of initial response and dynamic stability metrics for the transient response.

### 2.5.7 MIL-HDBK-1797

US military standard MIL-STD-1797(USAF) (1987), and its superseding, MIL-STD-1797A (1990), were the next generation of flying qualities specifications for piloted aircraft. Later, in December 1997 the MIL-STD-1797A was cancelled, and replaced by a new document, MIL-HDBK-1797 (1997), which has a handbook format and must be used only as guidance in a process of aircraft design. As stated in the MIL-HDBK-1797, this document is no longer to be cited as a requirement. The document also contains latest results on handling qualities research, providing the information to the reader in the form of background, discussion and suggestion. The sections of the standard where the longitudinal dynamic requirements and bandwidth/time delay criteria are discussed, are pertinent to this dissertation.

The short period dynamic requirements in MIL-HDBK-1797 are based on the concept of Control Anticipation Parameter (CAP), which was originally proposed by Bihrlé (1966, cited MIL-HDBK-1797, 1997, p.188). CAP is defined as a ratio of initial pitching acceleration to steady state normal acceleration, and can be expressed analytically in the following form

$$CAP = \frac{\ddot{\theta}(0)}{n_z(\infty)}, \quad (2.5)$$

where  $\ddot{\theta}(0)$  is the initial pitch acceleration, and  $n_z(\infty)$  is the steady state normal acceleration.

Obviously, the initial pitch acceleration depends on the damping and natural frequency of the short period mode, while steady state acceleration is a function of acceleration sensitivity, which was discussed in detail in Section 2.5.3. An expression for CAP can be derived from the second order differential equations describing short period mode of classical aeroplanes, see for example Cook (1997, p.224). Thus, CAP can be expressed as:

$$CAP = \frac{\omega_{sp}^2}{n_\alpha} \quad (2.6)$$

It should be emphasised that, as was mentioned in Section 2.5.3, the level boundaries in the MIL-F-8785C short period frequency and acceleration sensitivity criteria chart (Figure 2.10) are represented by the constant numbers of CAP in logarithmic scale.

As an example, Figure 2.16 shows the short period dynamic requirements for Category B Flight Phases, adapted from MIL-HDBK-1797. It can be seen, that these requirements combine the MIL-F-8785C requirements for both the short period frequency and acceleration sensitivity, and damping ratio. Therefore, as was discussed in Section 2.5.3, assuming that the short period dynamics of light gyroplanes can be described by second order transfer functions, it can be supposed that the CAP/damping ratio criterion is suitable for light gyroplanes.

The MIL-HDBK-1797 specification also suggests that the bandwidth of the open-loop pitch attitude response to pilot control force for Category C Flight Phases shall be within the bounds shown on Figure 2.17. There are no requirements for Category B Flight Phases; therefore, the criterion depicted in Figure 2.17 will be taken into consideration in this dissertation. The bandwidth and time delay parameters of this criterion are defined in the same way as in the ADS-33E-PRF design standard.

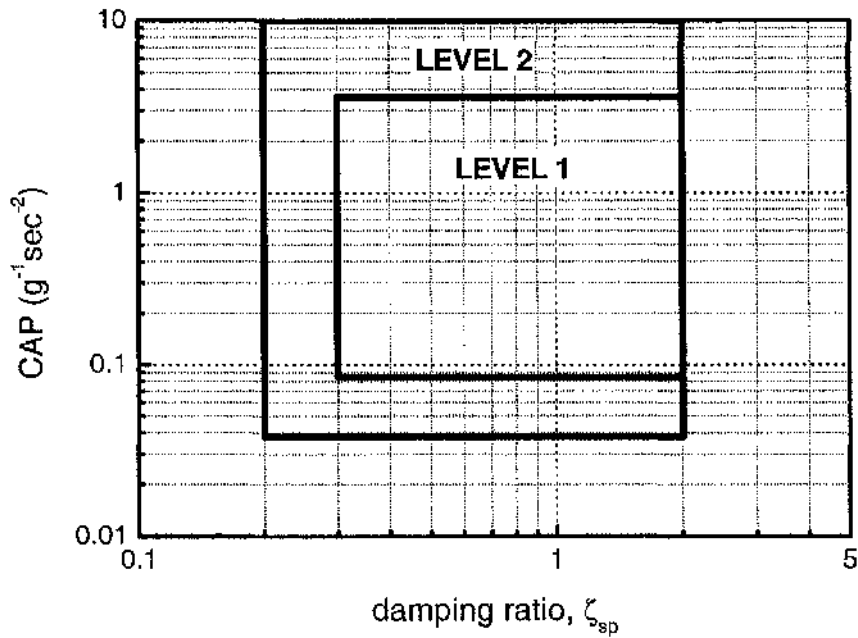


**Figure 2.16** Short period dynamic requirements for Category B Flight Phases, adapted from MIL-HDBK-1797 (1997)

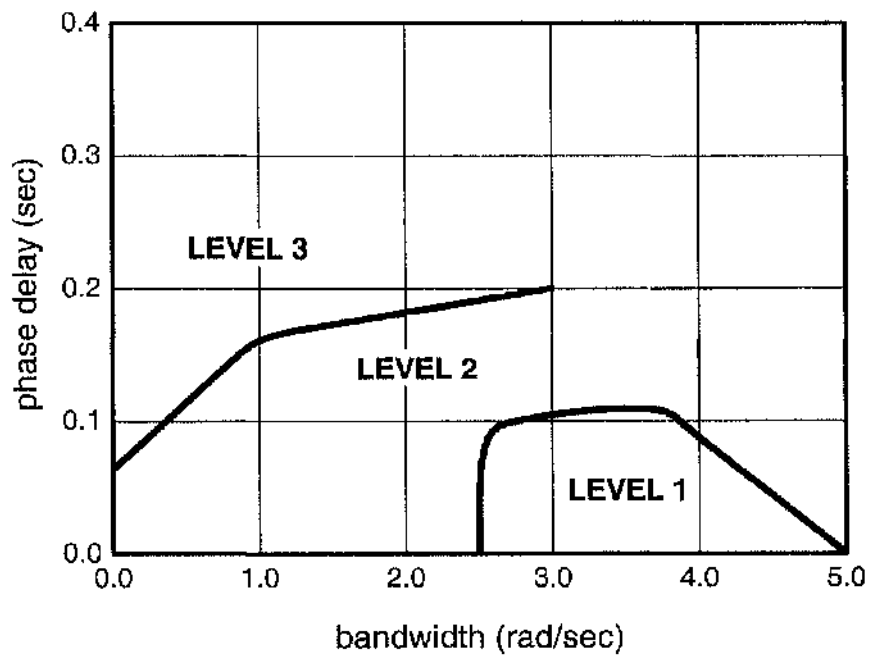


**Figure 2.17** Bandwidth requirements for Category C Flight Phases, adapted from MIL-HDBK-1797 (1997)

## 2.6 Chapter Summary

The chapter has provided general information about handling qualities and workload, and then has concentrated on the review and discussion of existing civil and military airworthiness and design standards, which can be used as a basis for developing handling qualities requirements for light gyroplanes. The longitudinal and lateral-directional handling qualities requirements from fourteen existing airworthiness and design standards, including BCAR Section T, have been thoroughly reviewed and analysed. The main conclusion that can be drawn from this review is that all the concepts for designing handling qualities requirements and criteria for aeroplanes, rotorcraft and V/STOL aircraft discussed in this chapter are suitable for light gyroplanes with some degree of certainty. Relying on limited flight test data and simulation results, it was assumed that gyroplane flight dynamics can be described in a similar manner to that of classical aeroplanes. For example, assuming that the short period dynamics of light gyroplanes can be described by second order transfer functions, it can be supposed that the concept of the MIL-F-8785C (1980) short period frequency and acceleration sensitivity criteria are suitable for light gyroplanes.

Nevertheless, extensive wind tunnel experiments, flight tests and simulation are essential for understanding the dynamic performance of light gyroplanes and form a database of objective and subjective assessments of handling qualities with the aim of developing new requirements and criteria in the future. The next consistent step towards developing gyroplane handling qualities requirements is to apply selected existing requirements and criteria to the available flight test data of the G-UNIV test gyroplane with the aim of assessing handling qualities levels and making further suggestions about the suitability of these requirements and criteria for a light gyroplane. Chapter 3 will provide results and detailed discussion of this process.

## ***Chapter 3***

# **Objective Assessment of Gyroplane Handling Qualities**

### **3.1 Introduction**

This chapter provides results of the objective assessment of the G-UNIV research gyroplane handling qualities against criteria reviewed in the previous chapter. The assessment is based on the flight test data for longitudinal and lateral-directional stick-fixed oscillations and frequency sweeps collected from the first flight trials of the G-UNIV research gyroplane during the period between autumn 2000 and winter 2001 (*Spathopoulos, 2001; Houston and Thomson, 2004*). As was noted in Chapter 2, only short period and Dutch roll characteristics of the G-UNIV test gyroplane are considered in this chapter.

### **3.2 Longitudinal Handling Qualities**

The short period mode of the G-UNIV gyroplane was tested using longitudinal control pulses to induce pitch oscillations. There were a number of pulse trials during the flight tests, but most of them did not satisfy the pulse criteria, where the pilot had to introduce a pulse signal and then return the stick to the trim position and keep it trimmed for a few seconds. It is very difficult to produce perfect pulses in such a small aircraft, because it is very sensitive to weather conditions. Furthermore, the G-UNIV test gyroplane does not have adjustable trim available during the flight; one can adjust the control stick only

on the ground. Finally, after careful inspection, only the two best pulse trials were selected for consideration.

At this point, it should be noted that for longitudinal stick position, the positive direction is defined aft, where full aft position represents 100% of stick travel (Figure 3.1). For lateral stick, the positive direction is set towards right position, where full right denotes 100% of stick travel. For directional control position, the positive direction is defined as right pedal forward, full right pedal represents 100% of pedals travel. Thus, Figure 3.2 shows an indicative example of the pitch rate response to longitudinal impulse disturbance input initiated from steady level flight at 40 mph. Even from this example, it can be noticed that the pulse is not perfect, because the pilot could not manage to maintain constant trim position of the stick after introducing the pulse signal.

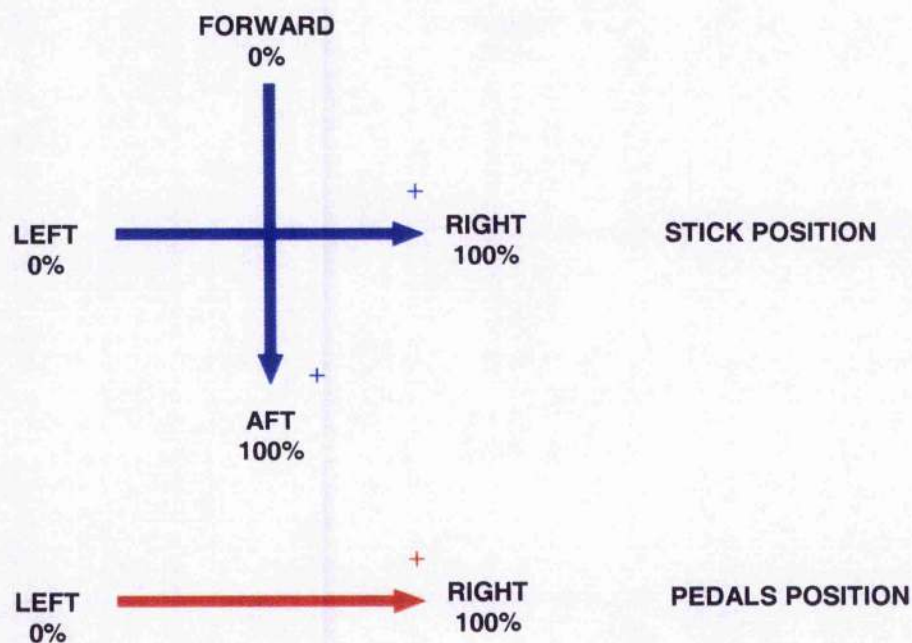


**Figure 3.1** Definition of control stick and pedals positions and directions

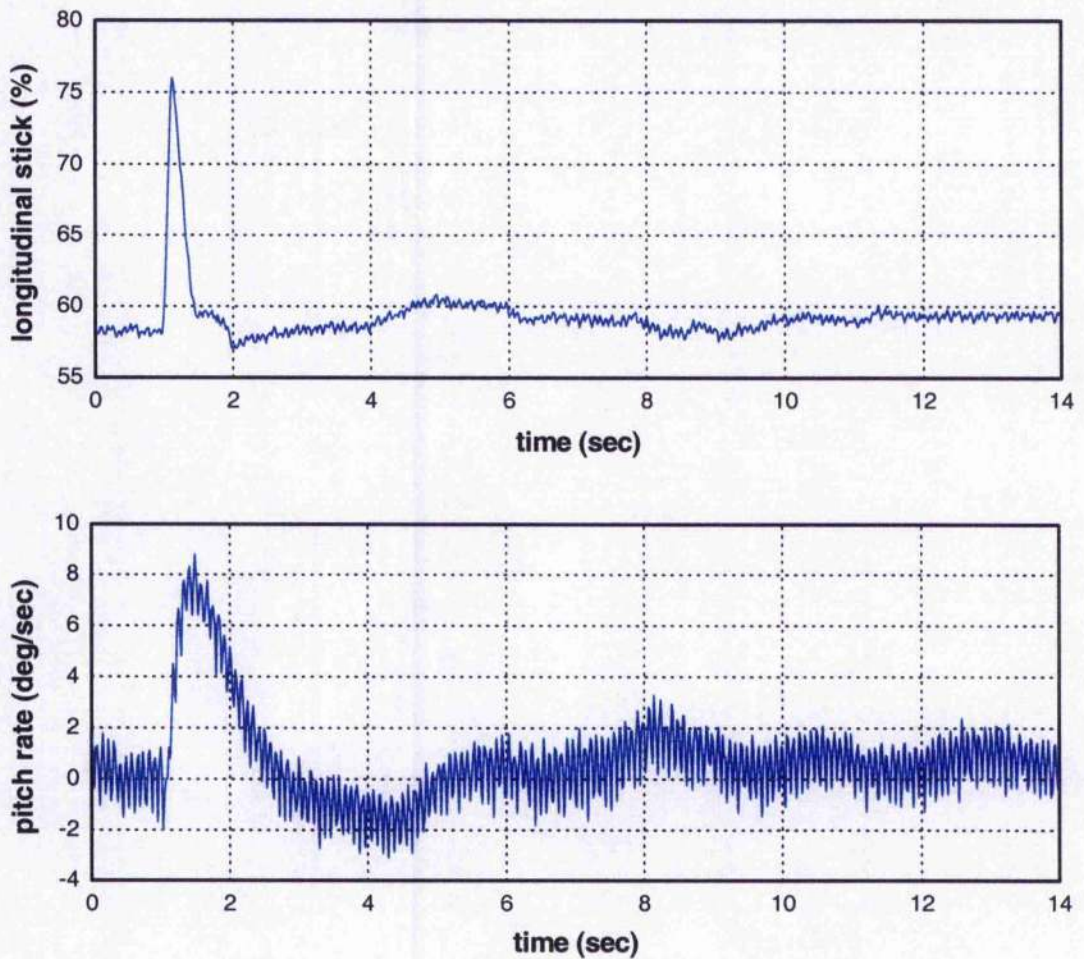


**Figure 3.2** Pitch rate response of the G-UNIV gyroplane to a pulse input

The short period response characteristics, obtained directly from the test data for two pulse trials, are presented in Table 3.1. It should be stated that the pitch rate data were used to obtain these dynamic response metrics. It is clear, that the values of the G-UNIV gyroplane's short period damping are low, and most likely will not meet requirements for satisfactory, or Level 1, handling qualities of most of the criteria reviewed in the previous chapter. The low short period damping can also be identified from Figure 3.3, where the short period mode of the G-UNIV gyroplane is depicted in the s-plane in comparison with the VPM M16 gyroplane (Houston, 2005), a Piper Cherokee aeroplane (Thomson, 2005), and a Puma helicopter (Padfield, 1996). In the Puma example, only the forward speed region, representing the short period mode, should be considered in the comparison. In spite of the fact that only limited number of examples of different

types of aircraft are depicted in Figure 3.3, the comparison allows us to make important inferences concerning the G-UNIV gyroplane stability characteristics, and thus handling qualities. It is obvious that the G-UNIV gyroplane's short period damping ratio is the lowest. Based on the results of the VPM M16 gyroplane for 30 mph and 70 mph, it can be predicted that the damping ratios of the G-UNIV gyroplane at higher speeds will most likely be even lower. Interestingly, the damping ratios of the VPM M16 gyroplane are in general similar to those of the Puma and Piper Cherokee. In addition, it can be seen from the s-plane that the undamped natural frequency of the G-UNIV research gyroplane is lower than that of other types of aircraft.

**Table 3.1** Characteristics of the short period response of the G-UNIV gyroplane

Trial No.	$\zeta_{sp}$	$\tau_{sp}$ (sec)	$\omega_{sp}$ (rad/sec)	$-\zeta_{sp}\omega_{sp}$ (rad/sec)
1	0.256	5.98	1.087	-0.278
2	0.275	6.37	1.026	-0.282

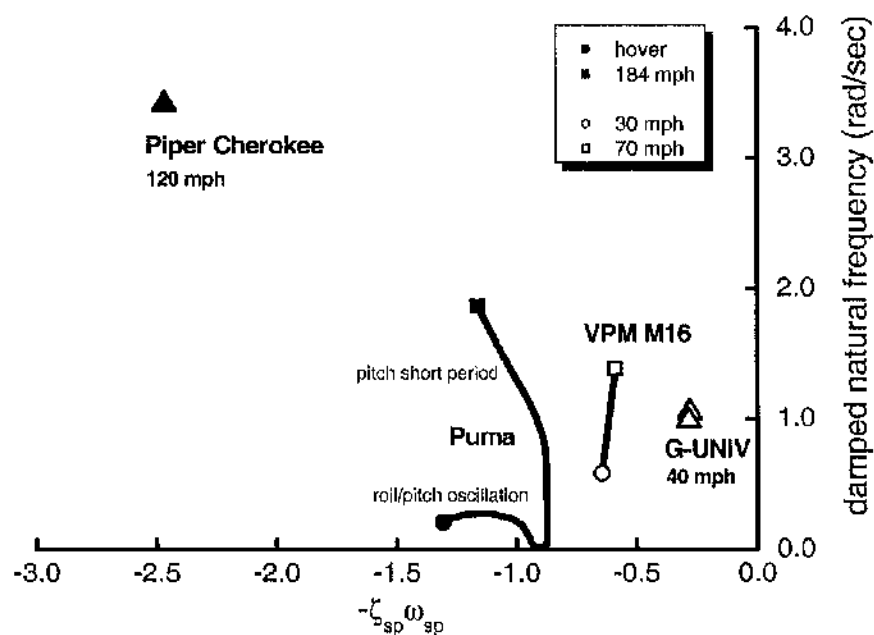


**Figure 3.3** Short period mode of the G-UNIV gyroplane in the s-plane in comparison with the VPM M16 gyroplane, a Piper Cherokee aeroplane and a Puma helicopter

The short period thumb print criterion, proposed by O'Hara (1967), predicts the unacceptable level of handling qualities for the research gyroplane (Figure 3.4). The G-UNIV results fall close to the region, characterised by O'Hara (1967) as "slow initially, then oscillatory; tendency to over-control". However, as was noted in Chapter 2, it should be borne in mind that the thumb print criterion is not universal; it was designed to assess handling qualities of classical aeroplanes, and therefore cannot be applied to all types of aircraft. Nevertheless, the concept of this criterion is fully suitable for light gyroplanes; only boundaries for handling qualities levels must be redesigned based on a database of pilot's subjective ratings of gyroplane performance.

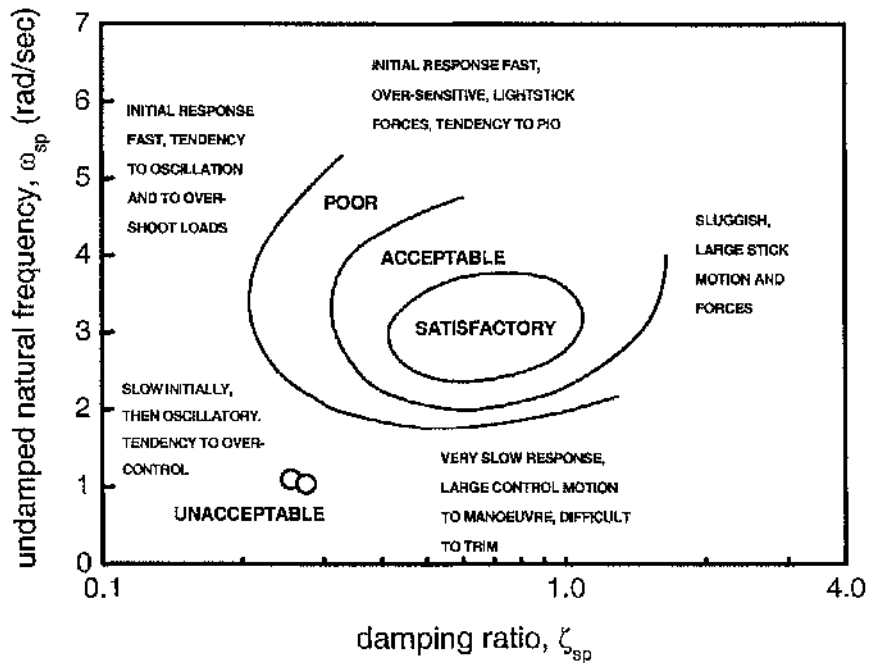


**Figure 3.4** Short period frequency and damping ratio of the G-UNIV gyroplane against requirements of the longitudinal short period thumb print criterion (O'Hara, 1967)

Next, all the longitudinal short period criteria, which were found suitable for a light gyroplane in Chapter 2, will be applied to the flight test data of the G-UNIV gyroplane in the following sections.

### 3.2.1 BCAR Section T

According to Subparagraph T 181 of BCAR Section T, "*Any short-period oscillations occurring under any permissible flight condition must be heavily damped with the primary controls fixed or free.*" The average damping ratio of the G-UNIV gyroplane is approximately 0.27 (Table 3.1), which definitely cannot be characterised as a high damping ratio. Therefore, most probably the G-UNIV research gyroplane does not satisfy the BCAR Section T requirements for short period oscillations. Nevertheless, it is not clear from the above requirements how to quantify the term "heavily damped". Houston and Thomson (2001, p.74), in discussing this issue, came to the conclusion that the Dynamic Stability subparagraph of BCAR Section T should "be amended to state that short period oscillations be "damped" and not "heavily damped", unless "heavily" can be further quantified". In addition, as was recommended in Chapter 2, the limits of damping ratio for short period, and also for phugoid and lateral-directional requirements should be specified in a manner used, for example, in MIL-F-8785C (1980) specification or DEF STAN 00-970 (2003) standard.

Since the average period of short period oscillations is equal to approximately 6.2 sec (Table 3.1), the G-UNIV gyroplane should be assessed under the following case of the Acceptable Means of Compliance requirements for longitudinal, lateral or directional oscillations: "*Any oscillation having a period between 5 and 10 seconds should damp to one half amplitude in not more than two cycles. There should be no tendency for undamped small amplitude oscillations to persist.*" It is obvious from Figure 3.2 that the G-UNIV gyroplane satisfies these requirements.

However, it should be emphasised that unusual phenomena have been encountered following longitudinal doublet inputs (Spathopoulos, 2001). In almost all doublet trials, gyroplane oscillations are badly damped, and in a few trials they are even divergent. The period of these oscillations was between 9 and 10 seconds, while the short period oscillations initiated by pulse inputs had an average period of oscillations of approximately 6 seconds, or 3 to 4 seconds less than these ones. Therefore, it can be hypothesised that these oscillations represent another oscillatory mode unique to light

gyroplanes, or at least unique to the G-UNIV test gyroplane. At this stage of research, it is very difficult to prove or argue against this hypothesis. More flight test data are needed for thorough investigation of these phenomena. As BCAR Section T requires impulse disturbance to assess short period dynamics (details are provided in Chapter 2, Section 2.3), these oscillations were not used in the assessment process.

### 3.2.2 MIL-F-8785C and DEF STAN 00-970

The frequency and acceleration sensitivity criteria from MIL-F-8785C (1980) specification and DEF STAN 00-970 (2003) standard were applied to the short period dynamic characteristics of the G-UNIV gyroplane (Table 3.2). Figure 3.5 shows results for this assessment. It can be seen that the G-UNIV research gyroplane attained Level 1 of handling qualities for Category B Flight Phases.

**Table 3.2** The undamped natural frequency and acceleration sensitivity of the short period oscillation of the G-UNIV gyroplane

Trial No.	$\omega_{sp}$ (rad/sec)	$n/\alpha$ (g/rad)
1	1.087	2.126
2	1.026	2.696

The equivalent short period damping ratio according to MIL-F-8785C specification should be within the limits of Table 2.2 presented in Chapter 2. Table 3.3 shows results of handling qualities Levels assessment. Both the MIL-F-8785C and DEF STAN 00-970 short period damping criteria predict Level 2 of handling qualities for Category B Flight Phases.

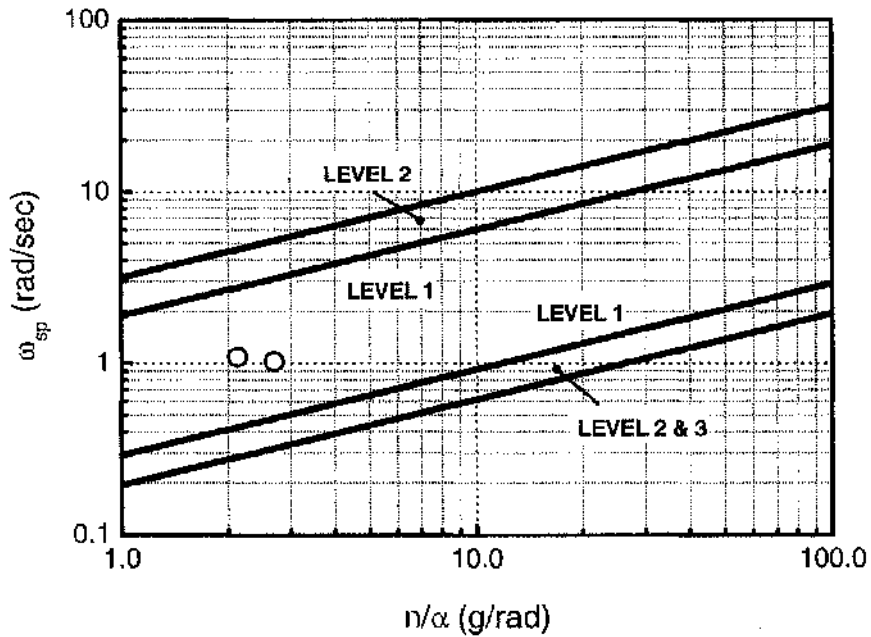


**Figure 3.5** Short period frequency and acceleration sensitivity of the G-UNIV gyroplane against MIL-F-8785C (1980) requirements for Category B Flight Phases

**Table 3.3** Assessment of the short period damping ratio of the G-UNIV gyroplane

Trial No.	$\zeta_{sp}$	Level Category B Flight Phases
1	0.256	2
2	0.275	2

Thus, summarising the results of the assessment, one can conclude that the frequency and acceleration sensitivity criteria predict Level 1 handling qualities for the G-UNIV research gyroplane, while short period damping meets only Level 2 of the handling qualities requirements. This proves the assumption that the gyroplane's short period damping is not high enough for Level 1 handling qualities. Nevertheless, the results of

the gyroplane handling qualities assessment indicate that these criteria are quite suitable to a light gyroplane, and probably minor changes will be required to transform them into proper light gyroplane criteria.

### 3.2.3 MIL-F-83300 and AGARD-R-577-70

Short period frequency-damping criteria from the MIL-F-83300 (1970) specification predict Level 2 handling qualities for the G-UNIV test gyroplane (Figure 3.6). It should be noted that points are very close to the boundary of Level 2. Obviously, these criteria do not predict Level 1 handling qualities because of the low values of damping ratio. For example, if the damping ratios were greater then the points in the chart would move into the Level 1 region.

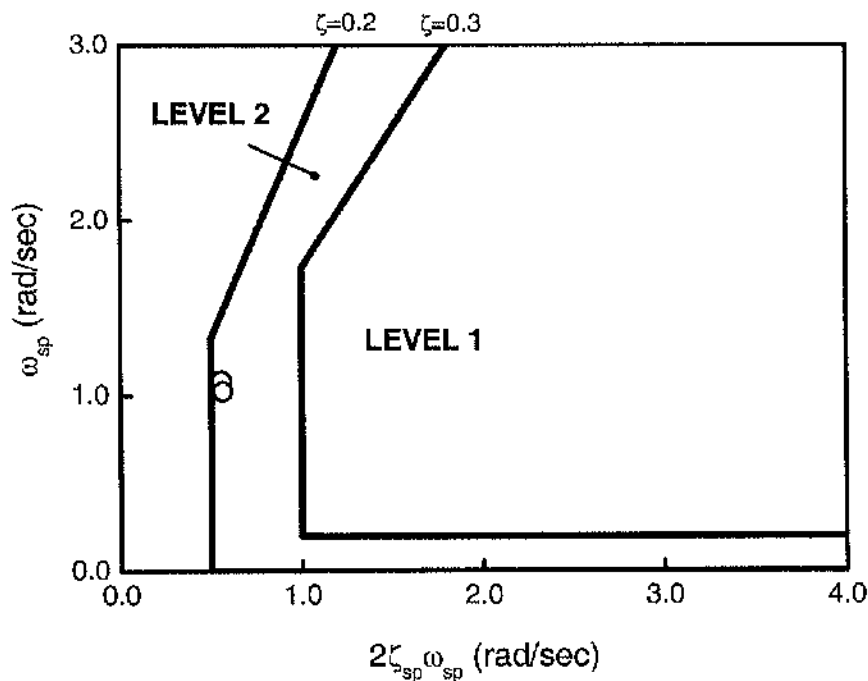


**Figure 3.6** The G-UNIV data points against MIL-F-83300 (1970) short-term longitudinal response requirements

The V/STOL requirements of AGARD Report 577 (AGARD-R-577-70, 1970) attain Satisfactory level of handling qualities for the G-UNIV gyroplane (Figure 3.7). The Satisfactory level defined by AGARD-R-577-70 can be compared to the Level 1 handling qualities of other specifications. In addition, the specification limits short period damping ratio, it should be at least 0.3. Since the average damping ratio of the G-UNIV research gyroplane short period oscillation is approximately 0.27 (Table 3.1), the AGARD-R-577-70 requirement for short period damping is not satisfied.

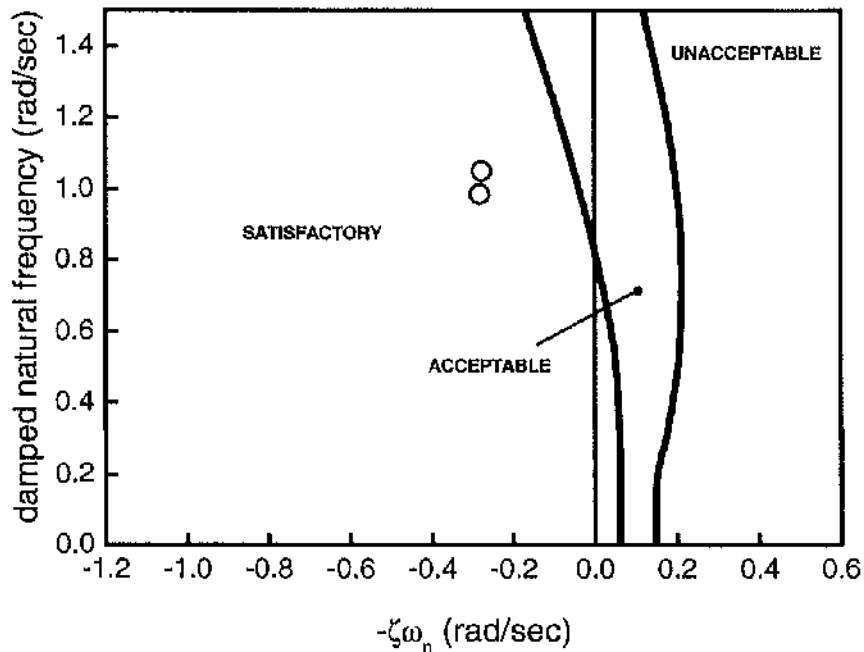


**Figure 3.7** The G-UNIV data points against AGARD-R-577-70 (1970) longitudinal dynamic stability criteria

### 3.2.4 DEF STAN 00-970 Rotorcraft

The pitch rate response of the G-UNIV gyroplane depicted in Figure 3.2 can be considered, according to DEF STAN 00-970 Rotorcraft (1984), as Aggressive manoeuvre. Therefore, the short period response characteristics were assessed against dynamic stability criteria for Aggressive Manoeuvres, as shown in Table 3.4. It can be seen that these criteria predict mostly Level 1 handling qualities for the G-UNIV test

gyroplane. Only peak response parameters for both trials, overshoot metric  $x_1$  % for trial 1 and second peak  $x_2$  % for trial 2 are within the limits of Level 2. Some of the parameters were out of the specified range or not available from the flight test data, and therefore were not judged. It is important to note that the standard requires that the input pulse be assumed to consist of a 10% full travel or one inch displacement, whichever is the least. As can be seen from Table 3.4, both trials have satisfied this limit.

**Table 3.4** The G-UNIV metrics against DEF STAN 00-970 Rotorcraft (1984) pitch short term initial response and dynamic stability criteria (Active Flight Phases, Aggressive Manoeuvres)

No of Trial	1		2	
Max Stick (%)	17.78		11.94	
Response Parameter	Pitch Rate		Pitch Rate	
Peak Response (deg/sec)	7.9	Level 2	7.25	Level 2
$T_1$ (sec)	0.5		0.5	
$y_1$ %	98.1	Level 1	86.48	Level 1
$y_2$ %	N/A*	N/A	N/A	N/A
$T_{30}$ (sec)	0.74	Level 1	0.8	Level 1
$T_{11}$ (sec)	1.12	Level 1	1.09	Level 1
$T_{01}$ (sec)	1.27	Level 1	1.26	Level 1
$x_1$ %	19.62	Level 2	32.83	N/A
$T_{02}$ (sec)	3.63	Level 1	5.57	Level 1
$x_2$ %	7.6	Level 1	14.48	Level 2
$T_F$ (sec)	N/A	N/A	N/A	N/A
$x_F$ %	N/A	N/A	N/A	N/A

\* N/A – not available

### 3.2.5 ADS-33E-PRF

As was already noted in Chapter 2, the ADS-33E-PRF (2000) bandwidth and phase delay criteria are of interest to the current research because they define the aircraft short period response to control inputs. To apply these criteria to the G-UNIV test gyroplane, the frequency domain attitude responses to pilot inputs are needed. The most appropriate approach to obtain frequency domain responses is to excite the frequency range of the aircraft response by inducing control input oscillations with various frequencies. A series of frequency sweeps were conducted at airspeeds of 30, 50 and 60 mph during the flight test trials of the research gyroplane in February 2001 (*Houston and Thomson, 2004*). At that time, the frequency-sweep technique was used to solve a gyroplane system identification problem, but later it was found that the test data were perfectly suitable for the handling qualities assessment purposes. The frequency sweeps were initiated by small amplitude longitudinal inputs, which had varying frequency of approximately 0.25 Hz at the beginning and between 2 and 3 Hz at the peak of each trial. The indicative results for the 50 mph pitch rate response to longitudinal sweeps are shown in Figure 3.8. The power spectral density (PSD) plots for this response (longitudinal stick and pitch rate) are depicted in Figure 3.9. PSD can be defined as the normalised energy distribution across the frequency spectrum. It can be seen that the input and output power spectrums show significant energy up to 10 rad/sec.

The pitch bandwidth and phase delay values were obtained from the seven most successful longitudinal frequency sweeps using a technique defined in ADS-33E-PRF (2000) standard and described in detail in Chapter 2, Section 2.4. These parameters were calculated from spectral analysis of the pitch rate response to pilot control inputs. The coherence functions for the frequency range up to 10 rad/sec was very nearly one, showing good enough correlation to use the test data for frequency domain analysis. The required pitch attitude frequency response was determined by integrating the pitch rate results. The bandwidth and phase delay results for different airspeeds are summarised in Table 3.5. It should be noted that only ACAH (Attitude Command/Attitude Hold) response-types approach was used to obtain these frequency domain metrics.

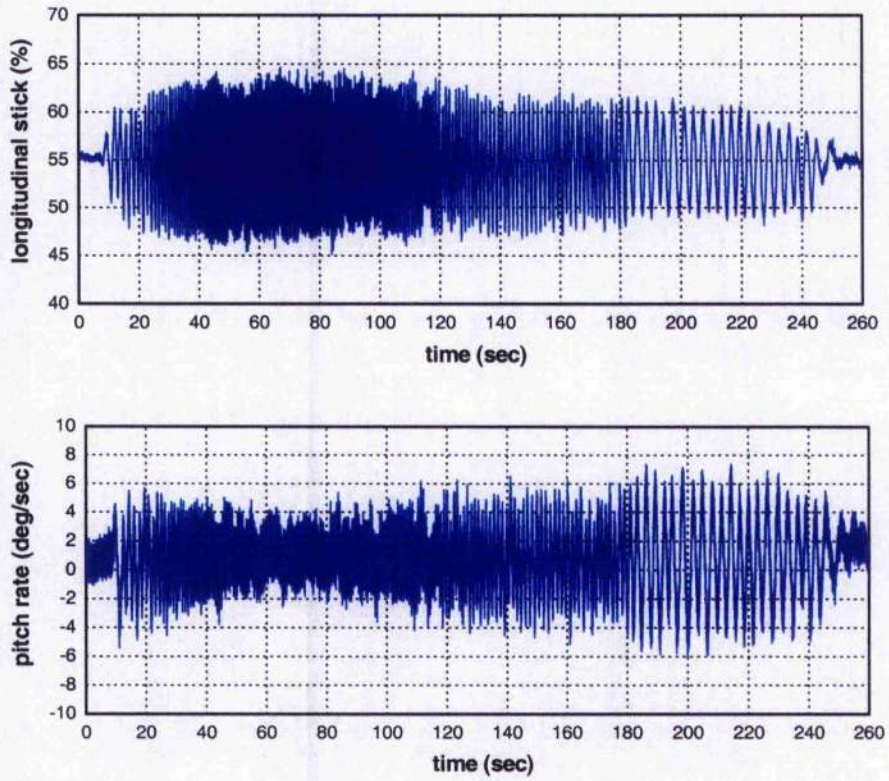


Figure 3.8 Longitudinal frequency sweeps of the G-UNIV gyroplane at 50 mph

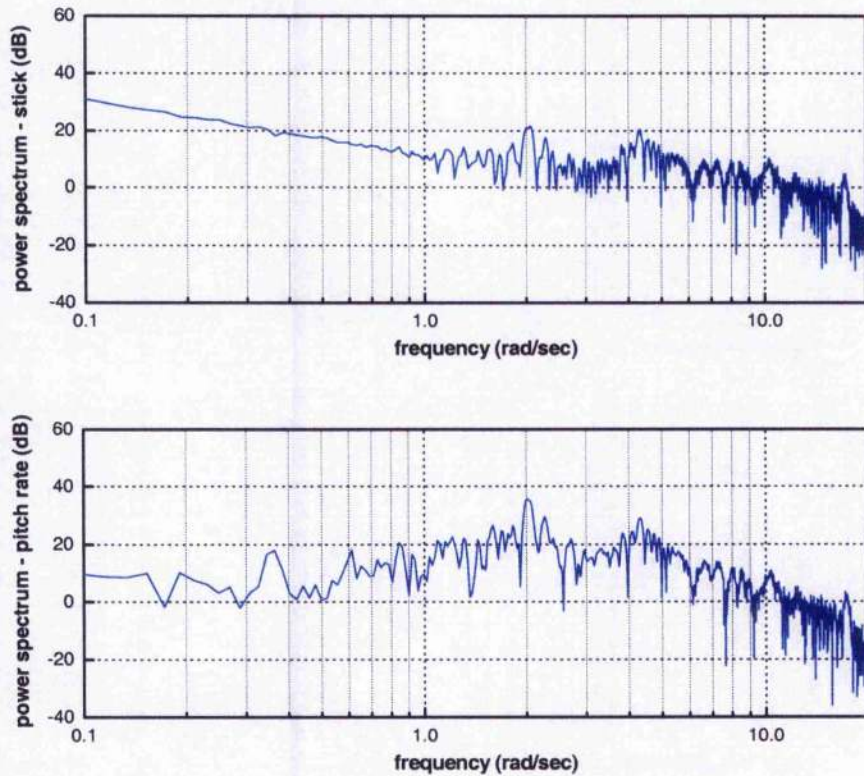


Figure 3.9 Longitudinal sweep power spectrums of the G-UNIV gyroplane

**Table 3.5** Longitudinal frequency sweeps characteristics of the G-UNIV gyroplane

Trial No.	Airspeed (mph)	Neutral stability frequency (rad/sec)	Phase bandwidth (rad/sec)	Phase delay (sec)
1	30	3.9	2.68	0.0494
2	50	5.0	2.25	0.0407
3	50	4.45	2.15	0.0429
4	60	4.3	1.54	0.0489
5	60	4.5	1.6	0.0458

ADS-33E-PRF standard defines bandwidth/phase-delay criteria for two speed ranges: (i) *hover and low speed* (up to 45 knots), and (ii) *forward flight* (greater than 45 knots). Thus, the results for 30 mph (26.07 knots) and 50 mph (43.45 knots) trials should be assessed against *hover and low speed* requirements, and the results for 60 mph (52.14 knots) trials should be estimated against *forward flight* requirements. However, as was noted in Chapter 2, requirements for small-amplitude pitch attitude changes - *hover and low speed* (All Other MTEs, UCE=1, Fully Attended Operations) completely coincide with those for *forward flight* (All Other MTEs, VMC, Fully Attended Operations). As a result, the small-amplitude pitch attitude criteria predict Level 1 handling qualities for the G-UNIV research gyroplane (Figure 3.10). The obtained results show that by increase in the airspeed, the bandwidth parameter is decreasing, indicating that the gyroplane becomes less agile, or less sharp.

Figure 3.11 shows results of the short period pitch oscillation assessment based on the data from Table 3.1. It can be seen that ADS-33E-PRF attains Level 2 handling qualities for the G-UNIV test gyroplane. It is clear that this criterion does not predict Level 1 handling qualities because of the low damping ratios. For instance, if the damping ratios were greater then the points in the chart would fall into the Level 1 region.

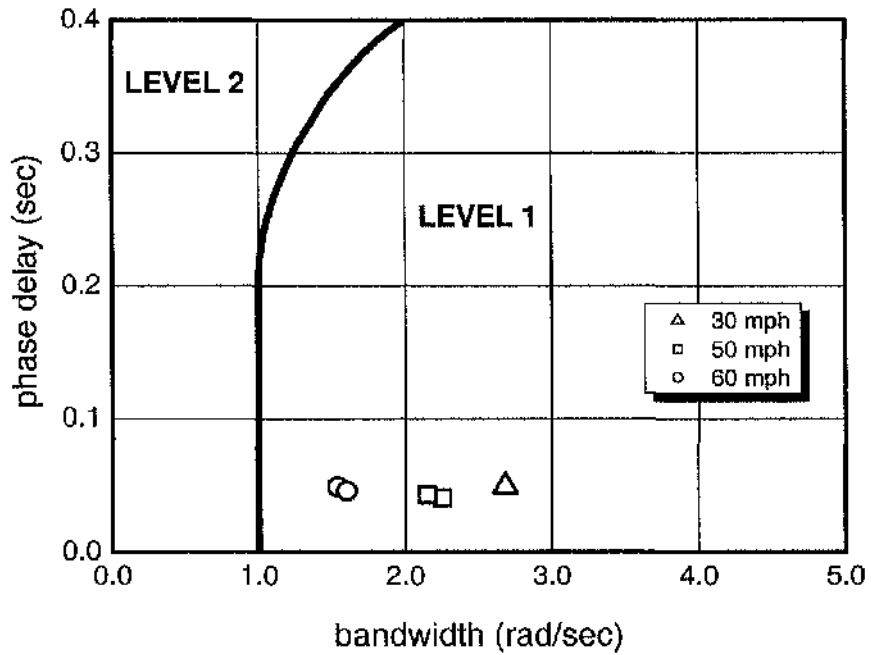


**Figure 3.10** The G-UNIV data points against ADS-33E-PRF (2000) requirements for small-amplitude pitch attitude changes (all other MTEs)

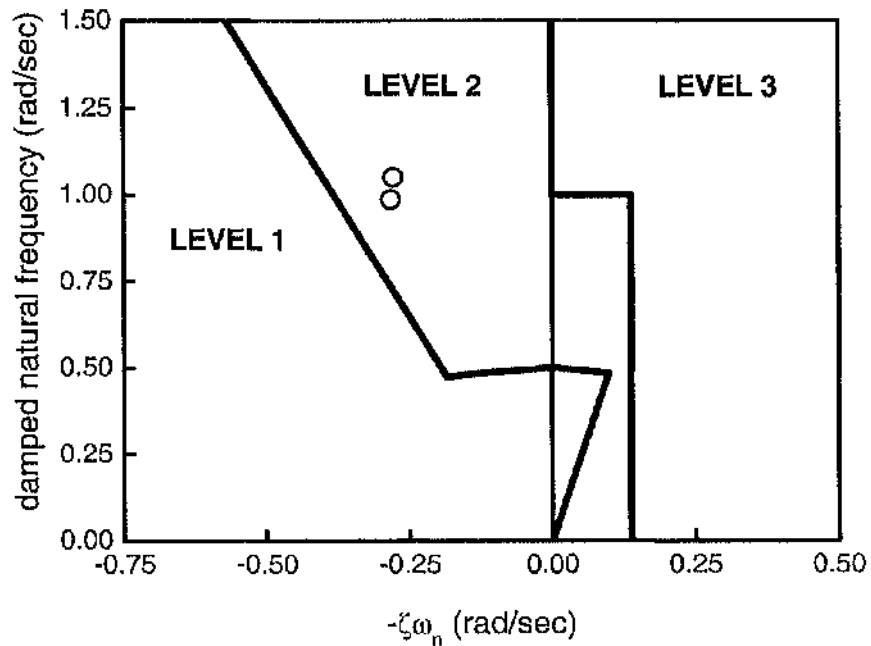


**Figure 3.11** The G-UNIV data points against ADS-33E-PRF (2000) limits on pitch oscillations (hover and low speed)

### 3.2.6 MIL-HDBK-1797

The MIL-HDBK-1797 short period dynamic requirements for Category B Flight Phases predict Level 2 handling qualities for the G-UNIV gyroplane (Table 3.6, Figure 3.12). It should be emphasised that the G-UNIV values for the CAP parameter lie in the middle line of Level 1 region of these criteria, thus indicating that Level 2 handling qualities caused only by poor damping characteristics.

**Table 3.6** Characteristics of the short period response of the G-UNIV gyroplane

Trial No.	$\zeta_{sp}$	$\omega_{sp}$ (rad/sec)	$n/\alpha$ (g/rad)	CAP ( $g^{-1}sec^{-2}$ )
1	0.256	1.087	2.126	0.556
2	0.275	1.026	2.696	0.390

MIL-HDBK-1797 specification also suggests using bandwidth and phase delay criteria in a longitudinal channel. It can be seen from Figure 3.13 that the MIL-HDBK-1797 criteria predict Level 1 (1 point, 30 mph) and Level 2 (4 points, 50 and 60 mph) handling qualities for the research gyroplane. A comparison between Levels defined by ADS-33E-PRF and MIL-HDBK-1797 shows that the latter standard is more stringent (Figure 3.13). However, it should be borne in mind that adapted MIL-HDBK-1797 requirements are defined for Category C Flight Phases (MIL-HDBK-1797 does not provide bandwidth/phase delay criteria for Category B Flight Phases).

As can be seen from the results of Table 3.5, the gyroplane phase delay parameter was no more than 0.05 seconds in all trials. It can be explained by the fact that the gyroplane has a simple mechanical control system in contrast to highly-augmented modern rotorcraft, where for example, delay in automatic control system or delay caused by flight control hydraulic actuators influence the phase delay parameter. For most conventional rotorcraft with simple mechanical control systems, this number is no more than 0.05-0.1 seconds (Houston, 2005). Therefore, it can be predicted that the phase delay of light gyroplanes will be no more than 0.1 seconds in all other test conditions. This led to the conclusion that there is no reason to specify this parameter for the light gyroplanes, while bandwidth metrics should be limited.

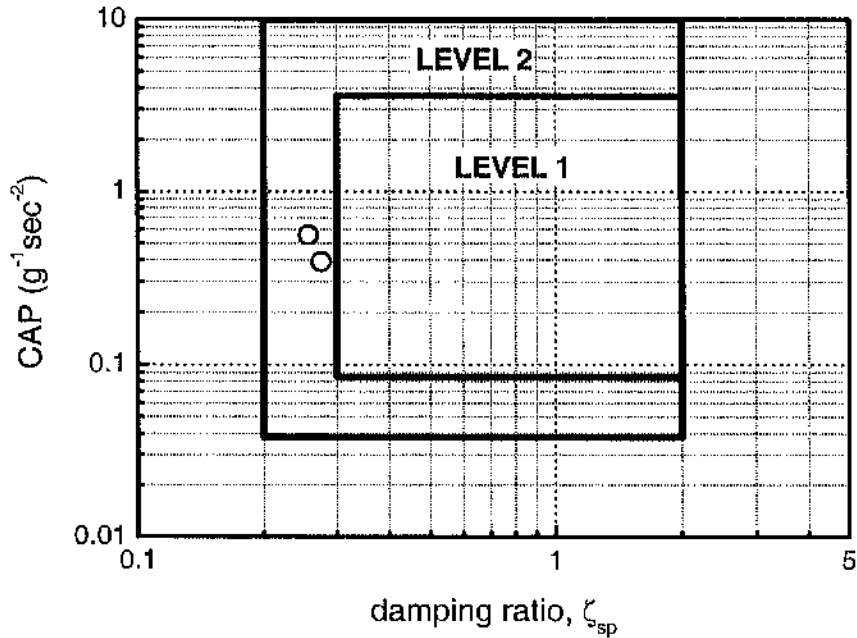


**Figure 3.12** The G-UNIV data points against MIL-HDBK-1797 (1997) short period dynamic requirements for Category B Flight Phases

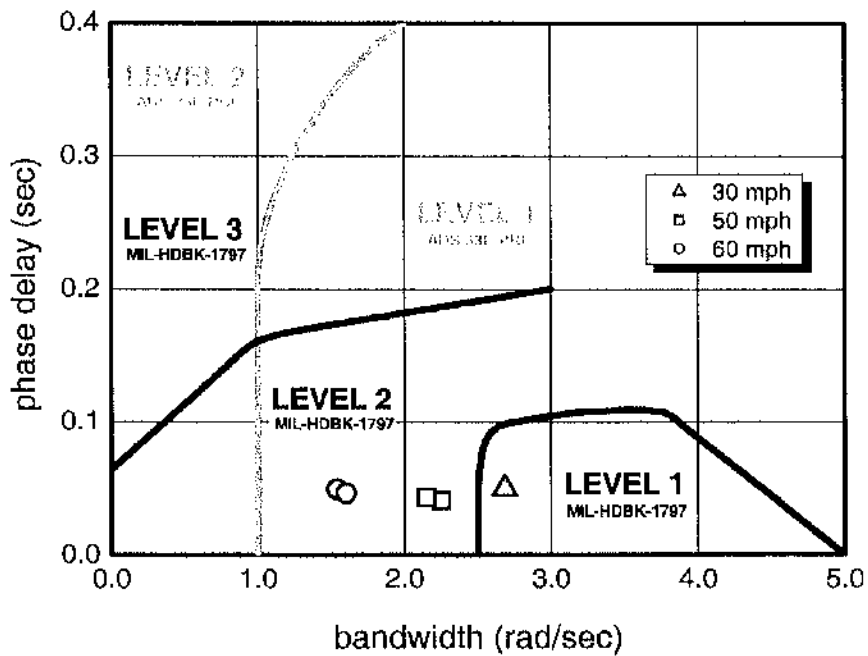


**Figure 3.13** The G-UNIV data points against MIL-HDBK-1797 (1997) and ADS-33E-PRF (2000) bandwidth requirements

### 3.3 Lateral-Directional Handling Qualities

The lateral-directional handling qualities of the G-UNIV test gyroplane were assessed in the same manner as the longitudinal handling qualities; therefore, this section discusses more briefly the techniques of assessment concentrating primarily on the results and discussion. The Dutch roll lateral-directional mode was tested using a yaw doublet (one right and left rudder cycle). Three most successful doublet trials at the airspeed of 40 mph were selected for consideration (Table 3.7). Figure 3.14 shows one of the selected responses of the test gyroplane to a doublet input initiated by the pedals. It should be noted that the pilot must use the rudder in a steady state flight to compensate the engine torque. Therefore, the trim position of the rudder is approximately 17.5 deg. In contrast to the pitch rate response to a pulse input presented in Section 3.2, the data of the response of the test gyroplane to a doublet input are more accurate since the test pilot could maintain the trim position of the rudder after initiating a doublet input.

**Table 3.7** Characteristics of the Dutch roll response of the G-UNIV gyroplane

Trial No.	$\zeta_d$	$\tau_d$ (sec)	$\omega_d$ (rad/sec)	$-\zeta_d\omega_d$ (rad/sec)
1	0.341	8.08	0.827	-0.282
2	0.321	6.82	0.972	-0.312
3	0.272	7.40	0.880	-0.239

Figure 3.15 shows characteristics of the Dutch roll mode of the G-UNIV research gyroplane depicted in the s-plane in comparison with those of a Piper Cherokee aeroplane (Thomson, 2005), Bo 105, Lynx and Puma helicopters (Padfield, 1996). It can be seen that the damping ratios and the undamped natural frequencies of the G-UNIV gyroplane are in general similar to those of the Bo 105, Lynx and Puma helicopters. Whilst the damping ratios of the G-UNIV gyroplane are higher than that of the Piper Cherokee aeroplane, and the undamped natural frequencies are lower, though it should be borne in mind that the Dutch roll mode for the Piper Cherokee is presented for a much higher speed (120 mph). Obviously, the G-UNIV Dutch roll mode in general is very similar to those of the presented helicopters, at least for the low speed region.

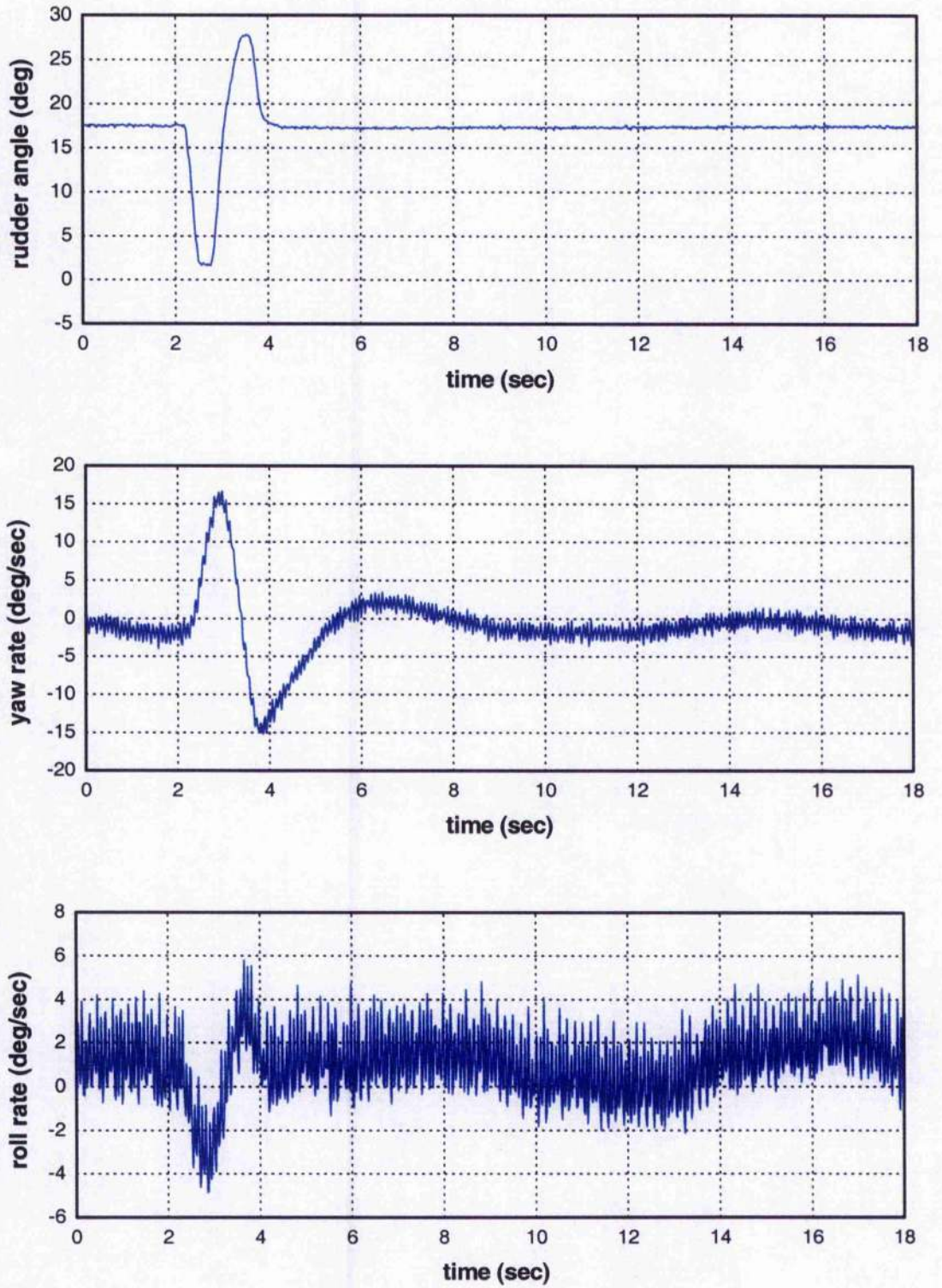
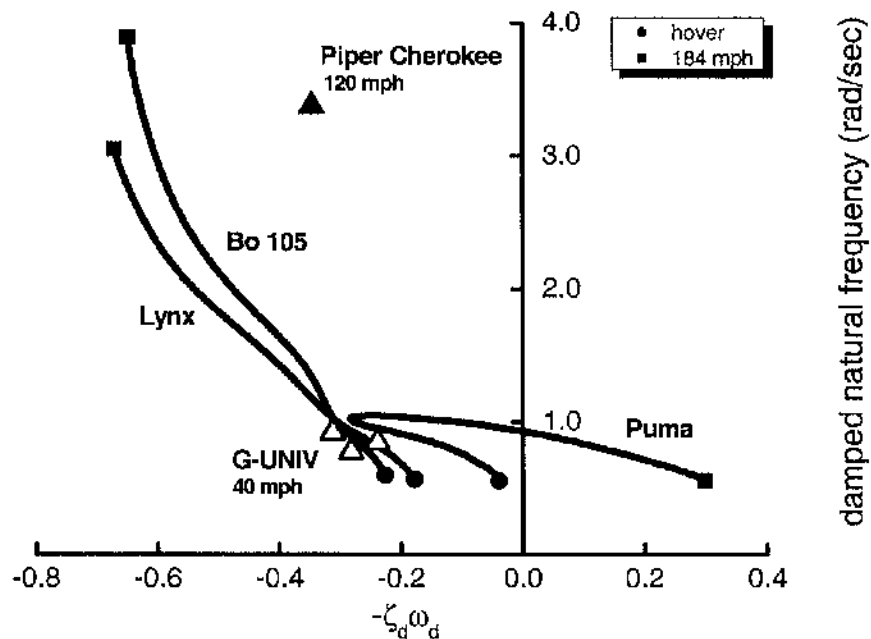


Figure 3.14 Roll and yaw rate response of the G-UNIV gyroplane to a rudder doublet



**Figure 3.15** Dutch roll mode of the G-UNIV gyroplane in the s-plane in comparison with a Piper Cherokee aeroplane and Bo 105, Lynx and Puma helicopters

### 3.3.1 BCAR Section T

As was demonstrated in Chapter 2, Section 2.3, BCAR Section T requires a pulse input to initiate the lateral oscillations. There were a number of lateral pulse trials during the flight tests, the indicative results for the airspeed of 40 mph are depicted in Figure 3.16. It can be seen that the initial pulse is not in good agreement with the BCAR Section T requirements, where it is stated that for those gyroplanes which do not have a variable trim control, after the initiating disturbance “*the control must be returned to the datum position and held fixed in that position*”. In the example presented in Figure 3.16 the test pilot could not hold the lateral stick in a fixed position after initiating the pulse input; the overshoot was about 30% of original pulse input.

Nevertheless, since the average period of Dutch roll oscillations is equal to approximately 7.4 sec (Table 3.7), the G-UNIV gyroplane should be assessed under the following case of the Acceptable Means of Compliance requirements for longitudinal, lateral or directional oscillations: "Any oscillation having a period between 5 and 10 seconds should damp to one half amplitude in not more than two cycles. There should be no tendency for undamped small amplitude oscillations to persist." It is clear from Figure 3.16 that the G-UNIV gyroplane satisfies these requirements.

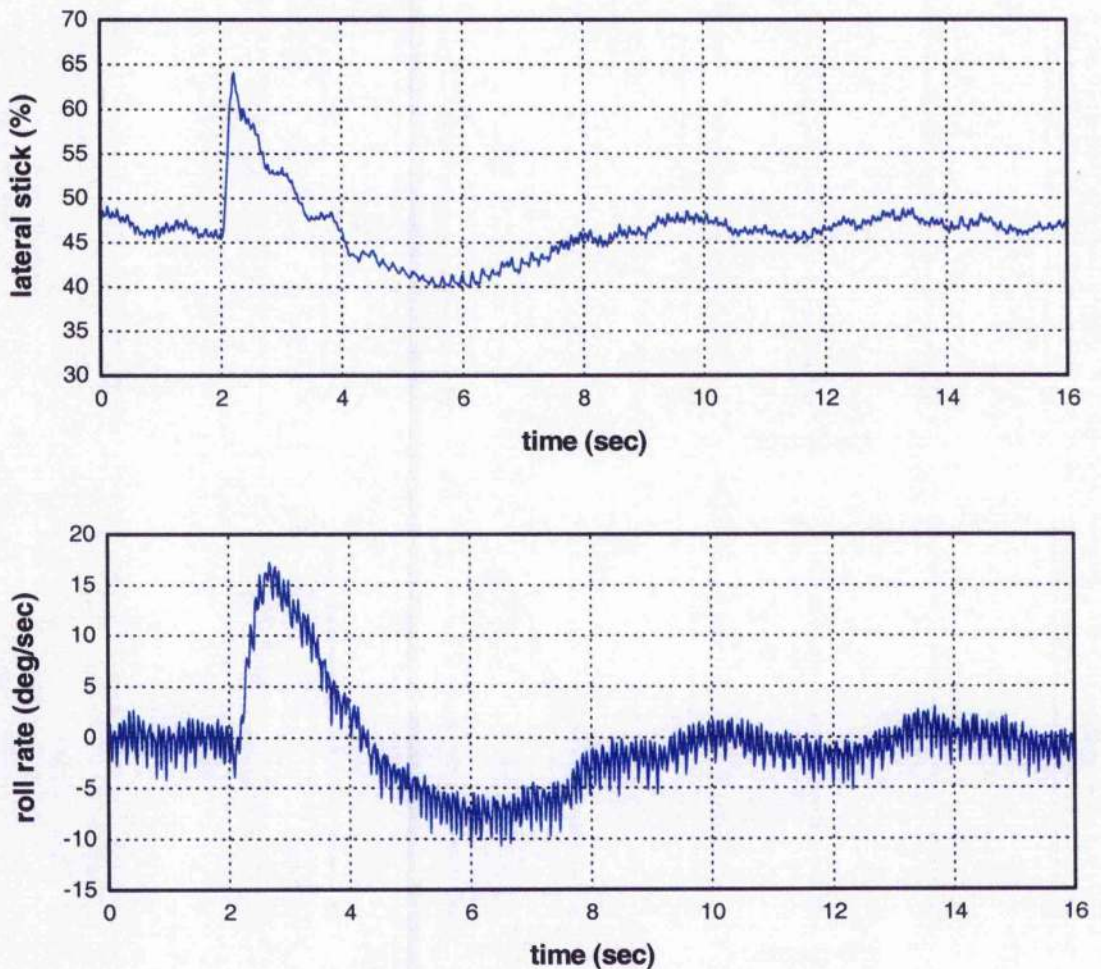


**Figure 3.16** Roll rate response of the G-UNIV gyroplane to a pulse input

### 3.3.2 MIL-F-8785C and DEF STAN 00-970

The frequency and damping ratio of the lateral-directional oscillations (Dutch roll) following a yaw disturbance input should exceed the minimum values of Table 2.3 presented in Chapter 2. Table 3.8 shows results of handling qualities Levels assessment. Both the MIL-F-8785C and DEF STAN 00-970 frequency/damping criteria predict Level 1 of handling qualities for all metrics (Category B Flight Phases).

**Table 3.8** Assessment of the Dutch roll frequency and damping ratio of the G-UNIV gyroplane

Trial No.	$\zeta_d$	$\zeta_d \omega_d$ (rad/sec)	$\omega_d$ (rad/sec)	Levels Category B Flight Phase
1	0.341	0.282	0.827	1/1/1
2	0.321	0.312	0.972	1/1/1
3	0.272	0.239	0.880	1/1/1

### 3.3.3 MIL-F-83300 and AGARD-R-577-70

The G-UNIV test gyroplane achieved Level 1 handling qualities for the lateral-directional oscillatory requirements of MIL-F-83300 (1970) specification (Figure 3.17). In contrast to the short period assessment, the high damping ratios of the Dutch roll were enough to achieve Level 1 handling qualities. The AGARD-R-557-70 (1970) lateral-directional requirements predict a Satisfactory level of handling qualities for the G-UNIV gyroplane (Figure 3.18).

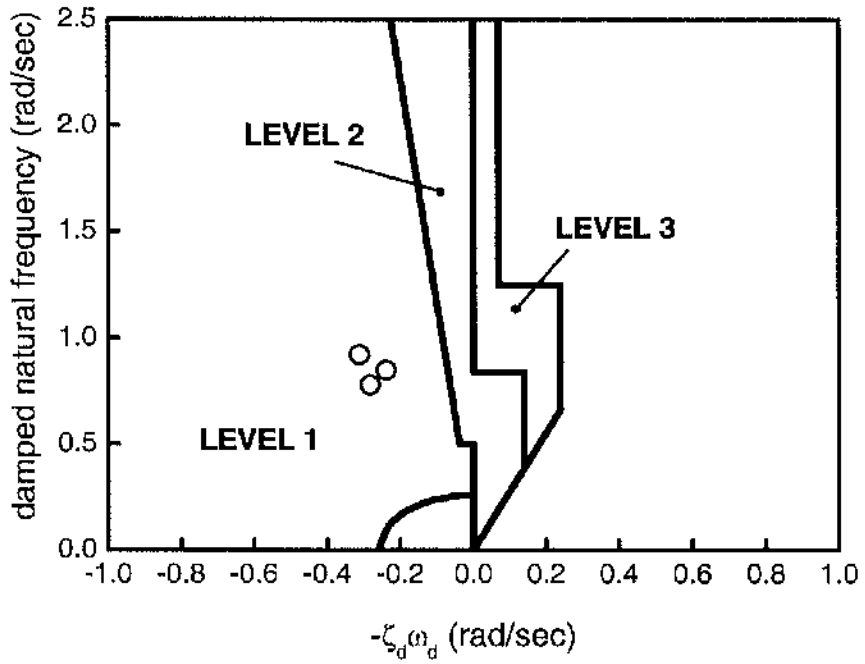


**Figure 3.17** The G-UNIV data points against MIL-F-83300 (1970) lateral-directional oscillatory requirements

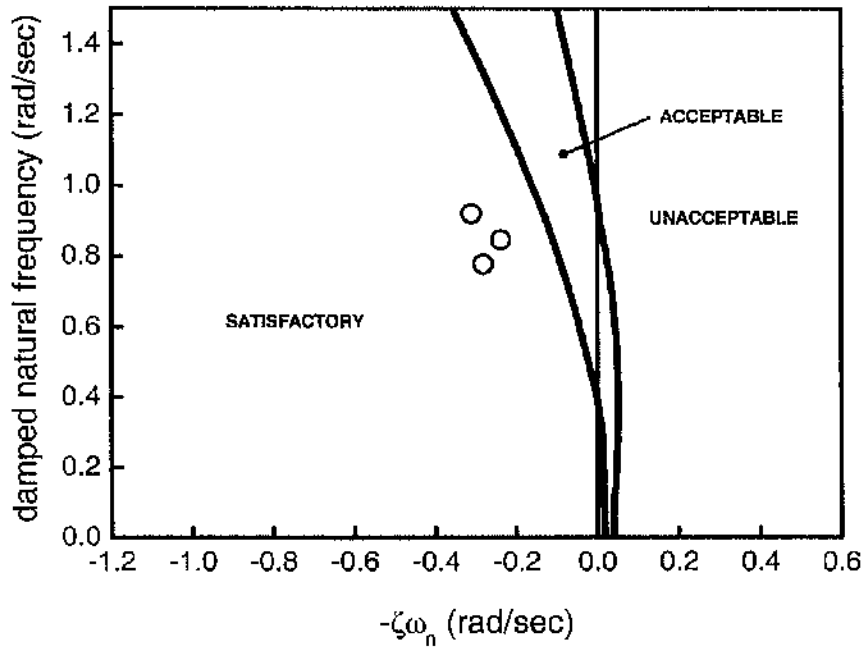


**Figure 3.18** The G-UNIV data points against AGARD-R-577-70 (1970) lateral-directional dynamic stability criteria

### 3.3.4 DEF STAN 00-970 Rotorcraft

The lateral-directional response to a rudder doublet of the G-UNIV gyroplane depicted in Figure 3.14 can be considered as an Aggressive manoeuvre, therefore the Dutch roll response characteristics were assessed against dynamic stability criteria for Aggressive Manoeuvres (Table 3.9). It can be seen that the initial roll response and dynamic stability criteria predict different Levels of handling qualities for the G-UNIV test gyroplane. It is clear that the first trial achieved better results (four metrics satisfied Level 1 requirements) than the second trial (only one parameter satisfied Level 1 requirements, while five metrics fall into limits of Level 3). It should be noted that some of the parameters were out of the specified range or not available from the flight test data, and therefore were not judged. As was mentioned in Section 3.2, DEF STAN 00-970 Rotorcraft standard requires that the input pulse be assumed to consist of a 10% full travel or one inch displacement, whichever is the least. As can be seen from Table 3.9, both trials have satisfied this limit.

**Table 3.9** The G-UNIV metrics against DEF STAN 00-970 Rotorcraft (1984) roll short term initial response and dynamic stability criteria (Active Flight Phases, Aggressive Manoeuvres)

No of Trial	1		2	
Max Stick (%)	18.61		17.78	
Response Parameter	Pitch Rate		Pitch Rate	
Peak Response (deg/sec)	17.02	Level 1	13.2	Level 2
T <sub>1</sub> (sec)	0.5		0.5	
y <sub>1</sub> %	90.1	Level 1	90.91	Level 1
y <sub>2</sub> %	N/A <sup>†</sup>	N/A	N/A	N/A

<sup>†</sup> N/A – not available

**Table 3.9** (cont.) The G-UNIV metrics against DEF STAN 00-970 Rotorcraft (1984) roll short term initial response and dynamic stability criteria (Active Flight Phases, Aggressive Manoeuvres)

No of Trial	1		2	
T <sub>30</sub> (sec)	1.15	Level 3	1.43	Level 3
T <sub>11</sub> (sec)	1.47	Level 2	3.1	Level 3
T <sub>01</sub> (sec)	1.61	Level 1	3.42	Level 3
x <sub>1</sub> %	37.53	Level 3	32.1	Level 3
T <sub>02</sub> (sec)	5.97	Level 1	6.25	Level 1
x <sub>2</sub> %	11.18	Level 2	18.36	Level 3
T <sub>F</sub> (sec)	N/A	N/A	N/A	N/A
x <sub>F</sub> %	N/A	N/A	N/A	N/A

### 3.3.5 ADS-33E-PRF

The roll bandwidth and phase delay metrics were obtained from the five most successful lateral frequency sweeps. The indicative results for the 50 mph pitch rate response to longitudinal sweeps are shown in Figure 3.19 and the pilot lateral stick and roll rate PSD plots are depicted in Figure 3.20. The input and output power spectrums show significant energy up to 10 rad/sec, while it should be noted that in both examples the power drops off distinctly at frequencies higher than 10 rad/sec. The coherence functions for the frequency range up to 10 rad/sec were very nearly one, showing good enough correlation to use the test data for frequency domain analysis. The roll attitude frequency response was determined by integrating the roll rate results. The bandwidth and phase delay results for different airspeeds are presented in Table 3.10. It is important to note that only ACAH (Attitude Command/Attitude Hold) response-types approach was used to obtain these frequency domain parameters.

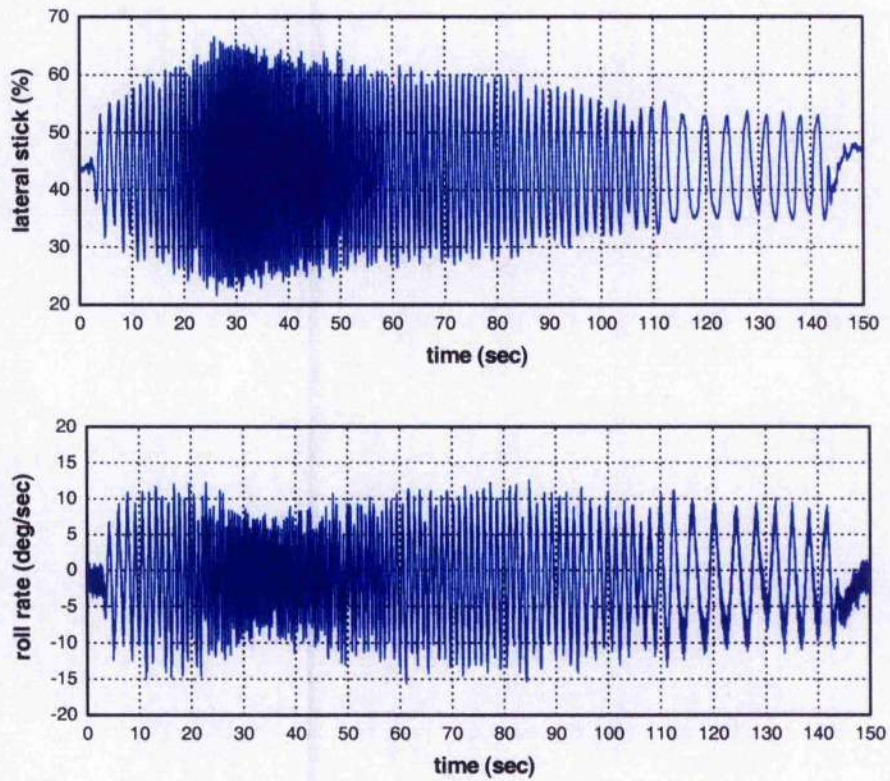


Figure 3.19 Lateral frequency sweeps of the G-UNIV gyroplane at 50 mph

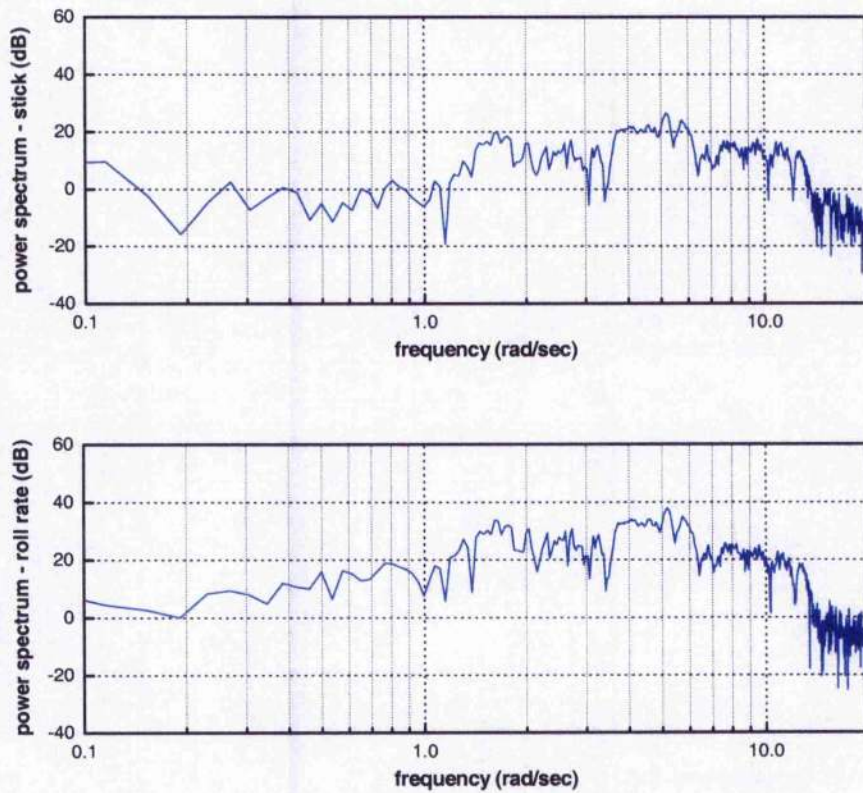


Figure 3.20 Lateral sweep power spectrums of the G-UNIV gyroplane

**Table 3.10** Lateral frequency sweeps characteristics of the G-UNIV gyroplane

Trial No.	Airspeed (mph)	Neutral stability frequency (rad/sec)	Phase bandwidth (rad/sec)	Phase delay (sec)
1	50	5.51	2.21	0.0551
2	50	5.53	2.43	0.0646
3	50	5.56	2.52	0.0672
4	60	5.35	2.35	0.0593
5	60	5.6	2.43	0.0591

As was noted in Chapter 2, the requirements for small-amplitude roll attitude changes - forward flight (All Other MTEs, UCE=1, Fully Attended Operations) fully coincide with those for forward flight (All Other MTEs, VMC, Fully Attended Operations). Thus, the small-amplitude roll attitude criteria predict Level 1 handling qualities for the G-UNIV research gyroplane (Figure 3.21). In contrast to the results for the pitch axis assessments, the results for the roll bandwidth/phase delay criteria do not depend on the airspeed, because points representing the 50 mph and 60 mph trials are very close to each other.

However, Pausder and Blanken (1992a; 1992b) suggested different Level boundaries for the roll axis criteria (Figure 3.22), which do not agree with those of ADS-33E-PRF standard. The suggestion is based on flight test results of DLR's variable-stability Bo 105 Advanced Technology Testing Helicopter System (ATTHes). Four experienced test pilots with different backgrounds conducted a high bandwidth slalom tracking task and assigned Cooper-Harper handling qualities ratings. The Level 1 of the DLR criterion requires not less than 2.5 rad/sec for the bandwidth, and defines the phase delay to be lower than approximately 0.09 sec. Requirements for the Level 2 are: not less than 1.5 rad/sec for the bandwidth, not greater than 0.17 sec for the phase delay. It is clear that both boundaries are more stringent than those of ADS-33E-PRF. Thus, the G-UNIV gyroplane meets only Level 2 handling qualities of the DLR criterion.

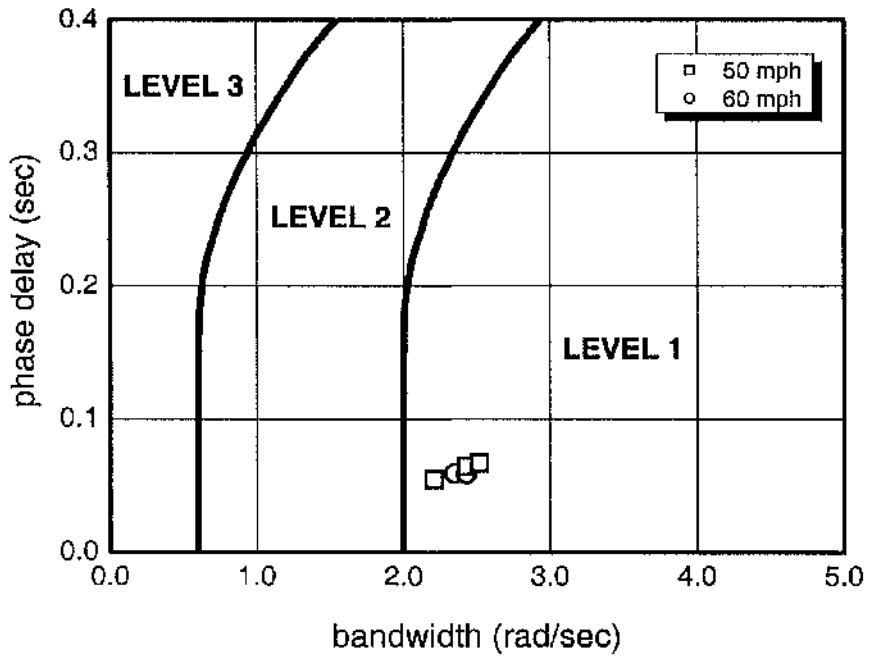


Figure 3.21 The G-UNIV data points against ADS-33E-PRF (2000) requirements for small-amplitude roll attitude changes (all other MTEs)

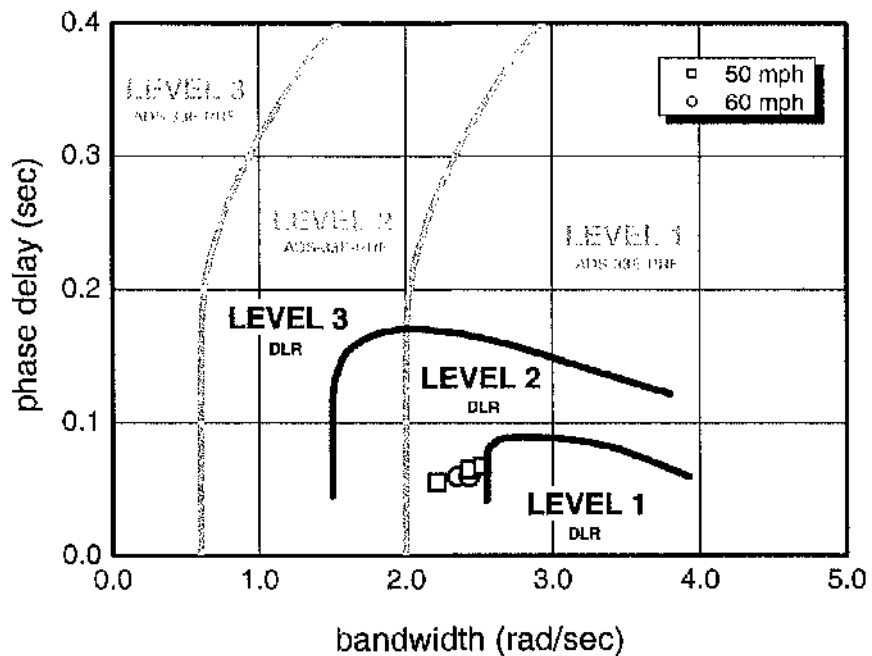


Figure 3.22 The G-UNIV data points against DLR (Pausder and Blanken, 1992) and ADS-33E-PRF (2000) bandwidth requirements

Pausder and Blanken (1992b) also recommended Level boundaries based on simulation results of NASA-Ames Vertical Motion Simulator (VMS) for the same slalom tracking task. Only one test pilot performed simulation trials and a limited number of configurations were tested. In this case, the boundaries were even more demanding for the bandwidth parameter in comparison with those based on flight test results, but still predicted Level 2 for the research gyroplane.

The test pilot, Roger Savage, who performed the gyroplane handling qualities tests, mentioned that the G-UNIV gyroplane in general is a good Level 2 aircraft in comparison to the VPM M16 gyroplane, which according to his words is a perfect (Level 1) gyroplane in terms of handling qualities. Hence, the G-UNIV handling qualities predicted by the DLR criterion coincide with the test pilot opinion. Presumably, the DLR bandwidth requirements are more applicable to light gyroplanes. It should be noted that this is just one pilot's subjective opinion; ideally, to design gyroplane handling qualities criteria, further flight tests and simulation trials are required.

Finally, results of lateral-directional oscillation assessments are shown in Figure 3.23. It can be seen that the G-UNIV gyroplane achieved Level 2 handling qualities. It is obvious that these criteria do not predict Level 1 handling qualities because of the low values of undamped natural frequency of lateral-directional oscillation. For example, if the natural frequency was greater then the points in the criteria chart would move towards the Level 1 region.

### 3.4 Chapter Summary

This chapter has been focused on the assessment of the objective handling qualities of the G-UNIV research gyroplane. The longitudinal and lateral-directional handling qualities have been estimated using criteria from the following standards and specifications: BCAR Section T (2003), MIL-F-8785C (1980), DEF STAN 00-970 (2003), MIL-F-83300 (1970), AGARD-R-577-70 (1970), DEF STAN 00-970 Rotorcraft (1984), ADS-33E-PRF (2000) and MIL-HDBK-1797 (1997).

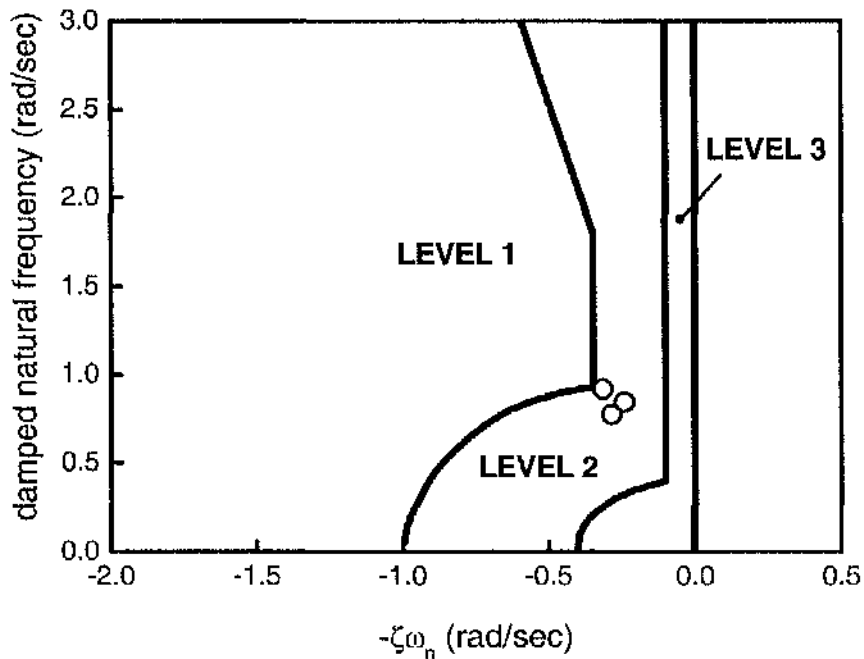


**Figure 3.23** The G-UNIV data points against ADS-33E-PRF (2000) lateral-directional oscillatory requirements

To summarise, the following results have been obtained. The G-UNIV research gyroplane has attained *unacceptable* level of handling qualities using the short period thumb print criterion (O'Hara, 1967). The test aircraft has *not satisfied* the BCAR Section T requirements for the short period oscillations, but has *satisfied* the general requirements for longitudinal and lateral-directional oscillations. The MIL-F-8785C and DEF STAN 00-970 short period frequency/acceleration sensitivity criteria have predicted *Level 1* of handling qualities (Category B Flight Phases), while the short period damping criteria have predicted only *Level 2*; the Dutch roll frequency/damping criteria have predicted *Level 1* handling qualities (Category B Flight Phases). The assessment against the MIL-F-83300 criteria have yielded *Level 2* handling qualities for the short period frequency/damping requirements and *Level 1* for the lateral-directional oscillatory criteria. The requirements of AGARD-R-577-70 have predicted *Satisfactory* level both for the longitudinal and lateral-directional handling qualities. The G-UNIV has met mostly *Level 1* handling qualities for the pitch dynamic stability criteria of

DEF STAN 00-970 Rotorcraft, and *Levels 1, 2 and 3* handling qualities for the roll dynamic stability criteria. The ADS-33E-PRF small-amplitude pitch and roll attitude criteria have predicted *Level 1* handling qualities; results of short period pitch and lateral-directional oscillation assessment against the ADS-33E-PRF criteria have yielded *Level 2*. The test aircraft has met *Level 2* handling qualities for the MIL-HDBK-1797 short period dynamic requirements (Category B Flight Phases); the bandwidth/phase delay criteria have predicted both *Level 1* and *Level 2*. Finally, the bandwidth/phase delay criteria for roll axis proposed by the DLR have predicted only *Level 2* handling qualities for the G-UNIV gyroplane.

It can be concluded from this thorough assessment against the criteria of different standards and specifications, that in general the G-UNIV research gyroplane is a good *Level 2* aircraft both in longitudinal and lateral-directional axes. Of course, it should be borne in mind that these criteria were designed for different types of aircraft and all the results are based only on limited flight test data, and therefore the obtained handling qualities levels of the G-UNIV gyroplane should be considered as a preliminary estimation. More importantly, it has been demonstrated that the gyroplane handling qualities can be estimated using the “classical” approaches from the existing standards for aeroplanes and rotorcraft, and moreover that gyroplane’s own criteria can be designed in the same manner as the criteria from these standards. As was stated in Chapter 2, extensive flight tests and simulation are essential to form a database of objective and subjective assessments of handling qualities of light gyroplanes with the aim of developing new gyroplane requirements and criteria in the future.

In spite of the fact that almost all specifications require data obtained from free and fixed stick responses, in this chapter, only fixed stick responses have been considered because of the lack of test data. Therefore, it is highly desirable to obtain flight test results for stick free responses as well. Most of the results for longitudinal and lateral-directional oscillations presented in this chapter have been obtained for the airspeed of 40 mph. It is also highly desirable to have experimental results for a full airspeed range of the G-UNIV research gyroplane.

## ***Chapter 4***

# **Development of a Gyroplane Simulation Model GSIM**

### **4.1 Introduction**

To create a usable set of handling qualities requirements and criteria, extensive flight tests are required. Furthermore, this process includes a tremendous amount of human resources, careful planning and organisation, and, because a flight test programme for handling qualities assessment usually includes aggressive manoeuvring at the edges of the aircraft flight envelope, safety issues must be paramount. This makes the process very expensive and time-consuming, especially for light gyroplanes that have still not found a wide practical application neither in the civil nor in the military sector. Mathematical modelling of the gyroplane's flight dynamics is therefore essential to reduce the required flight test effort.

The aim of this chapter is to describe the development and validation of the Gyroplane Simulation Model (GSIM); while the next chapter will discuss the principles and development of the inverse simulation technique. This chapter starts with a general overview of the GSIM model, providing the key properties and assumptions of the modelling process. This is followed by presenting the basic principles of simulation of aircraft rigid-body dynamics. A model of an autorotating rotor forms the core of the developed gyroplane mathematical model; therefore, a description of the calculation of rotor forces and moments is presented in detail, placing a considerable emphasis on the blade flapping dynamics and inflow modelling. The following sections document the

development of models for the rest of gyroplane's components, which include fuselage and empennage. The chapter ends with a discussion of the validation results, which include comparison of GSIM's steady state results with those obtained from the flight tests and the RASCAL model (Houston, 1994).

## 4.2 Overview of the Gyroplane Simulation Model

The gyroplane simulation model GSIM has been developed by studying and investigating the flight dynamics of the Montgomerie-Parsons and VPM M16 test gyroplanes at the Department of Aerospace Engineering, University of Glasgow, flight data obtained from the flight tests of these gyroplanes and wind tunnel tests of the scale model of VPM M14 gyroplane, simulation results evaluated by generic rotorcraft model RASCAL (Houston, 1994), and extensive literature review on this subject. Use was made of an existing helicopter individual blade rotor model IIBROM (Rutherford and Thomson, 1997), developed at Glasgow to incorporate into a generic inverse simulation algorithm GENISA (Rutherford and Thomson, 1996). This is not the first time a helicopter rotor model has been used as a basis for gyroplane simulation. For example, the generic rotorcraft model RASCAL developed by Houston (1994) uses the same rotor model for any type of rotorcraft, including gyroplanes. Moreover, Spathopoulos (2001) utilised the RASCAL model to investigate the autorotation mode of a gyroplane, and as a conclusion of this study it was emphasised that a rotorcraft mathematical model in general can be applied for gyroplane simulation if suitable induced velocity model is chosen and a rotor speed degree of freedom is incorporated. However, it should be noted that in contrast to RASCAL, the HIBROM model is not generic; therefore, significant changes were required to develop a new gyroplane model.

GSIM is an individual blade/blade element coupled rotor-fuselage model. This type of rotorcraft mathematical model has been successfully used in different studies (Houston, 1994; Rutherford and Thomson, 1997; Anderson, 1999; Celi, 1999). Combined blade element momentum theory was applied to calculate forces and moments of the autorotating rotor; aerodynamic and inertial loads were represented by 20 elements per blade. The G-UNIV gyroplane's teetering rotor has two blades with the NACA 8-H-12

aerofoil. The aerodynamic characteristics for the aerofoil section were obtained from NACA reports (*Stivers and Rice, 1946; Schaefer and Smith, 1949*) and CFD modelling. The constant-chord untwisted blades of the gyroplane's rotor are attached to the hub without flap and lag hinges, and have a zero pitch setting angle. Neither collective nor cyclic pitch can be applied.

Rotor inflow is calculated using the dynamic inflow model of Pitt and Peters (*1981*) improved later by Peters and HaQuang (*1988*). Blade flapping model is based on centre-spring equivalent rotor approach (*Padfield, 1996*). For modelling purposes, it was assumed that gyroplane blades are fully rigid and attached to the rotor shaft by a centre-spring; thereby blade elasticity is modelled by means of a centre-spring. Blade flapping dynamics is characterised by a second order nonlinear differential equation. Lookup tables of force and moment coefficients obtained from wind tunnel tests have been used for the fuselage, tailplane and fin aerodynamics. A model of International Standard Atmosphere (ISA) is utilised in the GSIM model; atmospheric turbulence is not modelled.

It should be noted that the GSIM modelling assumptions in general are similar to those of the HIBROM model (*Rutherford, 1997, p.51*). Key properties and assumptions of the GSIM model are summarised in Table 4.1. Apparently, the developed rotor model satisfies Level 2 modelling requirements (Table 4.2), proposed by Padfield (*1996, p.90*). However, in contrast to the RASCAL, the GSIM model is not generic, and was developed in the manner in which only the G-UNIV research gyroplane's flight dynamics is simulated. Nevertheless, the database of aircraft models can be easily extended, but would be restricted only by light gyroplanes with the design similar to the G-UNIV gyroplane. However, this does not exclude the possibility of further development of the GSIM model.

Finally, in the same manner as the HIBROM, the GSIM model was incorporated into the GENISA algorithm with the aim of using the inverse simulation package GENISA/GSIM for the process of designing gyroplane manoeuvres, which will be discussed in the next chapters.

**Table 4.1** Gyroplane mathematical model description

Model Item	Characteristics
Rotor dynamics	Rotor blades are fully rigid. Lead/lag freedom has been neglected. No hinge offset.
Rotor loads	Aerodynamic and inertial loads represented by 20 elements per blade.
Blade aerodynamics	NACA 8-H-12 aerofoil. Lookup tables for lift and drag as functions of angle of attack and Mach number.
Dynamic inflow	Peters and HaQuang dynamic inflow model. Effect of the rotor moments and the lag between application of the blade pitch and changes in the aerodynamic forces.
Airframe	Lookup tables and polynomial functions for fuselage, tailplane and fin aerodynamics.
Atmosphere	International Standard Atmosphere (ISA).

**Table 4.2** Levels of rotor mathematical modelling, reproduced from Padfield (1996)

	Level 1	Level 2	Level 3
<i>Aerodynamics</i>	linear 2-D dynamic inflow/local momentum theory analytically integrated loads	nonlinear (limited 3-D) dynamic inflow/local momentum theory local effects of blade vortex interaction unsteady 2-D compressibility numerically integrated loads	nonlinear 3-D full wake analysis (free or prescribed) unsteady 2-D compressibility numerically integrated loads
<i>Dynamics</i>	rigid blades (1) quasi-steady motion (2) 3 DoF flap (3) 6 DoF flap + lag (4) 6 DoF flap + lag + quasi-steady torsion	(1) rigid blades with options as in Level 1 (2) limited number of blade elastic modes	detailed structural representation as elastic modes or finite elements
<i>Applications</i>	parametric trends for flying qualities and performance studies  well within operational flight envelope  low bandwidth control	parametric trends for flying qualities and performance studies up to operational flight envelope  medium bandwidth appropriate to high gain active flight control	rotor design  rotor limit loads prediction  vibration analysis  rotor stability analysis  up to safe flight envelope

### 4.3 Aircraft Rigid Body Dynamics

The gyroplane is assumed to be a rigid body, therefore Euler rigid body equations of motion can be used to simulate the motion of the gyroplane's centre of gravity

$$\dot{U} = -(WQ - VR) + \frac{X}{m} - g \sin \Theta, \quad (4.1)$$

$$\dot{V} = -(UR - WP) + \frac{Y}{m} + g \cos \Theta \sin \Phi, \quad (4.2)$$

$$\dot{W} = -(VP - UQ) + \frac{Z}{m} + g \cos \Theta \cos \Phi, \quad (4.3)$$

$$I_{xx} \dot{P} = (I_{yy} - I_{zz})QR + I_{xz}(\dot{R} + PQ) + L, \quad (4.4)$$

$$I_{yy} \dot{Q} = (I_{zz} - I_{xx})RP + I_{xz}(R^2 - P^2) + M, \quad (4.5)$$

$$I_{zz} \dot{R} = (I_{xx} - I_{yy})PQ + I_{xz}(\dot{P} - QR) + N, \quad (4.6)$$

where  $U, V, W$  are the aircraft velocity components along the body fixed reference frame;

$P, Q, R$  are the aircraft roll, pitch and yaw rates about the body axes;

$\Phi, \Theta, \Psi$  are the aircraft roll, pitch and yaw attitudes;

$m$  is the aircraft mass;

$X, Y, Z$  are the external aerodynamic forces;

$L, M, N$  are the external aerodynamic moments acting about the centre of gravity;

$I_{xx}, I_{yy}, I_{zz}$  are the aircraft roll, pitch and yaw moments of inertia in the body axes;

$I_{xz}$  is the product of inertia in the body axes.

The rates of change of the attitude angles are related to the body axes angular velocities by the kinematic expressions

$$\dot{\Phi} = P + Q \sin \Phi \tan \Theta + R \cos \Phi \tan \Theta, \quad (4.7)$$

$$\dot{\Theta} = Q \cos \Phi - R \sin \Phi, \quad (4.8)$$

$$\dot{\Psi} = Q \sin \Phi \sec \Theta + R \cos \Phi \sec \Theta. \quad (4.9)$$

The earth fixed velocities can be derived from the translational body fixed velocities and the attitude angles through the Euler transformation equations

$$[\dot{x}_e \quad \dot{y}_e \quad \dot{z}_e]^T = T [U \quad V \quad W]^T, \quad (4.10)$$

where

$$T = \begin{bmatrix} \cos \Theta \cos \Psi & (\sin \Phi \sin \Theta \cos \Psi - \cos \Phi \sin \Psi) & (\cos \Phi \sin \Theta \cos \Psi + \sin \Phi \sin \Psi) \\ \cos \Theta \sin \Psi & (\sin \Phi \sin \Theta \sin \Psi + \cos \Phi \cos \Psi) & (\cos \Phi \sin \Theta \sin \Psi - \sin \Phi \cos \Psi) \\ -\sin \Theta & \sin \Phi \cos \Theta & \cos \Phi \cos \Theta \end{bmatrix}$$

is the Euler transformation matrix.

The dynamics of the rotating rotor and transmission system of the helicopter according to Padfield (1981; 1996) can be approximated by the following expression

$$\dot{\Omega} = \dot{R} + \frac{1}{I_R} (Q_e - Q_R - g_r Q_{tr}) \quad (4.11)$$

where  $\Omega$  is the rotor speed;

$R$  is the aircraft yaw rate;

$Q_e$  is the engine torque;

$Q_R$  is the rotor aerodynamic torque;

$Q_r$  is the tail rotor torque;

$g_r$  is the tail rotor gear ratio;

$I_R$  is the moment of inertia of the rotor.

Since a gyroplane operates only in the autorotation mode, i.e. the rotor is unpowered<sup>\*</sup>; equation (4.11) can be simplified in the following form

$$\dot{\Omega} = \dot{R} - \frac{Q_R}{I_R}. \quad (4.12)$$

It ought to be noted that in trimmed unaccelerated flight the rotor aerodynamic torque,  $Q_R$  must be equal to zero.

The aircraft external aerodynamic forces and moments from equations (4.1)-(4.6) can be calculated as a sum of the contributions from the aircraft subsystems

$$X = X_R + X_{fus} + X_{tp} + X_{fin} + X_P, \quad (4.13)$$

$$Y = Y_R + Y_{fus} + Y_{tp} + Y_{fin} + Y_P, \quad (4.14)$$

$$Z = Z_R + Z_{fus} + Z_{tp} + Z_{fin} + Z_P, \quad (4.15)$$

$$L = L_R + L_{fus} + L_{tp} + L_{fin} + L_P, \quad (4.16)$$

$$M = M_R + M_{fus} + M_{tp} + M_{fin} + M_P, \quad (4.17)$$

$$N = N_R + N_{fus} + N_{tp} + N_{fin} + N_P, \quad (4.18)$$

where the subscripts  $R$ ,  $fus$ ,  $tp$ ,  $fin$  and  $P$  correspond to rotor, fuselage, tailplane, fin and power respectively. It should be emphasised that the expressions in equations (4.13)-(4.18), in contrast to those of a helicopter (Padfield, 1996, p.92; Rutherford, 1997, p.49;

<sup>\*</sup> However, in some types of gyroplanes the rotor can be powered for a short period with the aim to pre-rotate it immediately before the take-off (for example, G-UNIV and VPM M16 gyroplanes). Moreover, some gyroplanes have a "jump" take-off capability, when after pre-rotating the rotor the collective pitch is applied to lift the aircraft from the ground. Because these modes are short and transient, they were not considered in the current research.

Cameron, 2002, p.144), contain components of power effect, which are typical for conventional aeroplane (Cook, 1997, p.61) or helicopter with thrust compounding (Rutherford, 1997, p.96; Leishman, 2003, p.232). In particular, the G-UNIV gyroplane is powered by a two-cylinder/two-stroke ROTAX TYPE 618 engine, driving a 62-inch diameter, three-bladed fixed pitch IVOPROP propeller (Table A2.1). Engine power, and therefore propeller thrust is controlled by a throttle lever, which is located on the left side of the pilot cockpit. In spite of the fact that, for an aircraft engine, the relationship between thrust and throttle lever position is usually represented by the first order lag transfer function (Cook, 1997, p.27; Houston, 2003), the GSIM has a simple engine model, where propeller thrust is assumed to have a linear functional dependence on throttle lever displacement. This assumption was made mainly due to the lack of test data for this type of aircraft engine.

Another contributing gyroplane subsystem is an autorotating rotor, which provides required lift force and control. The process of calculating forces and moments of the rotor is provided in detail in the following section.

#### 4.4 Rotor Forces and Moments

The study of gyroplane handling qualities requires accurate predictions of the vehicle dynamic response, and hence the rotor response, to mid-to-high frequency control inputs, which are typical for aggressive manoeuvres, such as slalom, acceleration-deceleration etc. Rutherford (1997) compared the two most widely used rotorcraft simulation approaches, a rotor disc model and an individual blade model, by the example of HGS (Thomson, 1992) and HIBROM (Rutherford and Thomson, 1997) models respectively, and noted that individual blade modelling provides a higher fidelity than rotor disc representation, and, furthermore, predicts more accurately an aircraft behaviour at the edges of the flight envelope. The latter statement is very important for the handling qualities study because it is aggressive manoeuvring which drives the vehicle to the edges of the flight envelope. Considering these conclusions, it was decided to utilise an individual blade technique for gyroplane simulation. It should be emphasised that the individual blade approach was successfully realised in two

rotorcraft models developed at Glasgow, RASCAL (Houston, 1994) and HIBROM (Rutherford and Thomson, 1997). These high-fidelity models were used for gyroplane flight dynamics research (Houston, 1996; 1998; Spathopoulos, 2001; Houston and Thomson, 2001; 2004), simulated “turbulence-induced” helicopter vibration analysis (Anderson, 1999), and helicopter manoeuvring study (Rutherford, 1997).

Aerodynamic and inertial forces and moments on the individual blade are calculated using the blade element theory. Detailed historical and theoretical development of the blade element theory can be found, for example, in the works by Johnson (1980, p.45), Prouty (1990, p.140), and Leishman (2003, p.78). The blade element theory is based on the assumption that each blade is divided into small sections, or elements, and each element of the blade is considered as a two-dimensional aerofoil with associated sectional lift and drag characteristics. It is also stipulated that the velocities and accelerations are uniform over each element. Then knowing the velocity and acceleration of each blade element, forces and moments can be calculated in each section, and finally integrated across span of the blade to find total forces and moments acting on the whole blade. Finally, the total rotor forces and moments can be obtained by summing the forces and moments from each blade.

It is worth noting at this point that the accuracy of calculation of rotor forces and moments depends on the reliability of the experimental data for aerodynamic characteristics of aerofoil sections. The lift and drag characteristics of the aerofoil section of the blade are usually obtained from wind tunnel tests and represented in the form of lookup tables.

#### 4.4.1 Blade Element Kinematics

A blade element analysis starts with calculating the velocities and accelerations at blade elements referred to the *blade* axes frame of reference. Therefore, known gyroplane velocities and accelerations in the *body* axes must be transferred through a number of axes transformations into the *blade* axes system.

## 4.4.1.1 Blade Element Velocity

The velocity of the pivot point in the *body* axes (Figure 4.1) can be calculated from the following expression

$$\mathbf{u}_{p.p.}^{body} = \mathbf{u}_{c.g.}^{body} + \boldsymbol{\omega}^{body} \times \mathbf{r}_{p.p. \leftarrow c.g.}^{body}, \quad (4.19)$$

where  $\mathbf{u}_{c.g.}^{body}$  is the vector of gyroplane velocity components  $U$ ,  $V$ ,  $W$  in the *body* axes;

$\boldsymbol{\omega}^{body}$  is the vector of gyroplane rotational velocity components  $P$ ,  $Q$ ,  $R$  in the *body* axes;

$\mathbf{r}_{p.p. \leftarrow c.g.}^{body}$  is the vector of the position of the pivot point relative to the gyroplane centre of gravity, and referred to the *body* axes;

and the subscript *p.p.* corresponds to pivot point.

The position vector  $\mathbf{r}_{p.p. \leftarrow c.g.}^{body}$  in equation (4.19) is formed in the following manner

$$\mathbf{r}_{p.p. \leftarrow c.g.}^{body} = [x_{c.g.} - x_{p.p.} \quad 0 \quad z_{c.g.} - z_{p.p.}]^T, \quad (4.20)$$

where  $x_{c.g.}$ ,  $z_{c.g.}$  are the distances along the *x*- and *z*-*body* axes from the gyroplane centre of gravity to the airframe reference point<sup>†</sup>;

$x_{p.p.}$ ,  $z_{p.p.}$  are the distances along the *x*- and *z*-*body* axes from the airframe reference point to the pivot point.

Since the *pivot* axes frame of reference is set with the origin at the pivot point and is not inclined with respect to the *body* axes (Figure 4.1), the translational and rotational velocities of the pivot point in the *pivot* axes are equal to those in the *body* axes

$$\mathbf{u}_{p.p.}^{pivot} = \mathbf{u}_{p.p.}^{body} = [U_{p.p.}^{pivot} \quad V_{p.p.}^{pivot} \quad W_{p.p.}^{pivot}]^T, \quad (4.21)$$

$$\boldsymbol{\omega}^{pivot} = \boldsymbol{\omega}^{body}. \quad (4.22)$$

<sup>†</sup> The airframe reference point of the G-UNIV gyroplane is taken as the intersection of the projection of the mast centreline and the keel centreline with the *x*-*body* axis aligned with the keel.

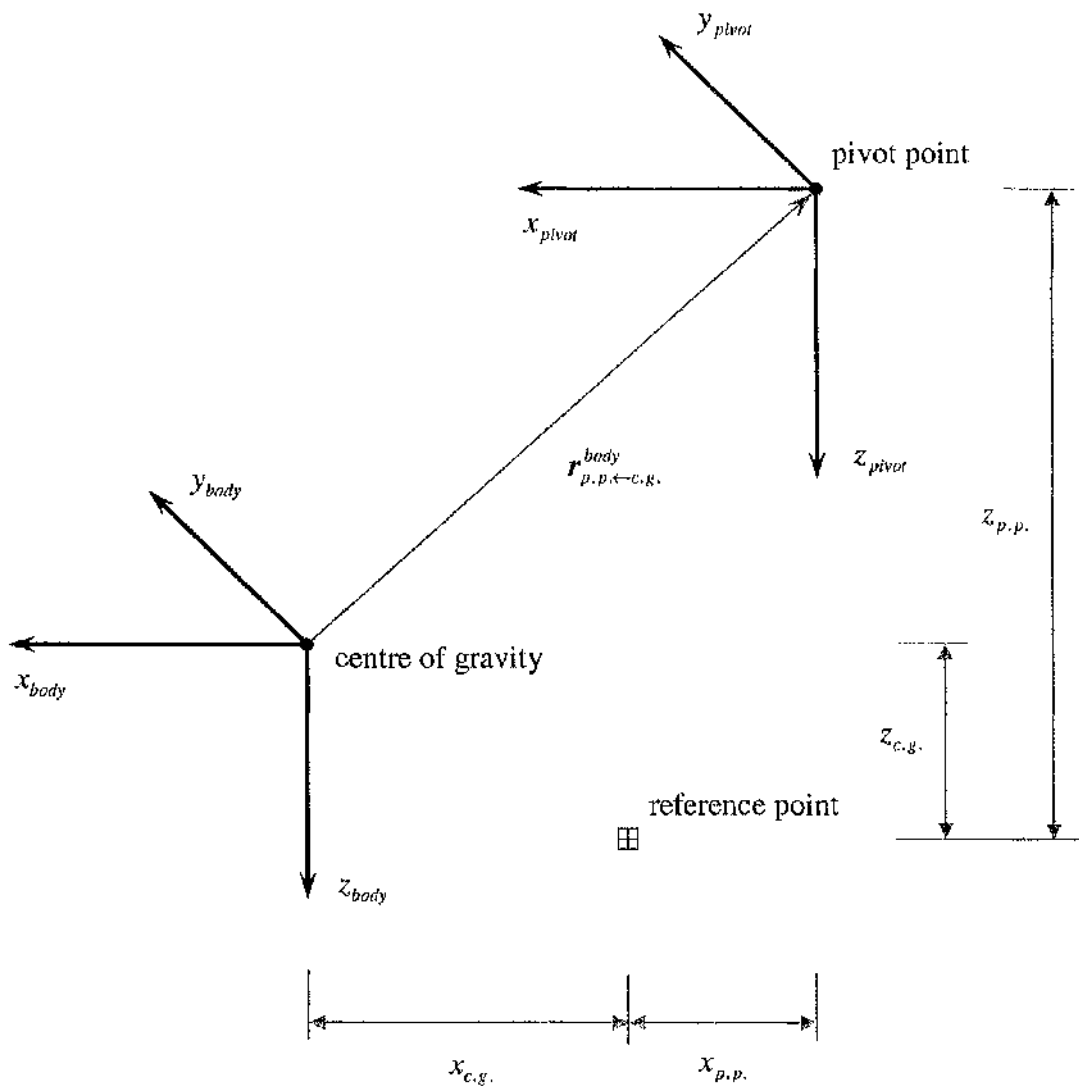


**Figure 4.1** Transformation from *body* to *pivot* axes

The rotor hub of the G-UNIV gyroplane is shifted with respect to the pivot point by longitudinal and vertical shaft offsets,  $l_{shaft}$  and  $h_{shaft}$  due to the fact that such a design reduces the forces acting on the pilot control stick. Thus, the *disc* axes frame of reference is defined with the origin at the hub, and rotated with respect to the *pivot* axes by the longitudinal and lateral rotor shaft angles,  $\theta_{shaft}$  and  $\phi_{shaft}$  (Figure 4.2). These two angles are the control angles that define the direction of the rotor thrust. Therefore the

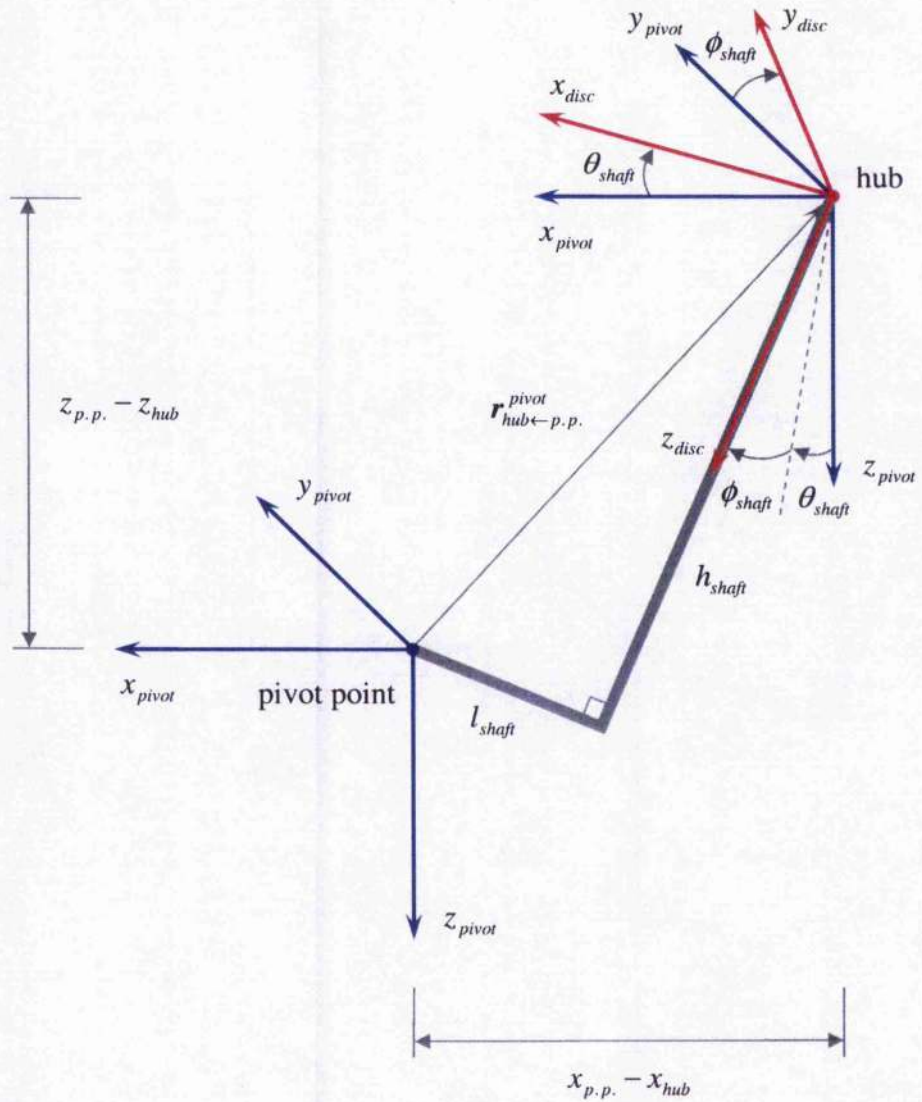


**Figure 4.2** Transformation from *pivot* to *disc* axes

next step is to transfer the translational and rotational velocities from equations (4.21) and (4.22) to the *disc* set of axes. The velocity of the hub in the *pivot* axes is then given as

$$\mathbf{u}_{hub}^{pivot} = \mathbf{u}_{p.p.}^{pivot} + \boldsymbol{\omega}^{pivot} \times \mathbf{r}_{hub \leftarrow p.p.}^{pivot}, \quad (4.23)$$

where

$$\mathbf{r}_{hub \leftarrow p.p.}^{pivot} = \begin{bmatrix} x_{p.p.} - x_{hub} & 0 & z_{p.p.} - z_{hub} \end{bmatrix}^T \quad (4.24)$$

is the vector of the position of the hub relative to the pivot point with reference to the *pivot* axes; and  $x_{hub}$ ,  $z_{hub}$  are the distances along the  $x$ - and  $z$ -*pivot* axes from the airframe reference point to the hub.

Hence, the translational and rotational velocities of the hub in the *disc* axes are

$$\mathbf{u}_{hub}^{disc} = \mathbf{T}^{disc \leftarrow pivot} \mathbf{u}_{hub}^{pivot} = \begin{bmatrix} U_{hub}^{disc} & V_{hub}^{disc} & W_{hub}^{disc} \end{bmatrix}^T, \quad (4.25)$$

$$\boldsymbol{\omega}^{disc} = \mathbf{T}^{disc \leftarrow pivot} \boldsymbol{\omega}^{pivot}, \quad (4.26)$$

where the transformation matrix from *pivot* to *disc* axes is given by

$$\mathbf{T}^{disc \leftarrow pivot} = \begin{bmatrix} \cos \theta_{shaft} & 0 & -\sin \theta_{shaft} \\ \sin \phi_{shaft} \sin \theta_{shaft} & \cos \phi_{shaft} & \sin \phi_{shaft} \cos \theta_{shaft} \\ \cos \phi_{shaft} \sin \theta_{shaft} & -\sin \phi_{shaft} & \cos \phi_{shaft} \cos \theta_{shaft} \end{bmatrix}.$$

The *shaft* axes frame of reference is also set with the origin at the hub, but in contrast to the *disc* axes set rotates about  $z$ -*disc* axis by the shaft azimuth angle  $\psi_{az}$  (Figure 4.3).

The velocity of the hub in the *shaft* axes is therefore

$$\mathbf{u}_{hub}^{shaft} = \mathbf{T}^{shaft \leftarrow disc} \mathbf{u}_{hub}^{disc}, \quad (4.27)$$

where the transformation matrix from *disc* to *shaft* axes is

$$\mathbf{T}^{shaft \leftarrow disc} = \begin{bmatrix} -\cos \psi_{az} & -\sin \psi_{az} & 0 \\ \sin \psi_{az} & -\cos \psi_{az} & 0 \\ 0 & 0 & 1 \end{bmatrix}.$$

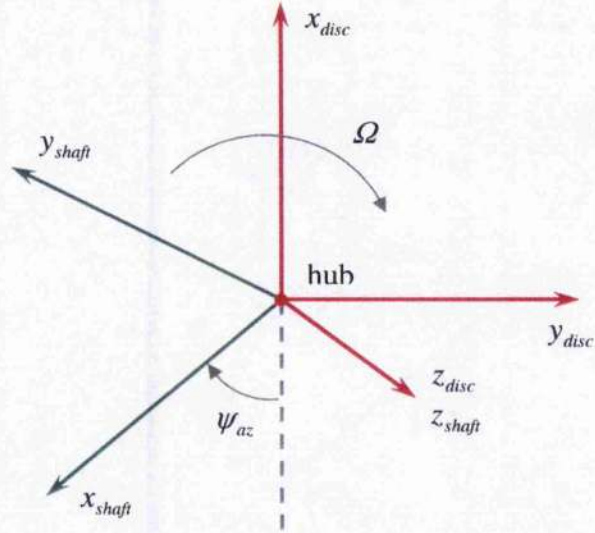


**Figure 4.3** Transformation from *disc* to *shaft* axes

The rotational velocity of the hub in the *shaft* axes is obtained by transforming the rotational velocity of the hub in the *disc* axes into the *shaft* axes, and adding then the rotor angular velocity,  $\Omega$

$$\omega^{shaft} = T^{shaft \leftarrow disc} \omega^{disc} + [0 \ 0 \ \Omega]^T = [P^{shaft} \ Q^{shaft} \ R^{shaft}]^T. \quad (4.28)$$

The final step includes transformation from *shaft* to *blade* axes as shown in Figure 4.4. Since the test gyroplane's blades have no hinge offset, and each blade rotates about *y-shaft* axis by blade flap angle,  $\beta$ , the translational and rotational velocities of the hub in the *blade* axes is then given as

$$\mathbf{u}_{hub}^{blade} = T^{blade \leftarrow shaft} \mathbf{u}_{hub}^{shaft}, \quad (4.29)$$

$$\omega^{blade} = T^{blade \leftarrow shaft} \omega^{shaft} + [0 \ \dot{\beta} \ 0]^T, \quad (4.30)$$

where the transformation matrix from *shaft* to *blade* axes is

$$\mathbf{T}^{blade \leftarrow shaft} = \begin{bmatrix} \cos \beta & 0 & -\sin \beta \\ 0 & 1 & 0 \\ \sin \beta & 0 & \cos \beta \end{bmatrix}.$$

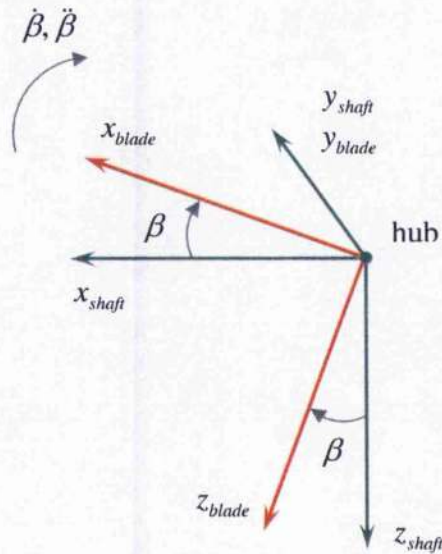


**Figure 4.4** Transformation from *shaft* to *blade* axes

The blade flap angle  $\beta$ , and the flapping rate  $\dot{\beta}$  are calculated from a second order nonlinear differential equation, which describes gyroplane's blade flapping dynamics. A detailed description of the blade flapping model is given in Section 4.5.

Finally, the translational velocity of a general blade element in the *blade* axes can be determined from

$$\mathbf{u}_{b.e.}^{blade} = \mathbf{u}_{hub}^{blade} + \boldsymbol{\omega}^{blade} \times \mathbf{r}_{b.e. \leftarrow hub}^{blade} = \begin{bmatrix} U_{b.e.}^{blade} & V_{b.e.}^{blade} & W_{b.e.}^{blade} \end{bmatrix}^T, \quad (4.31)$$

where

$$\mathbf{r}_{b.e. \leftarrow hub}^{blade} = [r_{b.e.} \quad 0 \quad 0]^T \quad (4.32)$$

is the vector of the position of the blade element relative to the hub with reference to the *blade* axes;  $r_{b.e.}$  is the distance along the *x-blade* axis from the hub to the blade element; and the subscript *b.e.* refers to the blade element.

#### 4.4.1.2 Blade Element Acceleration

The total forces acting on each blade can be calculated as a sum of the aerodynamic and inertial forces. A priori information about aerodynamic characteristics for the blade aerofoil section gives the aerodynamic forces of the individual blade as will be shown in the next subsection. In fact, the inertial forces acting on an individual blade depend on the accelerations of blade elements, which can be obtained from accelerations in the *body* axes through the series of axes transformations similar to those presented in the previous subsection.

Thus, the acceleration of the pivot point in the *body* axes is given by the following expression

$$\mathbf{a}_{p.p.}^{body} = \mathbf{a}_{c.g.}^{body} + \boldsymbol{\alpha}^{body} \times \mathbf{r}_{p.p. \leftarrow c.g.}^{body} + \boldsymbol{\omega}^{body} (\boldsymbol{\omega}^{body} \times \mathbf{r}_{p.p. \leftarrow c.g.}^{body}), \quad (4.33)$$

where  $\mathbf{a}_{c.g.}^{body}$  and  $\boldsymbol{\alpha}^{body}$  are the vectors of the gyroplane translational and rotational accelerations of the centre of gravity in *body* axes;  $\boldsymbol{\omega}^{body}$  is the vector of gyroplane rotational velocity components in the *body* axes; and  $\mathbf{r}_{p.p. \leftarrow c.g.}^{body}$  is given by equation (4.20). The vectors  $\mathbf{a}_{c.g.}^{body}$  and  $\boldsymbol{\alpha}^{body}$  are given by

$$\mathbf{a}_{c.g.}^{body} = \frac{\partial \mathbf{u}_{c.g.}^{body}}{\partial t} + \boldsymbol{\omega}^{body} \times \mathbf{u}_{c.g.}^{body} = \begin{bmatrix} \dot{U} + WQ - VR \\ \dot{V} + UR - WP \\ \dot{W} + VP - UQ \end{bmatrix}, \quad (4.34)$$

$$\alpha^{body} = [\dot{P} \quad \dot{Q} \quad \dot{R}]^T. \quad (4.35)$$

Since the *pivot* set of axes is defined with the origin at the pivot point and is not inclined with respect to the *body* axes, the translational and rotational accelerations of the pivot point in the *pivot* axes are equal to those in the *body* axes

$$\mathbf{a}_{pivot\ point}^{pivot} = \mathbf{a}_{pivot\ point}^{body}, \quad (4.36)$$

$$\alpha^{pivot} = \alpha^{body}. \quad (4.37)$$

The acceleration of the hub in the *pivot* axes can be obtained from the following expression

$$\mathbf{a}_{hub}^{pivot} = \mathbf{a}_{p.p.}^{pivot} + \alpha^{pivot} \times \mathbf{r}_{hub \leftarrow p.p.}^{pivot} + \omega^{pivot} (\omega^{pivot} \times \mathbf{r}_{hub \leftarrow p.p.}^{pivot}). \quad (4.38)$$

Therefore, the translational and rotational accelerations of the hub in the *disc* axes are respectively

$$\mathbf{a}_{hub}^{disc} = \mathbf{T}^{disc \leftarrow pivot} \mathbf{a}_{hub}^{pivot}, \quad (4.39)$$

$$\alpha^{disc} = \mathbf{T}^{disc \leftarrow pivot} \alpha^{pivot}. \quad (4.40)$$

Next, the accelerations of the hub in the *shaft* axes can be calculated

$$\mathbf{a}_{hub}^{shaft} = \mathbf{T}^{shaft \leftarrow disc} \mathbf{a}_{hub}^{disc}, \quad (4.41)$$

$$\alpha^{shaft} = \mathbf{T}^{shaft \leftarrow disc} \alpha^{disc} + [0 \quad 0 \quad \dot{\Omega}]^T, \quad (4.42)$$

where  $\dot{\Omega}$  is the rate of change of the rotorspeed.

The final transformation from *shaft* to *blade* axes allows obtaining the translational and rotational accelerations of the hub in the *blade* axes

$$\mathbf{a}_{hub}^{blade} = \mathbf{T}^{blade \leftarrow shaft} \mathbf{a}_{hub}^{shaft}, \quad (4.43)$$

$$\mathbf{a}^{blade} = \mathbf{T}^{blade \leftarrow shaft} \mathbf{a}^{shaft} + \begin{bmatrix} 0 & \ddot{\beta} & 0 \end{bmatrix}^T. \quad (4.44)$$

The second order derivative of the blade flap angle,  $\ddot{\beta}$  in equation (4.44) can be obtained from the blade flapping equation of motion, as will be detailed in Section 4.5. Finally, the translational acceleration of a general blade element in the *blade* axes is determined from the following expression

$$\mathbf{a}_{b.e.}^{blade} = \mathbf{a}_{hub}^{blade} + \mathbf{a}^{blade} \times \mathbf{r}_{b.e. \leftarrow hub}^{blade} + \boldsymbol{\omega}^{blade} (\boldsymbol{\omega}^{blade} \times \mathbf{r}_{b.e. \leftarrow hub}^{blade}). \quad (4.45)$$

#### 4.4.2 Blade Aerodynamic Forces

Aerodynamic lift and drag acting upon each blade element can be calculated from the velocity of a blade element given by equation (4.31). In the model, the blade aerodynamic coefficients depend on the local Mach number and angle of attack; therefore, the process of defining the blade aerodynamic forces must start with calculation of these parameters. The tangential and perpendicular components of the resultant velocity at the blade element (Figure 4.5) are given by

$$U_t = -V_{b.e.}^{blade}, \quad (4.46)$$

$$U_p = W_{b.e.}^{blade} - v_i \cos \beta, \quad (4.47)$$

where  $v_i$  is the induced velocity at the blade element. It is stipulated that the induced velocity at the blade element can be represented in the following form, proposed by Peters (1974, cited Gaonkar and Peters, 1988, p.217), that is

$$v_i(r_{b.e.}, \psi_{az}) = v_0^{disc} + \frac{r_{b.e.}}{R} (v_{1s}^{disc} \sin \psi_{az} + v_{1c}^{disc} \cos \psi_{az}), \quad (4.48)$$

where  $v_0^{disc}$ ,  $v_{1s}^{disc}$  and  $v_{1c}^{disc}$  are the uniform, longitudinal and lateral components of the rotor induced velocity in the *disc* set of axes, which can be calculated using dynamic inflow modelling. Detailed description of the rotor dynamic inflow model is presented in Section 4.6.

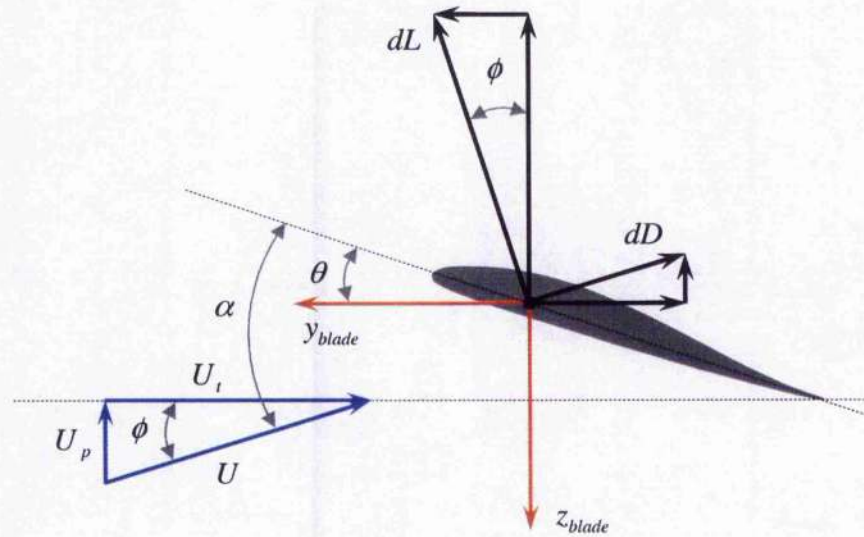


**Figure 4.5** Aerodynamic forces and incident velocities of a blade element

Therefore, the local Mach number can be determined

$$M = \frac{U}{a} = \frac{\sqrt{U_i^2 + U_p^2}}{a}, \quad (4.49)$$

where  $U$  is the resultant aerodynamic velocity of the blade element, and  $a$  is the local speed of sound.

The local angle of attack is given by

$$\alpha = \theta + \phi, \quad (4.50)$$

where  $\theta$  is the local geometric pitch angle, and  $\phi$  is the local inflow angle, which can be calculated from the tangential and perpendicular components of the resultant velocity at the blade element

$$\phi = \tan^{-1}\left(\frac{U_p}{U_t}\right). \quad (4.51)$$

The differential lift and drag forces are then defined in the conventional manner

$$dL = \frac{1}{2} \rho U^2 c C_l(\alpha, M) dr_{b.e.}, \quad (4.52)$$

$$dD = \frac{1}{2} \rho U^2 c C_d(\alpha, M) dr_{b.e.}, \quad (4.53)$$

where  $\rho$  is the local air density;

$c$  is the chord of the blade element;

$C_l$  and  $C_d$  are the lift and drag coefficients, respectively;

$dr_{b.e.}$  is the length of the blade element.

According to Figures 4.4 and 4.5, the aerodynamic forces acting on a blade element and referred to the *blade* set of axes can be determined from the sectional lift and drag forces and the local inflow angle

$$\mathbf{f}_{aero.}^{blade} = \begin{bmatrix} 0 \\ dL \sin \phi - dD \cos \phi \\ -dL \cos \phi - dD \sin \phi \end{bmatrix}. \quad (4.54)$$

Finally, the aerodynamic forces acting upon the whole blade are calculated by integration of the differential aerodynamic forces along the blade span

$$\mathbf{F}_{aero.}^{blade} = \int_0^R \mathbf{f}_{aero.}^{blade} dr_{b.e.} \quad (4.55)$$

#### 4.4.3 Blade Inertial Forces

The inertial forces acting on a blade element and referred to the *blade* set of axes are calculated from Newton's second law

$$\mathbf{f}_{inertial}^{blade} = m_{b.e.} \mathbf{a}_{b.e.}^{blade} = m_{b.e.} \begin{bmatrix} (a_{b.e.}^{blade})_x \\ (a_{b.e.}^{blade})_y \\ (a_{b.e.}^{blade})_z \end{bmatrix}, \quad (4.56)$$

where  $m_{b.e.}$  is the mass of the blade element.

Thus, the inertial forces acting upon the entire blade can be obtained by integration of the sectional inertial forces along the blade span, that is

$$\mathbf{F}_{inertial}^{blade} = \int_0^R \mathbf{f}_{inertial}^{blade} dr_{b.e.} \quad (4.57)$$

#### 4.4.4 Total Forces and Moments

From Newton's third law of motion the total force acting upon each blade is given by equilibrium

$$\mathbf{F}_{hub}^{blade} = \mathbf{F}_{aero.}^{blade} - \mathbf{F}_{inertial}^{blade}, \quad (4.58)$$

or

$$\mathbf{F}_{hub}^{blade} = \int_0^R \mathbf{f}_{aero}^{blade} dr_{b.e.} - \int_0^R \mathbf{f}_{inertial}^{blade} dr_{b.e.} \quad (4.59)$$

The moment of each blade about the hub can be written as

$$\mathbf{M}_{hub}^{blade} = \int_0^R \mathbf{r}_{b.e. \leftarrow hub}^{blade} \times \mathbf{f}_{inertial}^{blade} dr_{b.e.} \quad (4.60)$$

Next step involves backward transformations of the forces and moments from the *blade* axes to the *body* axes. This process includes transformation matrices and position vectors, which were defined earlier in this subsection. Thus, the total forces and moments of the autorotating rotor can finally be determined and used in equations (4.13) – (4.18) to calculate the total external forces and moments of the gyroplane.

The forces and moments at the hub with a reference to the *disc* axes are obtained from those of equations (4.59) and (4.60) through the transformations from *blade* to *shaft* and then from *shaft* to *disc* set of axes. It should be noted that contributions of each blade are now summed to determine the total forces and moments of the rotor:

$$\mathbf{F}_{hub}^{disc} = \sum_{n=1}^{N_b} (\mathbf{T}^{shaft \leftarrow disc})^{-1} (\mathbf{T}^{blade \leftarrow shaft})^{-1} \mathbf{F}_{hub}^{blade} \quad (4.61)$$

$$\mathbf{M}_{hub}^{disc} = \sum_{n=1}^{N_b} (\mathbf{T}^{shaft \leftarrow disc})^{-1} (\mathbf{T}^{blade \leftarrow shaft})^{-1} \mathbf{M}_{hub}^{blade} \quad (4.62)$$

where  $N_b$  is the number of blades on the rotor.

Thus, the forces and moments at the pivot point, referred to the *pivot* axes, are given by

$$\mathbf{F}_{p.p.}^{pivot} = (\mathbf{T}^{disc \leftarrow pivot})^{-1} \mathbf{F}_{hub}^{disc} \quad (4.63)$$

$$\mathbf{M}_{p,p.}^{pivot} = \left( \mathbf{T}^{disc \leftarrow pivot} \right)^{-1} \mathbf{M}_{hub}^{disc} + \mathbf{r}_{hub \leftarrow p.p.}^{pivot} \times \mathbf{F}_{p.p.}^{pivot}. \quad (4.64)$$

Finally, the rotor's contribution to the gyroplane external forces and moments can be calculated from the last transformation from *pivot* to *body* axes set:

$$\mathbf{F}_{c.g.}^{body} = \left( \mathbf{T}^{pivot \leftarrow body} \right)^{-1} \mathbf{F}_{p.p.}^{pivot} = [X_R \quad Y_R \quad Z_R]^T, \quad (4.65)$$

$$\mathbf{M}_{c.g.}^{body} = \left( \mathbf{T}^{pivot \leftarrow body} \right)^{-1} \mathbf{M}_{p.p.}^{pivot} + \mathbf{r}_{p.p. \leftarrow c.g.}^{body} \times \mathbf{F}_{c.g.}^{body} = [L_R \quad M_R \quad N_R]^T. \quad (4.66)$$

## 4.5 Blade Flapping Dynamics

Blade flapping motion can be described as the upward and downward movement of the rotor blades in a vertical plane. The Montgomerie-Parsons research gyroplane has hingeless teetering rotor with two blades attached firmly to the hub middle section. The elastic blades flap due to bending about the attachment point. The gyroplane blade flapping model is based on the original HIBROM model (*Rutherford, 1997; Rutherford and Thomson, 1997*), and uses the centre-spring equivalent rotor approach (*Padfield, 1996, p.96*). The approach is based on the assumption that the blade is rigid and attached to the shaft by a centre-spring. Such an approximation can be useful in generic rotor models, such as the gyroplane model, allowing simulation of different types of rotor system.

The blade flapping equation can be obtained from the equilibrium of moments about the centre hinge with spring stiffness  $K_\beta$ , that is

$$\int_0^R \mathbf{r}_{b.e. \leftarrow hub}^{blade} \times \int_{aero.}^{blade} d\mathbf{r}_{b.e.} - \int_0^R \mathbf{r}_{b.e. \leftarrow hub}^{blade} \times m_{b.e.} \mathbf{a}_{b.e.}^{blade} dr_{b.e.} + [0 \quad K_\beta \beta \quad 0]^T = 0, \quad (4.67)$$

where the first component is the blade aerodynamic moment

$$\mathbf{M}_{aero.} = [L_{aero.} \quad M_{aero.} \quad N_{aero.}] = \int_0^R \mathbf{r}_{b.e. \leftarrow hub}^{blade} \times \mathbf{f}_{aero.}^{blade} dr_{b.e.}, \quad (4.68)$$

and the second component is the blade inertial moment. The moment formed by blade weight force was neglected because "the mean lift and acceleration forces are typically one or two orders of magnitude higher" (Padfield, 1996, p.96).

To obtain the blade inertial moment, the blade acceleration vector  $\mathbf{a}_{b.e.}^{blade}$  is calculated in the way explained in the previous section:

$$\mathbf{a}_{b.e.}^{blade} = \mathbf{a}_{hub}^{blade} + \boldsymbol{\alpha}^{blade} \times \mathbf{r}_{b.e. \leftarrow hub}^{blade} + \boldsymbol{\omega}^{blade} (\boldsymbol{\omega}^{blade} \times \mathbf{r}_{b.e. \leftarrow hub}^{blade}), \quad (4.69)$$

where  $\boldsymbol{\omega}^{blade}$ ,  $\mathbf{r}_{b.e. \leftarrow hub}^{blade}$ ,  $\mathbf{a}_{hub}^{blade}$ , and  $\boldsymbol{\alpha}^{blade}$  were defined by equations (4.30), (4.32), (4.43), and (4.44) respectively. Then

$$\mathbf{a}_{b.e.}^{blade} = \begin{bmatrix} (\mathbf{a}_{hub}^{shaft})_x \cos \beta - (\mathbf{a}_{hub}^{shaft})_z \sin \beta \\ (\mathbf{a}_{hub}^{shaft})_y \\ (\mathbf{a}_{hub}^{shaft})_x \sin \beta + (\mathbf{a}_{hub}^{shaft})_z \cos \beta \end{bmatrix} + \begin{bmatrix} 0 \\ r_{b.e.} ((\alpha^{shaft})_x \sin \beta + (\alpha^{shaft})_z \cos \beta) \\ -r_{b.e.} ((\alpha^{shaft})_y + \dot{\beta}) \end{bmatrix} + \begin{bmatrix} r_{b.e.} (-(Q^{shaft} + \dot{\beta})^2 - (P^{shaft} \sin \beta + R^{shaft} \cos \beta)^2) \\ r_{b.e.} (P^{shaft} \cos \beta - R^{shaft} \sin \beta) (Q^{shaft} + \dot{\beta})^2 \\ r_{b.e.} (P^{shaft} \cos \beta - R^{shaft} \sin \beta) (P^{shaft} \sin \beta + R^{shaft} \cos \beta) \end{bmatrix}. \quad (4.70)$$

Thus, the equilibrium equation (4.67) can be rewritten

$$M_{aero.} + M_{\beta} \left( (\mathbf{a}_{hub}^{shaft})_x \sin \beta + (\mathbf{a}_{hub}^{shaft})_z \cos \beta \right) + I_{\beta} \left( (P^{shaft} \cos \beta - R^{shaft} \sin \beta) (P^{shaft} \sin \beta + R^{shaft} \cos \beta) - ((\alpha^{shaft})_y + \dot{\beta}) \right) + K_{\beta} \beta = 0, \quad (4.71)$$

where  $M_{\beta}$  and  $I_{\beta}$  are the blade mass moment and flap moment of inertia respectively

$$M_{\beta} = \int_0^R m_{b.e.} r_{b.e.} dr_{b.e.}, \quad (4.72)$$

$$I_{\beta} = \int_0^R m_{b.e.} r_{b.e.}^2 dr_{b.e.}. \quad (4.73)$$

Rearranging and solving equation (4.71) for  $\ddot{\beta}$  leads to

$$\begin{aligned} \ddot{\beta} = & \frac{M_{aero.}}{I_{\beta}} + \frac{M_{\beta}}{I_{\beta}} \left( (a_{hub}^{shaft})_x \sin \beta + (a_{hub}^{shaft})_z \cos \beta \right) \\ & + (P^{shaft} \cos \beta - R^{shaft} \sin \beta) (P^{shaft} \sin \beta + R^{shaft} \cos \beta) - (\alpha^{shaft})_y + \frac{K_{\beta}}{I_{\beta}} \beta. \end{aligned} \quad (4.74)$$

Equation (4.74) is the second order nonlinear differential equation, which describes blade flapping dynamics.

## 4.6 Rotor Dynamic Inflow Model

A correctness of representation of the inflow at the rotor disc is an important factor in the process of modelling rotary-wing aircraft, because it affects the local angle of attack in the blade element, and thus the entire rotor aerodynamics. The first model for the rotor induced velocity was proposed by Glauert (1926, p.15), as a result of comprehensive study of a gyroplane's autorotating rotor behaviour in the mid 1920s. The induced velocity was represented in the following manner, which included radial and azimuthal variations of inflow:

$$v_i = v_0 + v_1 \frac{r_{b.e.}}{R} \cos \psi_{az}, \quad (4.75)$$

where  $v_0$  and  $v_1$  are the uniform and longitudinal components of the rotor induced velocity.

This first attempt to model inflow distribution has led to the development of more sophisticated non-uniform inflow models. One of the most detailed reviews of non-uniform inflow modelling is available in the work of Chen (1990). However, static inflow models, such that developed by Glauert (1926) for example, assume that the airflow accelerates instantaneously across the plane of the rotor disc, and flow perturbations do not affect pitch and roll moments. This has led to the development of more advanced dynamic inflow models. Gaonkar and Peters (1988, p.215) stated that there are eight commonly used bases of dynamic inflow modelling: 1) simple momentum and vortex theories, 2) empirical models, 3) extended momentum theory, 4) mass effects or time delay, 5) equivalent Lock number and profile drag coefficient, 6) unsteady actuator disc theory, 7) prescribed wake theory, and 8) higher harmonic models.

The most widely used dynamic inflow model is that of Pitt and Peters (1981). This model uses principles of extended momentum theory, mass effects and unsteady actuator disc theory to obtain an unsteady flow, which has only three inflow degrees of freedom: uniform, longitudinal, and lateral. This model considers the effect of the rotor moments and the lag between application of the blade pitch and changes in the aerodynamic forces. The model was improved later by Peters and HaQuang (1988). The Pitt-Peters model initially was written in the wind-axis reference system for zero hub motions, Peters and HaQuang have rewritten this model in a general rotor frame making the model more convenient for practical applications. However, the original Pitt-Peters model has strict limitations; the model uses only two harmonics in the inflow distribution, and one or two functions of radial shapes for each harmonic.

Later, Peters and He developed and approved a generalised wake model (Peters *et al*, 1989). In this model, the inflow is represented as the sum of an unlimited number of radial shape functions for an unlimited number of harmonics. Such an approach is very useful practically; it is possible to choose a number of radial shape functions and a number of harmonics depending on an application task. In the following years, several efforts were made to improve the accuracy of this generalised wake model. For example, Krothapalli *et al* (1999, 2001) enhanced the original Peters-He model by including a wake curvature to augment the generalised wake model, and Peters *et al* (2001) extended the Peters-He inflow model to include effects of wake curvature and

ground plane interaction. All these sophisticated models are computationally expensive and therefore they are not entirely suitable to achieve the objectives of the current research. Use was made of the Peters-HaQuang dynamic inflow model, which is an improved version of the Pitt-Peters model as discussed above. Another deciding factor in choosing an inflow model for the current work was the fact that the HIBROM (Rutherford and Thomson, 1997), which formed the basis of the GSIM model, also utilises the Peters-HaQuang model, and therefore the applicability of this model in application to inverse simulation has already been proven. Moreover, the Peters-HaQuang model demonstrated high effectiveness in modelling of gyroplane's autorotating rotor behaviour (Houston, 2000; Spathopoulos, 2001).

The development of the Peters-HaQuang model is now detailed. As was noted earlier in this chapter, the induced velocity at the blade element is assumed to have the form of linear radial and first harmonic azimuthal distribution defined by equation (4.48), that is

$$v_i(r_{b.e.}, \psi_{az}) = v_0^{disc} + \frac{r_{b.e.}}{R} (v_{1s}^{disc} \sin \psi_{az} + v_{1c}^{disc} \cos \psi_{az}),$$

where  $v_0^{disc}$ ,  $v_{1s}^{disc}$  and  $v_{1c}^{disc}$  are the uniform, longitudinal and lateral components of the rotor induced velocity in the *disc* axes set.

The inflow states at the original Pitt-Peters model are related to the aerodynamic loads through the form of the first order differential equation written in the *wind* axes

$$\mathbf{M} \begin{Bmatrix} \lambda_0^{wind} \\ \lambda_{1s}^{wind} \\ \lambda_{1c}^{wind} \end{Bmatrix} + \mathbf{L}_{nd}^{-1} \begin{Bmatrix} \lambda_0^{wind} \\ \lambda_{1s}^{wind} \\ \lambda_{1c}^{wind} \end{Bmatrix} = \begin{Bmatrix} C_T^{wind} \\ -C_L^{wind} \\ -C_M^{wind} \end{Bmatrix}_{aero.}, \quad (4.76)$$

where

$$\mathbf{M} = \begin{bmatrix} \frac{8}{3\pi} & 0 & 0 \\ 0 & -\frac{16}{45\pi} & 0 \\ 0 & 0 & -\frac{16}{45\pi} \end{bmatrix} \quad (4.77)$$

is the apparent mass matrix, which can be considered as an inertia of the air mass; and  $L_{nl}$  is the nonlinear, inflow gains matrix.

Since the standard form of the inflow model presented in equation (4.76) uses non-dimensionalised components of the induced velocity, it is not unreasonable to utilise the same approach in this dissertation. The non-dimensionalised inflow components  $\lambda_0^{wind}$ ,  $\lambda_{1s}^{wind}$  and  $\lambda_{1c}^{wind}$  in the *wind* axes from equation (4.76) are determined from the  $v_0^{wind}$ ,  $v_{1s}^{wind}$  and  $v_{1c}^{wind}$  respectively, using the rotor speed,  $\Omega$  and the rotor radius,  $R$  in the following manner

$$\lambda_0^{wind} = \frac{v_0^{wind}}{\Omega R}, \quad (4.78)$$

$$\lambda_{1s}^{wind} = \frac{v_{1s}^{wind}}{\Omega R}, \quad (4.79)$$

$$\lambda_{1c}^{wind} = \frac{v_{1c}^{wind}}{\Omega R}. \quad (4.80)$$

At this point, it should be noted that since the rotor speed degree of freedom is implemented in the GSIM model (details are provided in Chapter 5), the rotor speed,  $\Omega$  used in the dynamic inflow model is updated at every time step. Therefore the above non-dimensionalisation with  $\Omega R$  is acceptable.

The nonlinear, static coupling matrix  $L_{nl}$  between induced flow and aerodynamic loads is defined by the following expression

$$L_{nl} = LV^{-1}, \quad (4.81)$$

where

$$L = \begin{bmatrix} \frac{1}{2} & 0 & \frac{15\pi}{64} \frac{\sqrt{1-\sin \chi}}{\sqrt{1+\sin \chi}} \\ 0 & \frac{-4}{1+\sin \chi} & 0 \\ \frac{15\pi}{64} \frac{\sqrt{1-\sin \chi}}{\sqrt{1+\sin \chi}} & 0 & \frac{-4\sin \chi}{1+\sin \chi} \end{bmatrix}, \quad (4.82)$$

and

$$V = \begin{bmatrix} V_T & 0 & 0 \\ 0 & V_m & 0 \\ 0 & 0 & V_m \end{bmatrix}. \quad (4.83)$$

It should be noted that the wake angle  $\chi$  in equation (4.82) is calculated in the same way as for the helicopter case proposed by Peters and HaQuang (1988)

$$\chi = \tan^{-1} \left[ \frac{|\lambda_m - \mu_z|}{\mu} \right], \quad (4.84)$$

and the components of the matrix  $V$  are determined by the following equations

$$V_T = \sqrt{\mu^2 + (\lambda_m - \mu_z)^2}, \quad (4.85)$$

$$V_m = \frac{\mu^2 + (2\lambda_m - \mu_z)(\lambda_m - \mu_z)}{V_T}, \quad (4.86)$$

where  $V_T$  is the resultant flow through the rotor disc;  $V_m$  is the mass-flow parameter due to cyclic disturbances;  $\lambda_m$  is the momentum theory non-dimensionalised induced velocity due to rotor thrust;  $\mu$  and  $\mu_z$  are the non-dimensionalised resultant forward and perpendicular component disc velocities respectively, which can be calculated by

$$\mu = \sqrt{\mu_x^2 + \mu_y^2}, \quad (4.87)$$

$$\mu_z = \frac{W_{hub}^{disc}}{\Omega R}, \quad (4.88)$$

where

$$\mu_x = \frac{u_{hub}^{disc}}{\Omega R}, \quad (4.89)$$

$$\mu_y = \frac{v_{hub}^{disc}}{\Omega R}, \quad (4.90)$$

The final step includes transformation from *wind* to *disc* set of axes. The inflow states and the force vector in the *wind* axes can be written in the following form

$$\begin{Bmatrix} \lambda_{\alpha}^{wind} \\ \lambda_{1s}^{wind} \\ \lambda_{1e}^{wind} \end{Bmatrix} = \mathbf{T}^{wind \leftarrow disc} \begin{Bmatrix} \lambda_{\alpha}^{disc} \\ \lambda_{1s}^{disc} \\ \lambda_{1e}^{disc} \end{Bmatrix}, \quad (4.91)$$

$$\begin{Bmatrix} C_T^{wind} \\ -C_L^{wind} \\ -C_M^{wind} \end{Bmatrix}_{aero.} = \mathbf{T}^{wind \leftarrow disc} \begin{Bmatrix} C_T^{disc} \\ -C_L^{disc} \\ -C_M^{disc} \end{Bmatrix}_{aero.} \quad (4.92)$$

The transformation matrix from *disc* to *wind* axes,  $\mathbf{T}^{wind \leftarrow disc}$  in equations (4.91) and (4.92) is defined as

$$\mathbf{T}^{wind \leftarrow disc} = \begin{bmatrix} 1 & 0 & 0 \\ 0 & \cos \delta & \sin \delta \\ 0 & -\sin \delta & \cos \delta \end{bmatrix},$$

where  $\delta$  is the difference between azimuth angles in the *disc* and *wind* sets of axes, and can be calculated from the following relationship

$$\delta = \tan^{-1} \left( \frac{\mu_y}{\mu_x} \right). \quad (4.93)$$

Finally, substituting the inflow states and the force vector in equation (4.76) by expressions from equations (4.91) and (4.92) yields

$$\mathbf{M} \begin{Bmatrix} \dot{\lambda}_0^{disc} \\ \dot{\lambda}_{1s}^{disc} \\ \dot{\lambda}_{1c}^{disc} \end{Bmatrix} + \mathbf{L}^{-1} \begin{Bmatrix} \lambda_0^{disc} \\ \lambda_{1s}^{disc} \\ \lambda_{1c}^{disc} \end{Bmatrix} = \begin{Bmatrix} C_T^{disc} \\ -C_L^{disc} \\ -C_M^{disc} \end{Bmatrix}_{\text{aero.}}, \quad (4.94)$$

where

$$\mathbf{L}^{-1} = \mathbf{V} \left( \mathbf{T}^{wind \leftarrow disc} \right)^T \mathbf{L}^{-1} \mathbf{T}^{wind \leftarrow disc}. \quad (4.95)$$

The first order differential equation (4.94) referred to the *disc* axes is considered throughout the thesis as the Peters-HaQuang dynamic inflow model. The model describes the time histories of the rotor dynamic inflow components, which contribute to the local angle of attack in the blade element, and therefore to the rotor aerodynamics, as shown in Section 4.4.2.

## 4.7 Fuselage Aerodynamic Forces and Moments

The fuselage aerodynamic forces and moments are determined from polynomial representations of them as the functions of fuselage angles of attack  $\alpha_{fus}$  and sideslip  $\beta_{fus}$ . It is apparent, that these angles are given by

$$\alpha_{fus} = \tan^{-1} \left( \frac{W_{fus}}{U_{fus}} \right), \quad (4.96)$$

$$\beta_{fus} = \sin^{-1} \left( \frac{V_{fus}}{V_{fus}} \right), \quad (4.97)$$

where the total velocity incident on fuselage is

$$V_{f_{fus}} = \sqrt{U_{fus}^2 + V_{fus}^2 + W_{fus}^2}, \quad (4.98)$$

and the components are obtained from the body axes total velocity components by

$$U_{fus} = U + Q(z_{fus} - z_{c.g.}), \quad (4.99)$$

$$V_{fus} = V - P(z_{fus} - z_{c.g.}) + R(x_{fus} - x_{c.g.}), \quad (4.100)$$

$$W_{fus} = W - Q(x_{fus} - x_{c.g.}), \quad (4.101)$$

The G-UNIV research gyroplane has never been wind tunnel tested. The only available data for a light gyroplane were from wind tunnel tests of the scale model of VPM M14 gyroplane at the Aeronautical Research and Test Institute of Prague (*Coton et al, 1998; Houston and Thomson, 2001*). Because the form and shape of the fuselages and empennages of these two gyroplanes can be assumed similar, the test data then were rescaled and used in the GSIM model.

The force and moment coefficients were obtained from wind tunnel tests at a reference dynamic pressure, and, therefore, must be corrected using a local dynamic pressure. It was assumed that the polynomials are linear, and the fuselage contributes only a pitching moment. Thus, the fuselage aerodynamic forces and moments can be written as

$$X_{fus} = \frac{P_{dyn}}{P_{dyn ref}} X_{fus 0}, \quad (4.102)$$

$$Y_{fus} = \frac{P_{dyn}}{P_{dyn ref}} Y_{fus 0} \beta_{fus}, \quad (4.103)$$

$$Z_{fus} = \frac{P_{dyn}}{P_{dyn ref}} Z_{fus 0} \alpha_{fus}, \quad (4.104)$$

$$L_{fus} = 0, \quad (4.105)$$

$$M_{fus} = \frac{P_{dyn}}{P_{dyn ref}} (M_{fus 0} + M_{fus 1} \alpha_{fus}), \quad (4.106)$$

$$N_{fus} = 0. \quad (4.107)$$

## 4.8 Empennage Aerodynamic Forces and Moments

The empennage of the research gyroplane is formed by a horizontal tailplane and a vertical fin. The empennage aerodynamic forces and moments were calculated in the same manner as for the fuselage, using polynomial representations.

The local incidence angle of the tailplane can be written in the form

$$\alpha_{tp} = \alpha_{tp_0} + \tan^{-1} \left( \frac{W_{tp}}{U_{tp}} \right), \quad (4.108)$$

where  $\alpha_{tp_0}$  is the geometric incidence angle of the tailplane, and the total velocity components are given by

$$U_{tp} = U - Q(z_{tp} - z_{c.g.}), \quad (4.109)$$

$$W_{tp} = W - Q(x_{tp} - x_{c.g.}). \quad (4.110)$$

Thus, the tailplane forces and moments are defined by

$$X_{tp} = 0, \quad (4.111)$$

$$Y_{tp} = 0, \quad (4.112)$$

$$Z_{tp} = \frac{P_{dyn}}{P_{dyn ref}} Z_{tp1} \alpha_{tp}, \quad (4.113)$$

$$L_{tp} = 0, \quad (4.114)$$

$$M_{tp} = \frac{P_{dyn}}{P_{dyn ref}} M_{tp1} \alpha_{tp}, \quad (4.115)$$

$$N_{tp} = 0. \quad (4.116)$$

The sideslip angle of the fin can be written as

$$\beta_{fin} = \beta_{fin0} + \sin^{-1} \left( \frac{V_{fin}}{V_{f fin}} \right), \quad (4.117)$$

where  $\beta_{fin0}$  is the geometric incidence angle of the fin, and the fin total velocity and its components are given by

$$V_{f fin} = \sqrt{U_{fin}^2 + V_{fin}^2 + W_{fin}^2}, \quad (4.118)$$

$$U_{fin} = U + Q(z_{fin} - z_{c.g.}), \quad (4.119)$$

$$V_{fin} = V - P(z_{fin} - z_{c.g.}) + R(x_{fin} - x_{c.g.}), \quad (4.120)$$

$$W_{fin} = W - Q(x_{fin} - x_{c.g.}). \quad (4.121)$$

Finally, the fin forces and moments are obtained from

$$X_{fin} = 0, \quad (4.122)$$

$$Y_{fin} = \frac{P_{dyn}}{P_{dyn ref}} Y_{fin1} \beta_{fin}, \quad (4.123)$$

$$Z_{fin} = 0, \quad (4.124)$$

$$L_{fin} = \frac{P_{dyn}}{P_{dyn ref}} L_{fin1} \beta_{fin}, \quad (4.125)$$

$$M_{fin} = 0, \quad (4.126)$$

$$N_{fin} = \frac{P_{dyn}}{P_{dyn ref}} N_{fin1} \beta_{fin}. \quad (4.127)$$

## 4.9 Validation of the GSIM

An important part in the mathematical modelling is the validation of a developed model. Flight tests measurements taken in steady level flight were compared with model results to validate the GSIM model. Flight test data were collected from the first flight trials of the G-UNIV research gyroplane during the period between autumn 2000 and winter 2001 (*Spathopoulos, 2001; Houston and Thomson, 2004*). In addition, GSIM trim results were compared to those obtained from the RASCAL model (*Houston, 1994*). This can be considered as a verification rather than validation process of the developed model because the RASCAL has been proven to be successful and reliable in simulating different types of rotorcraft, including the G-UNIV and VPM M16 test gyroplanes (*Houston, 1996; 1998; 2000; 2002; Anderson, 1999; Spathopoulos, 2001; Houston and Thomson, 2001; 2004*).

Before the comparison results will be presented and analysed, it is worthwhile at this point to discuss a number of complex issues regarding configuration of the test gyroplane. To begin with, the fuel mass could not be measured in flight, therefore the simulation results were calculated for two different configurations of the research gyroplane weight: maximum gross weight of 355 kg (full fuel) and minimum gross weight of 325 kg (zero fuel). For another thing, as was mentioned previously in the chapter, the accuracy of calculation of rotor forces and moments depends on the correctness and reliability of the experimental data for aerodynamic characteristics of aerofoil sections. The test gyroplane's teetering rotor has two blades with the

NACA 8-H-12 aerofoil. The only sources found with aerodynamic characteristics for this aerofoil, were NACA reports of the late 1940s (*Stivers and Rice, 1946; Schaefer and Smith, 1949*). Results provided in these papers were obtained from low-turbulence wind tunnel experiments at six Reynolds numbers from  $1.8 \times 10^6$  to  $11.0 \times 10^6$ . During these tests, the effect of leading-edge roughness (LER) was also investigated. As an example, results for Reynolds number of  $2.6 \times 10^6$  are presented in Figures 4.6 and 4.7.

In addition, the aerodynamic characteristics for the NACA 8-H-12 aerofoil generated by CFD simulation were kindly provided to the author by Dr George Barakos (University of Glasgow). These data were obtained for two Mach numbers, 0.1 and 0.5, from two different CFD models. Indicative results for  $M=0.1$  are shown in Figures 4.6 and 4.7. The first model was XFOIL from Mark Drela of the Massachusetts Institute of Technology (*XFOIL, 2001*). The model is based on a panel method coupled with a boundary layer solver. For all computations a simple transition model has been used, which was based on the  $e^N$  method. This allowed for laminar flow near the leading edge of the section and thus predicted the low drag bucket. The second model was a PMB (Parallel Multi-Block) solver of the University of Glasgow (*Badcock et al, 2000*). A full Navier-Stokes analysis was put forward with a two-equation eddy-viscosity turbulence model. The popular  $k-\omega$  model with no transition has been applied. Therefore, a fully turbulent solution was obtained with no laminar part near the leading edge. Due to this reason, drag values are higher and the low drag bucket is missing.

It can be seen from Figure 4.7 that the XFOIL predictions are closer to the NACA data with no leading-edge roughness, while simulation results of the PMB model are closer to the NACA data with leading-edge roughness. According to the surface condition of the blades and the local Reynolds number, both results may be valid. For example, the drag aerodynamics of used, eroded blades can be better described by the PMB model, while clean blades at low speed can produce the drag closer to the theory predicted by the XFOIL. Because it is difficult to predict the condition of the blades, lift and drag characteristics for the NACA 8-H-12 aerofoil were generated as mean values from the available NACA and CFD data (Figures 4.6 and 4.7). The technique proposed by Prouty (*1990, p.426*) was used to increase accuracy of calculations by representing the aerofoil

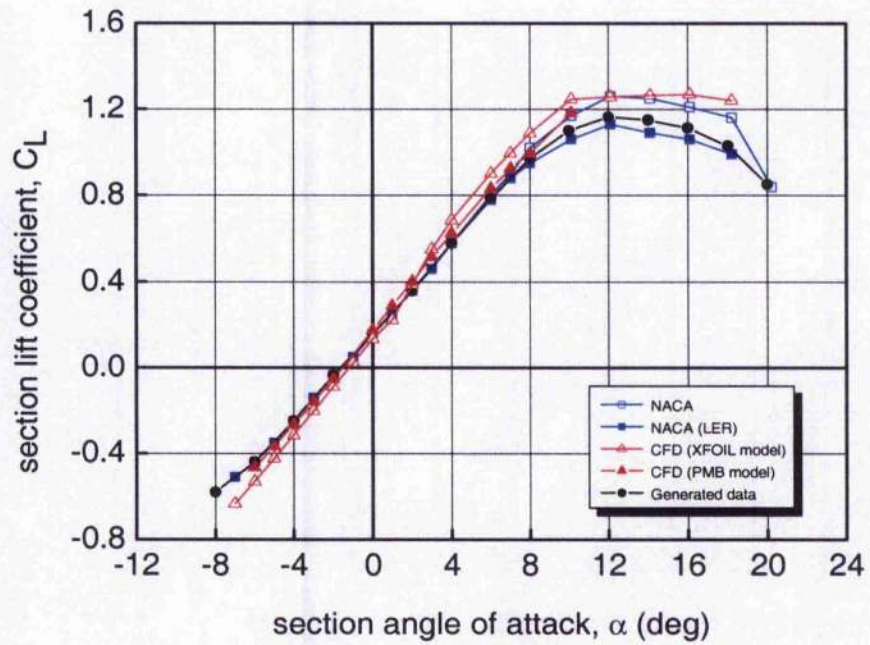


Figure 4.6 Lift coefficient of the NACA 8-H-12 aerofoil section

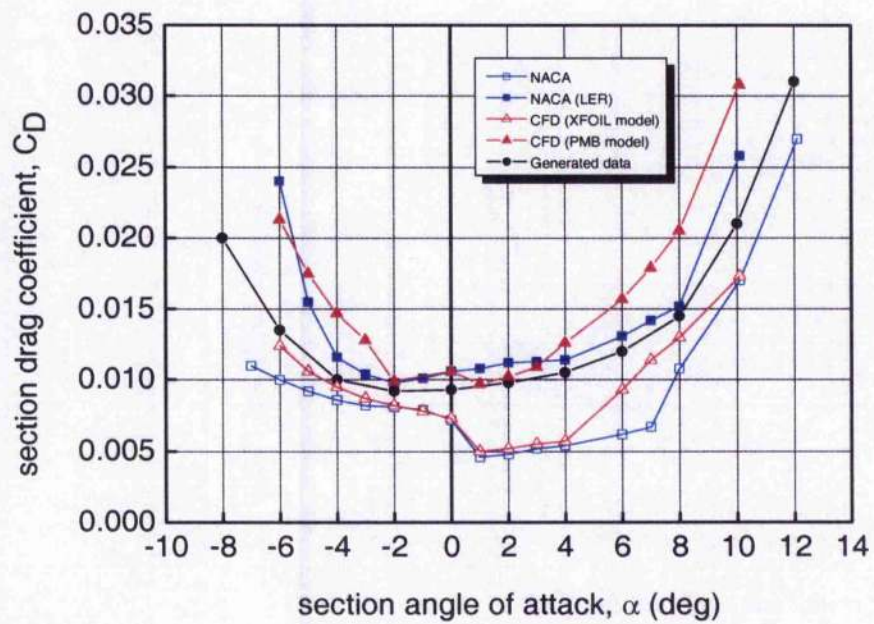


Figure 4.7 Drag coefficient of the NACA 8-H-12 aerofoil section

section lift and drag coefficients through 360 degrees of the section angle of attack. For the reason that the G-UNIV gyroplane's typical range of speed is not wide, it was assumed that the blade aerodynamic data do not depend on Mach number. Nevertheless, it should be noted that the GSIM model allows simulating dependence of the blade aerodynamic coefficients on the local Mach number.

To obtain steady state results the GSIM model uses a partial periodic trim algorithm originally proposed by McVicar and Bradley (1992), and then successfully utilised in the HIBROM model (Rutherford, 1997). This trimmer assumes that the trim solution must be found over a period of one rotor turn. The flight parameters must be averaged over this period and each of the aircraft's states must have the same value at the beginning and the end of the period. Then the aircraft controls must be calculated, which will produce the required trim state, and finally the periodic trim values of each of the states can be found. Rutherford (1997) implemented the original trimmer into an inverse simulation algorithm by considering each of the unknowns, which are the aircraft controls and the current state values, as components of a "pseudo" control vector, and using the flight parameters and the periodic states as functions in an error vector. A Newton-Raphson iterative method can then be applied in the same way as in the inverse simulation algorithm, which is detailed in the next chapter, to find the error vector for the unknown "pseudo" control vector.

The model validation results presented in Figures 4.8-4.12. All the coordinates of gyroplane subsystems used in the simulation are summarised in Table A2.2. Steady state results computed by the RASCAL model were kindly provided to the author by Dr Stewart Houston of University of Glasgow, and compared with those obtained from the GSIM model. Figure 4.8 shows the trim results for the pitch attitude as a function of forward airspeed. The simulation predicts an almost constant mismatch, but at least the trend in general is similar to the flight data. The RASCAL pitch results also do not match well with the test data, predicting lower values. It can be seen from Figure 4.8 that the flight test data were probably taken for two different aircraft configurations or different flight conditions, because the values for speed range 57-70 mph are slightly higher. It is interesting to notice that the RASCAL predictions are closer to the low-speed region of the test data, while the GSIM model shows better agreement at the high-speed range of the pitch attitude angles.

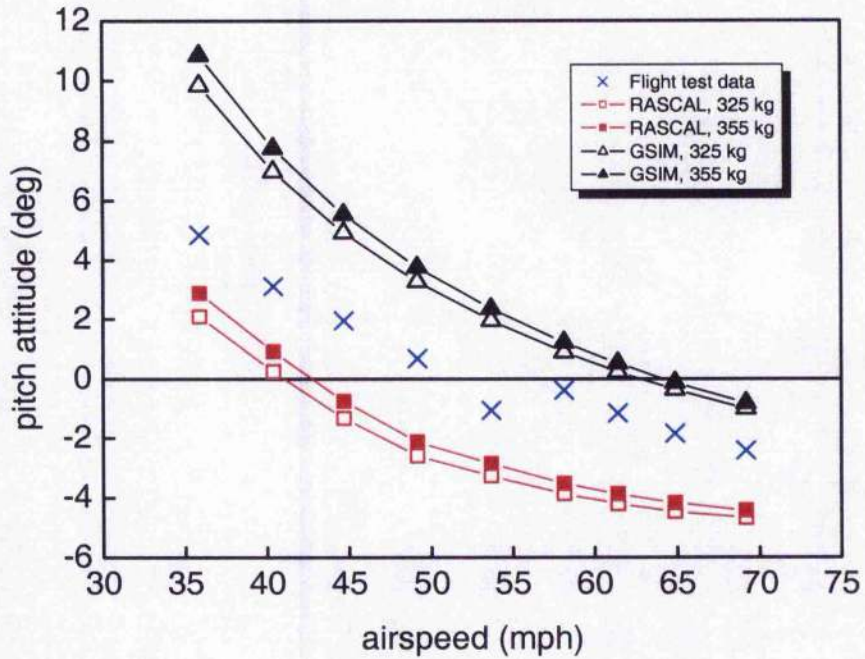


Figure 4.8 Comparison of steady state results for pitch attitude

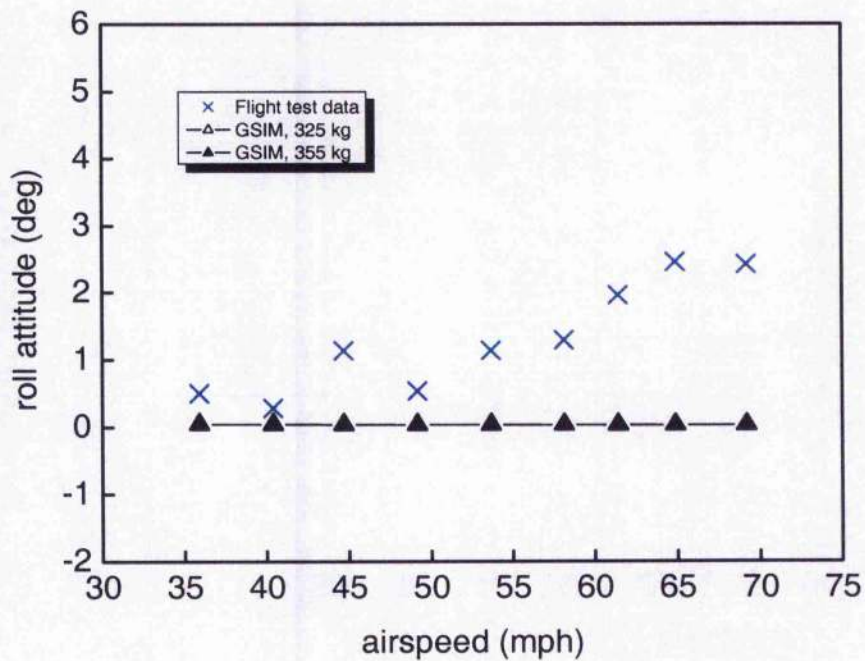
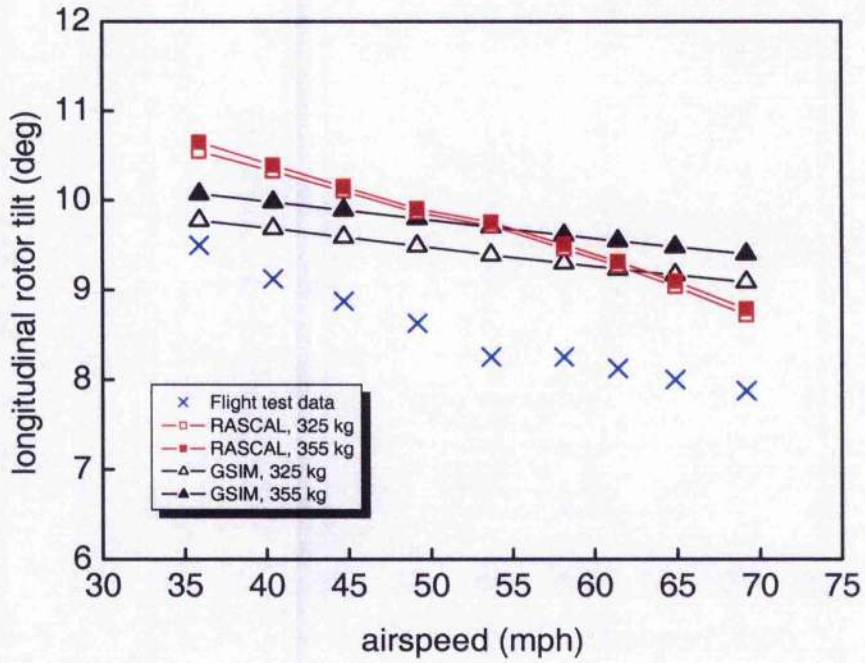
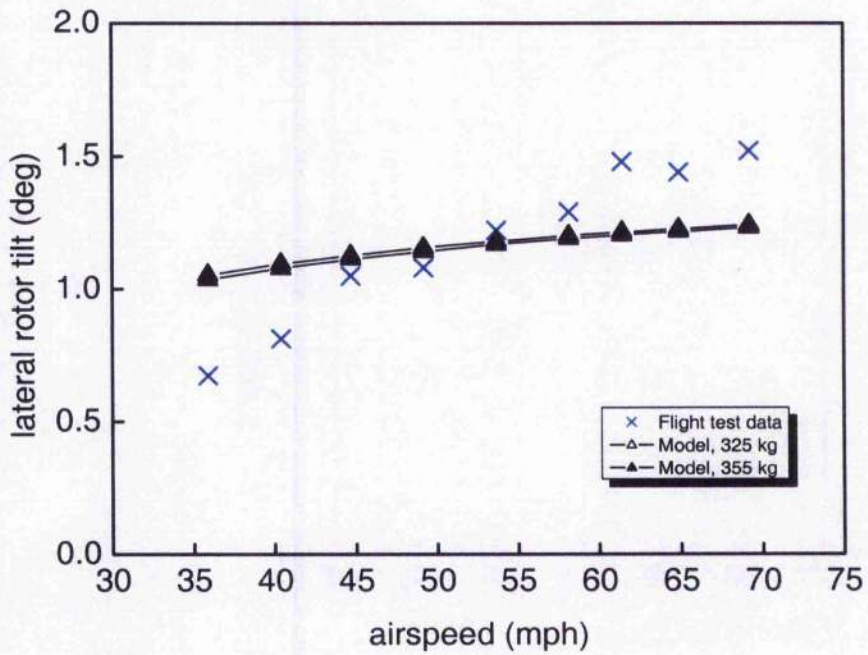


Figure 4.9 Comparison of steady state results for roll attitude



**Figure 4.10** Comparison of steady state results for longitudinal rotor tilt



**Figure 4.11** Comparison of steady state results for lateral rotor tilt

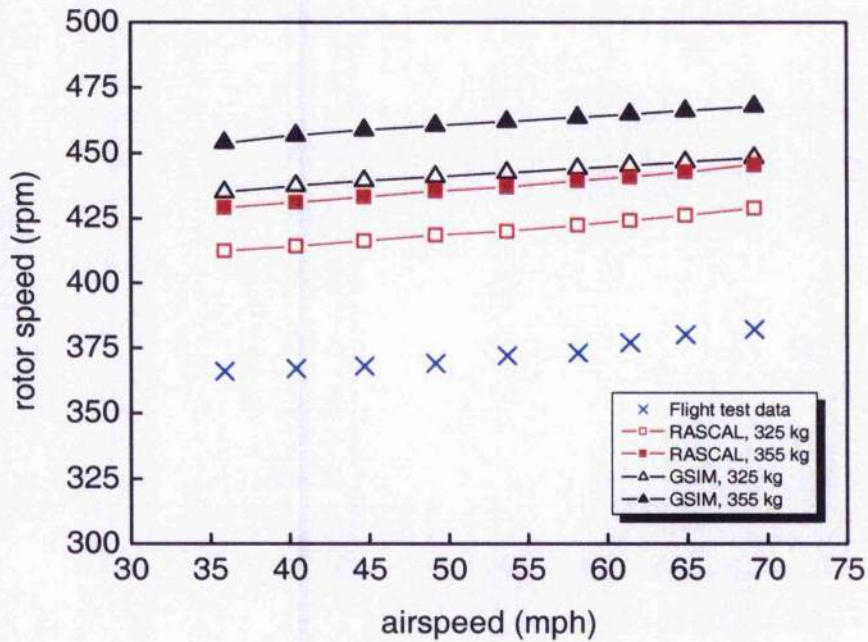


**Figure 4.12** Comparison of steady state results for rotor speed

In addition, the uniform mismatch in the pitch attitude conveys the suggestion that the discrepancy can be possibly caused by the calibration and measurement errors, though the model inadequacies must be also considered. Spathopoulos (2001, p.76), in discussing the steady state results obtained from the flight tests, noted that most likely the calibration errors are due to the fact that a conventional inclinometer was utilised to calibrate longitudinal and lateral channels for rotor tilt, as well as pitch and roll angle sensors (more detailed description of the calibration process is presented in Chapter 6). Since the fuselage and empennage aerodynamics do not contribute a lot to the total forces and moments of the gyroplane at the low-speed region where the discrepancy is largest, it is most probably that the rotor simulation model predicts forces and moments inaccurately. On the other side, in the high-speed region the airframe starts affecting the aerodynamics of the whole gyroplane, and it must be taken into consideration that the fuselage and empennage models are based on the wind tunnel data of the scale model of VPM M14 gyroplane as discussed in Section 4.7. Therefore, the wind tunnel tests of

the G-UNIV gyroplane are essential to simulate accurately the fuselage and empennage aerodynamics. Furthermore, Spathopoulos (2001, p.57) demonstrated that the pilot weight and fuel content affect the centre of gravity position of the gyroplane, which in turn affects the kinematics of the whole mathematical model.

The roll attitude (Figure 4.9) does not agree well with the test data at high speeds. This is likely because the G-UNIV test gyroplane did not have a sideslip indicator in the pilot cabin, and, therefore, in equilibrium flight it is very difficult for the test pilot, especially at high speeds, to maintain a zero sideslip angle, which in turn affects the roll attitude. It should be noted that a sideslip indicator has been installed recently in the pilot cockpit of the research gyroplane as a part of preparations for future flight tests.

It can be seen from Figure 4.10 that the comparison of longitudinal rotor tilt angles shows a good agreement at low speeds, and a small over prediction at higher speeds. It should be noted that the trend is similar only at high-speed region ( $-0.19 \text{ %/mph}$  from the flight data and  $-0.12 \text{ %/mph}$  from the simulation<sup>‡</sup>). A validation for lateral rotor tilt angles (Figure 4.11) shows a favourable flight/simulation comparison over most of the airspeed range. Predicted results lie within 2% of maximum available range of lateral tilt, although the gradient is slightly lower.

Figure 4.12 shows the validation results for the rotorspeed. It should be noted that the trend with the speed is similar and a uniform error is equal to approximately 70 and 90 rpm for the minimum and maximum weight respectively. The RASCAL results show a better agreement, though a consistent error of about 50/65 rpm remains. It is an incontestable fact that the rotorspeed is in inverse proportion to the blade drag. Probably lack of accurate initial data for the blade drag discussed earlier in this chapter causes the flight/simulation discrepancies in rotorspeed. In addition, it should be emphasised that the gyroplane model uses the centre-spring equivalent rotor model, assuming that a rotor blade is rigid. These factors, as well as others, such as complexity of autorotation conditions, possibly can be a reason for the rotorspeed mismatch.

---

<sup>‡</sup> As discussed in detail in Chapter 6, the measured full range for the longitudinal tilt is 17.73 deg, and the full range for the lateral tilt is 18.45 deg.

There is also a good probability that the flight/simulation discrepancies in the pitch and rotorspeed are caused by the fact that the GSIM uses the conventional, first-order, finite state dynamic inflow model discussed earlier in the chapter to calculate an induced velocity on the local airstream; while the more sophisticated wake models allow to simulate more realistically the behaviour of the airflow around the rotor, including wake distortion, blade-vortex interactions and specific for light gyroplanes rotor/propeller interaction. The gyroplane rotor/propeller interaction can be compared to the main rotor/tail rotor interaction in helicopter case, though the propeller operates in a plane, which is perpendicular to that of the tail rotor. For instance, Houston (2005) demonstrated that in applying a wake model instead of the conventional dynamic inflow model of Peters-HaQuang, the RASCAL predictions for the pitch and rotorspeed steady state results of the G-UNIV gyroplane are closer to the flight test data, the consistent error in rotorspeed for example decreases by about 15 rpm. The rotor wake model applied in this study was originally developed by Brown (2000) and is based on the numerical solution of the unsteady fluid-dynamic equations governing the generation and convection of vorticity through a domain enclosing the rotorcraft. Furthermore, Brown and Houston (2000) compared results calculated using the RASCAL model configured with two induced velocity models of Peters-HaQuang and Brown respectively with data obtained from flight experiments of the SA330 Puma helicopter, and demonstrated that the helicopter cross-coupling derivatives, response to control inputs, vibration levels and trim results have a better agreement with the test data in case if the Brown's wake model is applied.

To summarise, the comparison between the flight test data and simulation results for the trimmed flight state in general has given a good agreement. The observed flight/simulation discrepancies are due to the two possible factors: model inadequacies and calibration errors. It should be stated, however, that the validation process of the GSIM model was based only on one set of test data collected during the first phase of flight trials of the G-UNIV test gyroplane. It is highly demanded to obtain more test data for steady state flight in addition to already existing data to form a database of gyroplane trim results for different aircraft configurations and flight conditions. Only having such a database, a complete and adequate validation process of the gyroplane model would be possible.

Moreover, the inverse simulation results for slalom and acceleration-deceleration manoeuvres are compared with flight test data and then analysed in Chapter 5. Certainly, this process can be also considered as a validation of the GSIM model due to the fact that the developed simulation package GENISA/GSIM includes the gyroplane simulation model in conjunction with the inverse simulation algorithm GENISA, which is discussed in detail in the next chapter.

#### 4.10 Chapter Summary

This chapter has provided a detailed description of the gyroplane simulation model GSIM, which forms the basis of the developed inverse simulation package. A complex process of computation of the rotor forces and moments has been presented in great depth, with considerable importance been placed upon the blade flapping dynamics and the inflow modelling. The fuselage and empennage aerodynamics has been also discussed. Finally, the computational results for trimmed flight state have been validated against the experimental data. In addition, these results have been compared with those obtained from the RASCAL model. The flight/simulation discrepancies have been discussed and analysed, and it has been supposed that these discrepancies are caused by the two possible sources: model inadequacies and calibration errors. It has been shown that the realism of the GSIM model can be enhanced by a number of advanced features, such as blade elasticity and more sophisticated wake models. In addition, it has been stressed that wind tunnel tests of the G-UNIV gyroplane are essential to simulate accurately the fuselage and empennage aerodynamics. Nonetheless, in general, the comparison between the simulation results and flight test data has given a good agreement.

The following chapter will discuss the inverse simulation algorithm GENISA, and thereby complete the description of the developed inverse simulation package GENISA/GSIM.

## Chapter 5

# Gyroplane Inverse Simulation

### 5.1 Introduction

This chapter provides the first results of gyroplane inverse simulation. It should be emphasised that to the author's knowledge an inverse simulation has never been applied to a gyroplane simulation model before. The chapter starts with a discussion of the evolution of rotorcraft inverse simulation with a brief description of existing algorithms and methods of inverse problem applied to rotorcraft mathematical models with the aim of investigating different aspects of flight dynamics, including handling qualities study.

A description of modified inverse simulation algorithm GENISA is provided in detail, followed by a thorough discussion of mathematical modelling of gyroplane manoeuvres. Slalom and acceleration-deceleration manoeuvres are adapted from the ADS-33E-PRF (2000) standard, modified to suit a light gyroplane, and finally defined mathematically to implement them into the inverse simulation algorithm. This chapter proposes the inverse simulation algorithm GENISA in conjunction with the GSIM model described in the previous chapter, as a preliminary tool in the process of designing gyroplane test manoeuvres for handling qualities study. This includes an investigation of a performance of the G-UNIV test gyroplane flying selected manoeuvres with different levels of aggressiveness with the aim to make suggestions for the design of the slalom and acceleration-deceleration courses for the flight test programme. Finally, this chapter provides validation results for the developed inverse simulation package GENISA/GSIM.

## 5.2 Evolution of Rotorcraft Inverse Simulation

An inverse simulation algorithm calculates the pilot control inputs that will force a vehicle to fly a specified manoeuvre. The inverse simulation usually employs one of two different methods, numerical differentiation or numerical integration. The differentiation method was first successfully used by Thomson (1986) to quantify helicopter agility. Since this time, the University of Glasgow has become a centre of excellence in the development and research of the inverse simulation problem. The first inverse simulation algorithm was called HELINV (Thomson and Bradley, 1990a), which used the Royal Aerospace Establishment's helicopter mathematical model HELISTAB (Padfield, 1981). The HELINV algorithm was based on a numerical differentiation approach. Eleven state equations and four constraint nonlinear equations are reduced to seven nonlinear algebraic equations with seven unknowns (the four control inputs, roll and pitch attitude angles, and rotorspeed), and then solved using the discrete Newton-Raphson method (Thomson and Bradley, 1998). Backward differentiation of the aircraft attitude angles allows calculation of the attitude rotational rates; similarly, the rate of change of the rotorspeed is obtained by backward differentiation of the rotorspeed. Finally, the equations of motion can be solved for the unknown attitude angles, and control angles can be obtained from the rotor dynamics model. Nannoni and Stabellini (1989) used the same differentiation approach in the code NFPATH to solve the helicopter inverse problem for the preliminary design purposes. Similarly, Thomson and Bradley (1990b; 1998) proposed to use inverse simulation as a tool for the configurational design of the helicopter.

A helicopter generic simulation model, HGS (Thomson, 1992) was incorporated into the HELINV algorithm by Thomson and Bradley (1997b; 1998). The HGS model is nonlinear with seven degrees of freedom (six body modes and rotorspeed). This model has a disc representation of the main and tail rotors, and includes a multiblade description of main rotor flapping, dynamic inflow and look-up tables for helicopter fuselage aerodynamics.

The numerical integration technique for helicopter inverse simulation was proposed by Hess *et al* (1991). Dividing the initial flight trajectory into small intervals, the nonlinear equations of motion are integrated and compared with desired trajectories. A Newton-Raphson iterative scheme was applied to minimise the error vector. The advantages of the developed algorithm were demonstrated by examples from inverse simulation of F-4C and F-16 aircraft and Bo 105 helicopter manoeuvres (Hess *et al*, 1991; Hess and Gao, 1993; Gao and Hess, 1993).

Rutherford and Thomson (1996) used the same approach in a numerical integration algorithm called GENISA (Generic Inverse Simulation Algorithm). A comparison between HELINV and GENISA algorithms (Rutherford, 1997) showed that the two methods compare favourably, the only significant difference being that the GENISA algorithm is an order of magnitude slower than HELINV. However, GENISA demonstrated flexibility and scope for simulating different type of flying vehicles, which makes this algorithm suitable for a wide range of research applications, including the study of handling qualities. This was a principal reason for choosing the GENISA algorithm as a basis for the research described in this thesis.

A helicopter individual blade rotor model, HIBROM, was developed at Glasgow (Rutherford and Thomson, 1997). This model, in contrast to HGS, describes the helicopter blade dynamics separately. More detailed discussion of the model is provided in Chapter 4. Rutherford and Thomson (1997) compared inverse simulation results of the GENISA/HIBROM algorithm with those of the GENISA/HGS. The individual blade model showed several advantages in being incorporated into the GENISA algorithm. However, the HIBROM model made several assumptions, such as constant rotorspeed. Doyle and Thomson (2000) modified HIBROM by incorporating an engine governor model; thereby a rotorspeed degree of freedom was added to the model.

Helicopter inverse simulation has found many other applications. The inverse simulation technique was used to provide an improved simulation validation tool (Gray and von Grünhagen, 1998). A nonlinear helicopter simulation code SIMH, used in this research, was developed by the Institute of Flight Mechanics at DLR. The research

demonstrated a benefit in using the inverse simulation in the validation process of a helicopter simulation. The inverse simulation approach was also used for studying a helicopter in flight (Cao, 2000) and for helicopter gaming simulation (Cao and Su, 2002). In these papers, inverse simulation was based on the mathematical principle of solving nonlinear problems in least squares. The vehicle equations of motion were not linearised, hence making the algorithm flexible for simulating any kind of manoeuvring flight. Avanzini and de Matteis (2001) proposed the inverse simulation algorithm based on the integration approach and the time scale separation concept (Chen and Khalil, 1990). A six-degree-of-freedom model of the Bell AH-1G rotorcraft without engine dynamics and stability augmentation was used in this study. This method demonstrated high accuracy and numerical stability, and was approximately an order of magnitude faster than the numerical integration methods. Another way of looking at this problem was proposed by Celi (1999). The inverse simulation algorithm developed in this work was based on numerical optimisation. This methodology operates on a family of possible trajectories and control inputs, and by use of special criteria, the proper ones can be selected. The method was applied to the slalom manoeuvre from the ADS-33D (1994) standard.

Inverse simulation has become a very useful tool in estimating rotorcraft handling qualities and workload. In the ADS-33E-PRF (2000) handling qualities requirements flight test manoeuvres are provided in the form of precisely defined mission task elements. Mathematical representation of the MTEs (Thomson and Bradley, 1997a; 1997b) can be used as an input for the inverse simulation algorithm to calculate the pilot control inputs, which allows an estimate of handling qualities and workload. Using this technique, Thomson and Bradley (1994; 1997b; 1998) proposed the inverse simulation algorithm HELINV as a tool for preliminary assessment of helicopter handling qualities and workload. Attitude and control quickness parameters were estimated and compared for different levels of aggressiveness of the Lynx helicopter manoeuvres. It should be stated that an important conclusion was made from these studies that validity of inverse simulation is equivalent to validity of conventional simulation based on the same helicopter model.

### 5.3 Generic Inverse Simulation Algorithm GENISA

The detailed description of the GENISA algorithm was given by Rutherford and Thomson (1996), therefore in this thesis only primary aspects of the algorithm will be considered. In general, the aircraft dynamics may be described by the nonlinear equations of motion in the following standard form of the initial value problem

$$\dot{\mathbf{x}} = f(\mathbf{x}, \mathbf{u}); \quad \mathbf{x}(0) = \mathbf{x}_0 \quad (5.1)$$

$$\mathbf{y} = g(\mathbf{x}), \quad (5.2)$$

where  $\mathbf{x}$  is the system state vector,  $\mathbf{u}$  is the control vector, and  $\mathbf{y}$  is the output vector. The aim of inverse simulation algorithm is to calculate the control time histories  $\mathbf{u}$  from a predefined output vector  $\mathbf{y}$ . In particular, for the gyroplane application the state and control vectors are

$$\mathbf{x} = [U \quad V \quad W \quad P \quad Q \quad R \quad \Phi \quad \Theta]^T, \quad (5.3)$$

$$\mathbf{u} = [\theta_{shaft} \quad \phi_{shaft} \quad T_{prop} \quad \delta_{rud}]^T, \quad (5.4)$$

where  $\theta_{shaft}$  and  $\phi_{shaft}$  are the longitudinal and lateral rotor shaft angles,  $T_{prop}$  is the propeller thrust, and  $\delta_{rud}$  is the rudder angle.

It should be stated that the gyroplane controls differ from those of the helicopter, the gyroplane pilot controls the direction of rotor thrust by tilting the rotor shaft using the control stick. The gyroplane controls also include rudder pedals and throttle with operating principles similar to those of the small aeroplane.

The basic concept of the GENISA algorithm consists of the following. The initial flight trajectory is divided into small time intervals, forming the series of time points  $t_k$ .

Integrating the given system at the time point  $t_k$ , the estimates of state and output vectors can be calculated at the next time point

$$\mathbf{x}(t_{k+1}) = \int_{t_k}^{t_{k+1}} \dot{\mathbf{x}}(t_k) dt + \mathbf{x}(t_k), \quad (5.5)$$

$$\mathbf{y}(t_{k+1}) = \mathbf{g}[\mathbf{x}(t_{k+1})]. \quad (5.6)$$

The desired output vector is obtained from the mathematical representation of the manoeuvre (the next section describes this process in detail). Displacements  $x_e(t)$ ,  $y_e(t)$ ,  $z_e(t)$  relative to an Earth frame of reference can form an input for the inverse simulation algorithm. The aircraft's velocities and accelerations are obtained by differentiation. The desired output vector is then compared to the integrated equations of motion. Thus, the error function can be formed

$$\mathbf{y}_{error}(t_{k+1}) = \mathbf{y}(t_{k+1}) - \mathbf{y}_{desired}(t_{k+1}). \quad (5.7)$$

The Newton-Raphson method can be used to minimise the error vector and find the required control vector

$$\mathbf{u}(t_k)_{n+1} = \mathbf{u}(t_k)_n - \mathbf{J}^{-1} \mathbf{y}_{error}(t_{k+1})_n, \quad (5.8)$$

where  $n$  indicates the  $n$ th iteration of the Newton-Raphson solver at the current time point, and  $\mathbf{J}$  is the Jacobian matrix

$$\mathbf{J} = \left[ \frac{\partial \mathbf{y}_{error i}(t_{k+1})_n}{\partial \mathbf{u}_j(t_k)_n} \right]. \quad (5.9)$$

The Jacobian is calculated numerically using central differencing scheme. When actual and desired outputs match within defined tolerance, the process is repeated for the next time point.

To avoid inverting the Jacobian matrix the GENISA algorithm uses a modified form of the Newton-Raphson scheme

$$\mathbf{u}(t_k)_{n+1} = \mathbf{u}(t_k)_n - \mathbf{u}_{error}(t_k)_n, \quad (5.10)$$

where control error vector is evaluated by solving the system

$$\mathbf{J} \mathbf{u}_{error}(t_k)_n = \mathbf{y}_{error}(t_{k+1})_n. \quad (5.11)$$

The linear system (5.11) can be solved using LU factorisation, or singular value decomposition algorithms. Such an approach is more accurate and stable for a wider range of Jacobians (Rutherford, 1997).

Rutherford and Thomson (1996; 1997) demonstrated that the accuracy and stability of the GENISA algorithm are strongly affected by the calculation time step, which should be chosen carefully within limited range because of the two reasons. Too large a time step (approximately 0.05 sec or greater) is not acceptable in inverse simulation of modern, advanced rotorcraft models due to the fact that these models include high-frequency dynamics of rotor blade flapping. Conversely, too small a time step (approximately 0.01 sec or less) causes instability of the solution predicted by Lin *et al* (1993, cited Rutherford and Thomson, 1996; 1997). A proof of existence of these two types of instability was provided by Rutherford and Thomson (1996), results obtained from inverse simulation of the Lynx helicopter manoeuvres showed unstable oscillations of the solution.

To improve numerical stability, Rutherford and Thomson (1996; 1997) suggested that the error function  $\mathbf{y}_{error}$  from equation (5.7) should be based on aircraft's accelerations rather than displacements. Results from this study showed a significant improvement of

stability of inverse simulation solution. Thus, the flight trajectory can be defined in terms of the vehicle's Earth referenced accelerations  $\ddot{x}_e(t)$ ,  $\ddot{y}_e(t)$ ,  $\ddot{z}_e(t)$ , and, for example, heading attitude rate  $\dot{\Psi}(t)$ , thereby forming the desired output vector in a new form

$$\mathbf{y}_{desired}(t) = [\ddot{x}_e(t) \quad \ddot{y}_e(t) \quad \ddot{z}_e(t) \quad \dot{\Psi}(t)]^T. \quad (5.12)$$

As was noted by Cameron (2002, p.62), the fourth constraint as heading attitude rate  $\dot{\Psi}(t)$  in equation (5.12) is appropriate for manoeuvres where change of heading angle is not required (for example, the acceleration-deceleration). However, if manoeuvre definition requires a change in heading, then it is more relevant to use the sideslip rate  $\dot{\beta}(t)$  as a fourth constraint in equation (5.12). In that case, the desired output vector is defined as follows

$$\mathbf{y}_{desired}(t) = [\ddot{x}_e(t) \quad \ddot{y}_e(t) \quad \ddot{z}_e(t) \quad \dot{\beta}(t)]^T. \quad (5.13)$$

For some manoeuvres, such as the slalom, either heading attitude rate  $\dot{\Psi}(t)$  or sideslip rate  $\dot{\beta}(t)$  can be constrained depending on control strategy of the manoeuvre.

The helicopter individual blade rotor model HIBROM (Rutherford and Thomson, 1997) was developed at Glasgow for inclusion in the GENISA algorithm. This model, in contrast to disc models, describes the helicopter blade dynamics separately giving higher fidelity and range of applicability. Unfortunately, the GENISA/HIBROM algorithm has a constant rotorspeed assumption, in other words the time step for inverse simulation is equal to an integer number of main rotor revolutions.

Houston has had a considerable amount of success in investigating gyroplane stability and controllability using the generic simulation model RASCAL (Houston, 1996; 1998; 2000). A recent study (Houston, 1998) revealed that the rotorspeed degree of freedom is very significant for gyroplane simulation. To achieve autorotation, rotorspeed must be

adjusted to give a zero net torque. As the rotorspeed is not constant, the simulation time step is not fixed as it was in the initial GENISA/HIBROM algorithm. Hence, the manoeuvre time cannot be predicted a priori. Doyle and Thomson (2000) proposed a solution for this problem by adding an estimate of the next time point to the control vector. Consequently, the equation (5.4) can be rewritten in the following form

$$\mathbf{u}(t_k) = [\theta_{\text{shaft}}(t_k) \quad \phi_{\text{shaft}}(t_k) \quad T_{\text{prop}}(t_k) \quad \delta_{\text{rod}}(t_k) \quad t_{k+1}]^T. \quad (5.14)$$

Thus, the control time step is recalculated iteratively at each time point. To minimize the error between the actual and desired blade azimuth, the desired output vector is formed

$$\mathbf{y}_{\text{desired}}(t_k) = [\ddot{x}_e(t_k) \quad \ddot{y}_e(t_k) \quad \ddot{z}_e(t_k) \quad \dot{\Psi}(t_k) \quad \psi_{az}(t_k)]^T. \quad (5.15)$$

The next section provides description of the process of mathematical definition of gyroplane test manoeuvres for the handling qualities studies.

## 5.4 Mathematical Modelling of Gyroplane Manoeuvres

The ADS-33E-PRF (2000) standard specifies flight test manoeuvres in the form of precisely defined MTEs. To use the specific MTE as a desired flight path for inverse simulation it is necessary to develop a mathematical representation of it. Thomson and Bradley (1990b; 1997a; 1997b; 1998) proposed and described in detail the appropriate techniques for modelling helicopter manoeuvres, and verified validity of this approach by a comparison between flight test data and inverse simulation results. The approach is based on two methods: (1) global polynomial modelling, and (2) piecewise polynomial modelling. The first method employs polynomial representations of the helicopter parameters essential for the given task (for example, position, velocity and acceleration) for the whole length of the manoeuvre. In contrast to the first, the second method

divides the given course into individual sections, and fits simple polynomials to the desired profiles in each section. An important aspect of the process of choosing the proper polynomials in these two methods is that the polynomials must satisfy the boundary conditions, which are usually specified in the manoeuvre definition.

A library of models of helicopter basic Nap of the Earth manoeuvres was developed at Glasgow during the early stages of developing the inverse simulation package HELINV (Thomson and Bradley, 1990a; 1997a). Later this library was extended to include new manoeuvres from the ADS-33C (1989) and ADS-33D (1994) standards. However, not all rotorcraft manoeuvres are suitable for a light gyroplane mainly because of the fact that a gyroplane cannot hover and laterally reposition as a helicopter can. Thus, only two aggressive manoeuvres, slalom and acceleration-deceleration, were selected for consideration in this research. These manoeuvres were modified and modelled with the aim of using them in inverse simulation and flight test trials of the G-UNIV research gyroplane. Chapter 6, Section 6.5 provides a detailed description of the modified slalom and acceleration-deceleration manoeuvres, while in this section only minimum information essential for inverse simulation is presented.

Thomson and Bradley (1997a, p.308) stated that the global polynomial modelling method is adequate for studies of helicopter flight dynamics and performance, as well as for a validation process. Nevertheless, it was noticed that such an approach might not always be appropriate for the problem of estimation of helicopter handling qualities metrics. This was demonstrated in the example of assessment of helicopter quickness parameters using a sidestep MTE. The smooth profile of the global polynomial representation of the acceleration function did not permit modelling quick, aggressive changes in acceleration suggested by the ADS-33D (1994) document. The importance of adequate modelling of helicopter test manoeuvres for the handling qualities studies was emphasised later by Leacock (2000) and Cameron (2002). For instance, Leacock (2000, p.33) investigated an impact of these two methods of representing the MTEs on handling qualities of the Lynx helicopter flying a sidestep manoeuvre. The comparison revealed that the global polynomial method does not always permit modelling required aggressiveness of the sidestep MTE to meet desired performance requirements. These results are consistent with those of Thomson and Bradley (1997a, p.308). Here it should be noted, that the acceleration-deceleration task is similar to the sidestep in terms of

defining the input acceleration profile, but in contrast to the latter, must be performed on the longitudinal axis. According to the above-mentioned research conclusions, a piecewise polynomial representation of an acceleration profile for the gyroplane acceleration-deceleration manoeuvre was utilised in this dissertation.

However, Thomson and Bradley (1990, p.4), Leacock (2000, p.73) and Cameron (2002, p.19) demonstrated that the global polynomial modelling method is entirely adequate for modelling helicopter slalom manoeuvre. In contrast to the acceleration-deceleration, the slalom manoeuvre is defined by a track of the given course (time history of helicopter lateral displacement). In addition, as a consequence, an aggressiveness level of the slalom manoeuvre has a different nature, resulting from the fact that the slalom has an inherent global aggressiveness. For example, to change the level of aggressiveness of the slalom manoeuvre it is necessary to modify the conditions of the whole course. Meanwhile, in the acceleration-deceleration case, the aggressiveness can be defined locally, in some particular period, for example by decreasing the desired time of an acceleration part of the manoeuvre, initiating this by faster acceleration hence increasing the aggressiveness level of this part of the task. Therefore, from this example, the acceleration-deceleration manoeuvre would have a more aggressive first (or acceleration) part of the course; while the aggressiveness level for the rest of the manoeuvre would remain the same (more detailed discussion will be provided later in this section). The global aggressiveness level of the slalom manoeuvre is usually defined by varying the width and length of the course, with flight velocity to be maintained throughout the course.

In addition, it should be noted that to the best of the author's knowledge, a light gyroplane has never been flight tested for the slalom manoeuvre before, and consequently no flight test data are available to model accurately a flight path for this course. Therefore, one of the objectives of the flight test programme for this study is to record tracks of the slalom courses. To achieve this, the G-UNIV research gyroplane is equipped with a GPS receiver connected with an onboard recording system (Chapter 6, Section 6.3 provides a detailed description of the flight test instrumentation). Thus, at the stage when the gyroplane flight test programme was well advanced, and inverse simulation was used as a preliminary tool to prepare gyroplane manoeuvres and study

behaviour of the test aircraft during these manoeuvres, it was assumed that the global polynomial method would be adequate for modelling the gyroplane slalom manoeuvre.

The following two sections provide detailed description of the processes of modelling the gyroplane slalom and acceleration-deceleration manoeuvres.

### 5.4.1 Slalom Manoeuvre

The slalom manoeuvre (*ADS-33E-PRF, 2000*) must be started in steady level flight with a constant airspeed of at least 60 knots (~70 mph). Figure 5.1 shows the suggested course for the manoeuvre, reproduced from the ADS-33E-PRF standard. However, for a number of reasons (Chapter 6, Section 6.5) it was decided that the G-UNIV gyroplane flight test programme must include a shorter version of the slalom MTE, where the gyroplane pilot has to initiate only one turn to the left and one turn to the right to complete the course. Therefore, the shorter version of the slalom MTE, or minimum slalom, is considered in the process of manoeuvre design and in inverse simulation in general. The description, objectives and desired performance requirements for the gyroplane slalom manoeuvre are presented in more detail in Chapter 6, Section 6.5.

A flight path, or a track in the earth  $x_e - y_e$  plane, of the minimum slalom course is divided into three sections (Figure 5.2) as suggested by Thomson and Bradley (*1990b, p.5*), thus the lateral displacement  $y_e$  can be defined by a function of time, which has to satisfy ten boundary conditions:

$$1) t = 0, \quad y_e = 0, \quad \dot{y}_e = 0, \quad \ddot{y}_e = 0;$$

$$2) t = \frac{1}{3}t_m, \quad y_e = y_{\min}, \quad \dot{y}_e = 0;$$

$$3) t = \frac{2}{3}t_m, \quad y_e = y_{\max}, \quad \dot{y}_e = 0;$$

$$4) t = t_m, \quad y_e = 0, \quad \dot{y}_e = 0, \quad \ddot{y}_e = 0,$$

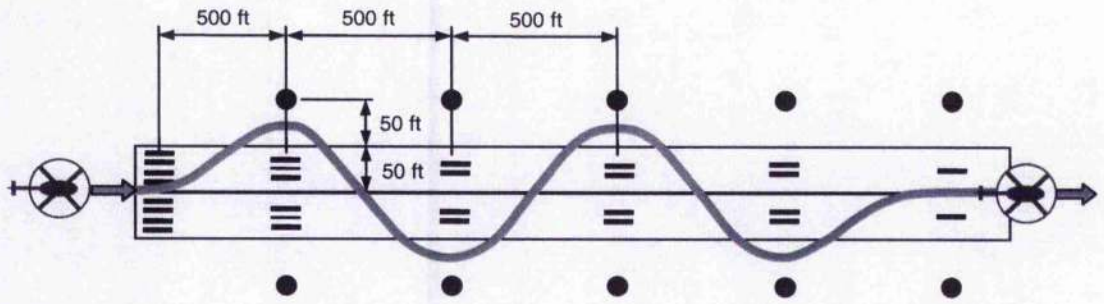


**Figure 5.1** Suggested course for slalom manoeuvre, reproduced from the ADS-33E-PRF (2000)

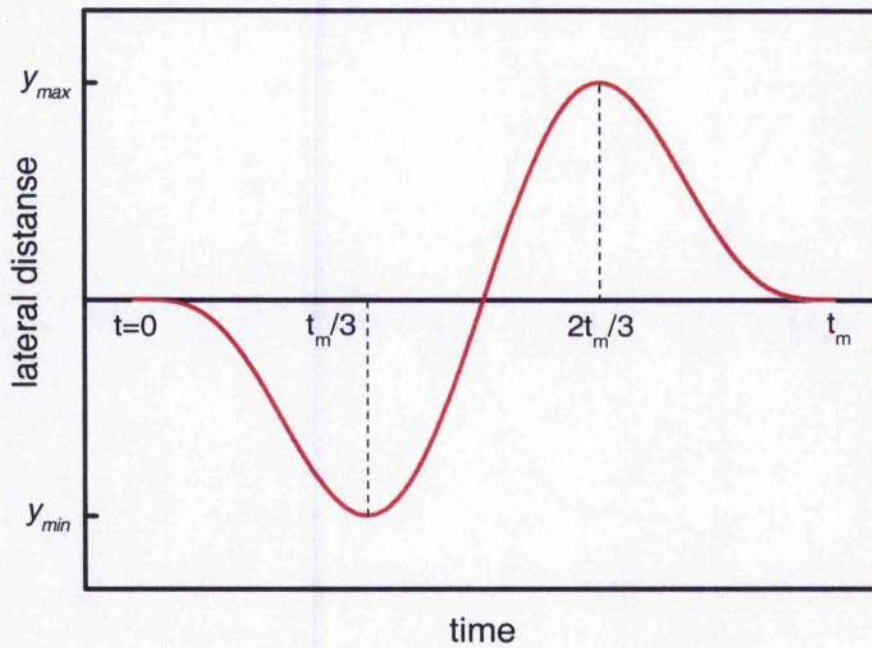


**Figure 5.2** Track for the slalom manoeuvre

where  $y_{\max}$  and  $y_{\min}$  are the maximum and minimum lateral distances from the centreline of the slalom course ( $y_{\max} = -y_{\min}$  for symmetrical track), and  $t_m$  is the time taken to complete the manoeuvre (Figure 5.2).

The simplest function to satisfy these boundary conditions is a polynomial of order nine. It was obtained in the following form

$$y_e(t) = \frac{y_{\max}}{16} \left[ 39366 \left( \frac{t}{t_m} \right)^9 - 177147 \left( \frac{t}{t_m} \right)^8 + 314928 \left( \frac{t}{t_m} \right)^7 - 275562 \left( \frac{t}{t_m} \right)^6 + 118098 \left( \frac{t}{t_m} \right)^5 - 19683 \left( \frac{t}{t_m} \right)^4 \right]. \quad (5.16)$$

The lateral velocity and acceleration can be obtained by differentiation of equation (5.16), and the longitudinal velocity can be found from

$$\dot{x}_e(t) = \sqrt{V_f^2(t) - \dot{y}_e(x)}, \quad (5.17)$$

because altitude is constant during the manoeuvre ( $\dot{z}_e(t) = 0$ ).

The longitudinal displacement  $x_e(t)$  and acceleration  $\ddot{x}_e(t)$  can be calculated by integration and differentiation of expression (5.17) respectively.

#### 5.4.2 Acceleration-Deceleration Manoeuvre

According to the ADS-33E-PRF (2000) standard, the acceleration-deceleration MTE is a linear repositioning manoeuvre in the longitudinal axis and must be started from the hover (Figure 5.3). However, a gyroplane cannot hover; therefore, the initial manoeuvre was modified to suit a light gyroplane such as the G-UNIV research gyroplane. The

pilot has to start this task not in hover, but at a specified airspeed, and fly the gyroplane as fast as possible acquiring maximum acceleration. When the aircraft achieved an adequate longitudinal velocity, an aggressive deceleration is initiated to return the aircraft to the initial airspeed at constant altitude. The detailed description, objectives and desired performance requirements for the gyroplane acceleration-deceleration manoeuvre are presented in Chapter 6, Section 6.5. Thus, the gyroplane acceleration-deceleration manoeuvre in the way it was defined is very similar to that of an aeroplane.

An acceleration function was utilised as a mathematical representation of the acceleration-deceleration course for two reasons: (1) as was noted in Section 5.3 of this chapter, it was revealed (*Rutherford and Thomson, 1996; 1997*) that a desired trajectory in the form of accelerations provides more stable solutions for the GENISA algorithm, and (2) the ADS-33E-PRF standard defines this manoeuvre in terms of accelerations. Thus, it was natural to represent the acceleration-deceleration MTE using an acceleration profile. The suggested profile is shown in Figure 5.4 indicating five sections into which the whole course is divided. It should be noted that the acceleration and deceleration periods,  $t_a$  and  $t_d$  respectively, are defined in the ADS-33E-PRF document such that for Good Visual Conditions (GVE)

$$t_a = t_1 \leq 1.5 \text{ sec}, \quad t_d = t_4 - t_2 \leq 3 \text{ sec}. \quad (5.18)$$

These two parameters, as well as maximum values of acceleration and deceleration,  $\dot{V}_{\max}$  and  $\dot{V}_{\min}$  correspondingly, can be used to model different levels of aggressiveness for the manoeuvre.

Having set the boundary conditions for the five sections of the course in the same way as shown in the subsection describing the slalom manoeuvre, the acceleration function for the acceleration-deceleration course is defined as a set of piecewise smooth polynomial functions in the following manner:

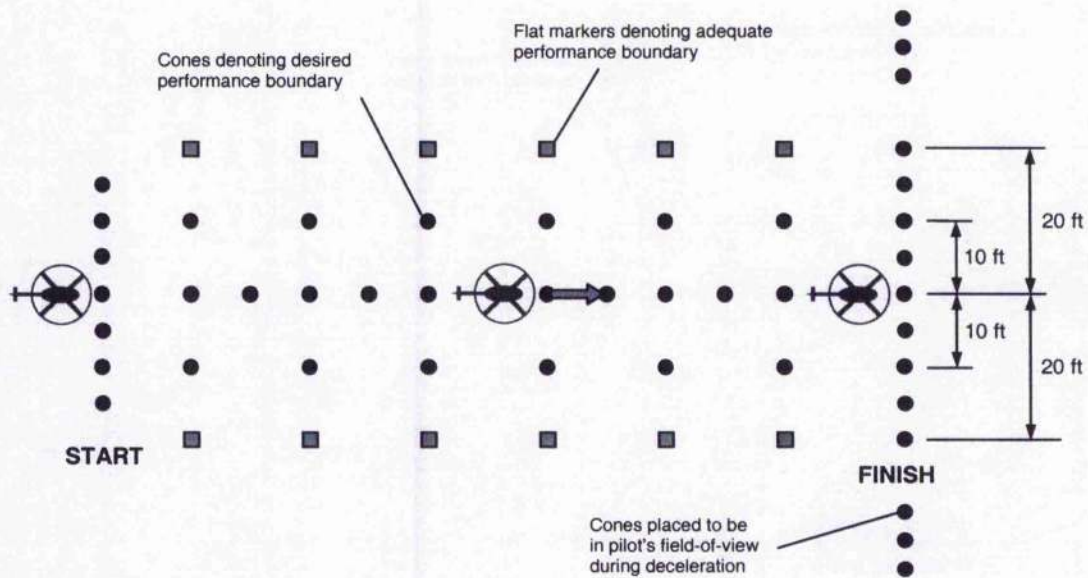


**Figure 5.3** Suggested course for acceleration-deceleration manoeuvre, reproduced from the ADS-33E-PRF (2000)

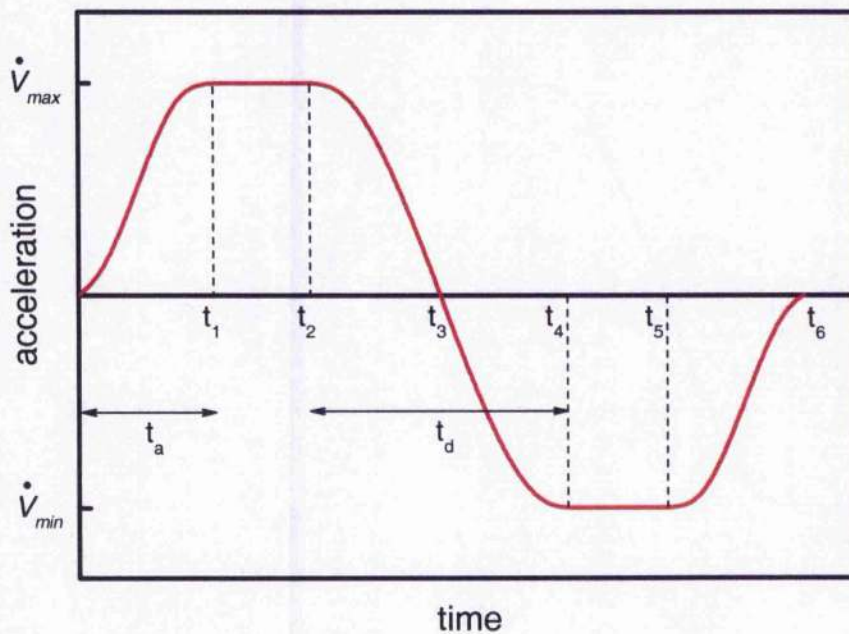


**Figure 5.4** Piecewise polynomial representation of an acceleration profile for the acceleration-deceleration manoeuvre

1) a rapid increase of longitudinal acceleration to a maximum value  $\dot{V}_{\max}$  after a time  $t_a$  seconds:

$$\dot{V}_f(t) = \dot{V}_{\max} \left[ -2 \left( \frac{t}{t_1} \right)^3 + 3 \left( \frac{t}{t_1} \right)^2 \right], \quad 0 \leq t < t_1; \quad (5.19)$$

2) a constant acceleration section to allow the flight velocity to achieve its maximum value  $V_{\max}$ :

$$\dot{V}_f(t) = \dot{V}_{\max}, \quad t_1 \leq t < t_2; \quad (5.20)$$

3) a rapid transition from maximum acceleration to maximum deceleration  $\dot{V}_{\min}$  in a time of  $t_d$  seconds:

$$\dot{V}_f(t) = \frac{\dot{V}_{\max}}{(t_2 - t_4)^3} \left[ (t_2 - t_4)^3 - 4t^3 + 6(t_2 + t_4)t^2 - 12t_2t_4t - 2t_2^2(t_2 - 3t_4) \right], \quad t_2 \leq t < t_4; \quad (5.21)$$

4) a constant deceleration section to allow the flight velocity to be reduced to zero:

$$\dot{V}_f(t) = -\dot{V}_{\max}, \quad t_4 \leq t < t_5; \quad (5.22)$$

5) a rapid decrease in deceleration to bring the gyroplane to the trimmed level flight at time  $t_m$ :

$$\dot{V}_f(t) = \frac{\dot{V}_{\max}}{(t_5 - t_6)^3} \left[ -(t_5 - t_6)^3 + 2t^3 - 3(t_5 + t_6)t^2 + 6t_5t_6t + t_5^2(t_5 - 3t_6) \right], \quad t_5 \leq t \leq t_6. \quad (5.23)$$

It is clear from Figure 5.4, that the time  $t_3$ , at what the flight velocity must achieve its maximum value can be obtained from

$$\int_0^{t_3} \dot{V}_f(t) dt = V_{\max}, \quad (5.24)$$

and the time taken to complete the manoeuvre,  $t_m$  can be calculated from the following condition

$$\int_0^{t_m} \dot{V}_f(t) dt = 0. \quad (5.25)$$

The longitudinal displacement  $x_e(t)$  is evaluated numerically from

$$x_e(t) = \int_0^{t_m} V_f(t) dt, \quad (5.26)$$

while lateral displacement  $y_e(t)$  and yaw angle perturbation  $\psi(t)$  are set to zero to satisfy the ADS-33E-PRF (2000) requirements for this manoeuvre. To be precise, the ADS-33E-PRF defines desired margins for the lateral track and heading angle,  $\pm 10$  ft ( $\sim \pm 3$  m) and  $\pm 10$  deg respectively for the GVE conditions (the same margins are defined for the gyroplane acceleration-deceleration manoeuvre in Chapter 6, Section 6.5), but for inverse simulation purposes, it was assumed that the acceleration-deceleration manoeuvre is performed in ideal conditions when these flight parameters are equal to zero. Vertical displacement  $z_e(t)$  is constant and equal to the given altitude of the manoeuvre (according to the definition of the acceleration-deceleration MTE (ADS-33E-PRF, 2000), altitude during the manoeuvre must be constant).

## 5.5 Inverse Simulation as a Preliminary Tool in Designing Gyroplane Manoeuvres

The culmination of the research presented in this dissertation is the flight test programme for the handling qualities study of the G-UNIV research gyroplane. Two aggressive manoeuvres, slalom and acceleration-deceleration have been chosen for this programme. However, at the initial stages of preparing these manoeuvres for the flight test programme questions have arisen regarding the proper definition of conditions and desired performance for these two gyroplane manoeuvres. To the author's knowledge, a

light gyroplane has never been flight tested for the slalom and acceleration-deceleration manoeuvres before; therefore, it was very difficult to predict the G-UNIV gyroplane behaviour during these courses. Thus, the inverse simulation was proposed as a preliminary tool in the process of designing gyroplane test manoeuvres for handling qualities studies. The gyroplane simulation model GSIM (Chapter 4), modified generic inverse simulation algorithm GENISA (Chapter 5, Section 5.3), and mathematical models of the slalom and acceleration-deceleration manoeuvres (Chapter 5, Section 5.4) form the core of the developed simulation package GENISA/GSIM, which allows the investigation of the performance of the test gyroplane during the tasks with different levels of aggressiveness, and, as a final result, suggests proper desired performance standards for the selected manoeuvres.

For both manoeuvres, the main parameters of the inverse simulation algorithm are selected as follows: solution time step,  $\Delta t$ , is set equal to the time of one rotor turn; number of intermediate integrations per interval,  $n_{int} = 25$ ; control perturbation size,  $\delta u = 1 \times 10^{-2} \times control$ ; convergence tolerance,  $\varepsilon = 1 \times 10^{-12}$ .

### 5.5.1 Slalom Manoeuvre

The aim of this part of the work is to investigate the performance of the G-UNIV gyroplane flying the slalom manoeuvre with different levels of aggressiveness. The metrics of aggressiveness of the slalom manoeuvre are the Aspect Ratio (AR) of the course and airspeed to be maintained throughout the task. The AR of the slalom course was defined as the ratio of width to length of the course, the same way as defined by Padfield *et al* (1994, p.5)

$$AR = \frac{W}{L} = \frac{2y_{max}}{L}, \quad (5.27)$$

where  $W$  is the width and  $L$  is the length of the slalom course. The approach used is to estimate boundaries of the aggressiveness levels of this manoeuvre in terms of the AR

and flight velocity. These results are essential for the process of designing the gyroplane slalom courses (Chapter 6, Section 6.5, and Chapter 7, Section 7.2).

The four gyroplane controls to be calculated from the GENISA/GSIM inverse simulation package are the longitudinal and lateral rotor shaft angles,  $\theta_{shaft}$  and  $\phi_{shaft}$  respectively, the propeller thrust  $T_{prop}$ , and the rudder angle  $\delta_{rud}$ . The first three constraints of the desired output vector are the gyroplane's Earth referenced accelerations  $\ddot{x}_e$ ,  $\ddot{y}_e$ ,  $\ddot{z}_e$ ; the fourth constraint can be either heading attitude rate  $\dot{\psi}$  or sideslip rate  $\dot{\beta}$ , as shown in equations (5.12) and (5.13) respectively. This choice fully depends on the pilot's subjective decision about what kind of control strategy must be employed to complete the manoeuvre. Thus, at this preliminary stage, it was decided to investigate both scenarios of the pilot control strategy.

Figure 5.5 shows comparison of inverse simulation results for the gyroplane minimum slalom manoeuvre ( $h = 20$  m;  $V_f = 70$  mph ( $\sim 60$  knots);  $AR = 0.067$ ;  $L = 450$  m ( $\sim 1500$  ft);  $y_{max} = 15$  m ( $\sim 50$  ft);  $t_m = 14.4$  sec) with the constrained sideslip rate and constrained heading attitude rate. It should be noted that the AR and flight velocity of this slalom course coincide with that of the ADS-33E-PRF (2000) depicted in Figure 5.1, the only difference is that the selected course is shorter.

It can be seen from Figure 5.5 that pilot workload in the lateral axis for the both control strategies is not high (the inverse simulation predicts only approximately 23% stick travel of available range of 18 degrees). Changes in lateral control input are higher than those in longitudinal input, though it should be noted that pilot workload in the longitudinal axis is quite significant (12% stick travel of available range of 18 degrees for the constrained sideslip rate case and 17% stick travel for the constrained heading rate case). These results indicate that the slalom manoeuvre in the form specified in the ADS-33E-PRF (2000) standard, demonstrate a low-moderate level of aggressiveness for the G-UNIV gyroplane.

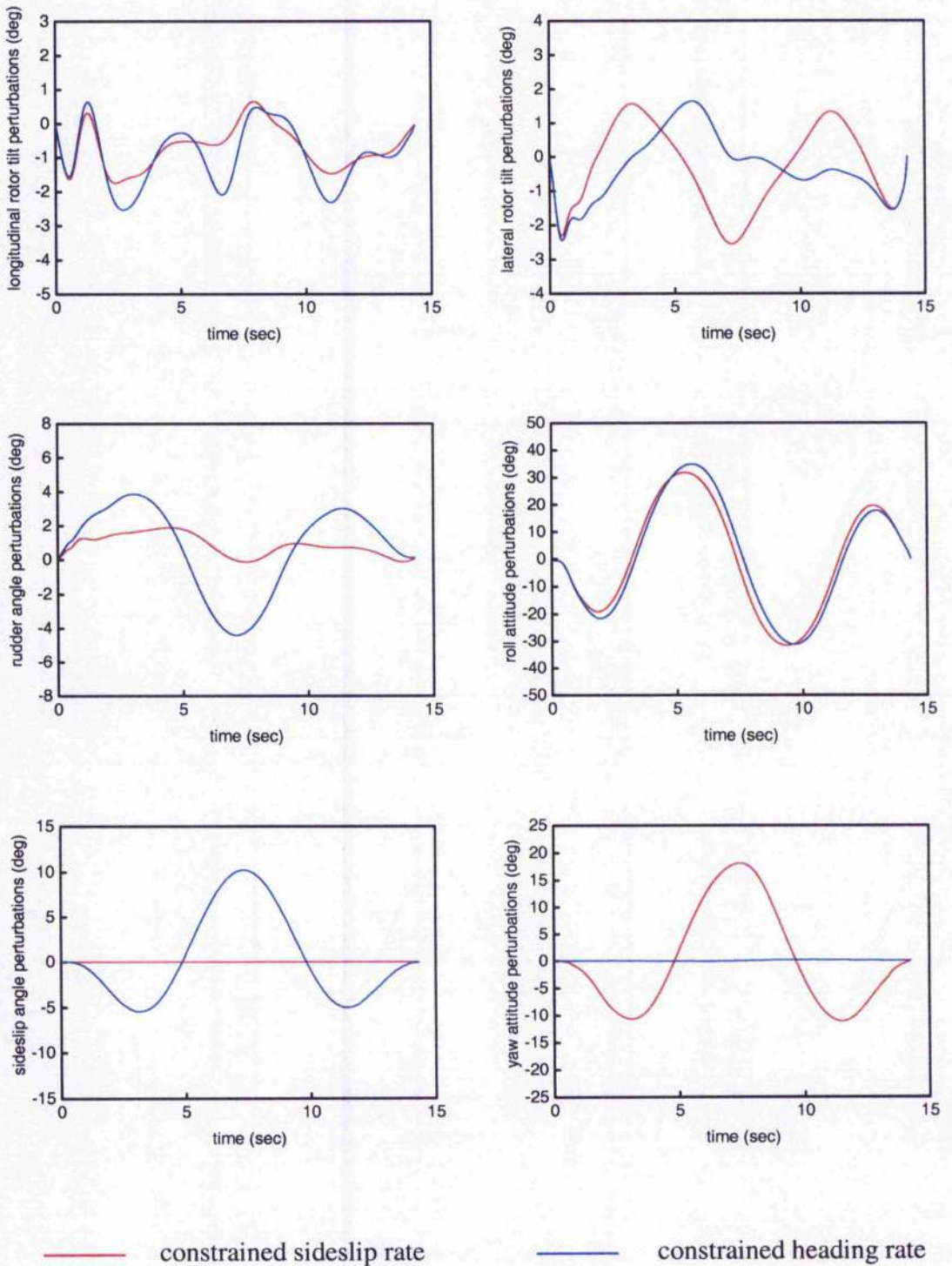


**Figure 5.5** Comparison of inverse simulation results for the G-UNIV gyroplane flying minimum slalom manoeuvre with constrained sideslip rate and constrained heading rate ( $h = 20$  m;  $V_f = 70$  mph;  $AR=0.067$ ;  $L=450$  m;  $y_{max} = 15$  m;  $t_m = 14.4$  sec)

Comparing the results of these two different control strategies, it is obvious that in the case when sideslip rate was constrained the sideslip angle is not changing, and consequently changes in rudder input are not high. Heading angle is changing in a range of approximately 30 degrees. In the constrained heading rate case, the yaw attitude is not changing, while sideslip angle is varying in the range of approximately 16 degrees, and changes in rudder angle are high. It is important to note that the inverse simulation predictions of the roll attitude perturbations are almost similar for both control strategies. Since a light gyroplane has never been flight tested for the slalom manoeuvre before, it was difficult to predict at this stage what control strategy would be chosen by the test pilot during the flight test programme for the G-UNIV gyroplane. It can be only supposed that the test pilot would most likely use both the sideslip and yaw to conduct the slalom task. This question will be discussed later in Chapter 7.

The first factor contributing to the aggressiveness level of the slalom manoeuvre is the AR. A comparison of inverse simulation results for the G-UNIV gyroplane flying the minimum slalom ( $h = 20$  m;  $V_f = 50$  mph;  $y_{\max} = 15$  m; constrained sideslip rate) with various ARs (0.067; 0.1; 0.13; 0.15) is presented in Figures 5.6 and 5.7. It can be seen that higher ARs require larger lateral control inputs, thereby increasing the level of aggressiveness of the course and pilot workload. At some point somewhere between  $AR = 0.13$  and  $AR = 0.15$  (Figure 5.6), the inverse simulation predicts that the rotor shaft would touch the lateral control limit, which is 9 degrees for the test gyroplane. It was stipulated for the purpose of preliminary analysis that only mechanical control limits restrict the ability of the G-UNIV gyroplane to perform the defined slalom course, though it ought to be noted that the frequency of lateral stick oscillations for AR 0.15 slalom (approximately 2.5 rad/sec) lies within the frequency bandwidth typical for the human pilot, which is about 10 rad/sec. Therefore, in this example, the gyroplane's control limits do not allow completion of the desired course, but the human pilot is still able to perform control stick oscillations predicted by inverse simulation. Figure 5.7 indicates that the maximum bank angle required for the slalom manoeuvre is larger for higher numbers of AR. For example, the maximum bank angle for the highly aggressive 50 mph slalom with AR 0.13 is about 50 degrees.

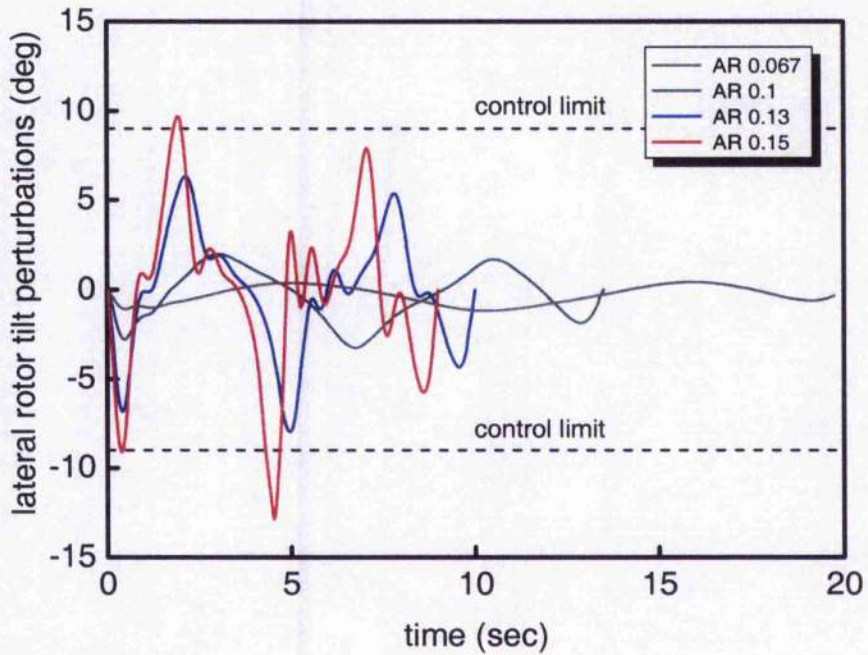


**Figure 5.6** Comparison of lateral rotor tilt perturbations predicted by inverse simulation for the 50 mph slalom with various ARs

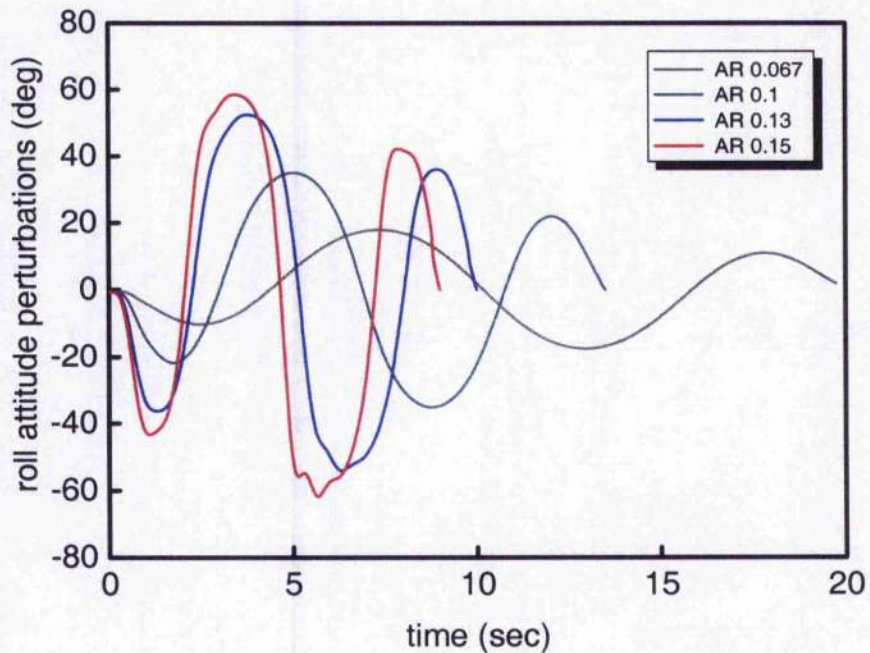


**Figure 5.7** Comparison of roll attitude perturbations predicted by inverse simulation for the 50 mph slalom with various ARs

As a final analysis, the effect of the flight velocity  $V_f$  on the level of aggressiveness of the slalom manoeuvre is investigated. Figures 5.8 and 5.9 show a comparison of inverse simulation results for the G-UNIV gyroplane flying the minimum slalom ( $h = 20$  m;  $AR = 0.11$ ;  $L = 275$  m;  $y_{max} = 15$  m; constrained sideslip rate) with various  $V_f$  (35 mph; 50 mph; 70 mph). It is obvious that airspeed has similar influence to the aggressiveness level of the course as AR has, the higher the airspeed the larger the lateral control inputs and consequently larger bank angles required to complete the task.

As can be seen from Figures 5.7 and 5.9, the maximum bank angles for most aggressive slalom courses do not exceed 50 degrees. It is worth noting that Thomson and Bradley (1990) and Rutherford (1997) defined the slalom manoeuvre for the Lynx and Puma helicopters in a way that the maximum bank angle should be greater than 50 degrees. In comparing the gyroplane performance during the slalom with that of a helicopter, it is obvious that the test gyroplane cannot produce such high roll attitude angles to complete the slalom courses with high level of aggressiveness.

From the above analysis, the inverse simulation predicts that 50 mph slalom with AR 0.15 and 70 mph slalom with AR 0.11 could not be completed by the G-UNIV gyroplane because control limits of the test gyroplane are exceeded. To estimate boundaries of the aggressiveness levels of this manoeuvre, a number of inverse simulation runs were performed with various ARs and  $V_f$ . The results are summarised in Figure 5.10. With a clear picture of the region where the test gyroplane can complete the slalom courses (i.e. where the gyroplane control limits are not exceeded), and the region where the test gyroplane cannot complete the slalom courses (i.e. where the gyroplane control limits are exceeded), it is possible to estimate the boundary of a flight envelope for the slalom manoeuvre. Figure 5.10 shows predicted flight envelope for the G-UNIV gyroplane minimum slalom course from inverse simulation results. It is noteworthy that constrained sideslip rate case was considered for these inverse simulation runs.

Next, the flight envelope was divided into three regions with low, moderate and high levels of aggressiveness for the slalom manoeuvre. Suggested levels of aggressiveness for the test gyroplane in terms of AR and flight velocity are depicted in Figure 5.11. The

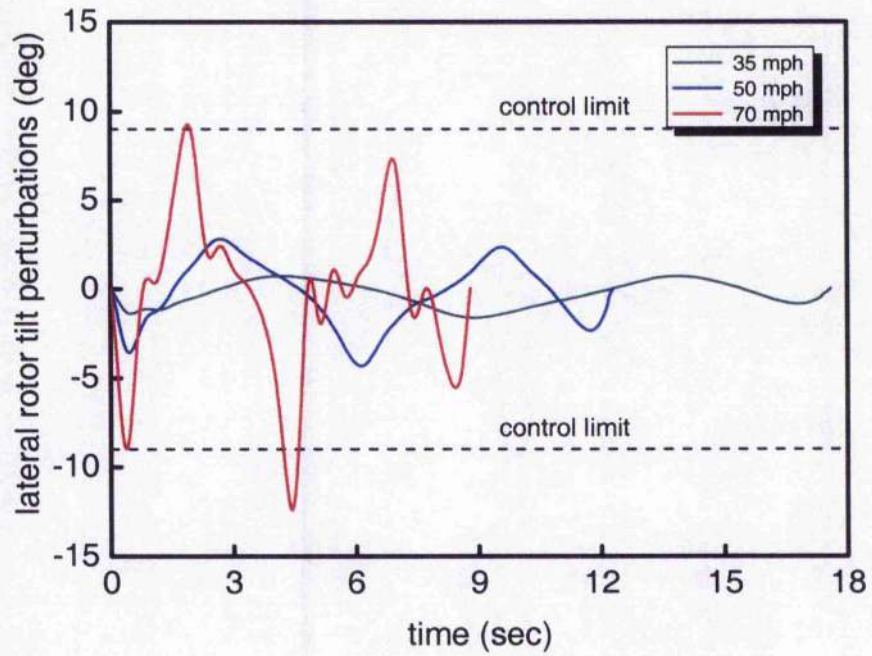


**Figure 5.8** Comparison of lateral rotor tilt perturbations predicted by inverse simulation for the AR 0.11 slalom with various airspeeds

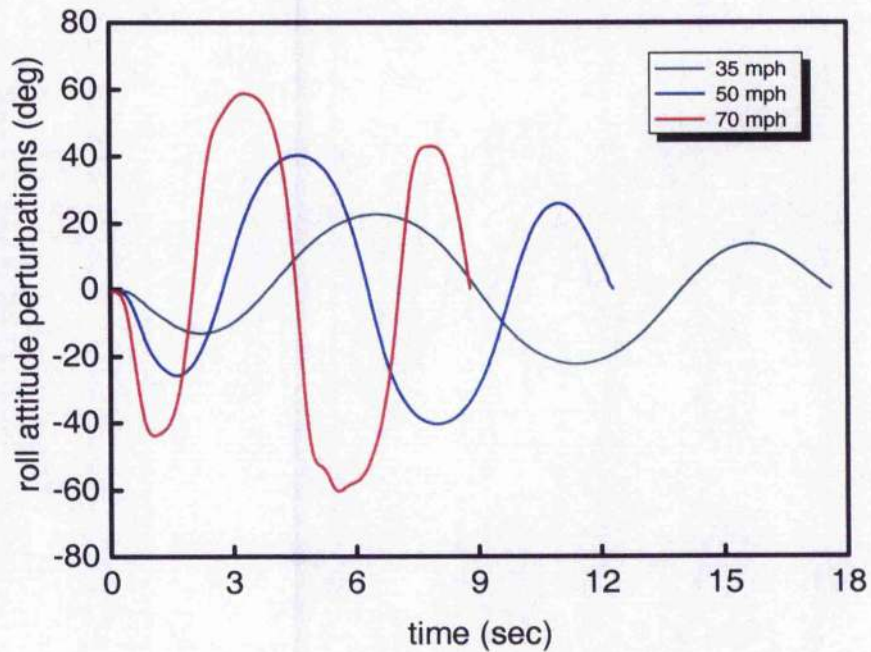


**Figure 5.9** Comparison of roll attitude perturbations predicted by inverse simulation for the AR 0.11 slalom with various airspeeds

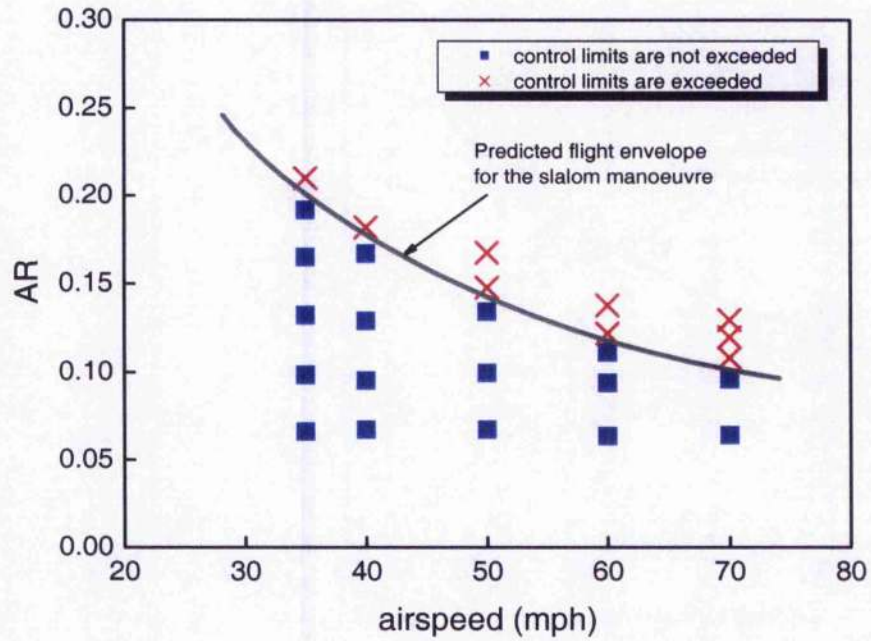


**Figure 5.10** Predicted flight envelope for the G-UNIV gyroplane minimum slalom course from inverse simulation results

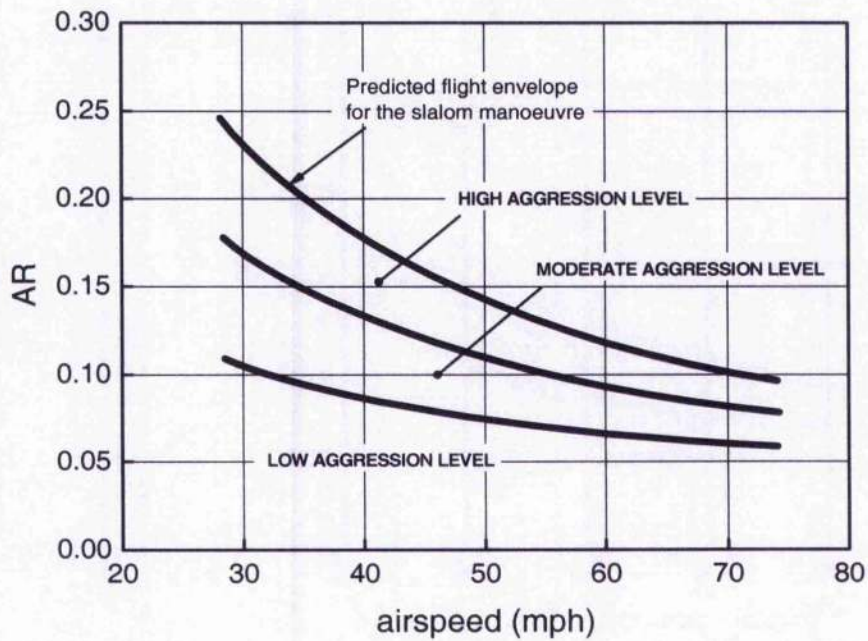


**Figure 5.11** Suggested levels of aggressiveness for the G-UNIV gyroplane minimum slalom course from inverse simulation results

proposed levels of aggressiveness are then used in the process of designing the gyroplane slalom manoeuvre (Chapter 6, Section 6.5), and validated by comparison with pilot subjective HQRs obtained from the flight tests of the G-UNIV research gyroplane (Chapter 7, Section 7.2).

### 5.5.2 Acceleration-Deceleration Manoeuvre

The main objective of the investigation of gyroplane performance during the acceleration-deceleration manoeuvre is to predict appropriate acceleration profile for the test aircraft, and then estimate distances needed to complete the manoeuvre with the selected profile for different speed ranges. The information about distances of the different courses is essential in the stage of preparing the ground course for the manoeuvre, which is discussed in details in Chapter 6, Section 6.5, and Chapter 7, Section 7.2.

The aggressiveness level of the acceleration-deceleration manoeuvre is affected by three parameters, which define the acceleration profile depicted in Figure 5.4. They are: the value of the maximum acceleration  $\dot{V}_{\max}$ , the acceleration period  $t_a$ , and the deceleration period  $t_d$ . For the G-UNIV research gyroplane, the value of maximum acceleration is limited by performance capabilities of a ROTAX TYPE 618 engine and three-bladed fixed pitch IVOPROP propeller, and it was stipulated that the maximum acceleration is approximately  $1 \text{ m/sec}^2$ . This assumption is mainly based on analysis of flight data collected in previous flight tests of the research gyroplane (*Houston and Thomson, 2004*).

The acceleration and deceleration periods of the manoeuvre are defined in the ADS-33E-PRF (2000) document as shown by equation (5.18),  $t_a \leq 1.5 \text{ sec}$ ,  $t_d \leq 3 \text{ sec}$ . These values make the acceleration profile very aggressive, but are still acceptable for modern helicopters. It should be borne in mind that these requirements were designed for the military rotorcraft, which usually have more advanced performance characteristics in comparison to civil ones, and all the more so in comparison with light gyroplanes. For

light gyroplanes, such as the G-UNIV test gyroplane, these requirements are too stringent, and most likely the test gyroplane would be unable to perform such aggressive manoeuvres mainly because of poorer engine performance characteristics. Thus, it was decided to increase the values of  $t_a$  and  $t_d$ , but the question has arisen, what values should be chosen for these metrics of aggressiveness? Figures 5.12 and 5.13 show various acceleration and airspeed profiles for the 40-60-40 mph acceleration-deceleration manoeuvre obtained for different combinations of these two parameters. The first profile (solid red line) satisfies the ADS-33E-PRF requirements ( $t_a \leq 1.5$  sec,  $t_d \leq 3$  sec), and as discussed above, this is a highly aggressive profile, not suitable for the test gyroplane. The test gyroplane would be able to perform, for example, the profiles represented by solid blue and green lines, with  $t_a = 3$  sec,  $t_d = 6$  sec, and  $t_a = 5$  sec,  $t_d = 10$  sec respectively. This can be observed clearly in Figure 5.13, where the airspeed profiles for these two cases are smooth and not saw-toothed. For study purposes, it was assumed that the least aggressive profile among these three, with  $t_a = 5$  sec and  $t_d = 10$  sec, would be the most appropriate to use in an inverse simulation of the G-UNIV gyroplane.

As was expected, the most significant control input of the test gyroplane flying the acceleration-deceleration manoeuvre is the propeller thrust  $T_{prop}$ , or engine power necessary to provide the required thrust. As an example, Figure 5.14 shows the engine power perturbations predicted by the inverse simulation package GENISA/GSIM for the 40-60-40 mph acceleration-deceleration manoeuvre ( $h = 50$  m;  $\dot{V}_{max} = 1$  m/sec<sup>2</sup>;  $t_a = 5$  sec;  $t_d = 10$  sec). A trim value of the G-UNIV gyroplane engine power at airspeed of 40 mph is about 40 kW, thus a maximum power perturbation of approximately 14 kW would not exceed the maximum available power of the ROTAX TYPE 618 engine, which is 55 kW (Table A2.1). It should be noted that the gradient of the engine power curve at the very beginning of the manoeuvre is unrealistically high due to the fact that the gyroplane model GSIM uses a simple engine model with no time lag between control input and simulated response. Most probably, in real flight, this curve would have the same shape but with a time lag of about 2-3 seconds, which is typical for conventional engines (Cook, 1997, p.27). Chapter 7, Section 7.2 provides flight test results for the G-UNIV gyroplane flying the acceleration-deceleration manoeuvre.

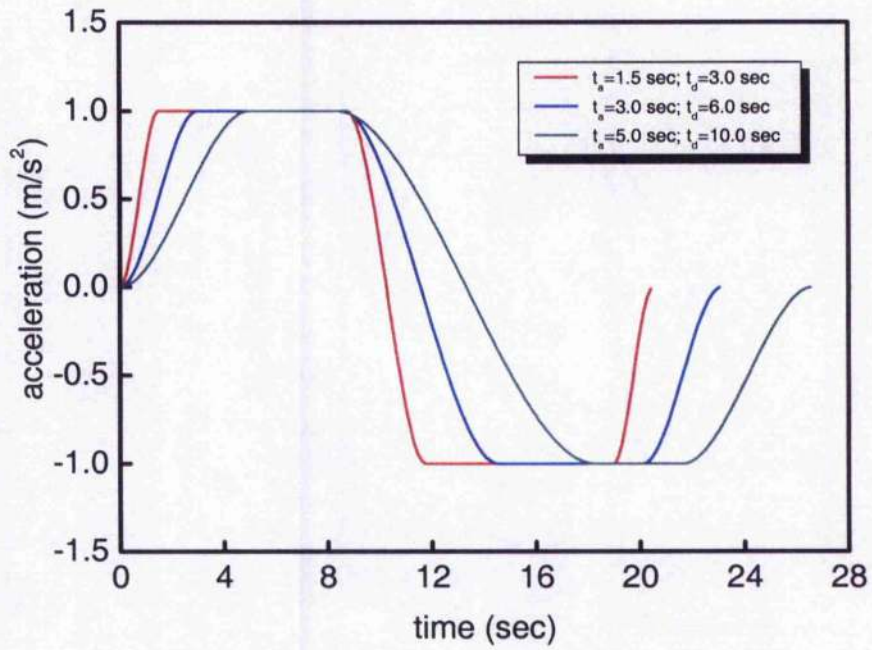


**Figure 5.12** Acceleration profiles for the acceleration-deceleration manoeuvre with different levels of aggressiveness

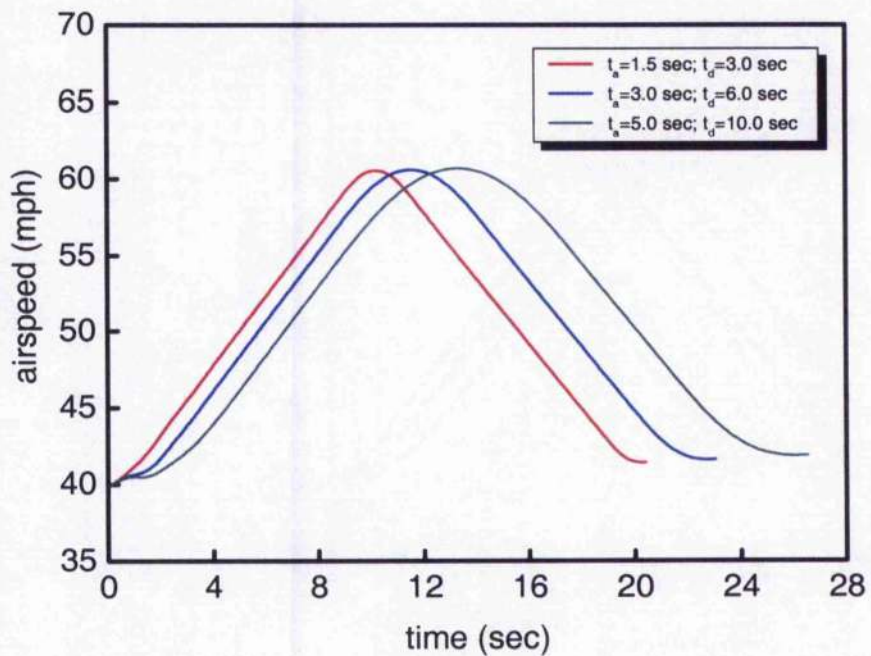


**Figure 5.13** Airspeed profiles for the acceleration-deceleration manoeuvre with different levels of aggressiveness

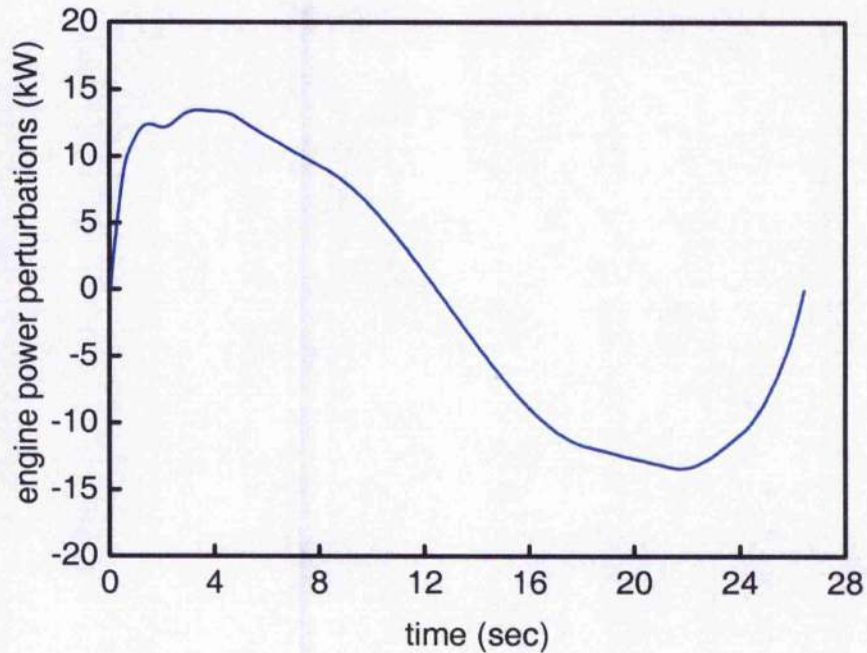


**Figure 5.14** Inverse simulation results for engine power perturbations of the G-UNIV gyroplane flying the acceleration-deceleration manoeuvre

The gyroplane, in contrast to the helicopter, does not use pitch attitude for either acceleration or deceleration. Figure 5.15 presents a comparison of inverse simulation results for the pitch attitude of the G-UNIV gyroplane and Lynx helicopter flying the 40-60-40 mph acceleration-deceleration manoeuvre ( $h = 50$  m;  $\dot{V}_{\max} = 1$  m/sec<sup>2</sup>;  $t_a = 5$  sec;  $t_d = 10$  sec). The results for the Lynx helicopter were calculated using the modified GENISA/HIBROM package (Rutherford, 1997; Doyle and Thomson, 2000). The gyroplane pilot has to decrease pitch angle (solid blue line) by approximately 6 degrees with aim to maintain constant altitude required for the desired performance rather than to initiate acceleration. It should be noted that the change in trim values of the pitch attitude for 40 mph and 60 mph is also about 6 degrees (Chapter 4, Section 4.9, Figure 4.8). As can be seen from Figure 5.15, the pitch attitude profile of the Lynx helicopter (solid red line) is different to the gyroplane's. The helicopter uses negative pitch angles for the acceleration part, and positive pitch angles for the deceleration. In comparison, Figure 5.16 shows inverse simulation results for the pitch attitude of the

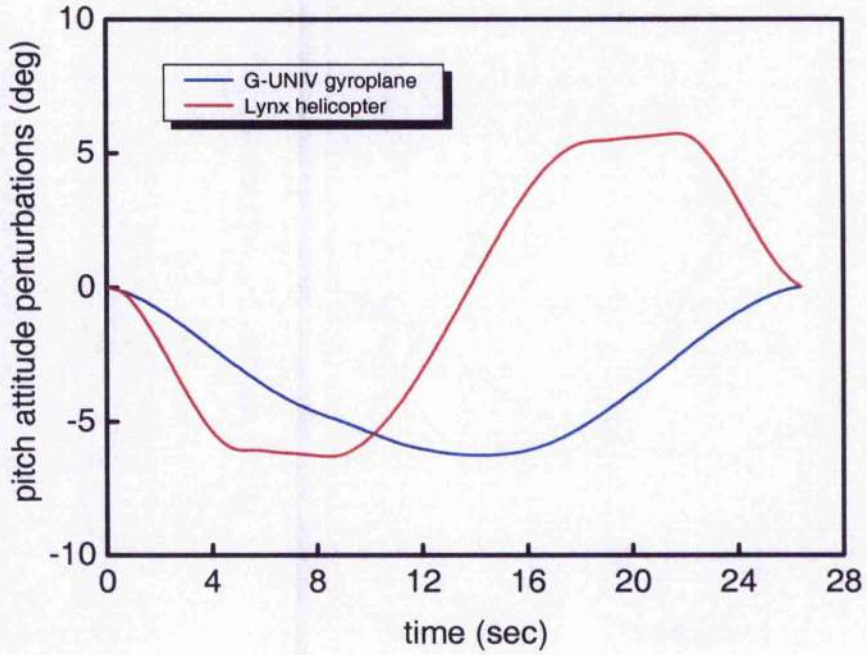


**Figure 5.15** Comparison of inverse simulation results for pitch attitude of the G-UNIV gyroplane and Lynx helicopter flying the acceleration-deceleration manoeuvre

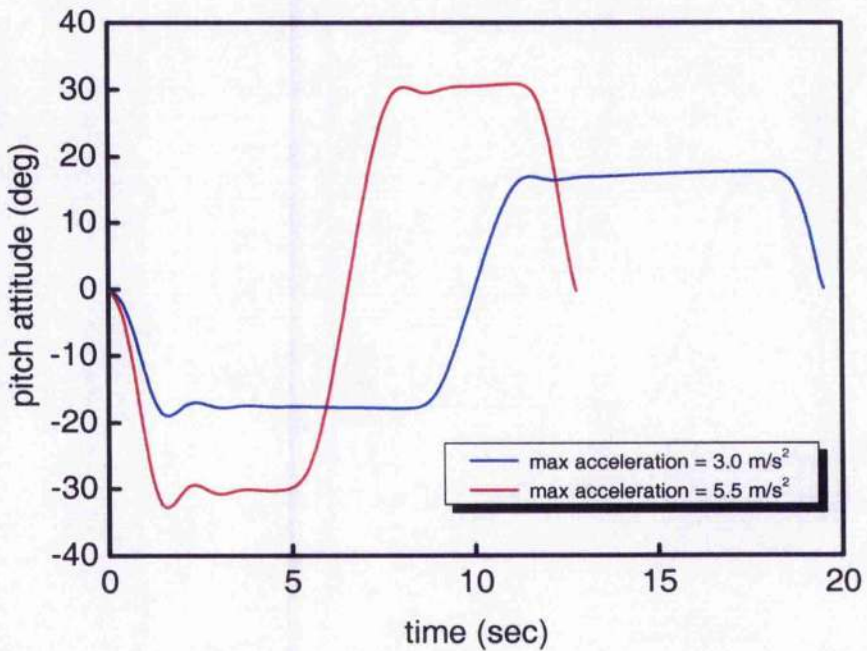


**Figure 5.16** Inverse simulation results for pitch attitude of the Lynx helicopter flying the acceleration-deceleration manoeuvre with two different acceleration profiles

Lynx helicopter flying the 0-50-0 knots acceleration-deceleration manoeuvre ( $h = 15$  m;  $t_a = 1.5$  sec;  $t_d = 3$  sec) with two different acceleration profiles ( $\dot{V}_{\max} = 3$  m/sec<sup>2</sup> and  $\dot{V}_{\max} = 5.5$  m/sec<sup>2</sup>). As can be seen from Figure 5.16, the second profile satisfies the ADS-33E-PRF requirements for the desired performance and GVE conditions (nose-up pitch attitude during the deceleration should be at least 30 degrees above the hover attitude).

Finally, the distance and time needed to complete the acceleration-deceleration manoeuvre with selected profile ( $\dot{V}_{\max} = 1$  m/sec<sup>2</sup>;  $t_a = 5$  sec;  $t_d = 10$  sec) for different speed ranges were estimated. The results are summarised in Table 5.1. The shortest distance was predicted for the 40-50-50 mph course (~357 m); while the longest distance was predicted for the 35-70-35 mph course (~ 954 m). This information about distances is then used in the stage of preparing the ground course for the gyroplane acceleration-deceleration manoeuvre, which is discussed in detail in the next chapter.

**Table 5.1** Estimation of the time and distance for the different acceleration-deceleration courses

Course	Speed range (mph)	$t_m$ (sec)	$x_e$ (m)
1	35 – 60 – 35	31.55	694.65
2	35 – 70 – 35	39.97	953.90
3	40 – 50 – 40	17.52	357.41
4	40 – 60 – 40	26.38	597.24
5	50 – 60 – 50	17.50	435.22
6	50 – 70 – 50	26.52	714.88

## 5.6 Validation of the Inverse Simulation Package GENISA/GSIM

As with most inverse simulation approaches, a key challenge involves the comparison of predicted pilot control inputs and state variables versus actual flight test measurements. In spite of the fact that a flight test technique for the handling qualities study and flight test results are presented in the following chapters (Chapters 6 and 7 correspondingly), it was considered reasonable to provide validation results of the GENISA/GSIM package in this chapter. The validation process is based on two manoeuvres, slalom and acceleration-deceleration, described in detail in the following subsections.

### 5.6.1 Slalom Manoeuvre

Inverse simulation results for the G-UNIV research gyroplane flying two different slalom manoeuvres, [AR 0.13,  $L$  225 m,  $W$  30 m, 70 mph] and [AR 0.2,  $L$  300 m,  $W$  60 m, 70 mph], were compared with the flight test data. To increase the accuracy of the inverse simulation, test data for the actual achieved slalom track (lateral displacement vs. longitudinal displacement) recorded by a GPS receiver (Figures 5.17 and 5.18) were used instead of polynomial representation of slalom tracks described in detail in Section 5.4. Figures 5.19 and 5.20 show comparison results, which can be considered as the validation of the GENISA/GSIM inverse simulation package. It should be emphasised that the sideslip rate was constrained for these inverse simulation runs, though the constrained heading rate can be used as well; a detailed discussion regarding this issue can be found in Section 5.4.

The inverse simulation predictions for the longitudinal and lateral rotor tilt for both examples are close to the flight data. Although some small discrepancies can be seen in longitudinal tilt angles, and the amplitude of lateral control inputs from the flight data is slightly higher than that of the simulation results, most importantly, the trend of these inputs is similar to the test data. The rudder angle perturbations from the flight test

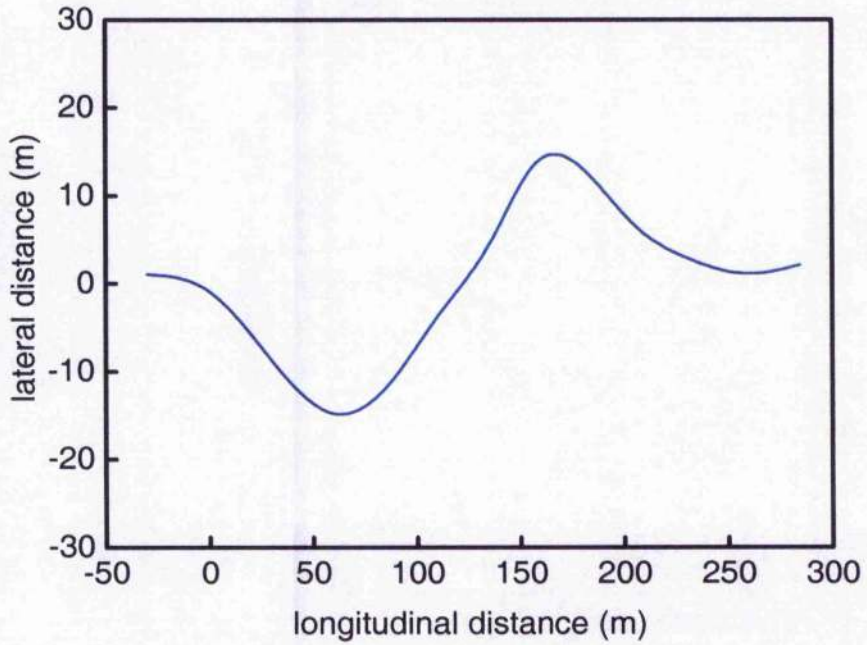


**Figure 5.17** GPS tracking for the gyroplane slalom manoeuvre  
[AR 0.13,  $L$  225 m,  $W$  30 m, 70 mph]

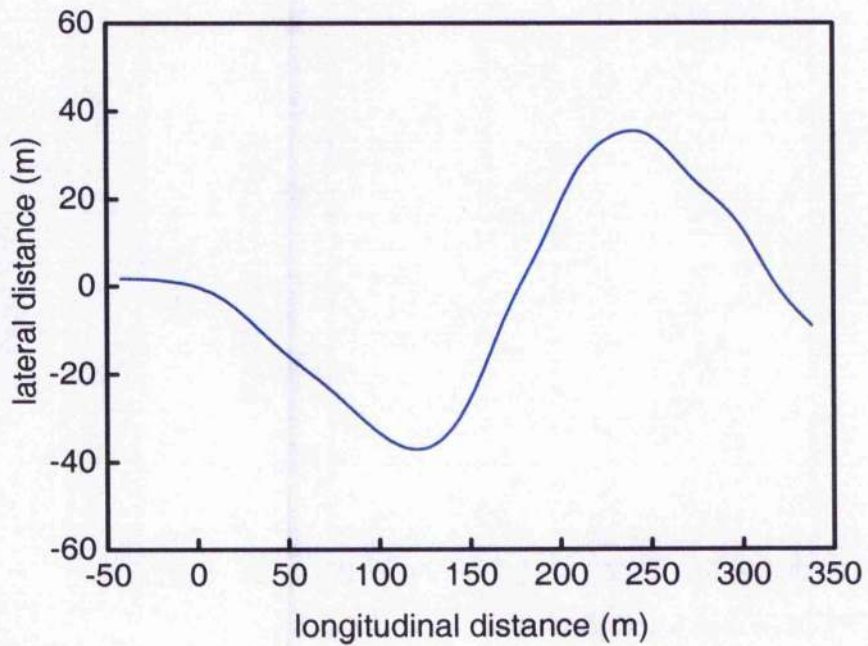


**Figure 5.18** GPS tracking for the gyroplane slalom manoeuvre  
[AR 0.2,  $L$  300 m,  $W$  60 m, 70 mph]

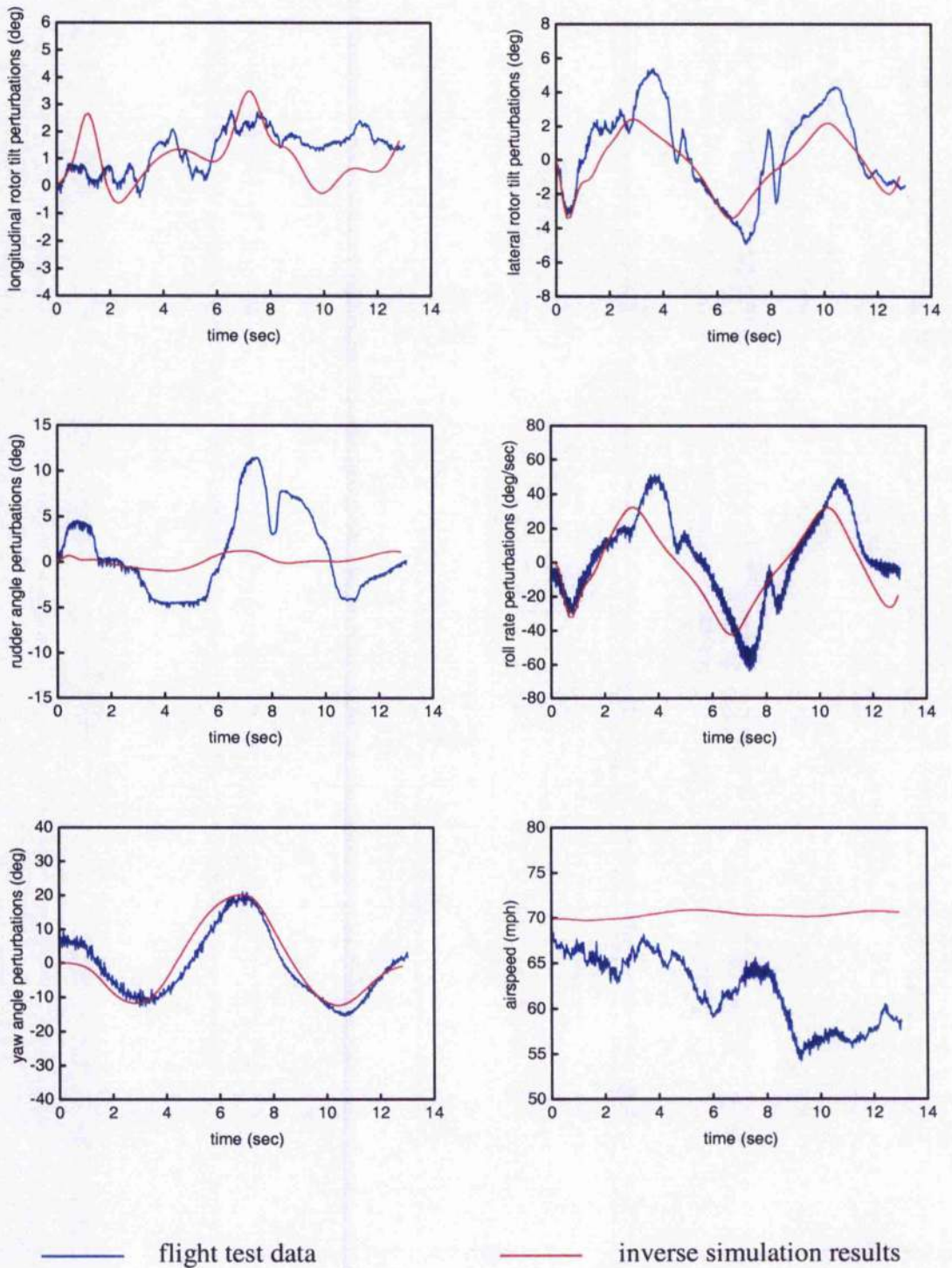


**Figure 5.19** Comparison of flight test data and inverse simulation results for the slalom manoeuvre [AR 0.13, L 225, W 30 m, 70 mph, Trial 1]

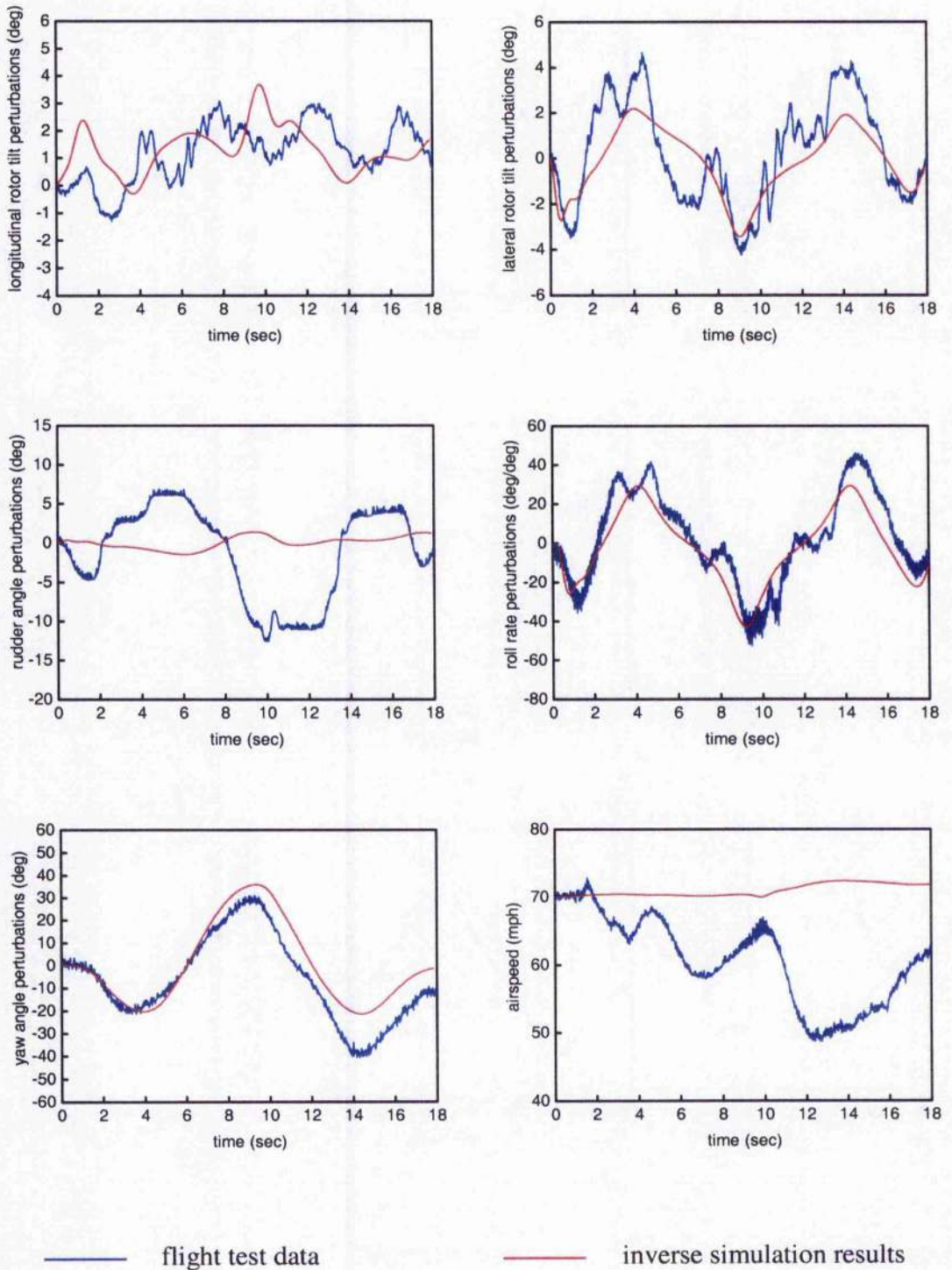


**Figure 5.20** Comparison of flight test data and inverse simulation results for the slalom manoeuvre [AR 0.2, L 300 m, W 60 m, 70 mph, Trial 2]

results are larger than those obtained from the GENISA/GSIM simulation package due to the fact that sideslip rate was constrained for these inverse simulation runs (note the almost constant rudder angles predicted by inverse simulation). A validation of the roll rate shows a favourable flight/simulation comparison for both manoeuvres. It is most important that maximum/minimum perturbations of the roll rate were predicted sufficiently accurately, because these quantities are essential in handling qualities study (for example, in calculation of aircraft quickness parameters).

A comparison of the yaw angle perturbations shows good agreement for both courses, though it should be noted that for the second course depicted in Figure 5.20 the test data indicate that the manoeuvre was finished with approximately -11.6 deg discrepancy of original flight path, which also can be seen in Figure 5.18; while the inverse simulation results predict as expected that yaw perturbations start and end at zero degrees. The flight test results for the yaw attitude do not meet the requirements for the slalom course; according to the requirements, the manoeuvre must be completed on the centreline, in coordinated straight flight.

It can be concluded from the validation results that the inverse simulation algorithm predicted control inputs and state variables fairly well, and the observed flight/simulation discrepancies, which can be seen in Figures 5.19 and 5.20, are most likely due to the inadequacies of the GSIM model. Chapter 4, Section 4.9 provides a detailed analysis of possible sources of modelling errors, and a discussion of how to enhance the gyroplane model. In addition, it should be noted that the test pilot could not maintain constant airspeed in both manoeuvres, which can be also a possible source for the observed discrepancies. Nevertheless, in general the comparison between the flight test data and inverse simulation results for the two different slalom courses has given a good agreement.

### 5.6.2 Acceleration-Deceleration Manoeuvre

Inverse simulation results for the 40-60-40 mph acceleration-deceleration manoeuvre were compared with those from the flight tests of the G-UNIV research gyroplane. Simulation results were calculated for the following conditions:  $\dot{V}_{\max} = 1.05 \text{ m/sec}^2$ ,  $t_a = 4 \text{ sec}$ ,  $t_d = 17$ , where  $\dot{V}_{\max}$  is the maximum value of acceleration, and  $t_a$ ,  $t_d$  are the acceleration and deceleration periods respectively. These parameters are the variables of piecewise polynomial representation of an acceleration profile discussed in detail in Section 5.4; and can be used to simulate different levels of aggressiveness for the acceleration-deceleration manoeuvre. The values for  $\dot{V}_{\max}$ ,  $t_a$ , and  $t_d$  were obtained by an experimental approach from acceleration profile, which was calculated by differentiating the airspeed from the flight test data.

Validation results are shown in Figure 5.21. Inverse simulation results for the longitudinal and lateral rotor tilt angles are sufficiently close to those from the flight data with minor discrepancies. The rudder angle perturbations also show good overall agreement with the test data, though the test pilot used small perturbations during the course. The inverse simulation results for the engine power show unrealistically high gradient at the very beginning of the course. As was discussed in Section 5.5, this is due to the fact that the gyroplane model GSIM uses a simple engine model with no time lag between control input and simulated response. As was predicted there is a small lag of few seconds between simulation results and those from the flight tests. However, in general flight/simulation comparison for the engine power is good.

It should be noted at this point that the pitch attitude was recorded incorrectly during the flight tests because the stabilising period of the angle sensor for the pitch channel was too high for such aggressive manoeuvres as slalom and acceleration-deceleration. Therefore, since the measurements of an angle of attack were recorded correctly, it was decided to compare the angles of attack instead of the pitch attitudes. The comparison depicted in Figure 5.21 shows excellent agreement between the flight and simulation results.

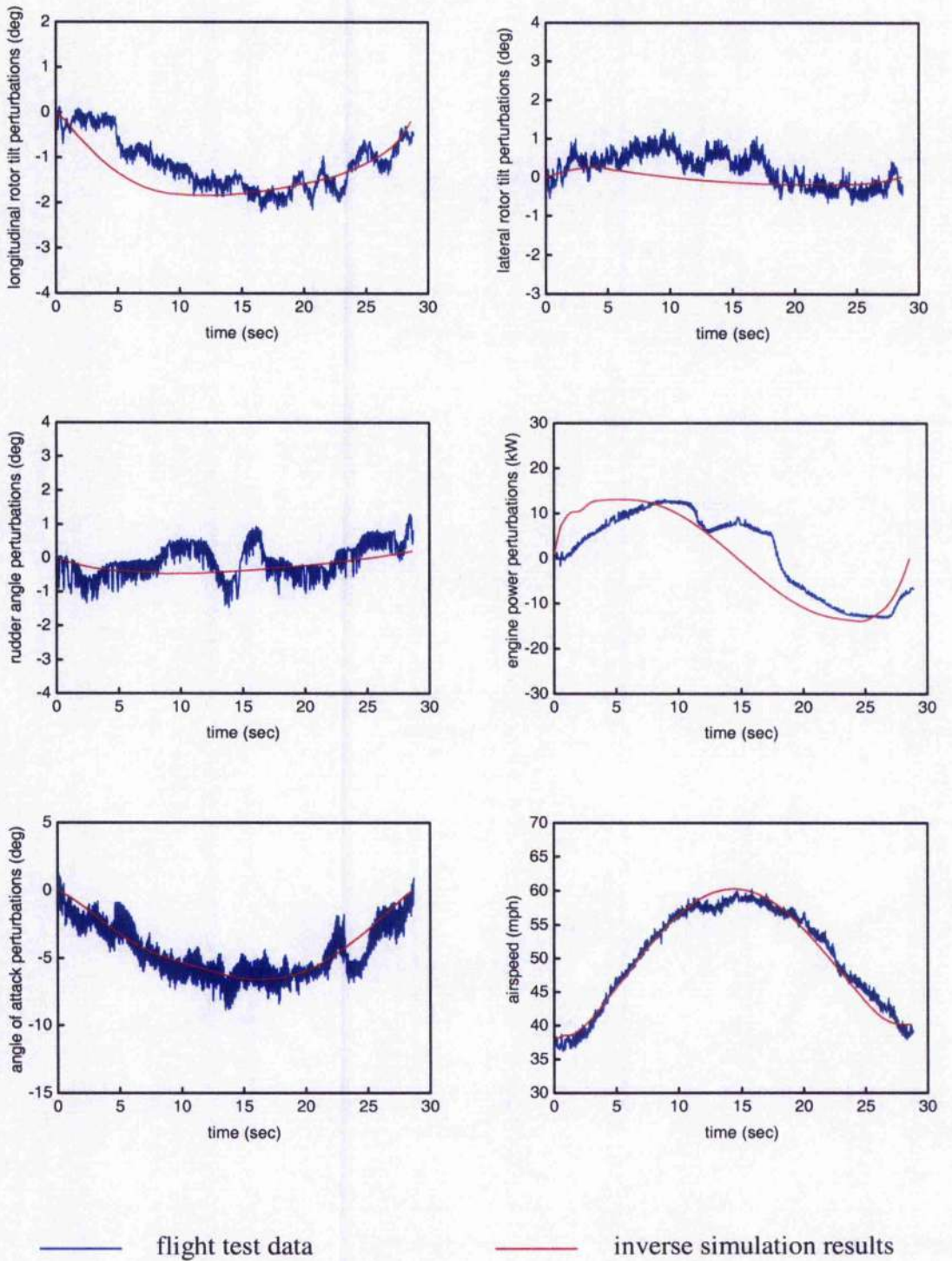


**Figure 5.21** Comparison of flight test data and inverse simulation results for the 40-60-40 mph acceleration-deceleration manoeuvre

## 5.7 Chapter Summary

The chapter has started with a discussion of the evolution of rotorcraft inverse simulation with a brief description of existing algorithms and methods of inverse problem applied to a wide range of rotorcraft flight dynamics studies. A detailed description of the modified inverse simulation algorithm GENISA has been provided with attention placed on improvements implemented to the original version of GENISA. The accuracy and stability of the developed algorithm has been also discussed.

Considerable emphasis has been placed on demonstration of how the slalom and acceleration-deceleration manoeuvres from the ADS-33E-PRF (2000) standard can be adapted to suit a light gyroplane, and then defined mathematically to incorporate them into the GENISA algorithm. As was emphasised in Chapter 4, to reduce the flight test effort required the inverse simulation has been proposed as a preliminary tool in the process of designing gyroplane test manoeuvres for handling qualities studies.

This chapter has provided the first results of the gyroplane inverse simulation. It should be noted that to the best of the author's knowledge the inverse simulation has never been applied to a gyroplane simulation model before. Two different control strategies (constrained sideslip rate and constrained heading attitude rate) for the slalom manoeuvre have been investigated. The effect of AR and airspeed of the slalom course on levels of aggressiveness has been also investigated. The higher the AR and airspeed the larger the lateral control inputs and consequently larger bank angles required to complete the slalom task. As a result, the flight envelope for the gyroplane slalom manoeuvre has been predicted, which must play a role in designing gyroplane slalom manoeuvres for the flight test programme. Finally, based on inverse simulation results the levels of aggressiveness for the gyroplane slalom manoeuvre have been proposed.

For the acceleration-deceleration manoeuvre, the influence of acceleration and deceleration periods of the acceleration profile on aggressiveness level has been investigated with the aim of choosing the most appropriate acceleration profile for the G-UNIV test gyroplane. In addition, the behaviour of the research gyroplane during the

acceleration-deceleration manoeuvre has been compared to that of the Lynx helicopter. It has been concluded that the G-UNIV gyroplane behaves more like an aeroplane rather than a helicopter during this manoeuvre, using mainly engine power, and thus propeller thrust, to accelerate and decelerate. At the end of the chapter, the distance and time needed to complete the acceleration-deceleration manoeuvre with different speed ranges have been estimated. This information is essential for preparing the ground course of this manoeuvre for the flight test programme.

Finally, this chapter has provided the validation results for the developed inverse simulation package GENISA/GSIM. The validation has been conducted by comparison of flight test results with predicted pilot control inputs and state variables. The comparison has been based on the gyroplane slalom and acceleration-deceleration manoeuvres. In conclusion, this chapter has demonstrated that the developed GENISA/GSIM package has proved to be valid for the purpose of designing gyroplane flight test manoeuvres for handling qualities studies.

## **Chapter 6**

# **Flight Testing Technique for Gyroplane Manoeuvres**

### **6.1 Introduction**

This chapter introduces a flight testing technique to study gyroplane handling qualities. The chapter starts with a description of the test aircraft, onboard instrumentation and ground preparations for the flight tests. The calibration procedures and other installation details, as well as calculation of mass, centre of gravity and moments of inertia, are also discussed. Finally, the chapter describes a process of design of gyroplane manoeuvres for the study of handling qualities. Two manoeuvres, slalom and acceleration-deceleration, based on those from the ADS-33E-PRF (2000) standard, are presented and discussed.

### **6.2 Description of the G-UNIV Research Gyroplane**

The research gyroplane was manufactured by Jim Montgomerie Gyrocopters (registration G-UNIV) and is owned by the Department of Aerospace Engineering, University of Glasgow for study and flight test purposes. In fact, the research gyroplane is a converted original two-seat Montgomerie-Parsons gyroplane. The second seat was removed and the space designed for the rear pilot's cockpit was used to house test instrumentation equipment. A picture of the G-UNIV research gyroplane is shown in Figure 6.1.



**Figure 6.1** Glasgow University research gyroplane (reg. G-UNIV)

The gyroplane has a teetering rotor with two blades attached to a hub without flap and lag hinges. The average gross mass during flight tests was approximately 387 kg. The aircraft is powered by a two-cylinder/two-stroke ROTAX TYPE 618 engine, driving a 62-inch diameter, three-bladed fixed pitch IVOPROP propeller. The aircraft has a mechanical control system, and the pilot's controls include the control stick, rudder pedals and throttle. Physical characteristics of the test gyroplane are presented in Table A2.1.

### 6.3 Flight Test Instrumentation

The test gyroplane was equipped with a range of sensors and a main instrumentation pallet, which was used to house a Kontron Elektronik industrial laptop PC and signal conditioning units. The main instrumentation pallet was located behind the pilot cockpit in the space left after removing the second seat. A specially designed glass fibre cover was used to protect all the equipment in the pallet (Figure 6.1). Digital on-board

recording system included National Instruments 12-bit DAQ card and Labview software. The recording system was able to acquire data from a number of channels and various types of transducers during the flight tests with the sampling frequency of 50 Hz. All channels were filtered with fourth order Butterworth low pass anti-aliasing filters at a cut-off frequency of 23 Hz.

Measured parameters and corresponding transducers are presented in Table 6.1. The angular rate sensors (Table A3.1) and angle indicators (Table A3.2) are manufactured by British Aerospace Systems & Equipment. The rate gyroscopes are used to measure the aircraft roll, pitch and yaw angular velocities ( $P$ ,  $Q$ ,  $R$ ), the angle indicators are used to record the Euler angles ( $\Phi$ ,  $\Theta$ ,  $\Psi$ ). The 3-axis accelerometer of Sumitomo Precision Products (Table A3.3) measures the aircraft linear accelerations. The test gyroplane instrumentation also includes a single axis accelerometer (Table A3.4), which is used to measure a vertical acceleration. The necessity to use the second accelerometer is due to the reason that the 3-axis transducer has a measuring range of  $\pm 2$  g in the  $z$ -axis, which is not enough for the gyroplane flight testing. The single axis accelerometer is manufactured by Seika, Scientific Electro Systems, and allows us to measure accelerations in a range of  $\pm 3$  g. All the rate gyroscopes, angle indicators and accelerometers were installed inboard of the main instrumentation pallet and aligned to corresponding gyroplane body axes.

The air data probe of SpaceAge Control includes an airspeed system pitot (Table A3.5) to record static and total air pressure, and hence aircraft velocity components; and two vanes to measure aerodynamic angles of attack and sideslip. The air data probe is mounted on the front of the fuselage to provide undisturbed air flow measurements (Figure 6.1). For the measurement of the ambient air temperature during flight tests, a temperature sensor (RS Components) was employed. Position transducers are manufactured by SpaceAge Control and are used to monitor the position of pilot control inputs for rotor tilt and rudder. Stick position sensors are installed under the pilot's cockpit and measure longitudinal and lateral stick positions, while the rudder sensor is placed at the fin pylon to measure the rudder deflections.

**Table 6.1** Measured parameters and corresponding transducers

Channel Number	Measured Variable	Description	Units	Transducer Type
1	$\theta_{shaft}$	longitudinal rotor tilt	deg	Position transducers (Space Age Control, Inc.)
2	$\phi_{shaft}$	lateral rotor tilt	deg	
3	$\delta_{rud}$	rudder angle	deg	
4	$\Phi$	roll attitude	deg	Angle sensor (Sumitomo Precision Products Ltd.)
5	$\Theta$	pitch attitude	deg	
6	$\Psi$	yaw attitude	deg	
8	$P$	roll rate	deg/sec	Angular rate sensor (British Aerospace Systems & Equipment)
9	$Q$	pitch rate	deg/sec	
10	$R$	yaw rate	deg/sec	
11	$a_z$	vertical acceleration	g	1-axis accelerometer (Seika, Scientific Electro Systems Ltd.)
12	$a_x$	x-axis acceleration	g	3-axis accelerometer (British Aerospace Systems & Equipment)
13	$a_y$	y-axis acceleration	g	
14	$a_z$	z-axis acceleration	g	
15	$T_{air}$	air temperature	deg	Thermocouple (RS components)
16	$\alpha_{vane}$	$\alpha$ -vane angle	deg	Air data probe (SpaceAge Control, Inc.)
17	$\beta_{vane}$	$\beta$ -vane angle	deg	
18	$P_{total}$	total pressure	mbar	
19	$P_{static}$	static pressure	mbar	
21	$h$	height	feet	
25	$\Omega$	rotor speed	rpm	Electro-optical sensors (RS Components)
0	$\Omega_{prop}$	propeller speed	rpm	

The rotor speed and propeller speed are measured by electro-optical sensors of RS Components. Small pieces made by reflective material are placed on the rotor and propeller plates, and the electro-optical devices are installed on static parts of both the rotor and propeller to capture a signal reflecting from rotating plates of the rotor and propeller. Spathopoulos (2001) gives a more detailed description of the test instrumentation, including an error analysis, transducers specifications and photographs.

The gyroplane test instrumentation and onboard computer are powered by an independent power source, which includes two 12 V DC batteries and a 150 W, 12 V to 24 V step-up DC/DC converter. It should be emphasised that this approach has been dictated by flight safety requirements, so in the case of instrumentation failure, none of the gyroplane systems should be affected. All the measured data are stored on the hard drive of the laptop PC. This allows immediate access to the recorded flight data, which is very useful practically, especially during flight tests. For example, the flight data can be checked and analysed after one flight trial to be sure that all the instrumentation devices operate well before performing the next test flight. It should be noted that this procedure takes only about 15 minutes to complete.

For the purposes of handling qualities flight tests, the G-UNIV gyroplane was also equipped with a GARMIN eTrex Summit personal navigator (Figure A3.1), based on GPS technology. Specifications of the personal navigator are summarised in Table A3.7. The GPS receiver was mounted on the top of the laptop PC inside the main instrumentation pallet (Figure 6.2) and connected with the onboard recording system. The GPS data were sampled at 1 Hz and used to track flight paths for slalom and acceleration-deceleration manoeuvres. To summarise, the instrumentation setup of the G-UNIV research gyroplane is shown in Figure 6.3.

It should be noted that the G-UNIV gyroplane has been flight tested previously (Spathopoulos, 2001; Houston and Thomson, 2004). The flight test programme included pre-trials verification of aircraft and instrumentation ("shakedown" flights) at first stage (Carlisle, July 2000); pre-trials test flights, trims and first step/doublet trials (Bournemouth, October 2000); and step/doublet, frequency sweep at the final stage of the programme (Carlisle, February 2001). Since that time, the G-UNIV gyroplane has not been flight tested.



Figure 6.2 The GPS receiver installed in the instrumentation pallet



Figure 6.3 The G-UNIV gyroplane instrumentation setup

## 6.4 Ground Preparations

Ground preparations included calculation of the test aircraft's mass, centre of gravity and moments of inertia, and calibration of the flight test instrumentation. The required calibration procedures of the flight test instrumentation were described in detail by Spathopoulos (2001). Appropriate calibration procedures for each sensor type have been completed during ground preparations of the test gyroplane.

### 6.4.1 Calculation of Mass and Centre of Gravity

Once the test gyroplane has been assembled, its mass and centre of gravity must be estimated. At the time of the flight tests, the research gyroplane's gross mass was estimated to be approximately 387 kg. Previous research (Houston, 1996; 1998; Spathopoulos, 2001) revealed that the position of the centre of gravity affects performance characteristics of a light gyroplane; therefore, the accurate estimation of this quantity was essential. The centre of gravity was measured experimentally along horizontal and vertical axes using weight and balance technique (Houston and Thomson, 2001). The detailed description of this process is given in Appendix 4.

### 6.4.2 Calculation of Moments of Inertia

Moments of inertia of the G-UNIV research gyroplane were estimated earlier using the specially designed test rig (Spathopoulos, 2001). The technique uses pendulum approach, and based on measurements of free oscillations of the aircraft/pilot system. Estimated moments of inertia are listed in Table A2.1. It should be noted, that the yaw moment of inertia was not measured, and was assumed to be of the same order of magnitude as the pitch one. Spathopoulos (2001) provides reasonable explanations for this assumption, based on VPM M16 gyroplane configuration data. The product of inertia  $I_{xz}$  was assumed equal to zero.

### 6.4.3 Calibration of the Flight Test Instrumentation

The air data probe included the airspeed system pitot and sensors for angle of attack and angle of sideslip, and was mounted on the front of the fuselage. Vane angle of attack and angle of sideslip were calibrated using a protractor provided by the manufacturer. The airspeed system was calibrated using a Duck-DPI 610 digital pressure calibrator.

The angle indicators were calibrated using a digital inclinometer. The 3-axis accelerometer was calibrated by measuring the gravity acceleration. This procedure was repeated for all three axes by turning the accelerometer and aligning the direction of measurements with the vertical axis. The rudder position transducer was calibrated using a specially prepared measuring scale.

Because the gyroplane control system is mechanical, i.e. the relationship between the shaft tilt angles and stick position is linear; the shaft tilt angles were used for the calibration procedure. The shaft tilt angles were measured using a dual axis digital clinometer AccuStar II/DAS 20 (Table A3.6). The manufacturer's range for tilt angles was 18 deg both for longitudinal and lateral axes, while the actual measured range for the longitudinal channel is 17.73 deg (maximum fore -0.13 deg, maximum aft 17.6 deg), and the range for the lateral channel is 18.45 deg (maximum left -7.69 deg, maximum right 10.76 deg). The reference point for the longitudinal channel is the maximum fore position of the rotor shaft, and the reference point for the lateral channel is +1.535 deg (right tilt). The rotor is designed this way to compensate for the engine and propeller torque, thus the pilot would have no, or very insignificant, torque to compensate in central position of the control stick.

The longitudinal and lateral rotor tilt angles were calculated as functions with two variables, longitudinal and lateral indications of position transducers. A rectangular slot in the bottom of the pilot cabin limits the travel of the control stick, and it was used to calibrate the stick position transducers. Using two rulers, 99 stick travel points (11 rows and 9 columns) were measured together with rotor tilt angles to form calibration meshes. Figures 6.4 and 6.5 show the calibration surfaces for the longitudinal and lateral channels, obtained from meshes using triangle-based cubic interpolation.

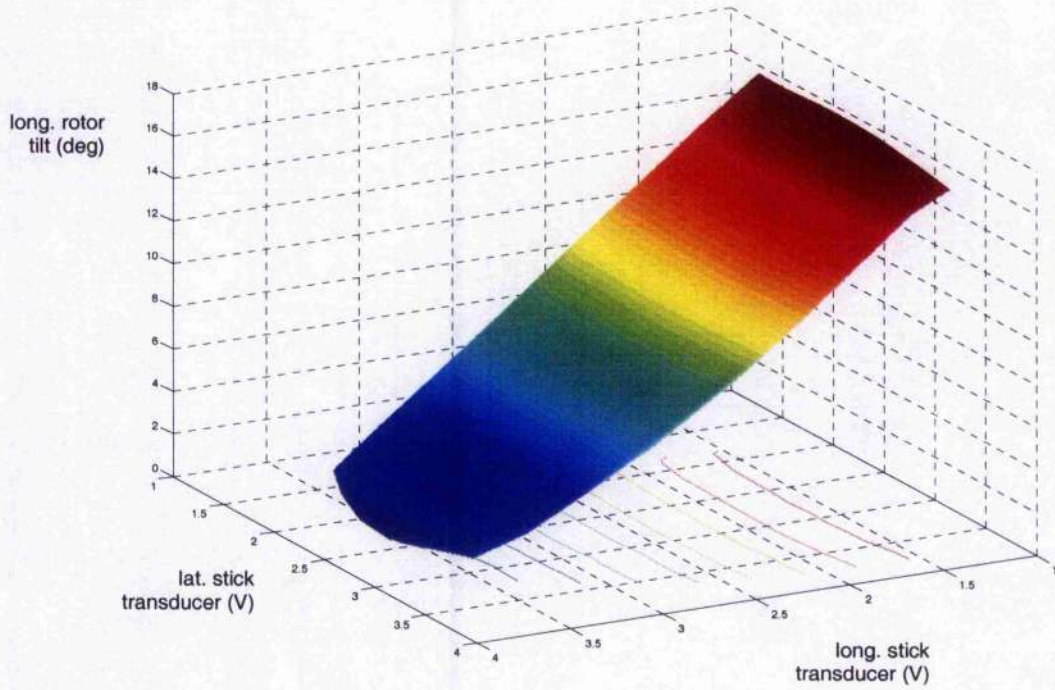


Figure 6.4 Control stick transducer calibration surface for longitudinal channel

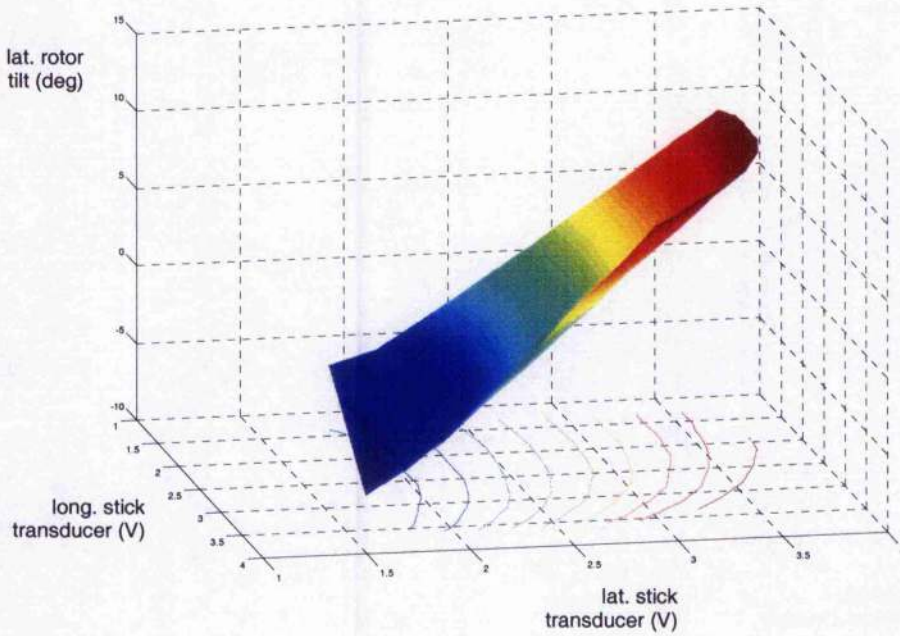


Figure 6.5 Control stick transducer calibration surface for lateral channel

#### 6.4.4 Airspeed Calculation Technique

The pitot probe transducer measures the difference between total and static pressure, which is the dynamic pressure. The velocity of the pitot probe in the wind axes can be calculated from Bernoulli's equation:

$$P_{static} + \frac{\rho V_{pitot}^2}{2} = P_{total} \quad (6.1)$$

Solving equation (6.1) for  $V_{pitot}$  gives

$$V_{pitot} = \sqrt{\frac{2(P_{total} - P_{static})}{\rho}} \quad (6.2)$$

or,

$$V_{pitot} = \sqrt{\frac{2P_{dyn}}{\rho}} \quad (6.3)$$

where  $\rho$  is the local air density, and  $P_{dyn}$  is the dynamic pressure.

The velocity obtained is a True Airspeed (TAS), as it was calculated for local air density. Equivalent Airspeed (EAS) can be calculated from equation (6.3) using air density for mean sea level instead of local one.

Local air density depends on static pressure and ambient air temperature, and was calculated using expression:

$$\rho = \frac{P_{static}}{R T_{air}} \quad (6.4)$$

where  $P_{static}$  is the static pressure;  $T_{air}$  is the air temperature; and  $R$  is the universal gas constant.

The components of velocity of the pitot probe in body axes were obtained from the following expressions:

$$U_{pitot}^{body} = V_{pitot} \cos \alpha_{pitot} \cos \beta_{pitot}, \quad (6.5)$$

$$V_{pitot}^{body} = V_{pitot} \sin \beta_{pitot}, \quad (6.6)$$

$$W_{pitot}^{body} = V_{pitot} \sin \alpha_{pitot} \cos \beta_{pitot}, \quad (6.7)$$

where  $\alpha_{pitot}$  and  $\beta_{pitot}$  are the pitot probe angle of attack and angle of sideslip.

Finally, using translational equation of motion:

$$\mathbf{u}_{pitot}^{body} = \mathbf{u}_{c.g.}^{body} + \boldsymbol{\omega}^{body} \times \mathbf{r}_{pitot-c.g.}^{body}, \quad (6.8)$$

components of absolute velocity of gyroplane centre of gravity in body axes were calculated

$$U = U_{c.g.}^{body} = U_{pitot}^{body} - Q(z_{pitot} - z_{c.g.}) + R(y_{pitot} - y_{c.g.}), \quad (6.9)$$

$$V = V_{c.g.}^{body} = V_{pitot}^{body} + P(z_{pitot} - z_{c.g.}) - R(x_{pitot} - x_{c.g.}), \quad (6.10)$$

$$W = W_{c.g.}^{body} = W_{pitot}^{body} - P(y_{pitot} - y_{c.g.}) + Q(x_{pitot} - x_{c.g.}). \quad (6.11)$$

### 6.4.5 Calculation of the Engine Power

The propeller rpm was measured using electro-optical sensor. The gearbox reduction ratio of the engine is 2.62, thus engine rpm can be calculated by multiplication of propeller rpm and gearbox reduction ratio. Finally, engine power was obtained using the performance curve provided in the engine specifications (Figure 6.6).

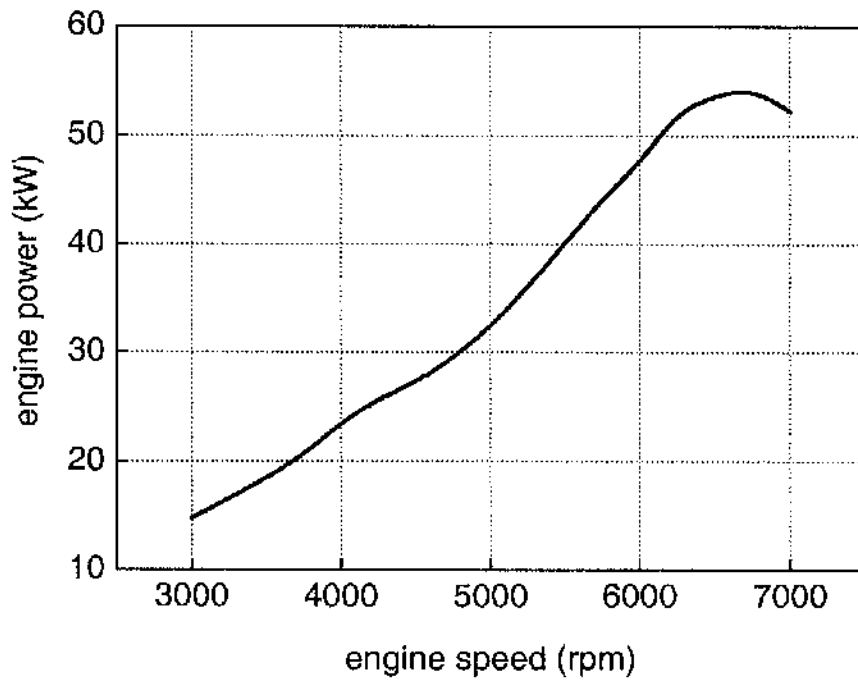


**Figure 6.6** ROTAX TYPE 618 engine performance

Once all the ground preparations were performed, the G-UNIV research gyroplane was ready for flight tests. The next section will discuss the design and preparation of the gyroplane test manoeuvres for handling qualities studies.

## 6.5 Design of Flight Test Manoeuvres

As was discussed in Chapter 2, the fact that the ADS-33E-PRF (2000) standard does not provide any categorisation according to rotorcraft size, allows the adaptation of the concept of mission task elements as a basis for the subjective handling qualities assessment of a light gyroplane. The two most appropriate manoeuvres from the ADS-33E-PRF standard, slalom and acceleration-deceleration, have been chosen for the current study. These MTEs were modified to suit a light gyroplane and prepared for the flight test programme. In the previous chapter, the inverse simulation was proposed as a preliminary tool in the process of designing gyroplane test manoeuvres for handling qualities studies. The original definition of these manoeuvres from the ADS-33E-PRF document in conjunction with the results obtained from the GENISA/GSIM simulation make good grounds for designing the MTEs for a light gyroplane. The objectives, descriptions and performance requirements for the gyroplane slalom and acceleration-deceleration manoeuvres are now described in more detail in the following subsections.

### 6.5.1 Slalom Manoeuvre

The ADS-33E-PRF defines the slalom manoeuvre in the following manner:

#### *a. Objectives.*

- *Check ability to manoeuvre aggressively in forward flight and with respect to objects on the ground.*
- *Check turn coordination for moderately aggressive forward flight manoeuvring.*
- *Check for objectionable interaxis coupling during moderately aggressive forward flight manoeuvring.*

*b. Description of manoeuvre. Initiate the manoeuvre in level unaccelerated flight and lined up with the centreline of the test course. Perform a series of smooth turns at 500-ft intervals (at least twice to each side of the course). The turns shall be at least 50 ft from the centreline, with a maximum lateral error of 50 ft. The manoeuvre is to be*

accomplished below the reference altitude. Complete the manoeuvre on the centreline, in coordinated straight flight.

**c. Description of test course.** The suggested test course for this manoeuvre is shown in Figure 6.7. Most runways have touchdown stripes at 500-ft intervals that can be conveniently used instead of the pylons. However, if the runway is not 100 ft wide, it will be necessary to use two cones to define each gate (as opposed to one cone and the runway edge as shown in Figure 6.7).

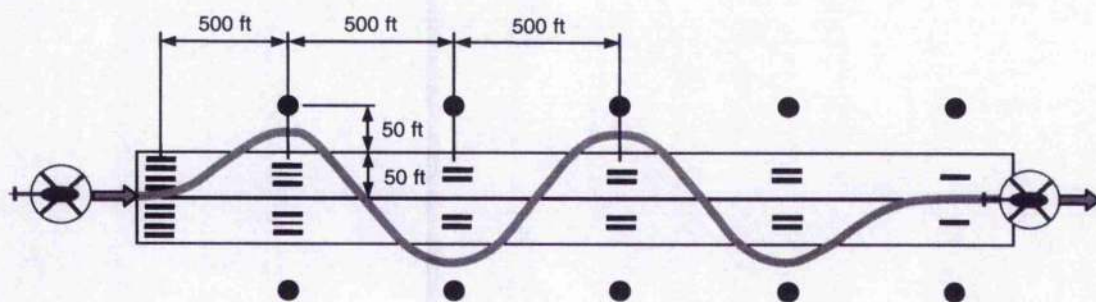


**Figure 6.7** Suggested course for slalom manoeuvre, reproduced from the ADS-33E-PRF (2000)

**d. Performance standards.** (Performance requirements presented in Table 6.2).

**Table 6.2** Desired and adequate performance for slalom manoeuvre, reproduced from the ADS-33E-PRF (2000)

	GVE	DVE
<b>DESIRED PERFORMANCE</b> <ul style="list-style-type: none"> <li>• Maintain an airspeed of at least X knots throughout the course</li> <li>• Accomplish manoeuvre below reference altitude of X ft:</li> </ul>	60 Lesser of twice rotor diameter or 100 ft	30 100 ft
<b>ADEQUATE PERFORMANCE</b> <ul style="list-style-type: none"> <li>• Maintain an airspeed of at least X knots throughout the course</li> <li>• Accomplish manoeuvre below reference altitude of X ft:</li> </ul>	40 100 ft	15 100 ft

The objectives of the ADS-33E-PRF slalom were applied without changes to the gyroplane slalom:

- 1) Check ability to manoeuvre aggressively in forward flight and with respect to objects on the ground;
- 2) Check turn coordination for moderately aggressive forward flight manoeuvring;
- 3) Check for objectionable interaxis coupling during moderately aggressive forward flight manoeuvring.

The slalom and acceleration-deceleration trials were conducted at the Carlisle airfield, UK. The administration of the airfield did not give the permission to perform the manoeuvres over the main runways because the Carlisle Airport is busy during the day with domestic flights. After discussions with the airfield administration, it was decided to fly the test manoeuvres over a site in a parallel course to the main runway. The length of the selected site was limited by the configuration of the airfield, which did not allow performing the suggested 2500 ft (~750 m) slalom course (Figure 6.7) in full. This was the reason why it was decided to conduct the minimum slalom, i.e. to initiate only one turn to left and one turn to right (Figure 6.8).

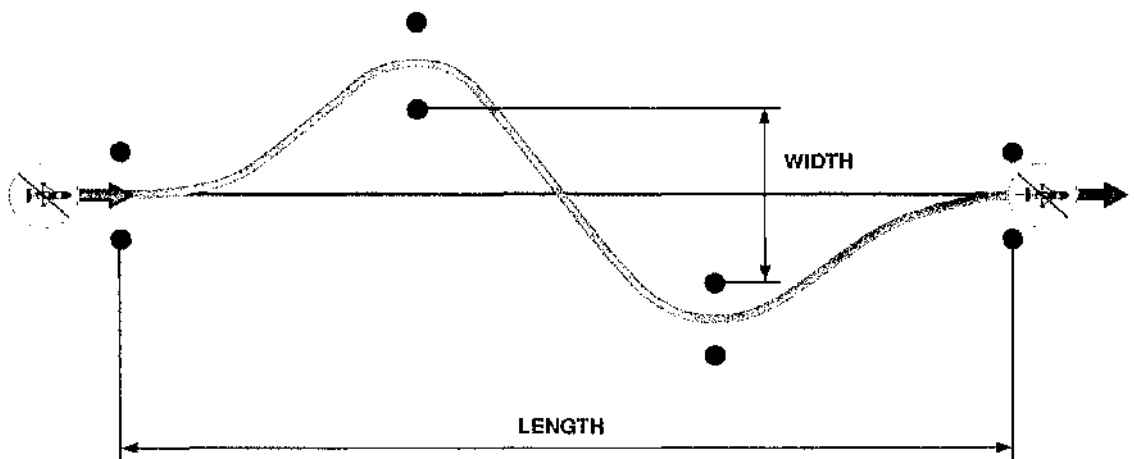


**Figure 6.8** Course for gyroplane minimum slalom manoeuvre

As can be seen from Table 6.2, the ADS-33E-PRF standard defines desired and adequate performance for two different flight conditions: Good Visual Conditions (GVE) and Degraded Visual Conditions (DVE). Since the BCAR Section T (2003) defines requirements applicable only to light gyroplanes, which are restricted to day VFR (Visual Flight Rules) conditions, and the G-UNIV research gyroplane falls into this category, the requirements for the gyroplane slalom and acceleration-deceleration manoeuvres were defined only for day VFR conditions.

Thus, the preliminary desired performance for the gyroplane minimum slalom manoeuvre was defined as follows:

“Initiate the manoeuvre in level unaccelerated flight at airspeed of 70 mph (~60 knots) and lined up with the centreline of the test course. Perform one smooth turn to left and one smooth turn to right at 150 m (~500 ft) intervals. The turns shall be at least 15 m (~50 ft) from the centreline, with a maximum lateral error of 15 m (~50 ft). The manoeuvre is to be accomplished below the reference altitude. Complete the manoeuvre on the centreline, in coordinated straight flight.”

In order to better understand the gyroplane behaviour and obtain the handling qualities and workload levels, the length and width, and thus the aggressiveness level, of the slalom course were varied. The ADS-33E-PRF (2000) standard specifies the minimum airspeed to be maintained throughout the task, which is 60 knots (~70 mph) for GVE conditions (Table 6.2). With the aim of revealing the airspeed requirements for the gyroplane slalom, the speed of the slalom course was also varied. Detailed descriptions of these courses along with flight test results and analysis are presented and discussed in Chapter 7.

### **6.5.2 Acceleration-Deceleration Manoeuvre**

The acceleration-deceleration MTE is defined in the ADS-33E-PRF document as follows:

**a. Objectives.**

- Check pitch axis and heave axis handling qualities:
  - (GVE): for aggressive manoeuvring near the rotorcraft limits of performance.
  - (DVE): for reasonably aggressive manoeuvring in the DVE.
- Check for undesirable coupling between the longitudinal and lateral-directional axes.
- Check for harmony between the heave axis and pitch axis controllers.
- Check for adequate rotor response to aggressive collective inputs.
- Check for overly complex power management requirements.

**b. Description of manoeuvre.** Start from a stabilized hover. In the GVE, rapidly increase power to approximately maximum, maintain altitude constant with pitch attitude, and hold collective constant during the acceleration to an airspeed of 50 knots. Upon reaching the target airspeed, initiate a deceleration by aggressively reducing the power and holding altitude constant with pitch attitude. The peak nose-up attitude should occur just before reaching the final stabilized hover. In the DVE, accelerate to a groundspeed of at least 50 knots, and immediately decelerate to hover over a defined point. The maximum nose-down attitude should occur immediately after initiating the manoeuvre, and the peak nose-up attitude should occur just before reaching the final stabilized hover. Complete the manoeuvre in a stabilized hover for 5 seconds over the reference point at the end of the course.

**c. Description of test course.** The test course shall consist of a reference line on the ground indicating the desired track during the acceleration and deceleration, and markers to denote the starting point and endpoint of the manoeuvre. The distance from the starting point to the final stabilized hover position is a function of the performance of the rotorcraft, and shall be determined based on trial runs consisting of acceleration to the target airspeed, and decelerations to hover as described above. The course should also include reference lines or markers parallel to the course centreline to allow the pilot and observers to perceive desired and adequate lateral tracking performance. A suggested test course is shown in Figure 6.9.

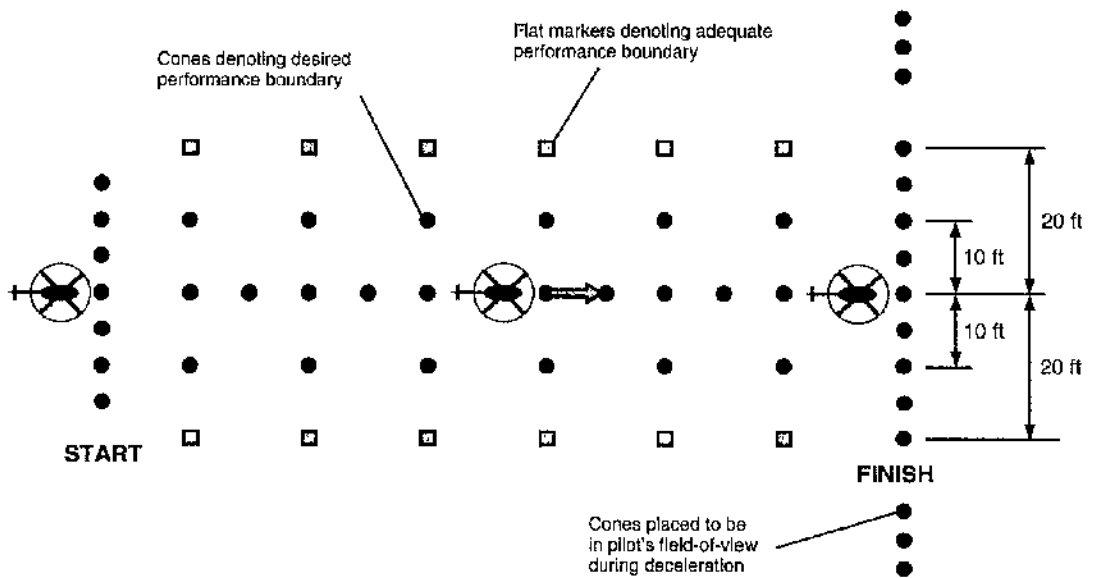


**Figure 6.9** Suggested course for acceleration-deceleration manoeuvre, reproduced from the ADS-33E-PRF (2000)

*d. Performance standards.* (Performance requirements presented in Table 6.3).

The objectives for the gyroplane acceleration-deceleration manoeuvre were defined by analogies with the ADS-33E-PRF document:

- 1) Check longitudinal handling qualities for aggressive manoeuvring near the gyroplane limits of performance;
- 2) Investigate couplings between the longitudinal and lateral-directional axes.

As a gyroplane cannot hover, it was decided to modify the manoeuvre, to start this task not at the hover, but at a specified airspeed, and fly the gyroplane as fast as possible acquiring maximum acceleration. When the aircraft achieved an adequate longitudinal velocity, an aggressive deceleration is initiated to return the aircraft to the initial airspeed at constant altitude. Thus, the preliminary desired performance for the acceleration-deceleration manoeuvre was defined as follows:

**Table 6.3** Desired and adequate performance for acceleration-deceleration manoeuvre, reproduced from the ADS-33E-PRF (2000)

	GVE	DVE
<b>DESIRED PERFORMANCE</b>		
<ul style="list-style-type: none"> <li>• Within X seconds from initiation of the manoeuvre, achieve at least the greater of 95% maximum continuous power or 95% maximum transient limit that can be sustained for the required acceleration, whichever is greater. If the 95% power results in objectionable pitch attitudes, use the power corresponding to the maximum nose-down pitch attitude that is felt to be acceptable. This pitch attitude shall be considered as a limit of the Operational Flight Envelope (OFE) for NOE flying.</li> </ul>	1,5 sec	NA
<ul style="list-style-type: none"> <li>• Achieve a nose-down pitch attitude during the acceleration of at least X deg below the hover attitude:</li> </ul>	NA	12 deg
<ul style="list-style-type: none"> <li>• Maintain altitude below X ft:</li> </ul>	50 ft	50 ft
<ul style="list-style-type: none"> <li>• Maintain lateral track within <math>\pm X</math> ft:</li> </ul>	10 ft	10 ft
<ul style="list-style-type: none"> <li>• Maintain heading within <math>\pm X</math> deg:</li> </ul>	10 deg	10 deg
<ul style="list-style-type: none"> <li>• Decrease power to less than 5% within X seconds to initiate deceleration.</li> </ul>	3 sec	NA
<ul style="list-style-type: none"> <li>• Significant increases in power are not allowed until just before the final stabilized hover.</li> </ul>	✓	✓
<ul style="list-style-type: none"> <li>• Achieve a nose-up pitch attitude during the deceleration of at least X deg above the hover attitude. The maximum pitch attitude should occur shortly before the hover.</li> </ul>	30 deg	15 deg
<ul style="list-style-type: none"> <li>• Longitudinal tolerance on the final hover point is plus zero, minus a distance equal to X % of the overall rotorcraft length.</li> </ul>	50 %	50 %
<ul style="list-style-type: none"> <li>• Rotor RPM shall remain within the limits of X without undue pilot compensation</li> </ul>	OFE	OFE
<b>ADEQUATE PERFORMANCE</b>		
<ul style="list-style-type: none"> <li>• Within X seconds from initiation of the manoeuvre, achieve at least the greater of 95% maximum continuous power or 95% maximum transient limit that can be sustained for the required acceleration, whichever is greater. If the 95% power results in objectionable pitch attitudes, use the maximum nose-down pitch attitude that is felt to be acceptable. This pitch attitude shall be considered as a limit of the Operational Flight Envelope (OFE) for NOE flying.</li> </ul>	3 sec	NA
<ul style="list-style-type: none"> <li>• Achieve a nose-down pitch attitude during the acceleration of at least X deg below the hover attitude.</li> </ul>	NA	7 deg
<ul style="list-style-type: none"> <li>• Maintain altitude below X ft:</li> </ul>	70 ft	70 ft
<ul style="list-style-type: none"> <li>• Maintain lateral track within <math>\pm X</math> ft:</li> </ul>	20 ft	20 ft
<ul style="list-style-type: none"> <li>• Maintain heading within <math>\pm X</math> ft:</li> </ul>	20 deg	20 deg
<ul style="list-style-type: none"> <li>• Decrease power to less than 30% of maximum within X seconds to initiate deceleration.</li> </ul>	5 sec	NA
<ul style="list-style-type: none"> <li>• Significant increases in power are not allowed until just before the final stabilized hover.</li> </ul>	✓	✓
<ul style="list-style-type: none"> <li>• Achieve a nose-up pitch attitude during the deceleration of at least X deg above the hover attitude.</li> </ul>	10 deg	10 deg
<ul style="list-style-type: none"> <li>• Longitudinal tolerance on the final hover point is minus a distance equal to X % of the overall rotorcraft length.</li> </ul>	100 %	100 %
<ul style="list-style-type: none"> <li>• Rotor RPM shall remain within the limits of the:</li> </ul>	SFE	SFE

“From level unaccelerated flight at an airspeed of 40 mph, rapidly increase power to approximately maximum, and maintain altitude constant during the acceleration to an airspeed of 60 mph (~50 knots). Upon reaching the target airspeed, initiate a deceleration aggressively reducing the power and holding altitude constant. Complete the manoeuvre in the initial airspeed of 40 mph. Maintain lateral track within  $\pm 3$  m ( $\sim \pm 10$  ft) and heading within  $\pm 10$  deg during the manoeuvre.”

For the GVE conditions, the ADS-33E-PRF document is very strict about nose-up pitch attitude during the deceleration period of this manoeuvre. The pitch angle must be at least 30 degrees above the hover attitude for desired performance, and at least 10 degrees for adequate performance (Table 6.3). Previous simulation results (*Bagiev et al, 2003; 2004*), and also those presented in Chapter 5, show that the gyroplane behaves differently in this manoeuvre, using mainly a propeller thrust for fast acceleration-deceleration. In addition, the gyroplane does not use nose-up pitch attitude for deceleration. Such behaviour resembles that of a conventional aeroplane or a helicopter with thrust compounding (*Rutherford, 1997, p.107*). Therefore, pitch attitude has not been specified in this task. For the investigation purposes, the start/finish and target airspeeds were varied. Altogether, six acceleration-deceleration tasks with different speed ranges were prepared for the flight tests. A detailed description of the prepared courses and flight test results of the G-UNIV gyroplane flying the acceleration-deceleration manoeuvres are presented and discussed in Chapter 7.

## 6.6 Chapter Summary

This chapter has presented preliminary stages of preparation for the flight test programme to study gyroplane handling qualities. A brief overview of the unique test aircraft, the G-UNIV gyroplane, has been given. This has been followed by a detailed description of the onboard flight test instrumentation and ground preparations for the flight tests, which included calibration procedures and processes of calculation of mass, centre of gravity and moments of inertia.

As was noted in Chapter 1, the basic premise of the current research is that the handling qualities requirements and prescribed manoeuvres from the ADS-33E-PRF (2000) document can be modified to suit a light gyroplane. In particular, in this chapter, considerable effort has been focused on the demonstration of how the ADS-33E-PRF slalom and acceleration-deceleration MTEs can be adapted to design gyroplane manoeuvres. Undoubtedly, a design of new, unique manoeuvres for light gyroplanes will be the subject of future work.

## ***Chapter 7***

# **Flight Testing of the G-UNIV Gyroplane for Subjective Assessment of Handling Qualities and Criteria Design**

### **7.1 Introduction**

A large part of the current research is focused on the flight test programme of the G-UNIV research gyroplane for handling qualities studies. This chapter starts with a description of pre-flight ground preparations, which is followed by thorough discussion of flight test results for the gyroplane slalom and acceleration-deceleration manoeuvres. Results of subjective assessment of handling qualities and workload based on pilot opinion are presented and analysed. The final section of this chapter is devoted to examples of designing of roll attitude quickness and pilot attack criteria for a gyroplane slalom manoeuvre.

### **7.2 Flight Tests of the G-UNIV Gyroplane for Handling Qualities and Workload Assessment**

Flight data were recorded during thirty slalom and six acceleration-deceleration tests performed in about 4 hours of flight time during three days (03-05 March 2004) at the Carlisle airfield, UK. It is suggested in the ADS-33E-PRF (2000) standard that the

manoeuvres must be flown by at least three test pilots. Unfortunately, due to time and financial limitations of this project, only one pilot examined the slalom and acceleration-deceleration manoeuvres. The test pilot was Roger Savage, who is presently a gyroplane flying instructor with over 4000 flying hours in gyroplanes, and over 7500 flying hours in total, including aeroplanes and helicopters. He is a holder of Private Pilot's Licenses (PPL) for Aeroplane, Helicopter and Gyroplane types of aircraft. Roger Savage is also a flight examiner for the UK Civil Aviation Authority PPL (Gyroplanes) and has been appointed a Panel Examiner to the Authority. However, it is important to note that he is not, and never has been, a qualified test pilot.

After the pre-flight ground preparations, which included engine test runs (Figure 7.1), instrumentation and software checks, radio communication unit and headset setup, maintenance and final inspection, the G-UNIV gyroplane was ready for the handling qualities flight tests. The slalom and acceleration-deceleration courses were prepared on the site in a parallel course with the main runway. This site was grass, and after discussions with the test pilot, it was agreed to use traffic cones with a height of 1 m to mark ground gates, and use sticks with a height of 0.5 m with red-coloured flags to indicate the centreline for the slalom course. For the acceleration-deceleration course, the sticks with flags were used to indicate both the centreline and the desired performance boundary. To mark the ground, a GPS receiver and measuring wheels were used. It should be noted that the GPS receiver used for these purposes was the one installed onboard the research gyroplane. It takes only few minutes to remove it from the instrumentation pallet, and install it back.

Before starting the slalom and acceleration-deceleration trials, the test pilot and the author flew over the site onboard a two-seat VPM M16 gyroplane to check the prepared courses from the air. Flight trials instruction forms (Appendix 5) were prepared and provided to the test pilot before each course trial. The pilot had also a shorter form of flight instructions, which was designed to fit into the pilot's flying suit thigh pocket, and thereby the pilot would have the description of the tasks in sight during the flight.



**Figure 7.1** The G-UNIV gyroplane at Carlisle airfield during pre-flight engine runs

### 7.2.1 Slalom Manoeuvre

The preliminary desired performance for the gyroplane minimum slalom manoeuvre was defined in Chapter 6, Section 6.5. In addition, the length and width of the slalom manoeuvre were varied in order to better understand the gyroplane behaviour and obtain subjective assessments of the handling qualities and workload. In such a manner, five different slalom courses were prepared for the flight tests (Table 7.1). Note, that the first course from Table 7.1 represents the desired performance requirements for the minimum slalom (length 450 m, width 30 m). The distance between gate's cones was constant for each slalom course and equal to 15 m (~50 ft) as required by the ADS-33E-PRF (2000) standard.

**Table 7.1** Slalom courses with various length and width

Course	Length (m)	Width (m)	AR
1	450	30	0.067
2	300	30	0.1
3	225	30	0.13
4	300	60	0.2
5	150	30	0.2

The metrics of aggressiveness of the slalom manoeuvre are the Aspect Ratio (AR) of the course and airspeed to be maintained throughout the task. The AR of the slalom course was defined in Chapter 5, Section 5.5 as the ratio of width ( $W$ ) to length ( $L$ ) of the course (Figure 6.8) to indicate aggressiveness level of the manoeuvre, the same way as defined by Padfield *et al* (1994, p.5). It should be noted that this is not the best way to indicate the aggressiveness level of slalom manoeuvre. For instance, courses 4 and 5 from Table 7.1 have the same ARs, while the length and width of the courses are different; moreover, as will be demonstrated later in this chapter, HQRs and WRs for these courses were different as well. Therefore, in this dissertation AR together with length are used to indicate the difference between these two particular courses. In addition, each slalom course was conducted for three different flight speeds of 35 mph, 50 mph and 70 mph. For each of these courses, the test pilot completed two evaluation runs to increase accuracy of subjective HQRs and WRs. In total, thirty slalom runs were performed.

It should be emphasised at this point that the inverse simulation results presented in Chapter 5 show that the courses [AR 0.2, 50 mph], [AR 0.13, 70 mph], and [AR 0.2, 70 mph] lie outside predicted flight envelope for gyroplane slalom manoeuvre (Figure

5.10). However, the results, which formed the basis for the slalom flight envelope, were obtained with the sideslip rate constrained, and therefore might be too stringent. Therefore, it was decided to prepare in advance all the courses from Table 7.1 and conduct flight tests in a stepwise manner, starting with the least aggressive course [AR 0.067, 35 mph], and then increasing the aggressiveness level step by step. After completing each test flight (one slalom course per one test flight), a thorough discussion with the test pilot regarding the behaviour of the test aircraft and safety issues took place. The test pilot also assigned handling qualities ratings using the Cooper-Harper rating scale (Figure 2.1) and workload ratings using the Bedford workload scale (Figure 2.2). Only after this discussion, a decision whether to go further and increase aggressiveness level of the next course or stop at this point was made. It should be stated, that due to the safety issues, the flight test programme was carefully planned and organised, and all the flight trials were prepared and conducted very carefully and in an incremental manner. All the five courses from Table 7.1 were prepared on the ground by placing small markers on the test site, thereby forming a distinctive mesh of markers on the ground, so the main markers (traffic cones and sticks with flags) can be easily and quickly placed at the proper positions depending on the chosen course.

As was noted above, after each test flight the test pilot assigned HQRs using the Cooper-Harper rating scale (Figure 2.1) and WRs using the Bedford workload scale (Figure 2.2). It should be stated that the pilot had no prior experience of either handling qualities or workload scales; therefore, the author spent some time explaining him the approach used in these rating scales. To the author's knowledge, this is the first time that the Cooper-Harper handling qualities rating scale and the Bedford workload rating scale have been applied to a light gyroplane. Finally, results for fifteen different configurations are summarised in Table 7.2 and Figures 7.2 and 7.3. It can be seen from the figures that by the increase in the airspeed and AR, the pilot subjective HQRs and WRs are degrading. That is to say, the higher the aggressiveness level of the slalom manoeuvre, the poorer the HQRs and WRs. The pilot had to turn more quickly on higher speeds and higher ARs. For example, for the most aggressive conditions (AR 0.2,  $L$  150 m, airspeed 70 mph) the pilot could not complete the slalom course, hence giving HQR 10 and WR 10.

**Table 7.2** Pilot subjective HQRs and WRs for the slalom courses

Course	AR	Airspeed (mph)	HQR	WR
1	0.067	35	2	2
		50	2.5	2.5
		70	4.5	4.5
2	0.1	35	4	3
		50	4.5	4.5
		70	6	6
3	0.13	35	3.5	4
		50	5	5
		70	7	7
4	0.2	35	4.5	5
	L 300 m	50	6	6
	W 60 m	70	8	8
5	0.2	35	7	7
	L 150 m	50	8	8
	W 30 m	70	10	10

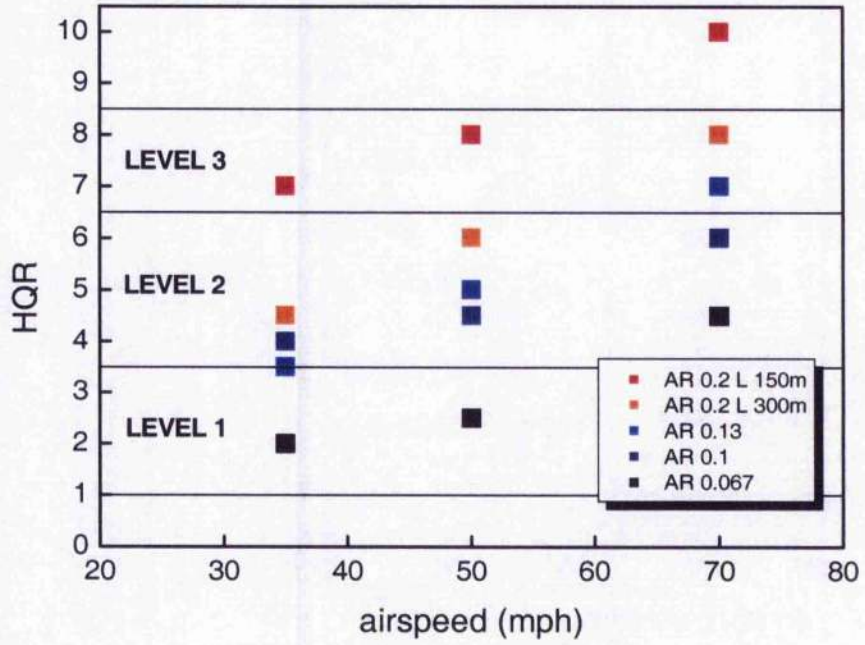


Figure 7.2 Pilot HQRs for the slalom manoeuvre

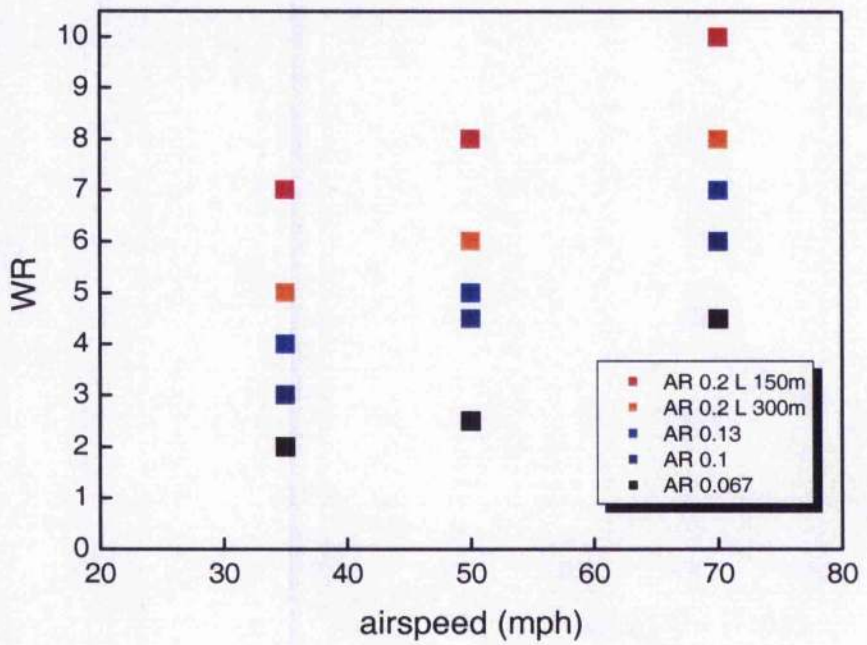
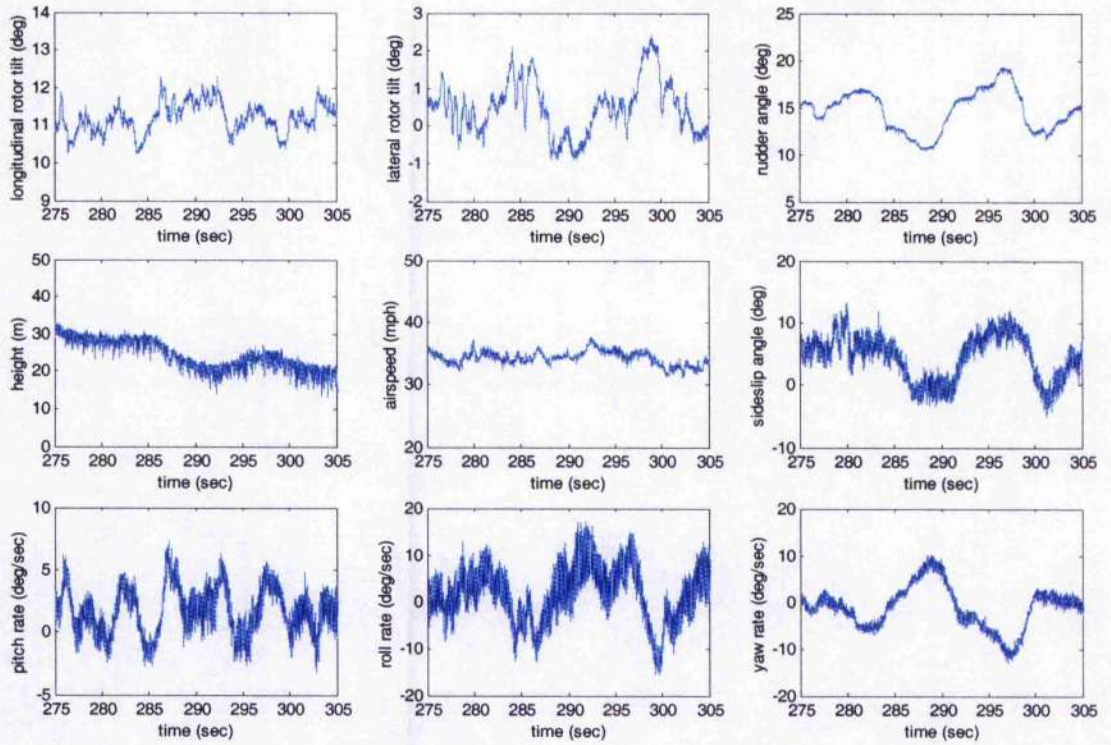


Figure 7.3 Pilot WRs for the slalom manoeuvre

Figures 7.4-7.6 show examples of flight test results for [AR 0.1, 35 mph], [AR 0.13, 70 mph], and [AR 0.2,  $L$  300 m, 50 mph] slalom courses respectively. As for example, referring to Figure 7.5, the test pilot started this manoeuvre at about 748 sec of recorded data, initiating large lateral rotor tilt perturbations for about  $\pm 5$  deg. The pilot strategy included a massive use of pedals to maintain the yaw attitude rate (note large sideslip angles). Maximum roll rate perturbations were about  $\pm 60$  deg/sec. The test pilot could not maintain the airspeed and height (note drop on airspeed of about 23 mph and height change of about 15 m), thus giving HQR 7 and WR 7 for this run.

Flight test results show that the test pilot used neither of the two control strategies (constrained sideslip rate and constrained heading attitude rate) discussed in detail in Chapter 5. Comparing the flight tests results (Figures 7.4-7.6) with those obtained from the inverse simulation (Figure 5.5), it can be seen from the flight data that the sideslip angles are large and changing fast, and at the same time, heading attitude rate is also not constant in all the examples. Therefore, it can be suggested for the future work that the slalom manoeuvre must be modelled in a more realistic manner. This example proves again the importance of accurate modelling of test manoeuvres stressed in Chapter 5. Because the pilot used a coupled control strategy, using stick and rudder, no conclusive comments can be made regarding cross-couplings for these data.

As a result of the analysis of different slalom courses, it is concluded that most suitable slalom courses to be considered as the slalom MTE for a light gyroplane are: [AR 0.067, 70 mph] and [AR 0.1, 50 mph]. It can be seen from Table 7.2 that the test pilot assigned HQRs 4.5 for these courses, which is equal to Level 2 of handling qualities as defined in the ADS-33E-PRF (2000) document. In one of the many post-flight discussions, the test pilot, Roger Savage, mentioned that the G-UNIV test gyroplane in general is a good Level 2 aircraft, and compared it to the VPM M16 gyroplane, which is according to his subjective opinion, is a better aircraft in terms of handling qualities and workload, and thus can be considered as a Level 1 gyroplane. It means, that selected courses, [AR 0.067, 70 mph] and [AR 0.1, 50 mph], are perfect choices for the gyroplane slalom MTE, because the Level 1 gyroplanes would most likely demonstrate Level 1 performance flying these courses.



**Figure 7.4** Flight test results for the G-UNIV research gyroplane flying the slalom manoeuvre [AR 0.1, 35 mph, Trial 1, HQR 4, WR 3]

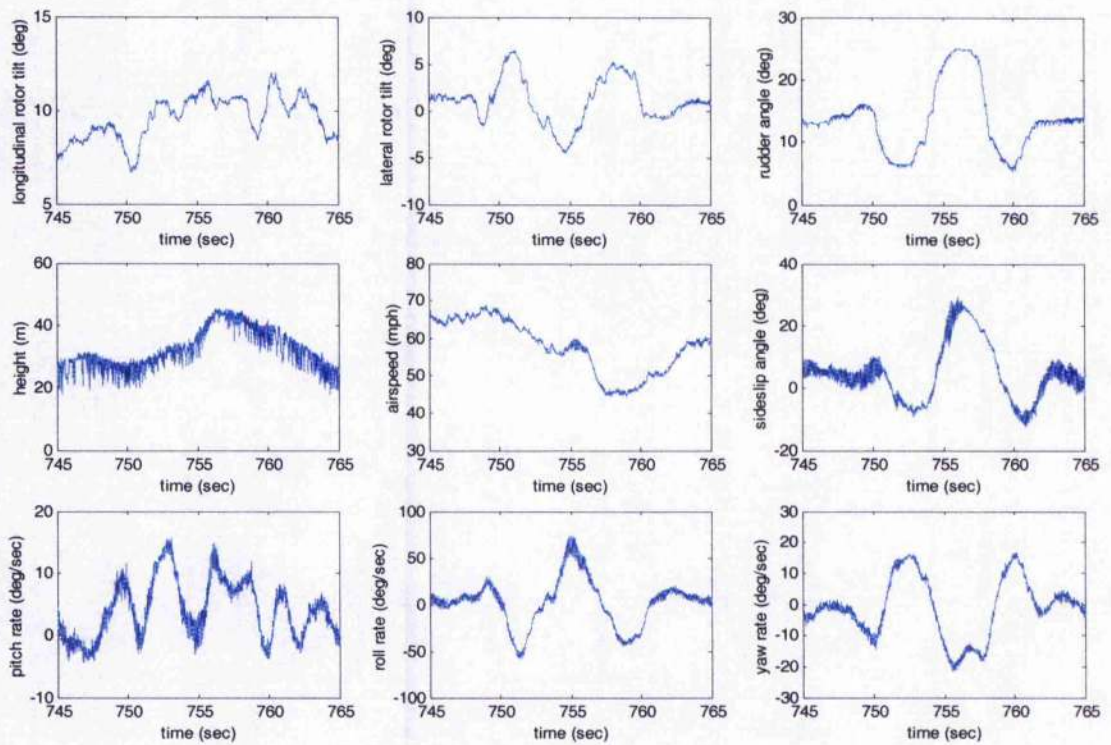


**Figure 7.5** Flight test results for the G-UNIV research gyroplane flying the slalom manoeuvre [AR 0.13, 70 mph, Trial 2, HQR 7, WR 7]

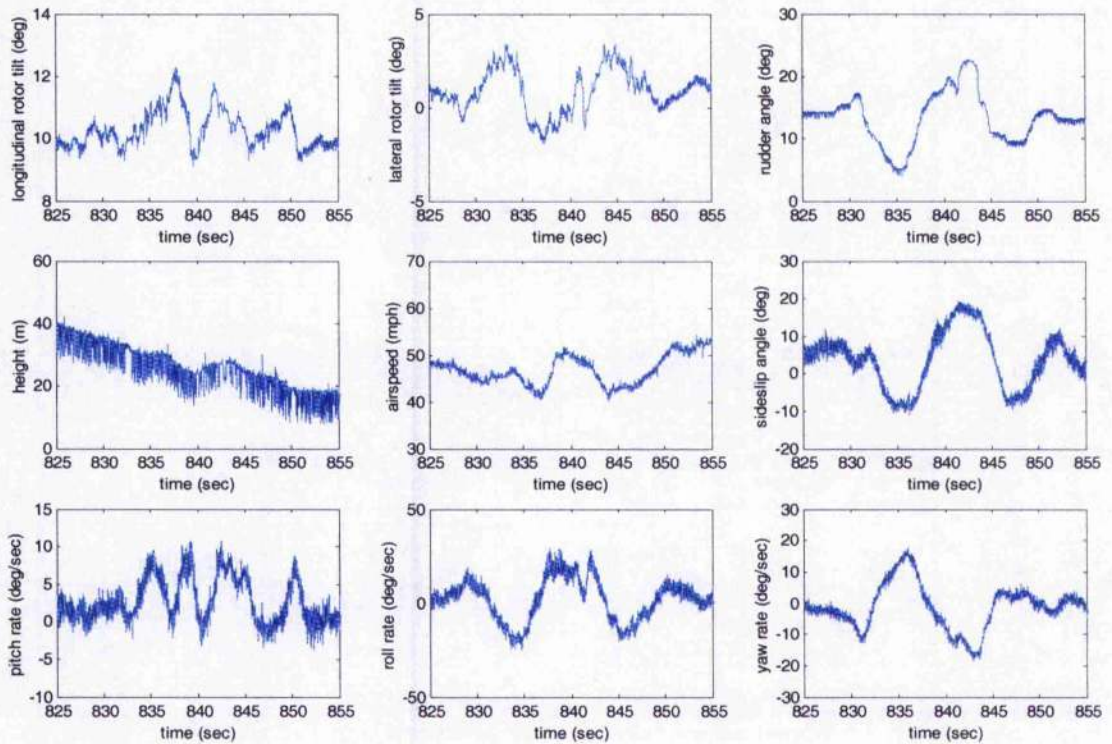


**Figure 7.6** Flight test results for the G-UNIV research gyroplane flying the slalom manoeuvre [AR 0.2,  $L$  300 m, 50 mph, Trial 2, HQR 6, WR 6]

Of course, all these conclusions are based only on one pilot's subjective opinion. In spite of the fact that the test pilot has a strong experience with gyroplanes, it is highly desirable to conduct more slalom trials with different test pilots to select the most appropriate course for the gyroplane slalom MTE. For example, as was noted above, the ADS-33E-PRF standard suggests that manoeuvres must be flown by at least three test pilots. In this particularly case, it would be very useful to have pilots with a different background, for example, one with gyroplane experience, second with light helicopter, and third with fixed wing aircraft.

In addition, the pilot HQRs were plotted against suggested levels of aggressiveness for the gyroplane slalom manoeuvre predicted by the inverse simulation (Figure 7.7). It can be seen that the low aggression level coincides well with the pilot's subjective ratings,

the test pilot assigned Level 1 handling qualities for the least aggressive slalom courses [AR 0.067, 35 mph, HQR 2] and [AR 0.067, 50 mph, HQR 2.5], which lie inside the predicted low aggression level. The moderate aggression region is also predicted well, four Level 2 courses fall into this region. Two Level 2 and one Level 3 points lie inside the high aggression level. However, the three most aggressive courses, [AR 0.13, 70 mph, HQR 7], [AR 0.2, 50 mph, HQR 8] and [AR 0.2, 70 mph, HQR 10], fall outside the predicted flight envelope. It seems that predicted lower and upper boundaries of the high aggression level must be shifted upwards to coincide with the subjective pilot ratings. Nevertheless, again, it should be remembered that handling qualities ratings are based only on one test pilot's opinion, therefore above conclusion must be proven by addition flight tests for the slalom manoeuvre.

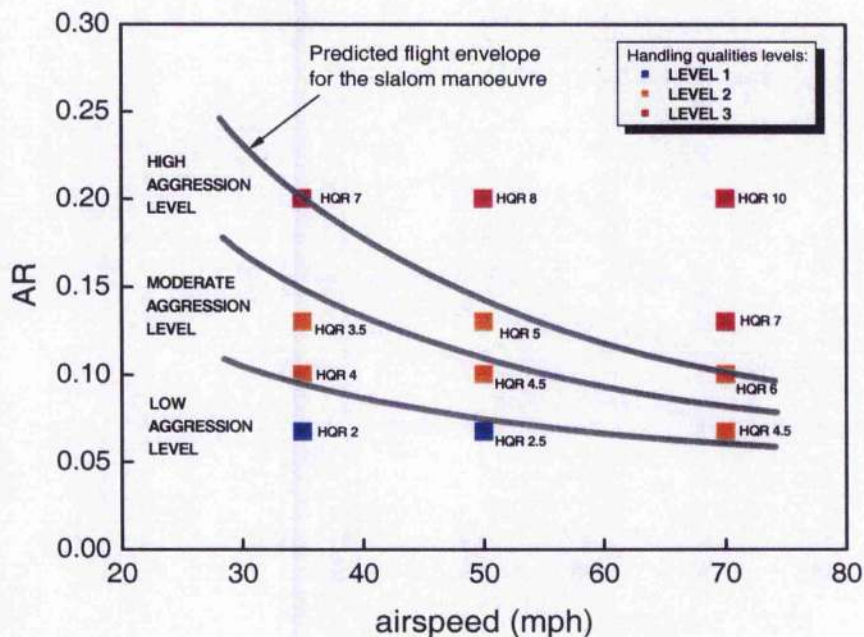


**Figure 7.7** Suggested levels of aggressiveness for the slalom course predicted by inverse simulation in comparison with pilot HQRs

In order to better understand the relationship between the pilot workload and aggressiveness of the manoeuvres, the maximum lateral rotor tilt angles were plotted against ARs. Figures 7.8-7.10 show the average results for three different flight speeds.

It can be seen that the higher the ARs, the closer rotor shaft is to its limits. However, the maximum tilt angles have decreased after AR 0.13 for airspeeds of 50 and 70 mph. This is almost certainly because the test pilot became more cautious feeling that he could hit the control limits. It can be predicted roughly from Figure 7.10 (dashed line) that the gyroplane would be unable to fly the 70 mph slalom course at ARs above 0.18/0.2. This proves again the fact that the flight envelope for gyroplane slalom manoeuvre predicted by inverse simulation (Figure 7.7) is too stringent most likely because only sideslip rate was constrained to obtain these results. Simulation results for the Lynx 60 knots (~70 mph) slalom (Padfield *et al*, 1994, p.6) predict a boundary AR of 0.11, which coincides with the inverse simulation predictions for the G-UNIV gyroplane (AR 0.1 at 70 mph as can be seen in Figure 7.7). However, it was noted that, if the pilot had more control authority, then the Lynx could be flown up to an AR of 0.2 without significant control problems. This example shows that the 70 mph slalom limitations for the test gyroplane obtained from flight tests and inverse simulation are similar to those for the Lynx helicopter.

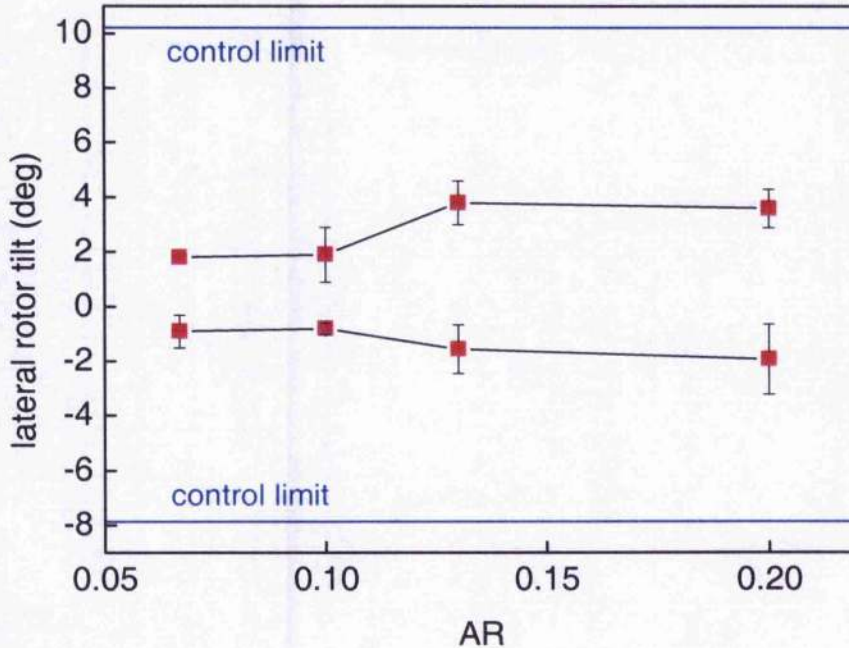


**Figure 7.8** Maximum lateral rotor tilt for the 35 mph slalom

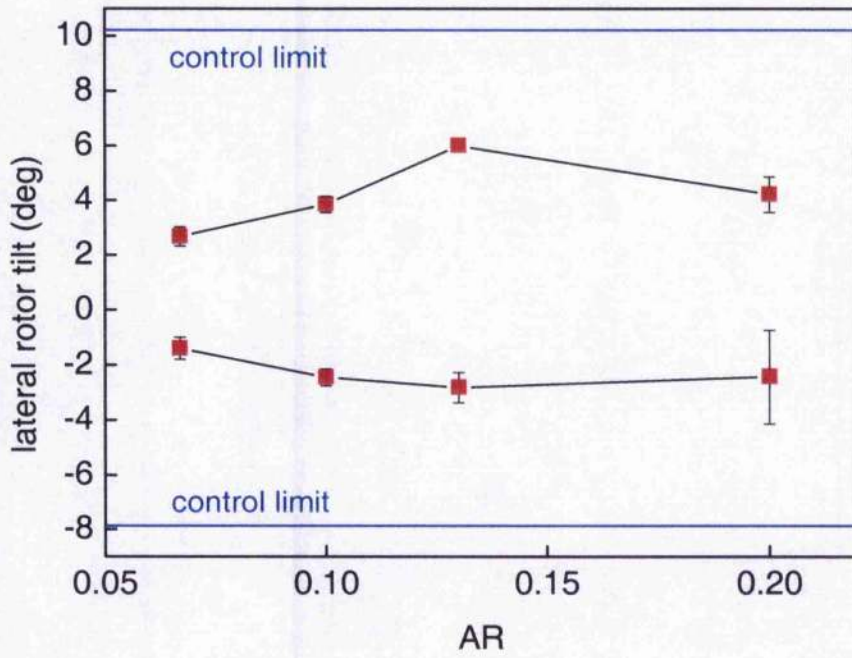


Figure 7.9 Maximum lateral rotor tilt for the 50 mph slalom

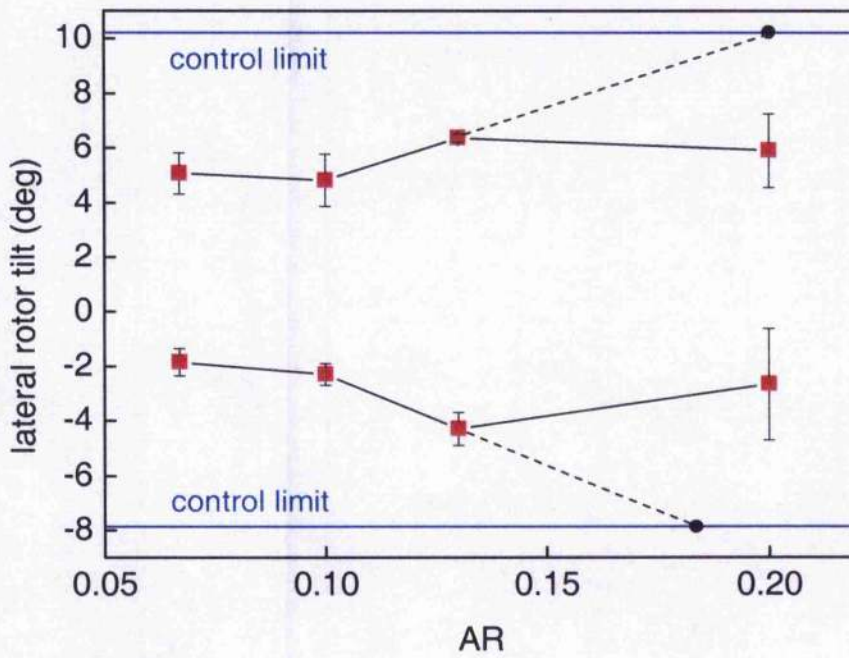


Figure 7.10 Maximum lateral rotor tilt for the 70 mph slalom

### 7.2.2 Acceleration-Deceleration Manoeuvre

The acceleration-deceleration manoeuvres were conducted during one test flight. It was possible, because, as was mentioned earlier in the section, the test pilot had a short form of the flight trials instructions onboard the gyroplane during these tasks. Speed ranges of start/finish and target airspeeds for these trials are shown in Table 7.3.

**Table 7.3** Acceleration-deceleration courses with various speed ranges

Course	Start/finish airspeed (mph)	Target airspeed (mph)
1	35	60
2	35	70
3	40	50
4	40	60
5	50	60
6	50	70

As in the slalom case, after the test flight for the acceleration-deceleration manoeuvres the test pilot assigned HQRs using the Cooper-Harper rating scale (Figure 2.1) and WRs using the Bedford workload scale (Figure 2.2). Summarised results are presented in Table 7.4 and Figures 7.11 and 7.12. Each bar in the figures represents the range between start/finish and target airspeeds. For five out of six trials the G-UNIV gyroplane achieved Level 1 of handling qualities (HQRs 1.5; 2; 2; 2; 2.5), and only one trial (50-70-50 mph) resulted of Level 2 (HQR 4). Pilot workload ratings distributed between WR 1.5 and WR 4, indicating that in general, the level of pilot workload was not high, and the pilot had no difficulties completing the acceleration-deceleration tasks. It can be seen from Figures 7.11 and 7.12 that the most difficult trial was the one where

the pilot had to accelerate and decelerate at high speeds (50-70-50 mph, HQR 4, WR 4). The easiest task according to the pilot ratings was the acceleration-deceleration manoeuvre at middle speeds (40-50-40 mph, HQR 1.5, WR 1.5). In general, the results of the subjective pilot assessment of handling qualities and workload show that the G-UNIV gyroplane meets Level 1 and Level 2 handling qualities and low level of workload for designed acceleration-deceleration manoeuvre.

**Table 7.4** Pilot subjective HQRs and WRs for the acceleration-deceleration courses

Course	Speed range (mph)	HQR	WR
1	35 – 60 – 35	2	3
2	35 – 70 – 35	2.5	3
3	40 – 50 – 40	1.5	1.5
4	40 – 60 – 40	2	2
5	50 – 60 – 50	2	2
6	50 – 70 – 50	4	4

As example, flight test results for the fourth trial from Table 7.3 are presented in Figure 7.13. The test pilot started the 40-60-40 mph acceleration-deceleration manoeuvre at about 741 sec of recorded data, initiating the power increase and changing longitudinal rotor tilt by about -2 deg. The pilot workload in lateral and yaw axes is not so significant. It can be seen that the airspeed was maintained well, while height drops. It should be noted that the requirements for the desired performance defined in Chapter 6, Section 6.5 state that the lateral track must be maintained within  $\pm 3$  m ( $\sim \pm 10$  ft) and the heading must be maintained within  $\pm 10$  deg during the manoeuvre. It is clear that requirements for the lateral track were failed (-15.5/+5 m), while the heading angle was maintained within required boundaries (-5/+3 deg).

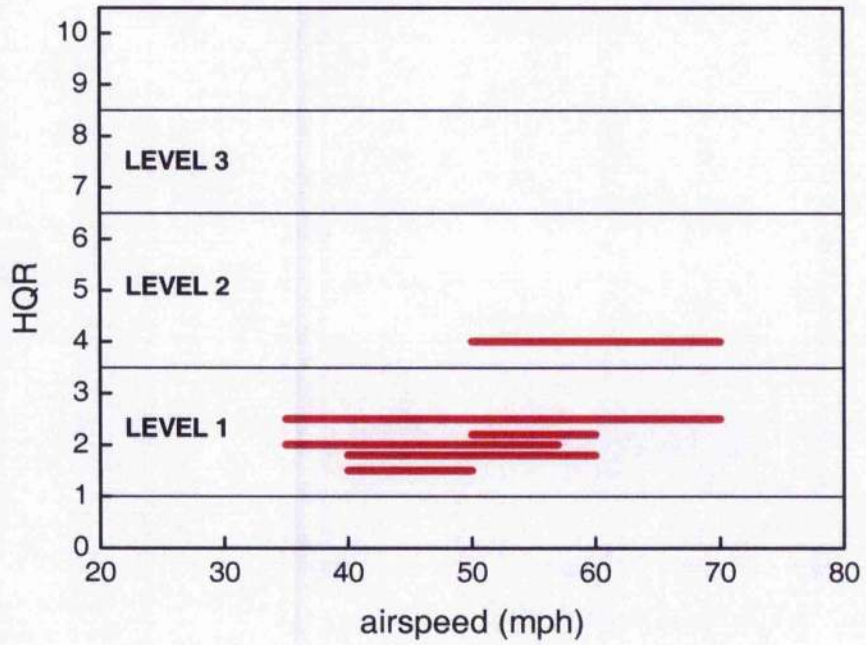


Figure 7.11 Pilot HQRs for the acceleration-deceleration manoeuvre

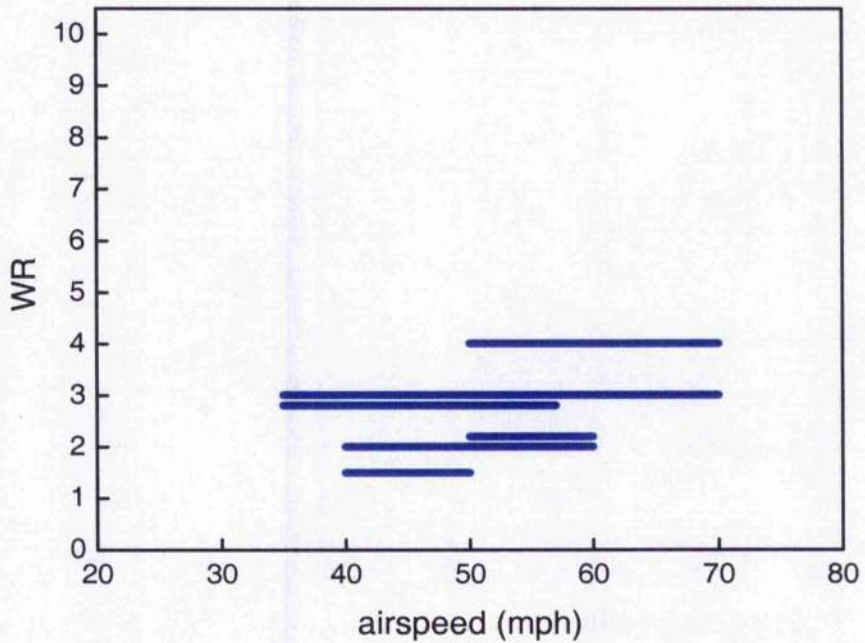
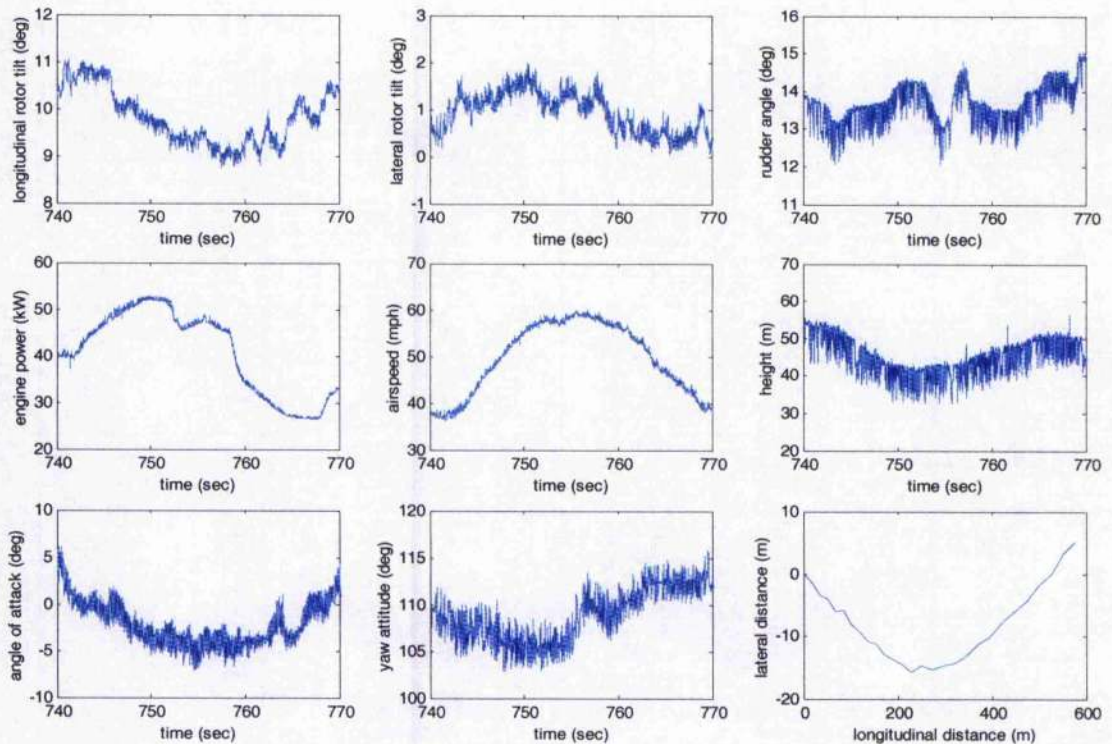


Figure 7.12 Pilot WRs for the acceleration-deceleration manoeuvre



**Figure 7.13** Flight test results for the G-UNIV research gyroplane flying the acceleration-deceleration manoeuvre [40-60-40 mph, HQR 2, WR 2]

Comparing the flight test data of the G-UNIV acceleration-deceleration (Figure 7.13) with simulation results of the Lynx helicopter for the same manoeuvre (Figure 5.15), it is obvious that the Lynx helicopter uses large pitch angles to accelerate and decelerate, while the gyroplane behaves more as an aeroplane rather than a helicopter, using mainly engine power for fast acceleration and deceleration. For example, to accelerate the gyroplane from 40 mph to 60 mph (fourth course from Table 7.3) the test pilot increased the engine power by approximately 12 kW (Figure 7.13), or 21.8% of maximum available power, which is 55 kW for the ROTAX TYPE 618 engine (Table A2.1). To decelerate, the test pilot decreased engine power by about 25 kW (45.5% of maximum available power). In comparison, the perturbation of longitudinal rotor tilt was approximately -2 deg (11.1% of maximum available range) to achieve the maximum angle of attack perturbation of about -7 deg. As was noted in Chapter 5, the angle sensor for the pitch channel (Chapter 6, Table 6.1) was not able to record flight

parameters correctly because the stabilising period of this transducer was too high for such aggressive manoeuvres as slalom and acceleration-deceleration. Therefore, it was stipulated that recorded angle of attack is equal to the pitch angle due to the fact that the height of the acceleration-deceleration manoeuvre is not changing a lot (Figure 7.13), and thus the flight path angle might be assumed equal to zero. As was discussed in Chapter 5, the gyroplane pilot has to decrease pitch angle mainly to maintain constant altitude required for the desired performance rather than to initiate acceleration. To prove this statement, it should be noted that the change in trim values of the pitch attitude for 40 mph and 60 mph is about 6 degrees (Chapter 4, Section 4.9, Figure 4.8). In comparison, for the Lynx acceleration-deceleration manoeuvre, the inverse simulation results show that the maximum pitch perturbation for the acceleration part was about -7 deg, and about +7 deg for the deceleration part (Figure 5.15).

Previous simulation results for the VPM M16 gyroplane obtained by using the RASCAL model (*Houston and Thomson, 2001*) showed cross-couplings between longitudinal and lateral-directional degrees of freedom for this gyroplane. Flight test results for the G-UNIV acceleration-deceleration task also indicated that undesirable couplings between the longitudinal and lateral-directional axes do exist. For example, during the 40-60-40 mph task (Figure 7.13) the test pilot had to tilt the rotor shaft to the right by about +1 deg to compensate increasing engine and propeller torque during the acceleration part, and tilt back to the trim position during the deceleration part of the manoeuvre. However, the pilot's ratings for handling qualities and workload were not high (HQR 2, WR 2) for this task, indicating that interaxis couplings did not affect pilot's ability to complete the task.

### **7.3 Examples of a Design of Handling Qualities Criteria for Light Gyroplanes**

The most important objective of the flight test programme for a handling qualities study is to form a database of flight test results and pilot subjective ratings for different manoeuvres with various levels of aggressiveness. This database, in conjunction with simulation results, can be used to develop handling qualities requirements and criteria. Of course, the flight test programme of the G-UNIV research gyroplane has provided

limited test data, which are in general not enough to develop any handling qualities requirements or criteria for light gyroplanes. In addition, it should be borne in mind that only one test pilot conducted all the flight experiments, and only one gyroplane was flight tested. Nevertheless, for demonstration purposes, it was decided to design gyroplane handling qualities criteria, which are based only on a limited set of flight test results and pilot subjective ratings.

As was demonstrated in Chapter 2, Section 2.4, the ADS-33E-PRF (2000) standard defines handling qualities levels for the roll attitude quickness parameter as a function of roll attitude change. This approach was adapted to design roll attitude quickness criteria for a gyroplane slalom manoeuvre. Figure 7.14 shows the results for roll attitude quickness calculated using the test data and plotted against roll attitude changes. Since every point in the chart is represented by a pilot's subjective HQR, handling qualities levels can be defined. The recommended level boundaries are depicted in Figure 7.14. It can be seen that the gyroplane level boundaries are shifted up and left in comparison with those of the ADS-33E-PRF (Chapter 2, Figure 2.7). It is clear from Figure 7.14 that, even for the most aggressive slalom manoeuvres, the G-UNIV gyroplane never achieved the 70 deg/sec boundary. Therefore, because of safety issues, it would be reasonable to specify a limit of aircraft capability represented by a roll rate boundary as demonstrated by Padfield (1996, p. 348).

The second criterion is based on a parameter called "pilot attack", which was proposed by Padfield *et al* (1994) as an objective metric of pilot workload. The pilot attack parameter is defined as follows

$$\text{pilot attack} = \frac{\dot{\eta}_{pk}}{\Delta\eta}, \quad (7.1)$$

where  $\dot{\eta}_{pk}$  is the peak value in the rate of change of lateral stick displacement and  $\Delta\eta$  is the corresponding change in net stick displacement. It was hypothesised by Padfield *et al* (1994) that workload levels for the pilot attack parameter can be defined as a function of change in net stick displacement. A gyroplane attack chart with the suggested levels of pilot workload is presented in Figure 7.15. It is clear that the trends

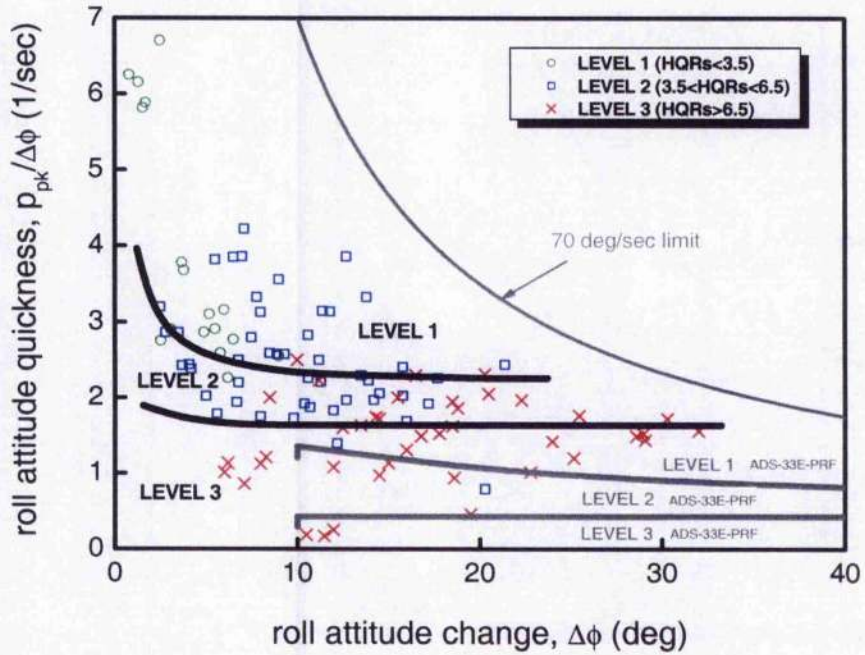


Figure 7.14 Suggested roll attitude quickness Levels for gyroplane slalom manoeuvre in comparison with those of ADS-33E-PRF

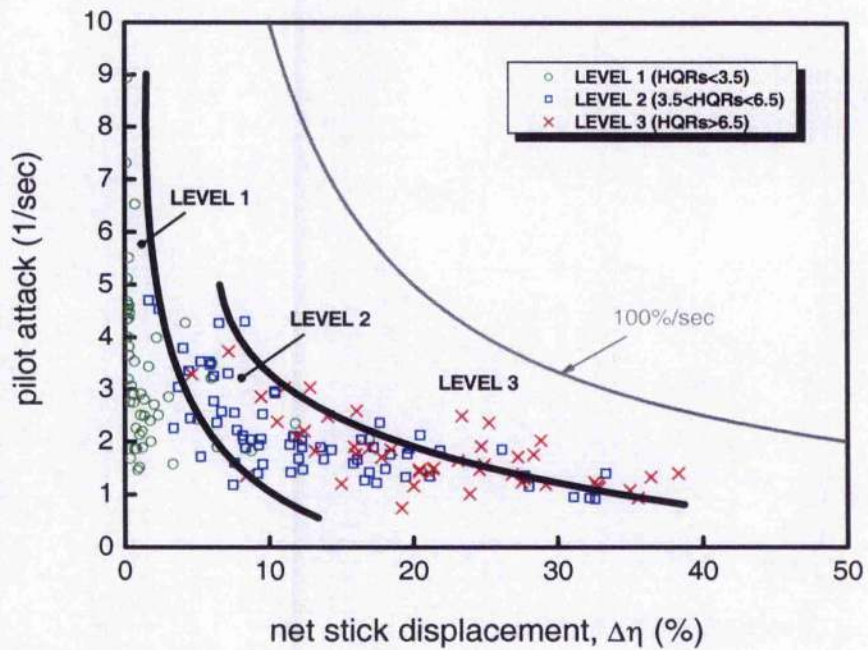


Figure 7.15 Suggested pilot attack Levels for gyroplane slalom manoeuvre

of the level boundaries and the limit of gyroplane capability (the 100 %/sec boundary) coincide with those predicted by Padfield *et al* (1994). It should be noted that even for helicopters there are no workload levels defined for the pilot attack chart, though some studies have provided experimental and simulation results of an assessment of the pilot attack metric (Padfield *et al*, 1994; Leacock, 2000; Macdonald, 2001; Cameron, 2002 for example). In conclusion, it should be emphasised that to the author's best knowledge, these two examples are the first documented handling qualities and workload criteria for gyroplanes.

## **7.4 Chapter Summary**

This chapter has presented results of a recently completed flight test programme for the G-UNIV gyroplane handling qualities assessment. Thirty slalom and six acceleration-deceleration manoeuvres with various levels of aggressiveness have been successfully completed during the flight tests. The chapter has presented time histories of slalom and acceleration-deceleration manoeuvres, as well as subjective pilot HQRs and WRs. It should be noted that gyroplane subjective handling qualities and workload ratings have been obtained and documented for the first time. Thus, a database of subjective pilot assessments for gyroplane slalom and acceleration-deceleration manoeuvres has been formed. An effect of slalom manoeuvre aggressiveness on pilot subjective handling qualities and workload ratings has been investigated. It has been revealed that by the increase in the airspeed and aspect ratio of the course, the pilot subjective handling qualities and workload ratings degrade. Flight testing has proven to be a most challenging part of the research project because a light gyroplane has never previously been flight tested for slalom and acceleration-deceleration manoeuvres. Therefore, all the test courses have had to be prepared very carefully and in an incremental manner, avoiding taking the test gyroplane to its limits. The final section of this chapter has proposed examples of designing handling qualities and workload criteria for light gyroplanes. It has been demonstrated how levels of handling qualities can be defined for roll attitude quickness and pilot attack criteria.

In conclusion, it should be emphasised that further investigations involving different types of gyroplanes and different test pilots are required to define proper requirements for gyroplane manoeuvres. Nevertheless, the author believes that the results of the flight test programme of the G-UNIV research gyroplane can be considered as a useful contribution to the time-consuming process of development of handling qualities standards for gyroplanes.

# Chapter 8

## Conclusions and Recommendations

### 8.1 Introductory Remarks

The main aim of this research as stated in Chapter 1 was to assess and study gyroplane handling qualities using flight testing and simulation techniques. To achieve this aim the following objectives of the research were set:

- i) *Objective Assessment of Gyroplane Handling Qualities;*
- ii) *Development of Inverse Simulation Package for Preliminary Design of Gyroplane Manoeuvres;*
- iii) *Subjective Assessment of Gyroplane Handling Qualities by Conducting a Series of Flight Tests;*
- iv) *Preliminary Recommendations Regarding the Structure and Organisation of Gyroplane Handling Qualities Requirements and Criteria.*

In this concluding chapter, the extent to which the main aim and objectives have been met is discussed.

## 8.2 Conclusions

Based on the results presented in this dissertation, the following conclusions can be drawn:

### *i) Objective Assessment of Gyroplane Handling Qualities*

Objective assessment of gyroplane handling qualities has been conducted. Longitudinal short period and lateral-directional Dutch roll characteristics of the G-UNIV gyroplane have been estimated against criteria and requirements from a series of standards and specifications. The assessment has been based on the flight test data obtained from previous studies. The G-UNIV research aircraft does not satisfy the BCAR Section T requirements for the short period oscillations because of its low pitch damping characteristics, but do satisfy the general requirements for longitudinal and lateral-directional oscillations. It has been concluded from the assessment that in general the G-UNIV research gyroplane is a good Level 2 aircraft both in longitudinal and lateral-directional axes. Of course, it should be borne in mind that the criteria used in the assessment process were designed for different types of aircraft and all the results are based only on limited flight test data, and therefore the obtained handling qualities should be considered as a preliminary estimation. More importantly, it has been demonstrated that gyroplane handling qualities can be estimated using the “classical” approaches from the existing standards for aeroplanes and rotorcraft, and that gyroplane’s own criteria can be designed in the same manner as the criteria from these standards.

### *ii) Development of Inverse Simulation Package for Preliminary Design of Gyroplane Manoeuvres*

A high fidelity, individual blade/blade element coupled rotor-fuselage mathematical model of a gyroplane, GSIM has been developed that includes a sophisticated dynamic inflow model and a blade flapping model based on centre-spring equivalent rotor

approach. Combined blade element momentum theory has been applied to calculate forces and moments of the gyroplane's autorotating rotor. The GSIM model has been validated against flight test data for steady state results. The study of gyroplane handling qualities requires accurate predictions of the vehicle dynamic response. Moreover, aggressive manoeuvres such as slalom and acceleration-deceleration drive the vehicle to the edges of the flight envelope. Therefore, the development of this high fidelity model, GSIM, has been successful.

The GSIM model has been successfully coupled with a generic inverse simulation algorithm GENISA to form an inverse simulation package GENISA/GSIM. To reduce the flight test effort required in the current research the GENISA/GSIM package has been proposed as a preliminary tool in designing gyroplane manoeuvres. The validation of the GENISA/GSIM has been conducted by comparison of flight test results with predicted pilot control inputs and state variables. It has been demonstrated that the slalom and acceleration-deceleration manoeuvres from the ADS-33E-PRF (2000) standard can be adapted to suit a light gyroplane, and then defined mathematically to incorporate them into the inverse simulation algorithm. To the author's best knowledge, inverse simulation has never been applied to a gyroplane simulation model before. The results presented in this dissertation has demonstrated that the GENISA/GSIM package has proved to be a valid, robust and reliable tool for designing gyroplane flight test manoeuvres for handling qualities studies and can be used in other applications.

Two different control strategies (constrained sideslip rate and constrained heading attitude rate) for the slalom manoeuvre have been investigated using the GENISA/GSIM package. An effect of AR and airspeed of the slalom course on levels of aggressiveness has been studied. The higher the AR and airspeed the larger the lateral control inputs and consequently larger bank angles required to complete the slalom task. As a result, a flight envelope and levels of aggressiveness for the gyroplane slalom manoeuvre have been proposed. A comparison of the G-UNIV gyroplane's behaviour during the acceleration-deceleration manoeuvre with that of the Lynx helicopter has led to the conclusion that the G-UNIV gyroplane behaves more like an aeroplane rather than a helicopter during this manoeuvre, using mainly an engine power, and thus a propeller thrust to accelerate and decelerate.

### *iii) Subjective Assessment of Gyroplane Handling Qualities by Conducting a Series of Flight Tests*

A flight test technique for handling qualities assessment of a light gyroplane has been developed. A detailed description of the test gyroplane, including onboard instrumentation and ground preparations for the flight test programme has been provided. The basic premise of the current research is that the handling qualities requirements and prescribed manoeuvres from the ADS-33E-PRF document can be modified to suit a light gyroplane. In particular, a considerable effort has been focused on demonstrating how gyroplane slalom and acceleration-deceleration manoeuvres can be designed based on those from the ADS-33E-PRF standard.

A flight test programme of the G-UNIV research gyroplane has been conducted to demonstrate the use of the designed gyroplane slalom and acceleration-deceleration manoeuvres based on those from the ADS-33E-PRF standard. Flight tests for handling qualities assessment usually include aggressive manoeuvring at the edges of the aircraft flight envelope, therefore safety issues must be paramount. The flight test programme has been carefully planned and organised, and all the flight trials have been prepared and conducted very carefully and in incremental manner. It should be emphasised that the flight test technique proposed in this dissertation can be easily adapted by gyroplane designers and testing engineers to assess handling qualities of gyroplanes in a stage of flight tests of first prototypes.

The concept of mission task elements from the ADS-33E-PRF standard has been used as a basis for subjective assessment of gyroplane handling qualities. After each test flight for the slalom and acceleration-deceleration manoeuvres, the test pilot assigned handling qualities ratings using the Cooper-Harper rating scale and workload ratings using the Bedford workload scale. It should be emphasised that for the first ever time gyroplane subjective handling qualities and workload ratings have been obtained and documented. Thus, a database of subjective pilot assessments has been formed and analysed. An effect of slalom manoeuvre aggressiveness on pilot subjective handling qualities and workload ratings has been investigated. It has been revealed that by the increase in the airspeed and aspect ratio of the course, the pilot subjective handling qualities and workload ratings are degrading. As was noted in Chapter 1, conducting

such a flight test programme has been challenging, as flying such tightly prescribed manoeuvres using a gyroplane has never previously been attempted.

*iv) Preliminary Recommendations Regarding the Structure and Organisation of Gyroplane Handling Qualities Requirements and Criteria*

Preliminary recommendations have been proposed regarding suitability of handling qualities criteria of fixed and rotary wing aircraft. Chapters 2 and 3 have provided a thorough discussion of a possible structure and organisation of the gyroplane handling qualities requirements for longitudinal and lateral-directional axes. In addition, this dissertation has proposed two handling qualities criteria for a light gyroplane, the roll quickness and pilot attack criteria for the slalom manoeuvre. The design of these criteria has been based on the flight test data obtained from the handling qualities flight tests of the G-UNIV research gyroplane. Currently available test data are insufficient to determine properly handling qualities levels because the flight test programme has provided only limited test data. In addition, it should be borne in mind that only one test pilot has been involved in the flight experiments, and only one gyroplane has been flight tested. Nevertheless, the author believes that the results of this flight test programme can be considered as a useful contribution to the time-consuming process of development of handling qualities requirements for gyroplanes.

Finally, it can be concluded that the main aim of the thesis, which was to assess and study gyroplane handling qualities using flight testing and simulation techniques, has been met successfully.

### **8.3 Recommendations for Future Work**

*i) Modelling and Simulation Improvements*

(a) The GSIM model has been developed to simulate uniquely the G-UNIV research gyroplane's flight dynamics. Nevertheless, this model can be easily applied to different types of gyroplanes.

(b) The GSIM rotor model can be enhanced by modelling blade elasticity and including free wake models.

(c) It has been demonstrated that the test pilot used neither of the two control strategies predicted by inverse simulation of the slalom manoeuvre. It would be therefore beneficial to define mathematically the slalom manoeuvre in a more realistic manner reflecting actual strategies.

(d) Only two gyroplane manoeuvres, the slalom and the acceleration-deceleration, have been considered in the thesis. It is recommended to enlarge a database of gyroplane manoeuvres by designing and flight testing new, specific to gyroplanes, test manoeuvres.

#### *ii) Issues Relating to the G-UNIV Research Gyroplane*

(a) The G-UNIV research gyroplane has never been wind tunnel tested. The only available aerodynamic data for a light gyroplane's fuselage and empennage were from wind tunnel tests of the scale model of VPM M14 gyroplane. Therefore, it would be advantageous to conduct wind tunnel tests of a scale model of the G-UNIV gyroplane.

(b) In this dissertation an objective assessment of the G-UNIV gyroplane's handling qualities has been mainly based on longitudinal and lateral-directional oscillations at the airspeed of 40 mph. It is highly desirable to obtain experimental results of the G-UNIV gyroplane's oscillations for a full airspeed range including stick fixed and stick free responses.

(c) It is suggested to investigate more thoroughly a phugoid mode and an "unusual oscillatory mode" of the G-UNIV gyroplane described in detail in Chapter 3.

*iii) Necessity for Further Flight and Simulation Experiments of Gyroplanes*

Further flight tests and simulation involving different types of gyroplanes and different test pilots are required to form a database of objective and subjective assessments of gyroplanes handling qualities with the aim of developing new gyroplane requirements and criteria in the future.

**8.4 Concluding Remarks**

The results presented in this dissertation are unique and significant, and reveal the behaviour of the gyroplane in terms of its handling qualities. Moreover, results in the area of gyroplane handling qualities are timely because of the poor gyroplane accident statistics in the UK. The author believes that the results, experience and knowledge, which have been gained during this research, can substantially contribute to the understanding of gyroplane flight dynamics and the development of new design and certification standards for gyroplanes.

# *Appendix 1*

## **A Review of Definitions of MIL-F-8785C Specification and DEF STAN 00-970 Rotorcraft Standard**

### **A1.1 MIL-F-8785C (1980)**

#### **A1.1.1 Classification of Aeroplanes**

<i>Class I</i>	<i>Small, light aeroplanes.</i>
<i>Class II</i>	<i>Medium weight, low-to-medium manoeuvrability aeroplanes.</i>
<i>Class III</i>	<i>Large, heavy, low-to-medium manoeuvrability aeroplanes.</i>
<i>Class IV</i>	<i>High-manoevrability aeroplanes.</i>

#### **A1.1.2 Flight Phase Categories**

##### Nonterminal Flight Phases

*Category A*     *Those nonterminal Flight Phases that require rapid manoeuvring, precision tracking, or precise flight-path control. Included in this Category are air-to-air combat, ground attack, weapon delivery/launch, aerial recovery, reconnaissance, in-flight refuelling (receiver), terrain following, antisubmarine search, and close formation flying.*

*Category B* Those nonterminal Flight Phases that are normally accomplished using gradual manoeuvres and without precision tracking, although accurate flight-path control may be required. Included in this Category are climb, cruise, loiter, in-flight refuelling (tanker), descent, emergency descent, emergency deceleration, and aerial delivery.

### Terminal Flight Phases

*Category C* Terminal Flight Phases normally accomplished using gradual manoeuvres and usually require accurate flight-path control. Included in this Category are takeoff, catapult takeoff, approach, wave-off/go-around, and landing.

### **A1.1.3 Levels of Flying Qualities**

- Level 1* Flying qualities clearly adequate for the mission Flight Phase.
- Level 2* Flying qualities adequate to accomplish the mission Flight Phase, but some increase in pilot workload or degradation in mission effectiveness, or both, exists.
- Level 3* Flying qualities such that the airplane can be controlled safely, but pilot workload is excessive or mission effectiveness is inadequate, or both. Category A Flight Phases can be terminated safely, and Category B and C Flight Phases can be completed.

## A1.2 DEF STAN 00-970 Rotorcraft (1984)

### A1.2.1 Short Term Dynamic Stability Criteria

Recommended criteria for Level 1 and Level 2 handling qualities (Figure 2.9):

- (i) *Maximum time ( $T_{30}$ ) to return within 30% peak disturbance from datum.*
- (ii) *Minimum and maximum limits on the time ( $T_{01}$ ) to first pass through datum.*
- (iii) *During the first return to datum there should be no obtrusive hesitation in the rate of return.*
- (iv) *Maximum percentage of peak disturbance for first peak overshoot ( $x_1$ ).*
- (v) *Minimum time ( $T_{02}$ ) for any second pass through datum (in same sense as initial disturbance) from any overshoot  $x_1$ , greater than 5%.*
- (vi) *Maximum percentage of peak disturbance for any second peak ( $x_2$ ) in the same sense as the initial disturbance.*
- (vii) *Maximum time ( $T_F$ ) to return and remain within  $\pm x_F\%$  of peak disturbance about datum.*

### A1.2.2 Pitch Short Term Response Characteristics

Levels of Handling Qualities for Aggressive Manoeuvres:

- Level 1*      *For Level 1 handling characteristics a pulse input through the longitudinal flying control should produce a pitch rate type of rotorcraft response in accordance with the first column of Table A1.1.*

- Level 2*            *Reduced handling qualities in terms of less responsiveness, greater sensitivity, larger overshoot and longer settling time are reflected in the wider parameter ranges quoted for Level 2 compared with Level 1.*
- Level 3*            *Is currently not addressed in Table A1.1. It would be inappropriate for the pilot to embark upon deliberately aggressive manoeuvres with the rotorcraft in a sufficiently degraded operating state that led to the workload in controlling the rotorcraft approaching the limits of the pilot's capability.*

#### Levels of Handling Qualities for Moderate Manoeuvres:

- Level 1*            *For Level 1 handling characteristics a longitudinal control input should also produce a pitch rate type of rotorcraft response. As shown in Table A1.1 the peak response to the standard control input does not have to be as high as for aggressive tasks, but no distinction is made for the dynamic stability criteria.*
- Level 2*            *If the longitudinal control input generates a pitch attitude, rather than a pitch rate, type of response the additional pilot anticipation required in accurately executing manoeuvres is likely to lead to Level 2 or 3 qualities, depending on control sensitivity or dynamic stability characteristics expressed in terms of pitch attitude as in Table A1.1.*
- Level 3*            *For Level 3 handling characteristics any short period oscillatory modes should be damped. Where flight under IFR is required, oscillations having a period of 5 sec or less should halve amplitude in less than 1 cycle, and those with a period greater than 5 sec in less than 2 cycles. For flight under VFR, oscillations with a period of 5 sec or less should halve amplitude in less than 2 cycles.*

**Table A1.1** Pitch short term initial response and dynamic stability criteria - Active Flight Phases, adapted from DEF STAN 00-970 Rotorcraft (1984)

Manoeuvre Classification	Aggressive			Moderate		
	1	2	3	1	2	3
Response Parameter	Pitch Rate	Pitch Rate		Pitch Rate	Pitch Attitude	Pitch Attitude
Peak Response	10-15 deg/sec	7-20 deg/sec		5-10 deg/sec	5-10 deg	3-5 deg
$T_1$ (sec)	0.5	0.5	N/A	0.5	0.5	0.5
$y_1$ %	>30	>30		>30	>30	>30
$y_2$ %	5	10		5	0	
$T_{30}$ (sec)	<1	<1	N/A	<1	<1.5	
$T_{11}$ (sec)	-	1-2		-	1.5-3	
$T_{01}$ (sec)	1-2	-		1-2	-	
$x_1$ %	15	20		15	25	-
$T_{02}$ (sec)	>2	>2		>2	>2.5	
$x_2$ %	10	15		10	15	
$T_F$ (sec)	3	5		3	5	
$x_F$ %	10	10		10	10	

### A1.2.2 Roll Short Term Response Characteristics

#### Levels of Handling Qualities for Aggressive Manoeuvres:

- Level 1* For Level 1 handling characteristics a pulse input through the lateral flying control should produce a roll rate type of rotorcraft response in accordance with the first column of Table A1.2.
- Level 2* Reduced handling qualities in terms of less responsiveness, greater sensitivity, larger overshoot and longer settling time are reflected in the wider parameter ranges quoted for Level 2 compared with Level 1.
- Level 3* Is currently not addressed in Table A1.2. It would be inappropriate for the pilot to embark upon deliberately aggressive manoeuvres with the rotorcraft in a sufficiently degraded operating state that led to the workload in controlling the rotorcraft approaching the limits of the pilot's capability.

#### Levels of Handling Qualities for Moderate Manoeuvres:

- Level 1* For Level 1 handling characteristics a lateral control input should also produce a roll rate type of rotorcraft response. As shown in Table A1.2 the peak response to the standard control input does not have to be as high as for aggressive tasks, but no distinction is made for the dynamic stability criteria.
- Level 2* If the lateral control input generates a roll attitude, rather than a roll rate, type of response the additional pilot anticipation required in accurately executing manoeuvres is likely to lead to Level 2 or 3 qualities, depending on control sensitivity or dynamic stability characteristics expressed in terms of roll attitude as in Table A1.2.

## Level 3

For Level 3 handling characteristics any short period oscillatory modes should be damped. Where flight under IFR is required, oscillations having a period of 5 sec or less should halve amplitude in less than 1 cycle, and those with a period greater than 5 sec in less than 2 cycles. For flight under VFR, oscillations with a period of 5 sec or less should halve amplitude in less than 2 cycles.

**Table A1.2** Roll short term initial response and dynamic stability criteria - Active Flight Phases, adapted from DEF STAN 00-970 Rotorcraft (1984)

Manoeuvre Classification	Aggressive			Moderate		
	1	2	3	1	2	3
Response Parameter	Roll Rate	Roll Rate		Roll Rate	Roll Attitude	Roll Attitude
Peak Response	15-20 deg/sec	10-15 deg/sec		10-15 deg/sec	8-12 deg	6-15 deg
T <sub>1</sub> (sec)	0.5	0.5	N/A	0.5	0.5	0.5
y <sub>1</sub> %	>30	>30		>30	>30	>30
y <sub>2</sub> %	5	10		5	0	0
T <sub>30</sub> (sec)	<1	<1		<1	<1.5	
T <sub>11</sub> (sec)	-	1-2		-	1.5-3	
T <sub>01</sub> (sec)	1-2	-		1-2	-	
x <sub>1</sub> %	15	20	N/A	15	25	-
T <sub>02</sub> (sec)	>2	>2		>2	>2.5	
x <sub>2</sub> %	10	15		10	15	
T <sub>F</sub> (sec)	3	5		3	5	
x <sub>F</sub> %	10	10		10	10	

## Appendix 2

### Configurational Data for the G-UNIV Research Gyroplane

Table A2.1 Physical characteristics of the G-UNIV research gyroplane

<i>General</i>	Gross mass Power (ROTAX TYPE 618) Moments of inertia: roll pitch yaw	387 kg 55 kW (73.8 hp)  72.96 kg m <sup>2</sup> 297.21 kg m <sup>2</sup> 300 kg m <sup>2</sup>
<i>Main Rotor</i>	Number of blades Blade radius Blade chord Blade mass Blade twist Flapping inertia Lift curve slope Acrofoil section Rotor direction	2 3.81 m 0.197 m 17.255 kg 0 deg 83.492 kg m <sup>2</sup> 5.75 rad <sup>-1</sup> NACA 8-H-12 Anti-clockwise
<i>Propeller</i>	Propeller blade radius Propeller blade chord Blade twist Orientation of thrust line	0.787 m 0.09 m 0 deg 1 deg
<i>Fuselage</i>	Side area Plan area Frontal area	0.798 m <sup>2</sup> 0.916 m <sup>2</sup> 0.448 m <sup>2</sup>
<i>Tailplane</i>	Area Lift curve slope Setting angle	0.356 m <sup>2</sup> 3.5 rad <sup>-1</sup> 0 deg
<i>Fin</i>	Area Lift curve slope Setting angle	0.281 m <sup>2</sup> 3.5 rad <sup>-1</sup> 0 deg

**Table A2.1** (cont.) Physical characteristics of the G-UNIV research gyroplane

<i>Endplate</i>	Area	0.107 m <sup>2</sup>
	Lift curve slope	3.5 rad <sup>-1</sup>
	Setting angle	0 deg
<i>Rudder</i>	Rudder area	0.368 m <sup>2</sup>
	Lift curve slope	3.5 rad <sup>-1</sup>

**Table A2.2** Coordinates (in metres) of the G-UNIV gyroplane subsystems used in the simulation\*

Nominal centre of mass	(0.174, 0, -0.83)
Rotor pivot point	(-0.013, 0, -1.968)
Rotor hub	(-0.038, 0, -2.105)
Propeller hub	(-0.95, 0, -0.795)
Fuselage c.p.	(1.626, 0, -0.48)
Tailplane c.p.	(-1.02, 0, -0.057)
Fin c.p.	(-1.0, 0, -0.268)
Endplate c.p.	(-1.09, ±0.45, -0.063)
Rudder c.p.	(-1.633, 0, -0.392)

\* Airframe reference point for coordinates presented in this table is taken as the intersection of the projection of the mast centreline and the keel centreline with the *x-body* axis aligned with the keel.

## Appendix 3

### Specifications of the Test Instrumentation

**Table A3.1** Specifications of the VSG 2000 angular rate sensors

<i>General Information</i>	Part Number Serial Number Manufacturer Description	292101-0100 30201, 30202, 30206 British Aerospace Systems & Equipment Solid state, single axis, angular rate sensor
<i>Performance</i>	Angular Rate Range Nominal Scale Factor Resolution Linearity Ready Time Bandwidth	$\pm 100$ deg/sec 20 mV/deg/sec 0.025 deg/sec $\pm 0.3$ deg/sec 0.3 sec 70 Hz (-90 deg phase)
<i>Environmental</i>	Temperature Range Shock Survival Vibration Survival	-40°C to +85°C 1000 g, 3 ms, 0.5 sine wave 10 g rms 20 to 1000 Hz
<i>Electrical</i>	Supply Voltage Range Output	9 to 18 V DC 0.5 V to 4.5 V DC unipolar

**Table A3.2** Specifications of the AD01-RP, AD01-Y angle sensors

<i>General Information</i>	Part Number Serial Number Manufacturer Description	AD01-RP (roll/pitch), AD01-Y (yaw) 6062350, 7053204, 7053155 Sumitomo Precision Products Ltd. Solid state, single axis, angle sensor
<i>Performance</i>	Angle Range Nominal Scale Factor Resolution Non-linearity Ready Time Bandwidth	$\pm 45$ deg (roll, pitch), $\pm 180$ deg (yaw) 44.2 mV/deg (roll, pitch), 11.1 mV/deg (yaw) 0.1 deg $\pm 1\%$ full scale 0.3 sec 3 Hz (-3dB gain)
<i>Environmental</i>	Temperature Range	-20°C to +70°C
<i>Electrical</i>	Supply Voltage Output	12 V DC 0.5 to 4.5 V DC unipolar

**Table A3.3** Specifications of the C3A-02 3-axes accelerometer

<i>General Information</i>	Part Number Serial Number Manufacturer Description	C3A-02 702111 Sumitomo Precision Products Ltd. Solid state, 3-axes, acceleration sensor
<i>Performance</i>	Acceleration Range Resolution Non-linearity  Ready Time Bandwidth	$\pm 2$ g 1 mg 0.5% full scale for x, y axes, 1.5% full scale for z axis  0.3 sec 30 Hz (-3dB gain) for x, y axes, 7 Hz (-3dB gain) for z-axis
<i>Environmental</i>	Temperature Range Shock Survival  Vibration Survival	-30°C to +75°C Drop to concrete floor from 1 m height (for all axes)  $\pm 4.5$ g 5 to 200 Hz (for all axes)
<i>Electrical</i>	Supply Voltage Range Output	4.75 to 5.25 V DC 0 to 5 V DC unipolar

**Table A3.4** Specifications of the Seika B1 single axis accelerometer

<i>General Information</i>	Part Number Serial Number Manufacturer Description	NB43R10, Seika B1 A7659 Seika Kempton Capacitive, single axis accelerometer
<i>Performance</i>	Acceleration Range Sensitivity Non-linearity Bandwidth	$\pm 3$ g 120.8 mV/g 1% full scale 200 Hz
<i>Environmental</i>	Temperature Range Shock Survival	-40°C to +85°C 10000 g
<i>Electrical</i>	Supply Voltage (Stabilised) Supply Voltage Range Output	5 V DC 3 to 5 V DC 2.4 to 2.6 V DC unipolar

**Table A3.5** Specifications of the Sensortechincs pressure transducers

<i>General Information</i>	Part Number Serial Number Manufacturer Description	144SC0811BARO, HCXM020D6 Not available Sensortechincs Precision pressure transducers
<i>Performance</i>	Pressure Range  Linearity Power Consumption	800-1100 mb (barometric), 0-20 mb (dynamic) 0.005% full scale 70 mW (barometric), 50 mW (dynamic)
<i>Electrical</i>	Output	0 to 5 V DC unipolar (barometric) 0.5 to 4.5 V DC unipolar (dynamic)

**Table A3.6** Specifications of the AccuStar II/DAS 20 dual axis clinometer

<i>General Information</i>	Part Number Serial Number Manufacturer Description	02119011-000 32969022 Schaevitz Sensors Capacitive, dual axes clinometer
<i>Performance</i>	Angle Range Nominal Scale Factor Resolution Linearity 0 to 10 deg 10 to 12 deg 12 to 15 deg 15 to 20 deg Bandwidth	$\pm 20$ deg 100 mV/deg 0.01 deg Monotonic $\pm 0.2$ deg $\pm 2.5\%$ $\pm 3.0\%$ 0.25 Hz (-3dB gain)
<i>Environmental</i>	Temperature Range	-20°C to +65°C
<i>Electrical</i>	Supply Voltage (Nominal) Supply Voltage Range Output	9 V DC 5 to 15 V DC 2.5 to 6.5 V DC

**Table A3.7** Specifications of the GARMIN eTrex Summit Personal Navigator

<i>General Information</i>	Part Number	190-00193-00
	Case	Fully-gasketed, high-impact plastic alloy, waterproof to 1 m for 30 min
	Size Weight	11.2x5.1x3.0 cm 150 g with batteries
<i>Performance</i>	Receiver	Differential-ready, 12 parallel channel
	Acquisition Time	Approx. 15 sec (warm start) Approx. 45 sec (cold start) Approx. 5 minutes (first start)
	Update rate	1/second, continuous
	Dynamics PC Interface	Performs to 6 g's RS-232
<i>Environmental</i>	Temperature Range	-15°C to +70°C
<i>Electrical</i>	Input	Two 1.5 V AA batteries
	Battery Life	Up to 16 hours of typical use

**Figure A3.1** GARMIN eTrex Summit Personal Navigator (*Garmin, 2005*)

## Appendix 4

### Experimental Measurement of Centre of Gravity Position

Since the location of the centre of gravity has been highlighted as an important design parameter for light gyroplanes, it is appropriate to consider a suitable method for determining this quantity. The method described here is easy to perform and provides fairly robust results. Equipment required includes three weight scales that each main wheel, plus nose (or tail) wheel is to rest upon. A tape measure is required to determine wheel track, and a clinometer is necessary for measuring the pitch angle of the aircraft. The method is performed in two separate stages. First, the aircraft is placed on the scales as shown in Figure A4.1, on a level surface. Position of the vertical reference line is arbitrary, and is a matter of choice. For a symmetric aircraft, the left and right wheel reactions should be the same – if they are not, advice should be sought. The wheelbase  $L$  should be measured, and then the longitudinal position of the c.g., with respect to the vertical reference line, is given by

$$x_{c.g.} = \frac{W_{nose}}{W} L, \quad (A4.1)$$

where  $W$  is the weight of the aircraft, i.e.  $W = W_{left} + W_{right} + W_{nose}$ .

The nose of the aircraft should then be raised so that the keel is inclined no less than 5 degrees to the level surface, and preferably 10 degrees. Note that the scales should not be inclined, and are to remain level. From geometry shown in Figure A4.2, the vertical location of the c.g. relative to the original level surface, is given by

$$z_{c.g.} = \frac{(W_{nose} - W'_{nose})}{W \tan \theta} L \quad (A4.2)$$

where  $\theta$  is the angle by which the keel has been raised;  $W_{nose}$  is the nose wheel reaction from stage one; and  $W'_{nose}$  is the nose wheel reaction from the inclined test.

It can be seen that only a few simple measurements need to be taken. However, equation (A4.2) emphasises the need for accuracy, especially in the measurement of the wheelbase. This is because of the  $\tan \theta$  term. For example, for inclined angles of around 5 degrees, a 0.001 m error in wheelbase will produce a 0.01 m error in  $z_{c.g.}$ ; for incline angles of 10 degrees, this error is reduced by half.

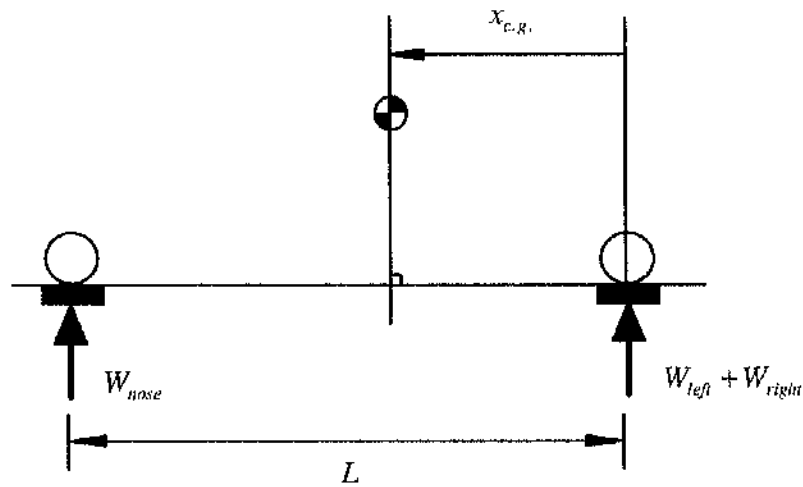


Figure A4.1 Measurement of longitudinal c.g. position

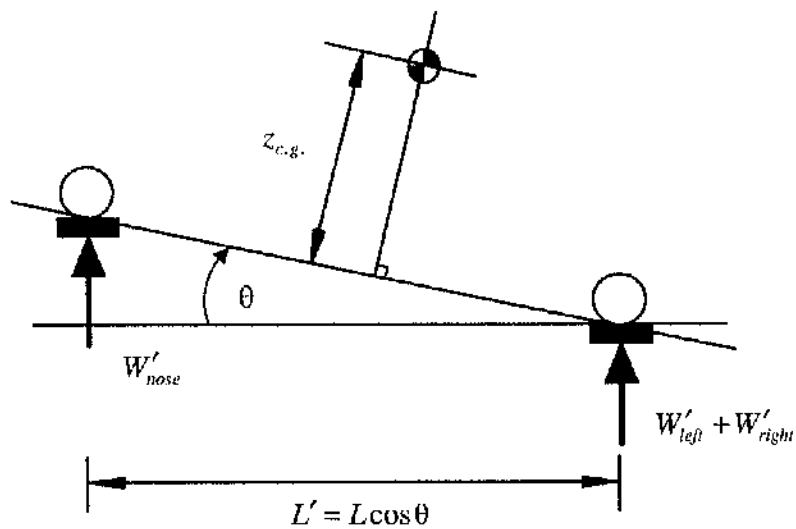


Figure A4.2 Measurement of vertical c.g. position

# Appendix 5

## Flight Trials Instruction Forms



### FLIGHT TRIALS INSTRUCTION FORM

FLIGHT TEST OBJECTIVE Slalom manoeuvre	FLIGHT No. 3/5	DATE 05 March 2004
---	-------------------	-----------------------

AIRCRAFT	MANUFACTURER Montgomerie	MODEL TYPE B8M-RT	SERIAL No. PFA/G08-1276
ENGINE	ROTAX	TYPE 618	4254311

PILOT Roger Savage	OBSERVER (GROUND) Marat Bagiev	AIRCRAFT REGISTRATION G-UNIV
-----------------------	-----------------------------------	---------------------------------

AIRCRAFT WEIGHT					
BASIC	CREW	FUEL	TOTAL TD	LONGITUDINAL CG	VERTICAL CG
272 kg	90 kg	~25 kg	387 kg	0.174	-0.83

FLIGHT CONDITIONS				T/O TIME	T/O FUEL
SURFACE WIND	SURFACE QAT	QFE	QNH	11:14	~25 kg
002/5	+5°C	1018 mb	1028 mb	LAND TIME	LAND FUEL
				11:30	~22 kg

#### TEST PLAN

1. Carry out normal take-off.
2. Initiate the manoeuvre in level unaccelerated flight at an airspeed of X mph and lined up with the centerline of the test course. Perform one smooth turn to left and one smooth turn to right at 150 m intervals. The turns shall be at least 15 m from the centerline, with a maximum lateral error of 15 m. The manoeuvre is to be accomplished below the reference altitude. Complete the manoeuvre on the centerline, in coordinated straight flight.

Press the EVENT button at the beginning of each trial.

N of trial	X
1	35
2	50
3	70

3. Carry out normal landing.



## FLIGHT TRIALS INSTRUCTION FORM

FLIGHT TEST OBJECTIVE Acceleration-deceleration manoeuvre		FLIGHT No. 2/AD	DATE 04 March 2004																					
AIRCRAFT	MANUFACTURER Montgomerie	MODEL TYPE B8M-RT	SERIAL No. PFA/G08-1276																					
ENGINE	ROTAX	TYPE 618	4254311																					
PILOT Roger Savage	OBSERVER (GROUND) Marat Bagiev	AIRCRAFT REGISTRATION G-UNIV																						
AIRCRAFT WEIGHT																								
BASIS 272 kg	CREW 90 kg	FUEL ~25 kg	TOTAL TO 387 kg																					
LONGITUDINAL CG 0.174		VERTICAL CG -0.83																						
FLIGHT CONDITIONS																								
SURFACE WIND 003/5	SURFACE QNT +5°C	QFE 1018 mb	QNH 1028 mb																					
TO TIME 15:54		TO FUEL ~25 kg																						
LAND TIME 16:14		LAND FUEL ~21 kg																						
TEST PLAN																								
1. Carry out normal take-off.																								
2. From level unaccelerated flight at an airspeed of X mph, rapidly increase power to approximately maximum, and maintain altitude constant during the acceleration to an airspeed of Y mph. Upon reaching the target airspeed, initiate a deceleration by aggressively reducing the power and holding altitude constant. Complete the manoeuvre in the initial airspeed of X mph. Maintain lateral track within $\pm 3$ m and heading within $\pm 10$ deg during the manoeuvre.																								
Press the EVENT button at the beginning of each trial.																								
<table border="1"> <thead> <tr> <th>N of trial</th> <th>X</th> <th>Y</th> </tr> </thead> <tbody> <tr> <td>1</td> <td>35</td> <td>60</td> </tr> <tr> <td>2</td> <td>35</td> <td>70</td> </tr> <tr> <td>3</td> <td>40</td> <td>50</td> </tr> <tr> <td>4</td> <td>40</td> <td>60</td> </tr> <tr> <td>5</td> <td>50</td> <td>60</td> </tr> <tr> <td>6</td> <td>50</td> <td>70</td> </tr> </tbody> </table>				N of trial	X	Y	1	35	60	2	35	70	3	40	50	4	40	60	5	50	60	6	50	70
N of trial	X	Y																						
1	35	60																						
2	35	70																						
3	40	50																						
4	40	60																						
5	50	60																						
6	50	70																						
3. Carry out normal landing.																								

# *References*

## **Part 1 – Standards and Specifications**

ADS-33C (1989), “Handling Qualities Requirements for Military Rotorcraft”,  
Aeronautical Design Standard ADS-33C, United States Army Aviation and Troop  
Command, August.

ADS-33D (1994), “Handling Qualities Requirements for Military Rotorcraft”,  
Aeronautical Design Standard ADS-33D, United States Army Aviation and Troop  
Command, July.

ADS-33D-PRF (1996), “Handling Qualities Requirements for Military Rotorcraft”,  
Aeronautical Design Standard ADS-33D-PRF, United States Army Aviation and Troop  
Command, May.

ADS-33E-PRF (2000), “Handling Qualities Requirements for Military Rotorcraft”,  
Aeronautical Design Standard ADS-33E-PRF, United States Army Aviation and Troop  
Command, March.

AGARD-R-577-70 (1970), “V/STOL Handling-Qualities Criteria”, Report No.  
AGARD-R-577-70, December.

BCAR Section S (2003), “British Civil Airworthiness Requirements, CAP 482, Section  
S, Small Light Aeroplanes”, UK Civil Aviation Authority, Issue 3, August.

BCAR Section T (1993), "British Civil Airworthiness Requirements, Section T, Light Gyroplane Design Requirements", UK Civil Aviation Authority, Paper T 860, Issue 2, July.

BCAR Section T (1995), "British Civil Airworthiness Requirements, CAP 643, Section T, Light Gyroplanes", UK Civil Aviation Authority, Issue 1, March.

BCAR Section T (2003), "British Civil Airworthiness Requirements, CAP 643, Section T, Light Gyroplanes", UK Civil Aviation Authority, Issue 2, August.

DEF STAN 00-970 (2003), "Design and Airworthiness Requirements for Service Aircraft", Defence Standard 00-970, Part 1, Section 2 - Flight, UK Ministry of Defence, October.

DEF STAN 00-970 Rotorcraft (1984), "Design and Airworthiness Requirements for Service Aircraft", Defence Standard 00-970, Volume 2 - Rotorcraft, UK Ministry of Defence, July.

FAR-23 (1993), "Federal Aviation Regulations, Part 23, Airworthiness Standards: Normal, Utility, Acrobatic, and Commuter Category Airplanes", Federal Aviation Administration, US Department of Transportation, Amendment 23-45, August.

FAR-27 (1983), "Federal Aviation Regulations, Part 27, Airworthiness Standards: Normal Category Rotorcraft", Federal Aviation Administration, US Department of Transportation, Amendment 27-19, January.

JAR-23 (2004), "Joint Aviation Requirements JAR-23, Normal, Utility, Aerobatic, and Commuter Category Aeroplanes", Joint Aviation Authorities, Amendment 2, November.

JAR-27 (2004), "Joint Aviation Requirements JAR-27, Small Rotorcraft", Joint Aviation Authorities, Amendment 4, November.

JAR-VLA (2004), "Joint Aviation Requirements JAR-VLA, Very Light Aeroplanes", Joint Aviation Authorities, Amendment 1, November.

JAR-VLR (2004), "Joint Aviation Requirements JAR-VLR, Very Light Rotorcraft", Joint Aviation Authorities, Amendment 1, November.

MIL-F-83300 (1970), "Flying Qualities of Piloted V/STOL Aircraft", Military Specifications MIL-F-83300, December.

MIL-F-008785A(USAF) (1968), "Flying Qualities of Piloted Airplanes", Military Specifications MIL-F-008785A(USAF), October.

MIL-F-8785B(ASG) (1969), "Flying Qualities of Piloted Airplane", Military Specifications MIL-F-8785B(ASG), August.

MIL-F-8785C (1980), "Flying Qualities of Piloted Airplanes", Military Specifications MIL-F-8785C, November.

MIL-H-8501A (1961), "General Requirements for Helicopter Flying and Ground Handling Qualities", Military Specifications MIL-H-8501A, September (superseding MIL-H-8501, November 1952).

MIL-HDBK-1797 (1997), "Flying Qualities of Piloted Aircraft", Department of Defence Handbook MIL-HDBK-1797, December.

MIL-STD-1797A (1990), "Flying Qualities of Piloted Aircraft", Military Standard MIL-STD-1797A, January (superseding MIL-STD-1797(USAF), March 1987).

## Part 2 – General

Anderson, D. (1999), "Active Control of Turbulence-Induced Helicopter Vibration", PhD Thesis, Department of Aerospace Engineering, University of Glasgow.

Anon. (1991), "Airworthiness Review of Air Command Gyroplanes", UK Air Accidents Investigation Branch Report, September.

Anon. (2002), "Aviation Safety Review 1992 - 2001", CAP 735, Safety Regulation Group, UK Civil Aviation Authority, October.

Anon. (2003), Bulletin 9/2003 (EW/C2002/05/05), UK Air Accidents Investigation Branch, September.

Ashkenas, I. L. (1984), "Twenty-Five Years of Handling Qualities Research", *Journal of Aircraft*, Vol. 21, No. 5, pp. 291-301.

Avanzini, G., de Matteis, G. (2001), "Two-Timescale Inverse Simulation of a Helicopter Model", *Journal of Guidance, Control, and Dynamics*, Vol. 24, No. 2, pp. 330-339.

Badcock, K. J., Richards, B. E., Woodgate, M. A. (2000), "Elements of Computational Fluid Dynamics on Block Structured Grids Using Implicit Solvers", *Progress in Aerospace Sciences*, Vol. 36, No. 5-6, pp. 351-392.

Bagiev, M., Thomson, D. G., Houston, S. S. (2003), "Autogyro Inverse Simulation for Handling Qualities Assessment", *Proceedings of the 29<sup>th</sup> European Rotorcraft Forum*, Friedrichshafen, Germany, 16-18 September.

- Bagiev, M., Thomson, D. G., Houston, S. S. (2004), "Autogyro Handling Qualities Assessment", Proceedings of the 60<sup>th</sup> Annual Forum of the American Helicopter Society, Baltimore, MD, 7-10 June.
- Bailey, F. J. (1938), "A Study of the Torque Equilibrium of an Autogyro Rotor", NACA Report 623.
- Bailey, F. J., Gustafson, F. B. (1939), "Observations in Flight of the Region of Stalled Flow Over the Blades of an Autogyro Rotor", NACA TN 741.
- Brown, R. E. (2000), "Rotor Wake Modelling for Flight Dynamic Simulation of Helicopters", AIAA Journal, Vol. 38, No. 1, pp. 57-63.
- Brown, R. E., Houston, S. S. (2000), "Comparison of Induced Velocity Models for Helicopter Flight Mechanics", Journal of Aircraft, Vol. 37, No. 4, pp. 623-629.
- Cameron, N. (2002), "Identifying Pilot Model Parameters for an Initial Handling Qualities Assessment", PhD Thesis, Department of Aerospace Engineering, University of Glasgow.
- Cao, Y. (2000), "A New Inverse Solution Technique for Studying Helicopter Manoeuvring Flight", Journal of the American Helicopter Society, Vol. 45, No. 1, pp. 43-53.
- Cao, Y., Su, Y. (2002), "Helicopter Manoeuvre Gaming Simulation and Mathematical Inverse Solution", Proceedings of the Institution of Mechanical Engineers, Part G, Journal of Aerospace Engineering, Vol. 216, No. G1, pp. 41-49.
- Carignan, S. J. R. P., Gubbels, A. W. (1998), "Assessment of Vertical Axis Handling Qualities for the Shipborne Recovery Task - ADS 33 (Maritime)", Proceeding of the 54<sup>th</sup> Annual Forum of the American Helicopter Society, Washington, DC, 20-22 May.

- Celi, R. (1999), "Optimization-Based Inverse Simulation of a Helicopter Slalom Maneuver", Proceedings of the 25<sup>th</sup> European Rotorcraft Forum, Rome, Italy, 14-16 September.
- Chalk, C. R., Wilson, R. K. (1969), "Airplane Flying Qualities Specification Revision", Journal of Aircraft, Vol. 6, No. 3, pp. 232-239.
- Charlton, M. T., Talbot, N. (1997), "Overview of a Programme to Review Civil Helicopter Handling Qualities Requirements", 23<sup>rd</sup> European Rotorcraft Forum, Dresden, Germany, 16-18 September.
- Chen, R. T. N. (1990), "A Survey of Non-Uniform Inflow Models for Rotorcraft Flight Dynamics and Control Applications", Vertica, Vol. 14, No. 2, pp. 147-184.
- Chen, F. C., Khalil, H. K. (1990), "Two-Time-Scale Longitudinal Control of Airplanes Using Singular Perturbation", Journal of Guidance, Control, and Dynamics, Vol. 13, No. 6, pp. 952-960.
- Cook, M. V. (1997), "Flight Dynamics Principles", London, Arnold.
- Cooper, G. E., Harper, R. P. (1969), "The Use of Pilot Rating in the Evaluation of Aircraft Handling Qualities", NASA TN D-5153.
- Coton, F. N., Smrcek, L., Patek, Z. (1998), "Aerodynamic Characteristics of a Gyroplane Configuration", Journal of Aircraft, Vol. 35, No. 2, pp. 247-279.
- Doyle, S. A., Thomson, D. G. (2000), "Modification of a Helicopter Inverse Simulation to Include an Enhanced Rotor Model", Journal of Aircraft, Vol. 37, No. 3, pp. 536-538.
- Etkin, B. (1972), "Dynamics of Atmospheric Flight", New York, John Wiley and Sons.

Fortenbaugh, R., King, D., Peryea, M., Busi, T. (1999), "Flight Control Features of the Bell-Agusta (BA) 609 Tiltrotor: A Handling Qualities Perspective", Proceedings of the 25<sup>th</sup> European Rotorcraft Forum, Rome, Italy, 14-16 September.

Fortenbaugh, R., Hopkins, R., King, D. (2004), "BA609 First Flight VSTOL Handling Qualities", Proceeding of the 60<sup>th</sup> Annual Forum of the American Helicopter Society, Baltimore, MD, 7-10 June.

Gao, C., Hess, R. A. (1993), "Inverse Simulation of Large-Amplitude Aircraft Manoeuvres", Journal of Guidance, Control, and Dynamics, Vol. 16, No. 4, pp. 733-737.

Gaonkar, G. H., Peters, D. A. (1988), "Review of Dynamic Inflow Modelling for Rotorcraft Flight Dynamics", Vertica, Vol. 12, No. 3, pp. 213-242.

Garmin (2005), Garmin eTrex Summit Personal Navigator web page. Available at <http://www.garmin.com/products/etrexsummit> [Accessed 25 January 2005].

Geddie, J. C., Boer, L. C., Edwards, R. J., Enderwick, T. P., Graff, N., Pfendler, C., Ruisseau, J.-Y., Van Loon, P. A. (2001), "NATO Guidelines on Human Engineering Testing and Evaluation", Report No. RTO-TR-021.

Gilruth, R. R. (1943), "Requirements for Satisfactory Flying Qualities of Aeroplanes", NACA Report 755.

Glauert, H. (1926), "A General Theory of the Autogyro", Reports and Memoranda No. 1111, Aeronautical Research Committee, London, November.

Glauert, H. (1927), "Lift and Drag of an Autogyro on the Ground", Reports and Memoranda No. 1131, Aeronautical Research Committee, London, July.

- Gray, G. J., von Grünhagen, W. (1998), "An Investigation of Open-Loop and Inverse Simulation as Nonlinear Model Validation Tools for Helicopter Flight Mechanics", *Mathematical and Computer Modelling of Dynamical Systems*, Vol. 4, No. 1, pp. 32-57.
- Ham, J. A. (1992), "Frequency Domain Flight Testing and Analysis of an OH-58D Helicopter", *Journal of the American Helicopter Society*, Vol. 37, No. 4, pp. 16-24.
- Ham, J. A., Gardner, Ch. K., Tischler, M. B. (1995), "Flight-Testing and Frequency-Domain Analysis for Rotorcraft Handling Qualities", *Journal of the American Helicopter Society*, Vol. 40, No. 2, pp. 28-38.
- Hess, R. A., Gao, C. (1993), "A Generalized Algorithm for Inverse Simulation Applied to Helicopter Maneuvering Flight", *Journal of the American Helicopter Society*, Vol. 16, No. 5, pp. 3-15.
- Hess, R. A., Gao, C., Wang, S. H. (1991), "Generalized Technique for Inverse Simulation Applied to Aircraft Maneuvers", *Journal of Guidance, Control, and Dynamics*, Vol. 14, No. 5, pp. 920-926.
- Hodgkinson, J. (1995), "The Relation of Handling Qualities Ratings to Aircraft Safety", Report No. AGARD-AR-335, Flight Vehicle Integration Panel Workshop on Pilot Induced Oscillations.
- Houston, S. S. (1994), "Validation of a Non-linear Individual Blade Rotorcraft Flight Dynamics Model Using a Perturbation Method", *Aeronautical Journal*, Vol. 98, No. 977, pp. 260-266.
- Houston, S. S. (1996), "Longitudinal Stability of Gyroplanes", *Aeronautical Journal*, Vol. 100, No. 991, pp. 1-6.

- Houston, S. S. (1998), "Identification of Autogyro Longitudinal Stability and Control Characteristics", *Journal of Guidance, Control, and Dynamics*, Vol. 21, No. 3, pp. 391-399.
- Houston, S. S. (2000), "Validation of a Rotorcraft Mathematical Model for Autogyro Simulation", *Journal of Aircraft*, Vol. 37, No. 3, pp. 403-409.
- Houston, S. S. (2002), "Analysis of Rotorcraft Flight Dynamics in Autorotation", *Journal of Guidance, Control and Dynamics*, Vol. 25, No. 1, pp. 33-39.
- Houston, S. S. (2003), Personal Communication.
- Houston, S. S. (2005), Personal Communication.
- Houston, S. S., Thomson, D. G. (1999), "Identification of Gyroplane Stability and Control Characteristics", Report No. RTO-MP-11, System Identification for Integrated Aircraft Development and Flight Testing.
- Houston, S. S., Thomson, D. G., Spathopoulos, V. M. (2001), "Experiments in Autogyro Airworthiness for Improved Handling Qualities", *Proceeding of the 57<sup>th</sup> Annual Forum of the American Helicopter Society*, Washington, DC, 9-11 May.
- Houston, S. S., Thomson, D. G. (2001), "The Aerodynamics of Gyroplanes", CAA Contract No. 7D/S/1125, Final Report.
- Houston, S. S., Thomson, D. G. (2004), "Flight Trials Using Montgomerie Gyroplane G-UNIV", CAA Contract No. 7D/S/1125/2, Final Report.
- Johnson, W. (1980), "Helicopter Theory", Princeton University Press.
- Key, D. L., Hoh, R. H., Blanken, C. L. (1998), "Tailoring ADS-33 for a Specific End Item", *Proceeding of the 54<sup>th</sup> Annual Forum of the American Helicopter Society*, Washington, DC, 20-22 May.

Krothapalli, K. R., Prasad, J. V. R., Peters, D. A. (1999), "Study of a Rotor Flap-Inflow Model Including Wake Distortion Terms", Report No. RTO-MP-11, System Identification for Integrated Aircraft Development and Flight Testing.

Krothapalli, K. R., Prasad, J. V. R., Peters, D. A. (2001), "Helicopter Rotor Dynamic Inflow Modelling for Manoeuvring Flight", *Journal of the American Helicopter Society*, Vol. 46, No. 2, pp. 129-139.

Leacock, G. R. (2000), "Helicopter Inverse Simulation for Workload and Handling Qualities Estimation", PhD Thesis, Department of Aerospace Engineering, University of Glasgow.

Leishman, J. G. (2000), "Principles of Helicopter Aerodynamics", Cambridge, Cambridge University Press.

Leishman, J. G. (2003), "The Development of the Autogiro: A Technical Perspective", Hofstra University Conference "From Autogiro to Gyroplane – The Past, Present & Future of an Aviation History", Hofstra University, NY, 25-26 April.

Lock, C. N. H. (1927), "Further Development of Autogyro Theory", Reports and Memoranda No. 1127, Aeronautical Research Committee, London, March.

Lock, C. N. H., Townend, H. C. H. (1928), "Wind Tunnel Experiments on a Model Autogyro at Small Angles of Incidence", Reports and Memoranda No. 1154, Aeronautical Research Committee, London, March.

Macdonald, C. A. (2001), "The Development of an Objective Methodology for the Prediction of Helicopter Pilot Workload", PhD Thesis, Department of Mathematics, Glasgow Caledonian University.

McVicar, J. S. G., Bradley, R. (1992), "A Partial Periodic Trim Algorithm for Application to Advanced Mathematical Models of Rotorcraft Vehicles", Proceedings of the Kinematics and Dynamics Multi-Body Systems Seminar, Institution of Mechanical Engineers Headquarters, London.

Meyer, M. A., Padfield, G. D. (2005), "First Steps in the Development of Handling Qualities Criteria for a Civil Tiltrotor", Journal of the American Helicopter Society, Vol. 50, No. 1, pp. 33-45.

Mitchell, D. G., Doman, D. B., Key, D. L., Klyde, D. H., Leggett, D. B., Moorhouse, D. J., Mason, D. H., Raney, D. L., Schmidt, D. K. (2004), "Evolution, Revolution, and Challenges of Handling Qualities", Journal of Guidance, Control, and Dynamics, Vol. 27, No. 1, pp. 12-28.

Nannoni, F., Stabellini, A. (1989), "Simplified Inverse Simulation for Preliminary Design Purposes", Proceedings of the 15<sup>th</sup> European Rotorcraft Forum, Amsterdam, the Netherlands, 12-15 September.

NASA (2005), "Aeronautics and Astronautics Chronology, 1915-1919", NASA's History Division website. Available at <http://www.hq.nasa.gov/office/pao/history/timeline/1915-19.html> [Accessed 03 February 2005].

Ockier, C. J. (1996), "Flight Evaluation of the New Handling Qualities Criteria Using the B0 105", Journal of the American Helicopter Society, Vol. 41, No. 6, pp. 67-76.

Ockier, C. J., Pausder, H.-J. (1995), "Experiences with ADS-33 Helicopter Specification Testing and Contributions to Refinement Research", Report No. AGARD-CP-560, Active Control Technology: Applications and Lessons Learned.

O'Hara, F. (1967), "Handling Criteria", Journal of the Royal Aeronautical Society, Vol. 71, No. 676, pp. 271-287.

- Padfield, G. D. (1981), "A Theoretical Model of Helicopter Flight Mechanics for Application to Piloted Simulation", Royal Aircraft Establishment, Technical Report 81048.
- Padfield, G. D. (1996), "Helicopter Flight Dynamics", Oxford, Blackwell Science.
- Padfield, G. D. (1998), "The Making of Helicopter Flying Qualities: Requirements Perspective", *Aeronautical Journal*, Vol. 102, No. 1018, pp. 409-437.
- Padfield, G. D., Jones, J. P., Charlton, M. T., Howell, S. E., Bradley, R. (1994), "Where Does the Workload Go When Pilots Attack Manoeuvres? An Analysis of Results from Flying Qualities Theory and Experiment", *Proceedings of the 20<sup>th</sup> European Rotorcraft Forum*, Amsterdam, the Netherlands, 4-7 October.
- Padfield, G. D., Meyer, M. A. (2003), "Progress in Civil Tilt-Rotor Handling Qualities", *Proceedings of the 29<sup>th</sup> European Rotorcraft Forum*, Friedrichshafen, Germany, 16-18 September.
- Pausder, H.-J., Blanken, C. L. (1992a), "Investigation of the Effects of Bandwidth and Time Delay on Helicopter Roll-Axis Handling Qualities", *Proceedings of the 18<sup>th</sup> European Rotorcraft Forum*, Avignon, France, 15-18 September.
- Pausder, H.-J., Blanken, C. L. (1992b), "Generation of Helicopter Roll Axis Bandwidth Data through Ground-Based and In-Flight Simulation", Report No. AGARD-CP-519, Flight Testing.
- Peters, D. A., HaQuang, N. (1988), "Dynamic Inflow for Practical Applications", *Journal of the American Helicopter Society*, Vol. 33, No. 4, pp. 64-68.
- Peters, D. A., Boyd, D. D., He, C. J. (1989), "Finite-State Induced-Flow Model for Rotors in Hover and Forward Flight", *Journal of the American Helicopter Society*, Vol. 34, No. 4, pp. 5-16.

- Peters, D. A., Morillo, J. A., Nelson, A. M. (2001), "New Developments in Dynamic Wake Modeling for Dynamic Applications", Proceedings of the 57<sup>th</sup> Annual Forum of the American Helicopter Society, Washington, DC, 9-11 May.
- Phillips, W. H. (1989), "Flying Qualities from Early Airplanes to the Space Shuttle", *Journal of Guidance, Control, and Dynamics*, Vol. 12, No. 4, pp. 449-459.
- Pitt, D. M., Peters, D. A. (1981), "Theoretical Prediction of Dynamic-Inflow Derivatives", *Vertica*, Vol. 5, No. 1, pp. 21-34.
- PRA (2004), "Safety Report: Gyroplane Accident Causes per NTSB Reports", Popular Rotorcraft Association website. Available at <http://www.pra.org> [Accessed 14 January 2004].
- Prouty, R. W. (1990), "Helicopter Performance, Stability, and Control", Robert E. Krieger Publishing Company, Malabar, Florida.
- Rutherford, S. (1997), "Simulation Techniques for the Study of the Manoeuvring of Advanced Rotorcraft Configurations", PhD Thesis, Department of Aerospace Engineering, University of Glasgow.
- Rutherford, S., Thomson, D. G. (1996), "Improved Methodology for Inverse Simulation", *Aeronautical Journal*, Vol. 100, No. 993, pp. 79-86.
- Rutherford, S., Thomson, D. G. (1997), "Helicopter Inverse Simulation Incorporating an Individual Blade Rotor Model", *Journal of Aircraft*, Vol. 34, No. 5, pp. 627-634.
- Schaefer, R. F., Smith, H. A. (1949), "Acrodynamic Characteristics of the NACA 8-H-12 Airfoil Section at Six Reynolds Numbers from  $1.8 \times 10^6$  to  $11.0 \times 10^6$ ", NACA Technical Note 1998.

- Shomber, H A., Gertsen, W. M. (1967), "Longitudinal Handling Qualities Criteria: An Evaluation", *Journal of Aircraft*, Vol. 4, No. 4, pp. 371-376.
- Soule, H. A. (1937), "Flight Measurements of the Dynamic Longitudinal Stability of Several Airplanes and a Correlation of the Measurements with Pilots' Observations of Handling Characteristics", NACA Report 578.
- Spathopoulos, V. M. (2001), "The Assessment of a Rotorcraft Simulation Model in Autorotation by Means of Flight Testing a Light Gyroplane", PhD Thesis, Department of Aerospace Engineering, University of Glasgow.
- Stivers, L. S., Rice, F. J. (1946), "Aerodynamic Characteristics of Four NACA Airfoil Sections Designed for Helicopter Rotor Blades", NACA Wartime Report, RBL5K02.
- Tate, S. J., Padfield, G. D., Tailby, A. J. (1995), "Handling Qualities Criteria for Maritime Helicopter Operations – Can ADS-33 Meet the Need?", Proceedings of the 21<sup>st</sup> European Rotorcraft Forum, Saint-Petersburg, Russia, 30 August – 1 September.
- Thomson, D. G. (1986), "An Analytical Method of Quantifying Helicopter Agility", Proceedings of the 12<sup>th</sup> European Rotorcraft Forum, Garmisch-Partenkirchen, Germany, 22-25 September.
- Thomson, D. G. (1992), "Development of a Generic Helicopter Mathematical Model for Application to Inverse Simulation", Internal Report No. 9216, Department of Aerospace Engineering, University of Glasgow.
- Thomson, D. G. (2005), "Aircraft Handling Qualities and Control 5", Lecture Notes, Department of Aerospace Engineering, University of Glasgow.
- Thomson, D. G., Bradley, R. (1990a), "Development and Verification of an Algorithm for Helicopter Inverse Simulation", *Vertica*, Vol. 14, No. 2, pp. 185-200.

- Thomson, D. G., Bradley, R. (1990b), "The Use of Inverse Simulation for Conceptual Design", Proceedings of the 16<sup>th</sup> European Rotorcraft Forum, Glasgow, UK, 18-20 September.
- Thomson, D. G., Bradley, R. (1994), "The Contribution of Inverse Simulation to the Assessment of Helicopter Handling Qualities", Proceedings of the 19<sup>th</sup> ICAS Conference, Anaheim, CA, 18-23 September.
- Thomson, D. G., Bradley, R. (1997a), "Mathematical Definition of Helicopter Manoeuvres", Journal of the American Helicopter Society, Vol. 42, No. 4, pp. 307-309.
- Thomson, D. G., Bradley, R. (1997b), "The Use of Inverse Simulation for Preliminary Assessment of Helicopter Handling Qualities", Aeronautical Journal, Vol. 101, No. 1007, pp. 287-294.
- Thomson, D. G., Bradley, R. (1998), "The Principles and Practical Application of Helicopter Inverse Simulation", Simulation Practice and Theory, International Journal of the Federation of European Simulation Societies, Vol. 6, No. 1, pp. 47-70.
- Wheatley, J. B. (1932), "Lift and Drag Characteristics and Gliding Performance of an Autogiro as Determined in Flight", NACA Report 434.
- Wheatley, J. B. (1933), "Wing Pressure Distribution and Rotor-Blade Motion of an Autogiro as Determined in Flight", NACA Report 475.
- Wheatley, J. B. (1934), "The Aerodynamic Analysis of the Gyroplane Rotating Wing System", NACA TN 492.
- Wheatley, J. B. (1935), "An Aerodynamic Analysis of the Autogiro Rotor with a Comparison between Calculated and Experimental Results", NACA Report 487.
- Wheatley, J. B. (1936a), "The Influence of Wing Setting on the Wing Load and Rotor Speed of a PCA-2 Autogiro as Determined in Flight", NACA Report 523.

Wheatley, J. B. (1936b), "A Study of Autogiro Rotor-Blade Oscillations in the Plane of the Rotor Disc", NACA TN 581.

Wheatley, J. B. (1937a), "An Analytical and Experimental Study of the Effect of Period Blade Twist on the Thrust, Torque, and Flapping Motion of an Autogiro Rotor", NACA Report 591.

Wheatley, J. B. (1937b), "An Analysis of the Factors that Determine the Periodic Twist of an Autogiro Rotor Blade, with a Comparison of Predicted and Measured Results", NACA Report 600.

Wheatley, J. B., Bioletti, C. (1936a), "Analysis and Model Tests of Autogiro Jump Take-off", NACA TN 582.

Wheatley, J. B., Bioletti, C. (1936b), "Wind Tunnel Tests of a 10-foot-Diameter Gyroplane Rotor", NACA Report 536.

Wheatley, J. B., Bioletti, C. (1937), "Wind Tunnel Tests of a 10-foot-Diameter Autogiro Rotors", NACA Report 552.

Wheatley, J. B., Hood, M. J. (1936), "Full-Scale Wind Tunnel Tests of a PCA-2 Autogiro Rotor", NACA Report 515.

Wheatley, J. B., Windler, R. (1935), "Wind Tunnel Tests of a Cyclogiro Rotor", NACA TN 528.

XFOIL (2001), XFOIL website, Massachusetts Institute of Technology. Available at <http://raphael.mit.edu/xfoil/> [Accessed 10 January 2005].

